Multimorbidity in the ageing human brain: associations between Alzheimer's disease pathology and white matter hyperintensities

Kirsty Elizabeth McAleese
BSc Hon Biomedical Sciences

Institute for Ageing and Health
Newcastle University
Campus for Ageing and Vitality
Newcastle-Upon Tyne
NE4 5PL

Thesis submitted for the degree of Doctor of Philosophy in
Newcastle University
May 2014

“I have no special talents. I am only passionately curious”
Albert Einstein (1879-1955)

Abstract

Background: In the brains of both demented and non-demented subjects the most common pathologies are Alzheimer's disease (AD) related pathologies and white matter lesions (WML). It is widely assumed that small vessel disease (SVD) is the main cause of WML, although evidence suggests neurodegenerative pathologies may also be involved in the pathogenesis of WML. However, investigation of these pathologies is hindered due lack of standardized histological criteria for WML assessment and the current use of semi-quantitative assessment is incapable of detecting subtle variations in pathologic burden across cases. The main aim of this study was to improve the *post mortem* assessment of WML/WMH and AD-related pathology in the ageing human brain by the use of *post mortem* MRI and quantitative neuropathological assessment, and to investigate possible associations between AD pathology and white matter integrity.

Methods: Formalin fixed brains underwent *post mortem* MRI and white matter hyperintensitites (WMH) were assessed according to the Age-Related White Matter Change (ARWMC) scale. ARWMC scores were compared with corresponding semi-quantitative neuropathological scores obtained by an extensive assessment of the white matter. In a cohort of AD and control brains semi-quantitative and quantitative assessment of hyperphosphorylated tau (HPT), amyloid-beta (Aβ) pathology and SVD were compared. The influence of AD-related pathology and SVD on white matter integrity was then investigated using a combination of *post mortem* MRI-based WMH assessment, quantitative neuropathological assessment using Tissue Micro Array (TMA) methodology and Sclerotic Index.

Key findings: MRI-based assessment of fixed *post mortem* brains was found to be a practical method that reliably reflects WML in the frontal, parietal and occipital WM comparable with an extensive histological assessment at 7 mm intervals. Digital quantification of cortical HPT, Aβ and SVD pathology revealed widespread variations in pathological burden. HPT, Aβ pathology and SVD had a significant influence on WMH severity in both non-demented normal aged and AD brains, however, HPT, but not SVD, was the most significant predictor of WMH score.

Conclusion: This study showed that MRI-based assessment of fixed *post mortem* brains is a practical method for the assessment of white matter integrity and TMA is a practical method for quantitative neuropathological assessment of degenerative neocortical pathologies. HPT was found to be the strongest predictor of WMH. However, further studies are required to elucidate the different patho-physiological mechanisms that may underlie WM damage in the ageing brain.

Acknowledgements

I would like to express my special appreciation to my supervisor Professor Johannes Attems for his support, knowledge and enthusiasm. I thank him for his continuous encouragement and belief in me and for the opportunity to complete a PhD and begin a career in research.

I feel truly privileged to have worked with such an encouraging and friendly group of people throughout my PhD. I would like to give a special thanks to Mrs Mary Johnson for all of her guidance, support and endless patience Mrs Ros Hall and Mrs Lynn Ramsay for taking their time to share their expertise in immunohistochemistry and histology. I thank my fellow PhD colleagues, particularly Miss Lauren Walker for her support and friendship, and Mr Shane McParland, Mr Daniel Erskine and Miss Elizabeth Gemmell for all of their help and advice.

I also wish to extend my gratitude to Mr Arthur Oakley for sharing his many words of wisdom, Mr Josh Beverley and Miss Madhurima Dey for their analytical assistance, to my second supervisor Professor Raj Kalaria, my progress supervisors Dr Elizabeta Mukaetova-Ladinska and Dr Chris Morris for their guidance and support, and to all the staff at the Newcastle Brain and Tissue Resource for their assistance during my studies. None of this research would have been possible without the generosity of the donors and families, and I hope my work will help to inspire further important research in this field.

Finally I would like to thank Mr Steven Hardy and all my family and friends, particularly Miss Kirsty Parkins, for their encouragement and support throughout my studies, and to let them know how much I appreciate all that they have done to help me achieve my PhD.

My PhD was funded by the Dunhill Medical Trust.

Kirsty E. McAleese

April 2014

Contribution of others to this thesis

I, Kirsty E. McAleese, performed and/or supervised all histological analysis, and performed all statistical analysis, data interpretation, literature research and writing of this thesis. I contributed to technical histological work, including tissue sectioning, histological staining and immunohistochemistry, used in all chapters of this thesis. Concept and design of the project was a joint collaboration with my supervisor Prof. Johannes Attems.

Mrs Ross Hall contributed to the technical histological work, including tissue sectioning and histochemical staining, used for analysis in Chapter 3.

Mrs Lynne Ramsay contributed to technical histological work inclusive of tissue processing of all cases used in this thesis and tissue sectioning, histological staining and immunohistochemical staining of tissue used for analysis in Chapters 4 and 5.

Mr Joshua Beverley and Miss Madhurima Dey both assisted in the vascular Sclerotic Index measurements used for analysis in Chapters 4 and 6.

Prof. Johannes Attems, Mr Shane McParland, Miss Lauren Walker and Mrs Mary Johnson contributed the concept and design of the TMA methodology used for analysis in Chapter 6.

Mrs Mary Johnson contributed to the technical histological work, including production of TMA blocks, sectioning of TMA blocks and histological and immunohistochemical staining of TMA sections used for analysis in Chapter 6.

Contents

Figure and table legends

Abbreviations

%BF	Percentage binary area fraction
3R	3 repeat tau
4R	4 repeat tau
A-syn	Alpha-synuclein
Aβ	Amyloid-beta
AD	Alzheimer's disease
AID	The Alzheimer's disease International
ApoE	Apolipoprotein E
APP	Amyloid precursor protein
ARWMC	Age-related white matter change
AS	Atherosclerosis
BACE 1	Beta-site APP cleaving enzyme 1
BR	Brain reserve
CAA	Cerebral amyloid angiopathy
CBD	Corticobasal degeneration
CBS	Corticobasal syndrome
CC	Corpus collosum
CERAD	Consortium to Establish a Registry for Alzheimer's Disease
cdk5	Cyclin dependent kinase 5
CNS	Central nervous system
CR	Cognitive reserve
C99	Carboxyl terminal 99 fragment
CVD	Cerebral vascular disease
CVL	Cardiovascular lesions
DGM	Deep grey matter
DLB	Dementia with Lewy bodies
DTI	Diffusion tensor imaging
EPVS	Enlarged perivascular space
FA	Fractional anisotropy
FI	Fragmentation Index
FTLD	Frontotemporal lobar degeneration

FUS	Fused in sarcoma RNA-binding protein
GCI	Glial cytoplasmic inclusion
GFAP	Glial fibrillary acidic protein
GVD	Granulovacuolar degeneration
GSK-3β	Glycogen synthase kinase 3β
H&E	Haematoxylin and eosin
HIF	Hypoxia Inducible Factors
HPT	Hyperphosphorylated tau
HS	Hippocampal sclerosis
IDE	Insulin degrading enzyme
IHC	Immunohistochemistry
LB	Lewy body
LBD	Lewy bodies disease
LFB	Luxol fast blue
LN	Lewy neurite
MAP2	Microtuble-associated-protein-2
MBD	Microtuble binding domain
MCI	Mild cognitive impairment
mDext	Mean external diameter
mDint	Mean internal diameter
MRI	Magnetic resonance imaging
MTL	Medial temporal lobe
NBTR	Newcastle Brain and Tissue Resource
NCI	Neuronal cytoplasmic inclusion
NFT	Neurofibrillary tangle
Ngb	Neuroglobin
Ni	No inclusion
NII	Neuronal intranuclear occlusion.
NT	Neuropil thread
OxS	Oxidative stress
PD	Parkinson’s disease
PDD	Parkinson’s disease dementia
PHF	Paired helical filament
PP2A/5	Protein phosphatase 2A/5
PSP	Progressive surpanuclear palsy

PVD	Perivascular drainage
PVS	Perivascular space
PVWMH	Periventricular white matter hyperintensities
PVWML	Periventricular white matter lesions
sAPPβ	Secreted APP-beta
SI	Sclerotic Index
SLF	Superior longitudinal fasciculus
SMC	Smooth muscle cell
SVD	Small vessel disease
SVP	Subcortical vascular pathology
TBS	Tris buffered saline
TDP	Trans-activation response DNA-binding protein
TMA	Tissue MicroArray
UPS	Ubiquitin-proteasome system
VCI	Vascular cognitive impairment
VP	Vascular pathology
WLD	Wallerian-like degeneration
WM	White matter
WMH	White matter hyperintensities
WML	White matter lesion
WMs	White matter score
wt	Wild type

Original publication

The study described in Chapter 3 of this thesis is based on the following original publication.

McAleese KE, Firbank M, Hunter D, Sun L, Neal JW, Mann DM, Esiri M, Jellinger KA, O'Brien JT, Attems J (2013) Magnetic resonance imaging of fixed post mortem brains reliably reflects subcortical vascular pathology of frontal, parietal and occipital white matter. *Neuropathol Appl Neurobiol* 39:485-97.

Chapter 1 – Introduction

1.1 Population ageing and age-related dementias

Global population ageing has been a defining process for the 20th century and the socio-economical burdens resulting from this process are continuing to increase in the 21st century. Population ageing is the result of a demographic transition from high to low mortality rates and increased life expectancy; together with a steady decline in fertility population ageing results in profound social, economical and political challenges (Sosa-Ortiz et al., 2012, Olshansky, 1985). The increase in the global ageing population is the driving force behind the current pandemic of dementia. Dementia amongst the elderly is a fundamental problem, and remains the main cause of disability among older adults (Sosa-Ortiz et al., 2012).

The Alzheimer's Disease International (AID) 2010 report estimated a global prevalence of dementia in the over 60's at 35.6 million (4.7%), doubling every 20 years to 65.7 million by 2030 and 115.4 million by 2050 (AID, 2009). The estimated annual global economic cost of dementia was estimated at $604 billion, or 1% of global gross domestic product in 2010, of which 89% was from high-income countries reflecting the cost of care to suffers (AID, 2010, AID, 2013). The economic burden of dementia is increasing in parallel with its prevalence and is predicted to cost the global economy $1,117 billion by 2030. These problems are also reflected in the UK, with over 800,000 people thought to be suffering some form of dementia at a cost of £23 billion to the National Health Service (Lakey, 2012).

Dementia can have a devastating impact on suffers, their families and care-givers and is being recognized as a critical issue, with world wide governments prioritizing funding for dementia research and ensuring health and social care systems are adequately structured and prepared. On December 2013 at the G8 dementia summit, the UK formally joined the Global Dementia Innovation Envoy, accepting dementia as a public health priority. In partnership with various national and international health organisations, the UK government acknowledged dementia as a global disease with high socio-economic burden

and agreed to increase funding into the innovation of cure/disease-modifying therapies and to improve the quality of life for suffers and carers (G8UK, 2013).

1.2 Dementia

Dementia is a syndrome caused by various disorders affecting the cerebral structure and function, resulting in progressive deterioration of memory, behavior and mental functions to a point were the individuals ability to perform everyday tasks is impaired, comprising autonomy and capacity for independent living (Sosa-Ortiz et al., 2012).

There are 2 main types of dementia; age-related (senile) dementia and early onset dementia. Age-related dementias occur in the majority of cases as a result of the progression of sporadic neurodegenerative or cerebrovascular diseases (CVD) and manifest usually after the age of 65 years. Early onset dementias generally occur before the age of 65 years, are much less common than age-related types and are attributed to genetic mutations that result in cerebral disease; e.g. early onset Alzheimer's disease (AD) may be caused by autosomal dominant mutations of *presenilin 1* gene on chromosome 14 or by mutations of the β-amyloid precursor protein gene on chromosome 21 (Jefferies and Argrawal, 2009); early-onset vascular dementia (VaD) CADASIL (cerebral autosomal dominant arterio-pathy with subcortical infarcts and leuko-encephalopathy) is caused by *Notch3* gene mutation on chromosome 19 (Chabriat et al., 2009). Other types of early-onset dementias can results from alcohol abuse, Huntington's disease, prion diseases and HIV/AIDS amongst others. This study will focus on age-related dementias only.

1.3 Neurodegeneration

Neurodegenerative diseases share common clinical features and pathogenic mechanisms, characterized by progressive neuronal dysfunction that can lead to dysfunction and/or death of specific neuronal populations in distinct anatomically related functional systems. Therefore, the clinical presentation of neurodegenerative diseases is generally dependent on the region affected and not on the underlying molecular nature of the pathological lesion. This leads to an overlap of clinical symptoms in different neurodegenerative diseases which potentially impairs the accuracy of *pre-mortem* diagnosis of neurodegenerative diseases; e.g. pigmented neuron loss in the substantia nigra presents clinically as parkinsonism, irrespective of the neuropathology which could be for example

α-synuclein (α-syn) or hyperphosphorylated tau (HPT) aggregates (Attems and Jellinger, 2013b).

The unifying feature of neurodegenerative diseases is the insidious accumulation of insoluble aggregates of physiologically soluble proteins of the central nervous system (CNS) (Skovronsky et al., 2006). The native function of various proteins is lost and proteins misfold and oligomerize into fibrils, which further accumulate and deposit intracellular in neurons and/or neuroglia or extracellular. The molecular nature of the respective protein deposit, in conjunction with the topographical localization, is the basis of the classification of neurodegenerative disease (Table 1.1).

Disease	Protein	Form	Localization
Alzheimer's disease	tau (3R, 4R) Aβ (1-40, 1-42) tau (3R, 4R) and Aβ (1-40, 1-42)	NFT, NT Aβ plaque neuritic plaque	Neuronal soma (NFT) and dendrites (NT) extracellular tau, neuronal processe; Aβ, extracellular
Lewy body diseases			
Parkinson disease	α-synuclein	LB, LN	Neuronal soma (LB) and dendrites (LN)
Dementia with Lewy bodies	α-synuclein	LB, LN	Neuronal soma (LB) and dendrites (LN)
Multiple system atrophy	α-synuclein	GCI	Cytoplasm of glial cells
Frontotemporal lobar degeneration			
Tauopathies			
Picks disease	tau (3R)	Pick bodies	Neuronal soma
Corticobasal degeneration	tau (4R)	Astrocytic plaques	Distal segements of astrocytes
Progressive supranuclear palsy	tau (4R)	Globose NFT, tufted astrocytes	Neuronal and astroctye soma
Agyrophilic grain disease	tau (4R)	Grains	Neuronal dendrites
Neurofibrillary tangle dominante dementia	tau (3R, 4R)	NFT, NT	Neuronal soma (NFT) and dendrites (NT)
Others			
FTLD-TDP	TDP-43	NCI, NII	Neuronal cytoplasm and nuclei
FTLD-UPS	Ubiquitin	NCI, NII	Neuronal cytoplasm and nuclei
FTLD-FUS	FUS	NCI, NII	Neuronal cytoplasm and nuclei
FTLD-ni	none known	-	-

Table 1.1. Classification of neurodegenerative diseases. FTLD, frontotemporal lobar degeneration; TDP, trans-activation response DNA-binding protein; UPS, ubiquitin-proteasome system; FUS, fused in sarcoma RNA-binding protein; ni, no inclusion; 3R, 3 repeat tau; 4R, 4 repeat tau; Aβ, amyloid-beta; NFT, neurofibrillary tangle; NT, neuropil thread; LB, Lewy body; LN, Lewy neurite; GCI, glial cytoplasmic inclusion; NCI, neuronal cytoplasmic inclusion; NII, neuronal intranuclear occlusion.

Despite considerable advances in our knowledge and understanding of the patho-mechanisms of neurodegeneration, the exact cause for the accumulation of these proteins in age-related diseases still remains unknown. The causes are likely to be multifactorial, with the involvement of environmental, lifestyle factors and individual epigenetics. Variations in specific gene expression and activity may cause higher production of a specific protein or an isoform and/or its related regulatory enzymes, or a decrease in the activity of the protein degradation and/or elimination pathways e.g. ubiquitin-proteasome system, all of which may lead to an increased formation of protein aggregates (Figure 1.1). Furthermore, the exact mechanisms as to how these protein aggregates cause

neuronal dysfunction and/or loss remain to be elucidated. Neurodegenerative disease itself usually does not lead to fatal brain lesions; it rather predisposes the sufferer to acquire fatal diseases (Attems et al., 2005b).

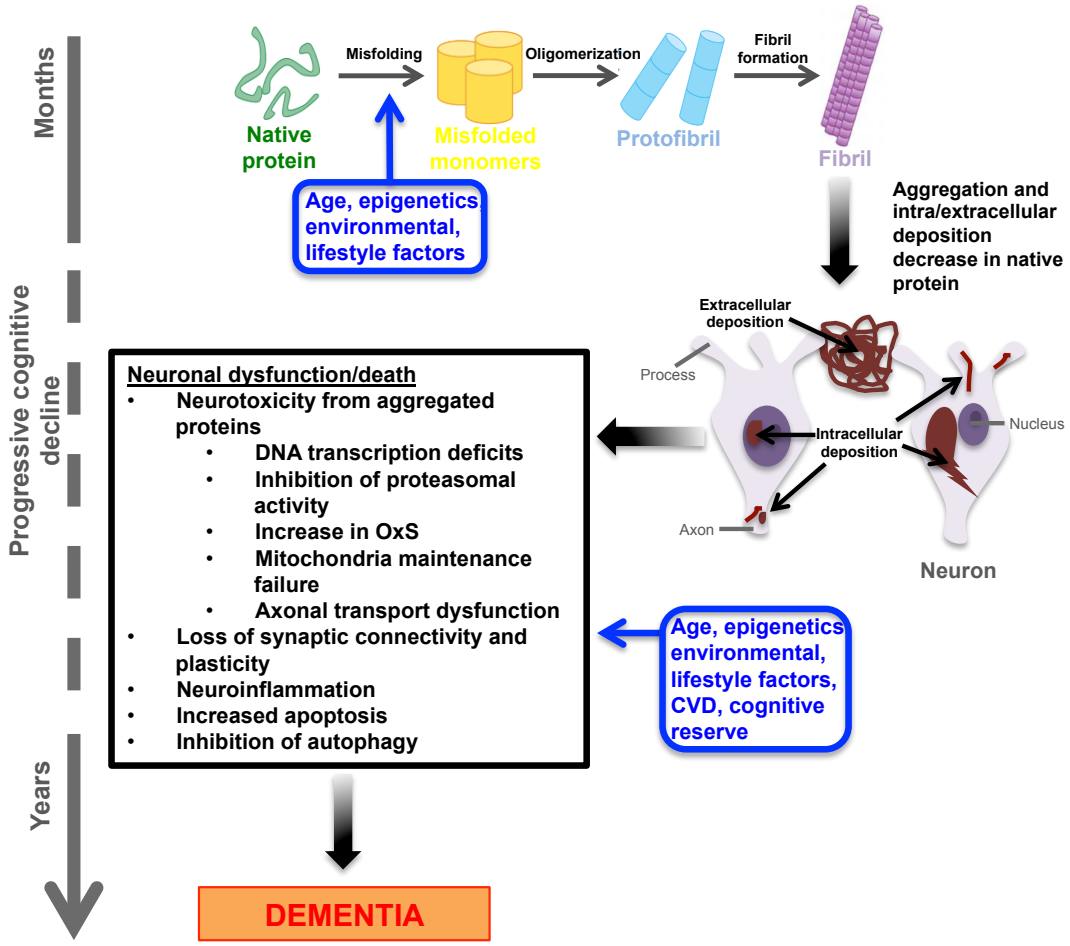

Figure 1.1 Schematic diagram illustrating the potential patho-mechanisms involved in neurodegeneration. Native proteins undergo conformational change and aggregation as a result of various genetic and environmental factors. Protein accumulations are deposited intracellular in cell soma, processes, axons and nucleus in neurons and neuroglia, and/or extracellular in the brain parenchyma. Protein deposits, in conjunction with various factors, may cause a wide range of neuronal dysfunctions and eventual neuronal death, resulting in the clinical syndrome dementia over a long period of time. OxS, oxidative stress; CVD, cerebral vascular disease

The amount of pathology, as well as the location, is crucial for the development of clinical symptoms (Attems and Jellinger, 2013b). However, neuropathological lesions are commonly present in non-demented elderly, although to a lesser extent. It is still unknown why in some individuals the neurodegenerative processes develops to dementia while others show only limited pathology and remain cognitively intact. This has led to an ongoing debate as to whether age-associated neurodegenerative pathologies are a consequence of ageing rather than a distinct disease; in a disease context some individuals would never develop dementia, regardless of their age. If neurodegeneration would be an inevitable consequence of ageing, everyone would eventually develop dementia

if the individual "threshold" age would be reached. The variation between individual susceptibility to age-related changes and pathological burden and the age of dementia onset has been attributed to cognitive reserve (CR) and brain reserve (BR) (Stern, 2012). CR is a hypothetical concept suggesting that differences in cognitive processes are a consequence of lifetime intellectual activities and environmental factors (Stern, 2002). CR cannot be measured, only estimated based on lifetime factors and intellectual testing, but extensive epidemiological and experimental evidence has shown that higher cognitive reserve and successful cognitive ageing is associated with a higher education, more leisure activities and occupation complexity (Barulli and Stern, 2013, Suchy et al., 2011). BR is a similar concept based on the individual variation in quantitative measures e.g. brain size (Perneczky et al., 2012, Whitwell, 2010), neuronal number, synaptic connections. Once BR has decreased beyond a certain threshold functional decline occurs (Barulli and Stern, 2013). CR, unlike BR, is dynamic and can be actively altered throughout life; therefore, CR is believed to account for the differences in cognitive state despite predisposed or equal BR and pathological burden (Figure 2.1).

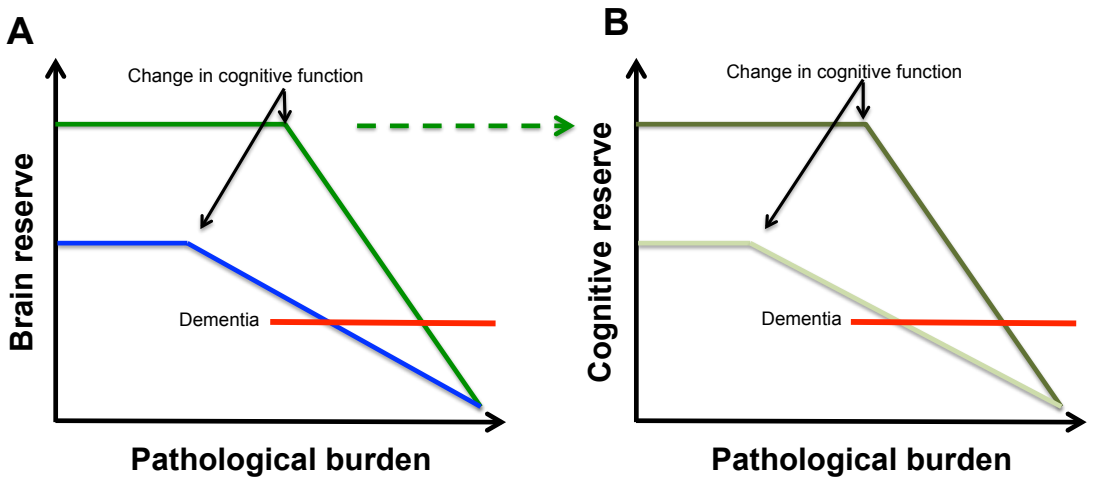

Figure 1.2. Graphical representation of how brain reserve and cognitive reserve mediate decline in cognitive function in non-demented, and decline to dementia in demented elderly. A) *x-axis* represents cerebral pathology accumulating over time, *y-axis* represents brain reserve, green line represents a high brain reserve and the blue line a low brain reserve. We assume cerebral pathology increases with increasing age at the same rate for the two individuals. The amount of pathology needed before cognitive function declines to dementia (red line) is greater in the individual with higher brain reserve than the lower brain reserve leading to a later changing point. B) *x-axis* represents cerebral pathology accumulating over time, *y-axis* represents cognitive reserve, dark green line represents a high cognitive reserve and the lighter green line a low cognitive reserve. If we take two individuals with the same brain reserve and equally increasing cerebral pathology, the amount of pathology needed before cognitive function is affected is greater in the individual with higher cognitive reserve than the lower cognitive reserve leading to a later changing point. More pathology is required for the individual with higher brain reserve and cognitive reserve to meet clinical diagnosis of dementia, thus delaying the onset of disease. However, once cognitive decline begins it is more rapid in the person with higher brain reserve and cognitive reserve. Modified from Barulli and Stern 2013.

1.4 Major age associated dementias and their associated lesions

Firstly, I will discuss the major neurodegenerative diseases, their associated hallmark pathologies and current criteria used for the *post mortem* neuropathological diagnosis; confirmed disease diagnosis is based on a standardized practice of *post mortem* brain sampling to access known predilection areas of hallmark lesions and stage the most dominant pathology.

1.4.1 Alzheimer's Disease

AD is the most common age-related neurodegenerative dementia subtype representing 60-80% of cases globally (Mayeux and Stern, 2012, Nowrangi et al., 2011, Reitz et al., 2011), and prevalence increases with age, affecting up to 50% of the over 85 year olds (AID, 2009). In 1906, Alois Alzheimer first described the clinical symptoms and presence of 'chemical changes of fibrillary substance' and 'miliary foci…in the cortex' (Alzheimer, 1907), corresponding to

what we know now as neurofibrillary tangles (NFT) and amyloid-beta (Aβ) plaques. This was followed by the discovery of senile plaques by Divry in 1930 (Maccioni et al., 2001) but it wasn't until the mid-1980's that the core proteins were identified as microtubule protein tau (Brion et al., 1986, Grundke-Iqbal et al., 1986) and Aβ peptide derived from the amyloid precursor protein (APP) (Glenner and Wong, 1984).

Clinically AD is characterized by impairment in memory, including short- term, semantic and implicit memories. In addition oral and written language impairment, as well as impairment in visual and spatial recognition may be present. Symptoms become increasingly severe as the disease progresses, interfering with daily life activities (Thies and Bleiler, 2013). Neuropathologically AD is characterized by the presence of both intracellular HPT, in the form of NFT and neuropil threads (NT) and extracellular Aβ deposits. Macroscopically, AD brains present with characteristic cortical atrophy (thinning of the gyri and deepening of the sulci) especially in the temporal lobe (Halliday et al., 2003) and commonly exhibit enlarged lateral ventricles (Figure 1.3).

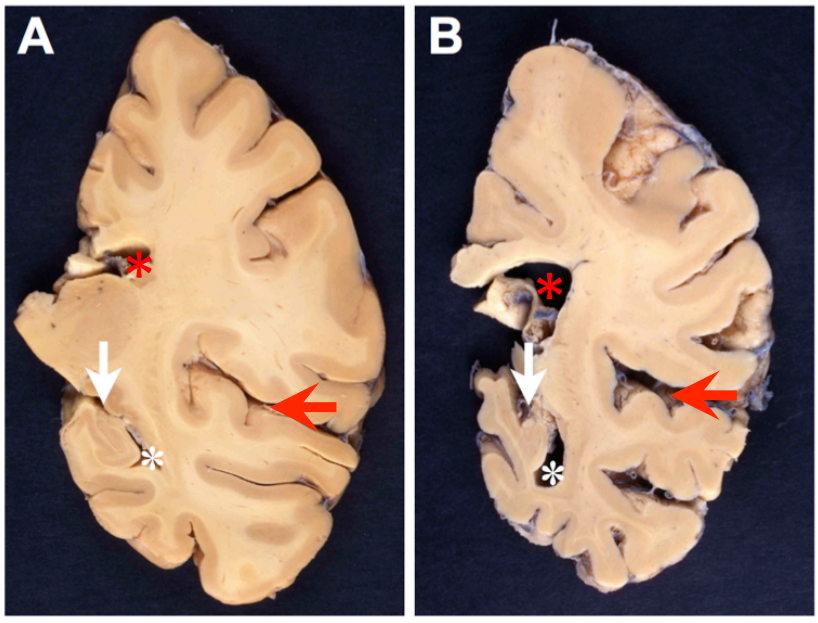

Figure 1.3. Formalin fixed brain slices of the left hemispheres (level of posterior hippocampus) of an aged non-demented individual (A) and an AD patient (B). Note the marked atrophy in B, especially hippocampal atrophy (arrow) and the lateral sulcus (red arrow) with widening of the lateral ventricle (red asterisk) and inferior horn of the 2nd ventricle (white asterisk). Photographs courtesy of Simon Fraser and Arthur Oakley, modified from (Attems and Jellinger, 2013b).

Tau is a multifunctional microtubule associated protein in axons and dendrites involved in the assembly, stabilization and linking to various cytoskeleton filaments required for axonal morphology (Maccioni and Cambiazo, 1995, Mandelkow et al., 1995, Ittner et al., 2010). Tau is also thought to have roles in neuronal development, neuronal signal transduction and polarity (Shahani and Brandt, 2002) especially in the postsynaptic compartments of the dendrites (Ittner et al., 2010). Alternative splicing of the microtubule associated protein tau (*MAPT*) gene on chromosome 17 (Goedert et al., 1989) yields 6 isoforms of mRNA, which differ by the presence of 3-repeat (3R; microtubule binding repeats) or 4-repeat (4R) of the C-terminus and the presence or absence or one or two inserts of amino acids in exon 2 and 3 or the N-terminus (Gong et al., 2005). Tau protein is modulated by phosphatases (dephosphorylation) and kinases (phosphorylation) causing tau microtubule binding and un-binding from the microtubulus, respectively. Under physiological conditions both de-phosphorylation and phosphorylation are required for tau's physiological function, hence, tau phosphorylation states are under a constant dynamic equilibrium. However, abnormal hyperphosphorylation causes complete dissociation of tau from the microtubule, leading to depolymerized microtubules and, crucially, tau looses its biological function (Iqbal et al., 1986, Lindwall and Cole, 1984) and is termed HPT, undergoing conformational change and aggregation into filaments and subsequently paired helical filaments (PHF) occur (Metcalfe and Figueiredo-Pereira, 2010) (Figure 1.4). Phosphorylation is up to 4-fold higher in AD brains compared to normal (Ksiezak-Reding et al., 1992). The cause of tau hyperphosphorylation remains to be fully elucidated; theoretically up regulation of kinase activity and down regulation of phosphatase activity would generate hyperphosphorylation, however, studies are inconsistent and as of yet all attempts to induce NFT in animal model via alteration of phosphorylation have failed (Gong et al., 2005). Furthermore, other post-translational modifications of tau e.g. glycosylation, ubiquitination etc., may also play an important role in the pathogenesis of NFT formation (Gong et al., 2005, Garcia-Sierra et al., 2008, Metcalfe and Figueiredo-Pereira, 2010, Wang et al., 2007).

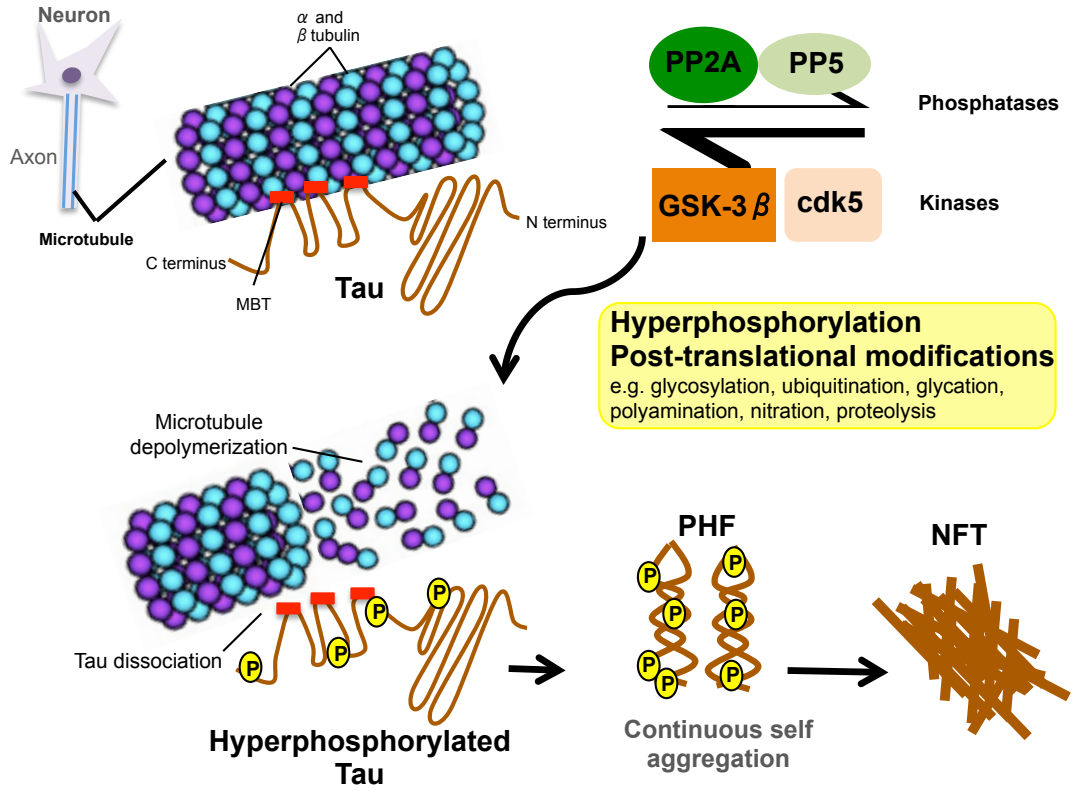

Figure 1.4. Schematic diagram illustrating the proposed pathogenesis of NFT. Tau is a microtubule-associated protein primarily located in the neuronal axon. Dephosphorylated tau binds to microtubule components α and β tubulin at the MBD. Phosphorylation of tau protein, via serine and/or threonine residues, is controlled by kinases such as GSK-3β and cdk5, and phosphatases PP2A and PP5. It is proposed that when the dynamic equation favors kinases, hyperphosphorylation of tau occurs. In conjunction with various post-translational modifications, HPT dissociates from the microtubule, causing microtubule breakdown. HPT undergoes self-aggregation in to PHF, which compose NT in neuronal dendrites, and eventually form NFT in the neuronal soma. MBD, microtubule binding domain; GSK-3β, glycogen synthase kinase 3β; cdk5, cyclin dependent kinase 5; HPT, Hyperphosphorylated tau; NFT, neurofibrillary tangles; NT, neuropil threads PP2A/5, protein phosphatase 2A/5; PHF, paired helical filaments;

Using immunohistochemical antibodies (e.g., AT8) accumulations of HPT can be visualized in *post mortem* tissue. In AD, accumulations are seen in neurons and encompass both 3R and 4R HPT variants. HPT accumulates in the neuronal soma as NFT (also non-aggregated HPT can accumulate as pre-tangles; considered a precursor of NFT), and in the dendrites and processes of the tangle containing neurons as NT, which are short, fragmented fiber-like accumulations of HPT (Braak and Braak, 1988) (Figure 1.5). Ghost-tangles are a form of extracellular NFT found in severely effected areas after neuronal loss (Cras et al., 1995). Importantly the extent of NFT/NT correlates with cognitive deficits (Giannakopoulos et al., 2003). In AD, NFT/NT are predominantly found in the entorhinal cortex, hippocampus and layer III and VI of the isocortex, the olfactory bulb and locus ceruleus (Attems et al., 2012, Braak and Del Tredici,

2011, Attems et al., 2005c). It is widely accepted that NFT/NT initially manifest in the transentorhinal and entorhinal cortices and gradually spread to the hippocampus and isocortex in a specific pattern, which is the basis for the neuropathological grading system used for the diagnosis of AD (see section 2.2.2) NFT are associated with both neuronal death (Gomez-Isla et al., 1997) and cognitive impairment in AD (Braak and Braak, 1996, Giannakopoulos et al., 2003, Ince, 2001, Rossler et al., 2002).

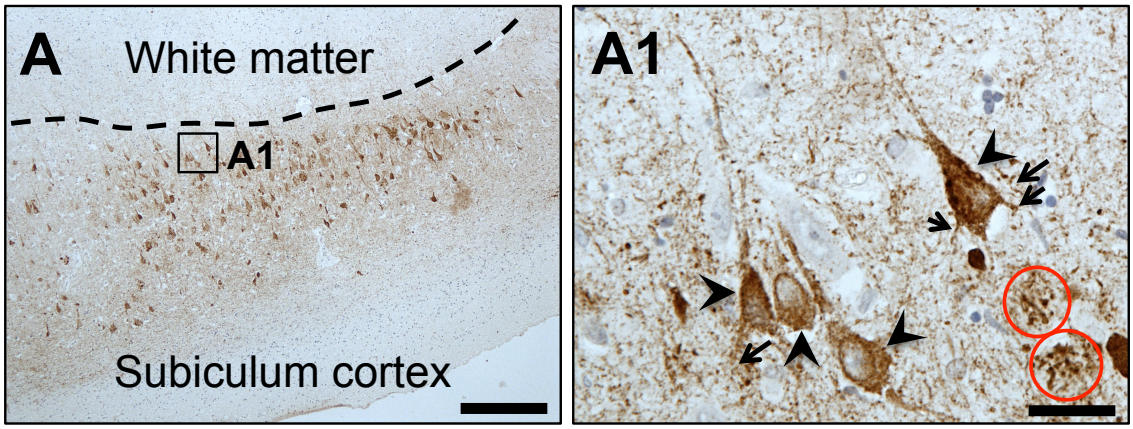

Figure 1.5. A) NFT and NT in the subiculum of the hippocampus . A1) Arrow heads indicate neuronal soma that comprises the NFT. Arrows indicate NT in neuronal processes. Red ovals highlight neuritic plaques. Immunohistochemistry AT8; NFT, neurofibrillary tangles; N, neuropil threads; Scale bars: A 500μm; A1 50μm.

APP, a type-1 transmembrane protein highly expressed in neurons, undergoes enzymatic cleavage by α or β secretase and secondary cleavage by the γ-secretase complex to produce various peptides required for cellular function e.g. APP-intracellular cytoplasmic domain for DNA transcription regulation. Under physiological conditions the α-secretase, or non-amyloidogenic pathway, is dominant and does not result in the formation of Aβ peptide (40kDa). By contrast, in AD the β secretase, or amyloidogenic pathway, is more prevalent and abnormal amounts of the Aβ peptide are produced that eventually forms extracellular Aβ deposits. β-secretases cleave the extracellular APP domain, followed by secondary cleavage by γ-secretase complex, resulting in the formation of Aβ peptides (Selkoe, 2008). Various isoforms of Aβ exist, the most common being the 1-40 (95% of peptides (Naslund et al., 1994)) and 1-42 variants (Citron et al., 1996), with the latter having 2 supplementary amino acids which renders it more hydrophobic and prone to precipitate in water and initiate

oligomerization and self-aggregation into plaques (Naslund et al., 1994) (Figure 1.6).

The physiological function of Aβ is unknown although recent evidence has indicated roles in positive synapse activity (Puzzo et al., 2008). However, deletion of APP in transgenic mice does not have a significant effect on life expectancy (Zheng et al., 1995). Degradation of Aβ occurs via multiple enzymes, the most important ones being neprilysin and insulin degrading enzyme (IDE). In addition Aβ may be cleared via interstitial fluid and perivascular spaces, which is considered the brains lymphatic drainage system (Weller et al., 2009). Aβ deposition is related to the imbalance of production and clearance of the Aβ peptide. It has been postulated that slight variations/alterations in this equilibrium, as a result of (epi)-genetic and environmental factors, cause an increase in Aβ plaque deposition over time. A study by Tyler and colleagues (Tyler et al., 2002) found that in 15 neuropathologically confirmed AD brains, 80% had either a decrease in α-secretase activity (81% of normal activity), an increase in β-secretase activity (average 185% of normal activity) or both compared to control brains, highlighting the implications of an imbalance in Aβ peptide production.

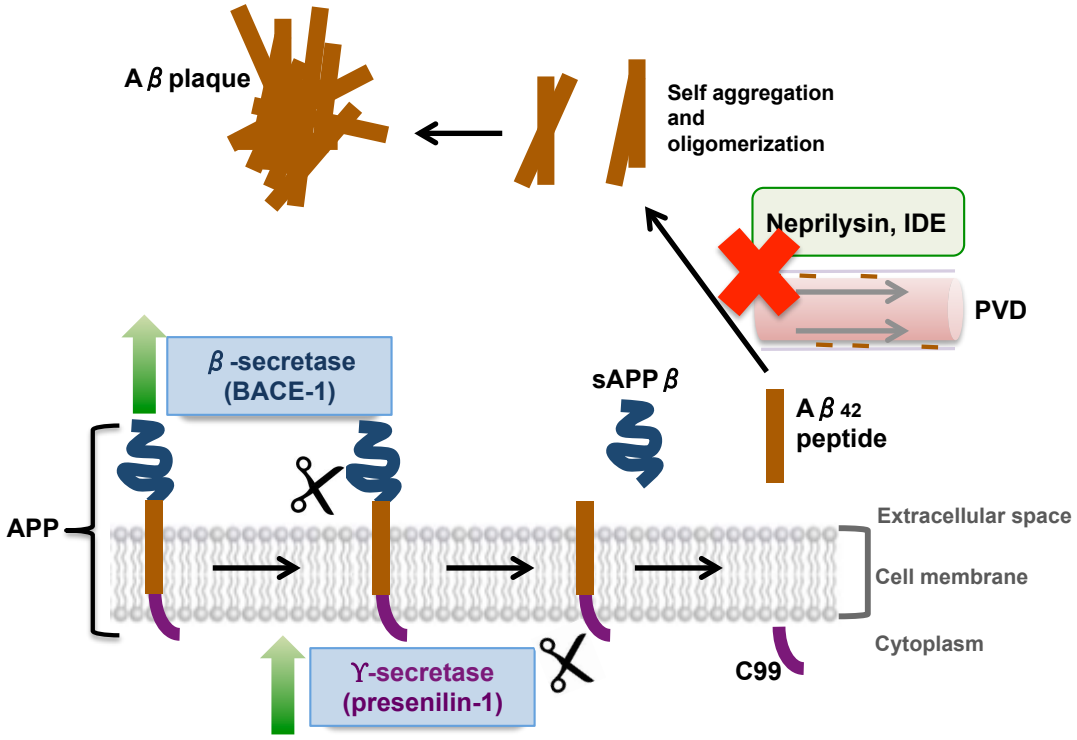

Figure 1.6. Schematic diagram illustrating the proposed pathogenesis of Aβ deposits (focusing on Aβ-42 only). The transmembrane protein APP is first cleaved in the extracellular domain by a BACE-1, a β-secretase, releasing sAPPβ fragment. Subsequent intramembrane cleavage by presenilin-1, a ϒ-secretase , produces the extracellular Aβ-42 peptide and C99 fragment. Increased production or activity of β and ϒ secretases, and/or failure of PVD, and/or decreased enzymatic clearance via neprilysin or IDE, results in an increase of endogenous Aβ-42. Aβ-42 undergoes self-aggregation and oligomerization to form an extracellular Aβ plaque. APP, amyloid precursor protein; BACE-1, beta-site APP cleaving enzyme 1; sAPPβ, secreted APP-beta; Aβ, amyloid-beta; C99, carboxyl terminal 99 fragment; IDE, insulin degrading enzyme; PVD, perivascular drainage.

In recent years a plethora of anti- Aβ antibodies for use in immunohistochemistry has been developed (e.g. 4G8), revealing the different morphological forms of extracellular Aβ aggregates. There are 2 main types of parenchymal deposits; i) diffuse Aβ deposits are usually large (50-100's μm) with continuous ill-defined borders, also termed as 'lake-like' or 'fleecy' (Duyckaerts et al., 2009) (Figure 1.7 A-A3**)**, while ii) focal Aβ deposits incorporate a dense, spherical accumulation of Aβ peptide that may contain focal deposits of activated microglia (Arends et al., 2000) with/without a neuritic corona. Focal deposits with a neuritic corona are referred to as neuritic plaques; the central deposit is virtually always Aβ-42 (Guntert et al., 2006) with an external halo (the corona) of HPT from dystrophic neurites (Figure 1.7 B**)**. Neuritic plaques are strongly associated with AD, while diffuse and non-tau containing focal deposits are also frequently seen in controls both in *post*

mortem brains and *in vivo* using Pittsburgh compound-B (PIB) PET scans (Lockhart et al., 2007). However, Aβ deposits have no significant correlation with clinical dementia symptoms (Delaere et al., 1990, Dickson et al., 1992). The large majority of Aβ deposits are located in the grey matter (although there may be diffuse deposits in the white matter (WM) (Duyckaerts et al., 2009)) and neuritic plaques are preferentially found in cortical cell layers II and III (Duyckaerts et al., 1986). The topographical locations of Aβ deposits are not random and follow a distinct sequence based on the stage of disease, which is used in the neuropathological diagnosis of AD and described in section 2.2.

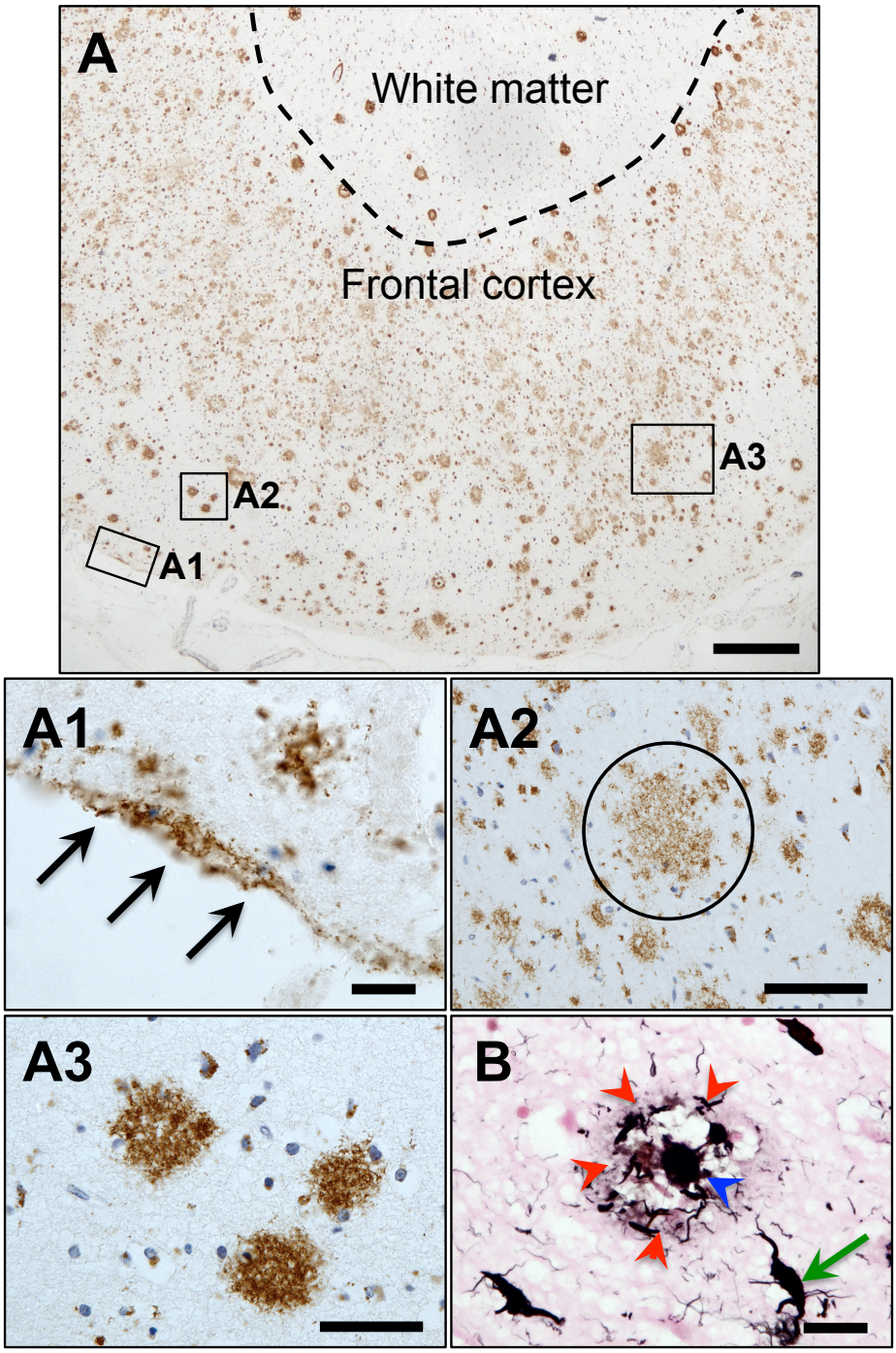

Figure 1.7. Different morphology of Aβ deposition in the pre-frontal cortex (A-A3). Subpial band-like Aβ (arrows, A1); fleecy Aβ (oval, A2), focal Aβ plaques (A3). Neuritic plaques (B) contain a dense aggregated Aβ core (blue arrow head) surrounded by a neuritic coronal (red arrow heads) made of dystrophic neurites (green arrow). A 4G8, B Gallyas silver stain; Scale bars: A 500μm; A1, B 20μm; A2 100μm; A3 50μm.

Both Aβ and HPT have been studied in great detail. Most therapeutic approaches for AD target Aβ deposition due to the 'amyloid cascade hypothesis', that proposes Aβ accumulation, in the form of oligomers, is the primary event in AD pathogenesis (Hardy and Selkoe, 2002, Hardy and Higgins, 1992) (Figure 1.8). Evidence for this theory stems from Trisomy 21 and various mutations of APP and presenilins genes in familial AD cases that clearly exhibit both HPT and Aβ pathologies. However, subjects with a tau gene mutation, such as those involved in taupathies e.g. familial forms of frontotemporal lobar degeneration (FTLD) characterized by severe NFT, do not exhibit Aβ pathology, suggesting that APP metabolism alteration may trigger HPT (Munoz and Ferrer, 2008), as severe HPT pathology in tauopathies does not result in Aβ accumulation (Hutton et al., 1998). Furthermore, Aβ oligomers have been shown to promote phosphorylation of tau in primary hippocampal neurons (De Felice et al., 2008) and activate specific cell signaling triggering NFT pathogenesis (Alvarez et al., 1999, Patrick et al., 1999, Alvarez et al., 2001) suggesting HPT formation in AD is secondary to Aβ accumulation and directly affected by Aβ species.

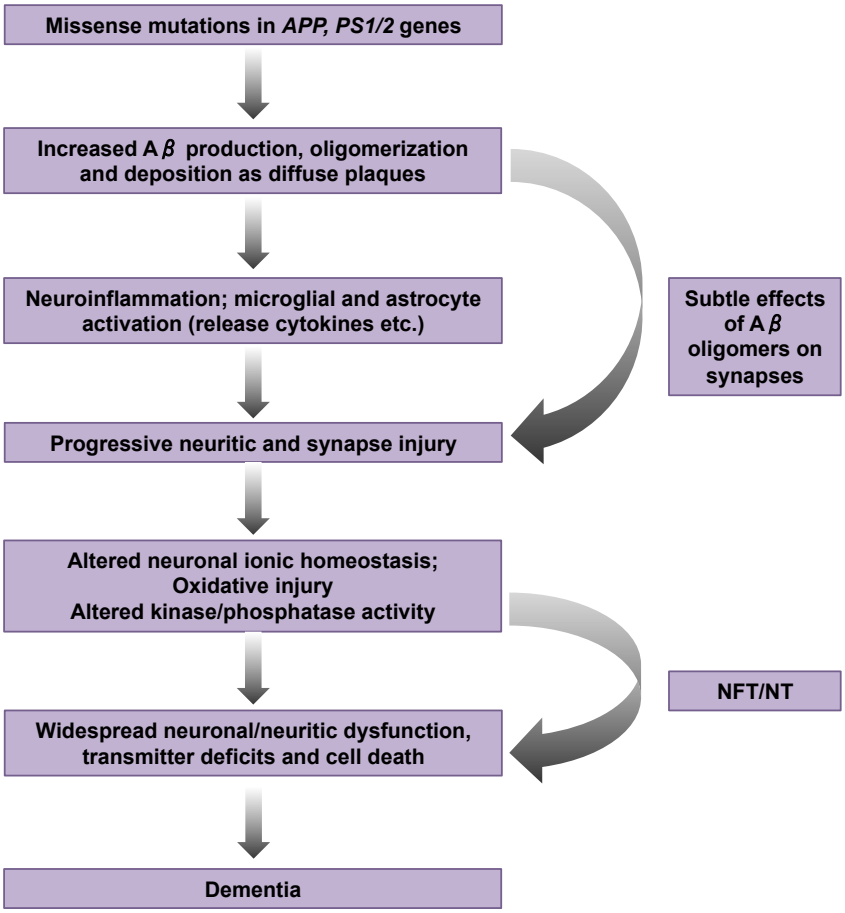

Figure 1.8. 'The amyloid cascade hypothesis'. A sequence of proposed pathological events that lead to AD. Adapted from (Hardy, 2002).

Although, contrary evidence suggests that in age-related AD the 'amyloid cascade hypothesis' may not always apply as large autopsy studies have shown that HPT pathology predates Aβ depositions by decades (Duyckaerts and Hauw, 1997). In transgenic animal studies, mice that express human APP exhibit abundant Aβ deposition but no tau pathology (Oddo et al., 2003) and transgenic tau knock-out mice exhibit no neuronal degeneration indicating tau is required for neurodegeneration in AD and is not merely a 'secondary' pathology (Rapoport et al., 2002). Most importantly there is a lack of correlation between Aβ deposition and cognitive deficits, and it is not uncommon for elderly individuals with severe Aβ pathology to maintain normal cognitive function (Braak and Braak, 1991), further supporting HPT as main instigator of neurodegeneration in AD. Furthermore, the 'amyloid cascade hypothesis' has been the backbone to the vast majority of drug research into AD; however, no therapies designed to prevent and/or reverse amyloid accumulation have passed Phase III clinical trials (Karran et al., 2011).

Although the relationship of HPT and Aβ is not yet fully determined, the co-occurrence of pathologies in AD suggests a synergistic relationship. Recently, the 'tau axis hypothesis of Alzheimer's disease' (Ittner and Gotz, 2011) was proposed linking the 2 pathologies to the dendritic compartments of the neuron (Ittner et al., 2010) with both pathologies playing a part in neurotoxicity (Figure 1.9). This hypothesis is supported by the presence of neuritic plaques (HPT is present in dystrophic neurites) and co-localization studies, which show that at least 25% of neuritic plaques occur at synapses (Fein et al., 2008).

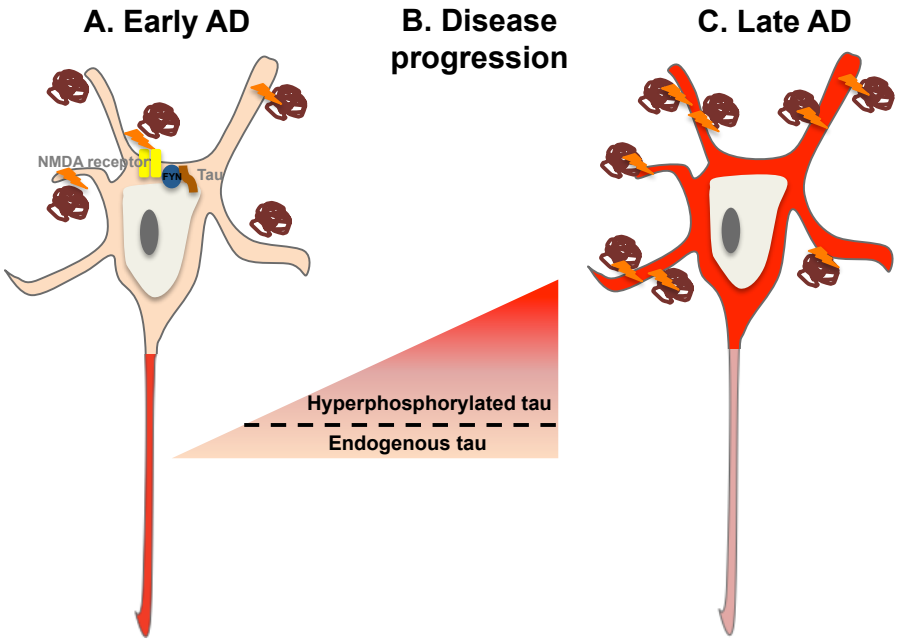

Figure 1.9. Schematic diagram illustrating the 'tau axis hypothesis', which was recently proposed due to the discovery of tau in neuronal dendrites under physiological conditions, suggesting a role as a scaffolding compartment in post-synaptic compartments. The hypothesis has 3 stages: 1) Early AD: postsynaptic toxicity of Aβ is tau-dependent; tau interacts with tyrosine protein kinase FYN, thereby, increases FYN's targeting to the posy-synaptic compartment. FYN in turn activates NMDA receptors, and this increase causes sensitization of NMDA receptors and makes them responsive to Aβ. 2) Disease progression: continued exposure of Aβ triggers tau phosphorylation and NFT/NT accumulate in the dendrites and soma. 3) Late AD: high levels of hyperphosphorylated tau in the dendritic and soma compartments and the toxic effects of Aβ lead to neuronal vulnerability and eventually loss of synaptic connections and death. Modified from Ittner and Gotz, 2011.

Although the neuropathological diagnosis of AD relies on the staging of both NFT/NT and Aβ deposition, additional pathological lesions associated with AD may be present including cerebral amyloid angiopathy (CAA), hippocampal sclerosis (HS) and granulovacuolar degeneration (GVD).

CAA is characterized by the deposition of Aβ in vessel walls of leptomeningeal and cortical arteries, arterioles and, rarely, veins (Vinters, 1987) and is strongly associated with AD-related pathology, present in 80-100% of AD cases (Attems and Jellinger, 2004, Attems et al., 2005a). Morphologically, moderate/severe amounts of predominantly Aβ-40 (Glenner and Wong, 1984) is initially deposited in the *tunic media*, eventually spreading into all vessel wall layers causing thickening, loss of smooth muscle cells (SMC) and disruption of vessel architecture, with the preservation of endothelial cells. There are 2 types of CAA; CAA-type 1 characterized by the presence of capillary CAA with or without CAA in in other vessels; CAA-type 2 is restricted to leptomeningeal and cortical arteries, arterioles and rarely veins, without capillary involvement (Thal et al., 2002a). CAA primarily affects the leptomeningeal and cortical vessels of neocortical regions (Thal et al., 2003) and somewhat resembles distribution pattern of Aβ deposition. However, in CAA the occipital lobe is frequently and severely affected, followed by parietal, frontal and temporal cortices (Attems et al., 2005a), cerebellum and finally basal ganglia and thalamus (Vinters, 1987). CAA is thought to arise due to the physiologically drainage of Aβ and it's transporter apolipoprotein E (apoE) (Mahley, 1988), via perivascular spaces (PVS) and vascular basement membranes. It is suggested that alteration of this mechanism or variants of apoE (*APOE ε4* allele is a significant risk factor for AD and CAA) (Deane et al., 2008), contributes to the development of CAA. In addition, smooth muscle cell derived Aβ is thought to contribute to the Aβ deposition in vessel walls (Mazur-Kolecka et al., 2006). As to date, no standardized neuropathological consensus criteria for the scoring of CAA are established but several methods have been published to describe the severity of CAA in *post mortem* brains (Thal et al., 2003, Chalmers et al., 2009, Attems et al., 2005a).

HS is defined as severe astrogliosis and neuronal loss in CA1, a region vulnerable to hypoxic damage, and the subiculum. Autopsy series reports have shown the prevalence of HS can be up to 26 % in the demented elderly (Attems and Jellinger, 2006) and is a frequently seen in AD cases (Jellinger, 2007). HS is strongly linked to aberrant TDP-43 pathology (Nelson et al., 2013); a neuropathological study showed that almost 90% of HS cases demonstrated aberrant TDP-43 pathology compared to 10% of controls (Nelson et al., 2011). HS is also suggested to have a pathogenic link to coronary heart disease and

concurring occult hypoxic-ischemic episodes (Attems and Jellinger, 2006).

GVD is characterized by vacuolar cytoplasmic changes of neurons of the medial temporal lobe (MTL) (Ball and Lo, 1977) and regions of the neocortex and deep grey matter (DGM) nuclei (Steele et al., 1964). There are 5 stages of GVD, based on a hierarchy distribution pattern beginning in the hippocampal subfields (CA1/2 and subiculum), spreading to the entorinhinal cortex, CA4 and temporal neocortex, eventually percolating the thalamic nuclei and frontal/parietal neocortex (Thal et al., 2011). GVD is frequently seen in AD cases compared to normal aged control cases (Ball, 1977), and most importantly the GVD stages correlate with AD-specific pathology i.e. NFT and Aβ deposition, but not other neurodegenerative disorders (Thal et al., 2011), indicating a possible role in the chronic stress response in AD pathogenesis.

A definitive diagnosis of AD is given *post mortem* via histological assessment of both HPT and Aβ deposition. With disease progression, the neuropathological lesions of AD increase step-wise following a hierarchical pattern. Several criteria are available for the neuropathological diagnosis of AD. The topographical distribution pattern of NFT/NT pathology is central to the disease progression and staging of AD. Braak neurofibrillary stages describe the progression of NFT/NT and (Braak et al., 2006, Braak and Braak, 1991) (section 2.2.2 and Thal Aβ phases describe the progression of parenchymal Aβ depositions (Thal et al., 2002b) (section 2.2.3). The Age adjusted criteria of the Consortium to Establish a Registry for Alzheimer's Disease (CERAD) is a practical and standardized neuropathology protocol based on age and semi-quantitative assessment of neuritic plaques providing neuropathological definitions; A: "possible AD", B: "probable AD", C: "definite Alzheimer's disease" and "normal brain" to indicate levels of diagnostic certainty (Mirra et al., 1991) (section 2.2.4). The above criteria are combined into the NIA-Alzheimer's Association guidelines to yield a ‘ABC’ score from the Aβ plaque score (Thal phases), Braak neurofibrillary stage, and CERAD neuritic plaque score to reflect the amount of ‘Alzheimer Disease Neuropathological Change’ on a four-tiered scale (Montine et al., 2012) (section 2.2.5).

1.4.2 Lewy body diseases

Lewy body diseases (LBD) include dementia with Lewy bodies (DLB), Parkinson's disease (PD), and Parkinson's disease dementia (PDD) (McKeith et al., 2005). Pathologically the 3 disorders are characterized by hallmark neuronal inclusion of alpha-synuclein (α-syn) in the form of Lewy bodies (LB) in neuronal soma, and Lewy neurites (LN) in the neuronal processes (Spillantini et al., 1997), therefore LBD may also be referred to as a synuclenopathies.

α-syn is a 140 amino acid lipid binding protein of the brain, localized in presynaptic terminals (Goedert, 2001). Its physiological function(s) remain(s) elusive, although, evidence suggests α-syn plays a role in the modulation of synaptic transmissions, particularly supporting conformational changes of the synaptic SNARE protein complex (Chandra et al., 2005) and neuronal plasticity (Waxman and Giasson, 2009). Little is known about the mechanism(s) that drive(s) α-syn aggregation under pathologic conditions. Phosphorylation at serine residue 129 is thought to play a key role in the production of the pathological variant (Anderson et al., 2006) in conjunction with nitration and reactive oxygen species alterations (Giasson et al., 2000, Paik et al., 2000, Paxinou et al., 2001, Uversky et al., 2001). The pathological impact of LB and LN and whether they are detrimental to normal cellular functions or a manifestation of a cytoprotective response remains unresolved (Jellinger, 2010). Toxicity of α-syn oligomers has been demonstrated (Winner et al., 2011) specifically in the direct binding and fragmentation of mitochondria that can lead to neuronal death (Nakamura et al., 2011). However, formation of α-syn oligomers has been shown to predate the formation of LB/LN which are composed of aggregated α-syn (Galvin et al., 2001). LB/LN do not always correlate with the pathology (Jellinger, 2009), showing an inconsistent relationship to the clinical disease (Colosimo et al., 2003, Zaccai et al., 2008, Burke et al., 2008, Parkkinen et al., 2008), though, others have found a correlation of LB/LN with cognitive impairment (Bertrand et al., 2004, Apaydin et al., 2002).

LB inclusions occur in 2 forms (Figure 1.10); 1) classical LB are spherical cytoplasmic inclusions approximately 8-30μm in diameter, with a pale hyaline eosinophilic core surrounded by concentric lamellar bands. Classic LB are

predominantly seen in the pigmented neurons of the subtantia nigra, locus ceruleus and dorsal motor nucleus of nervus vagus, and neurons may contain multiple inclusions. 2) cortical LB are angular, rounded or reniform eosinophilic structures without a halo, frequently seen in the iso- and allocortical areas of PD brains (Jellinger, 2012, Attems and Jellinger, 2013b). LN are curvilinear or dot like processes in dystrophic neuritis (Saito et al., 2003) found in close proximity to LB.

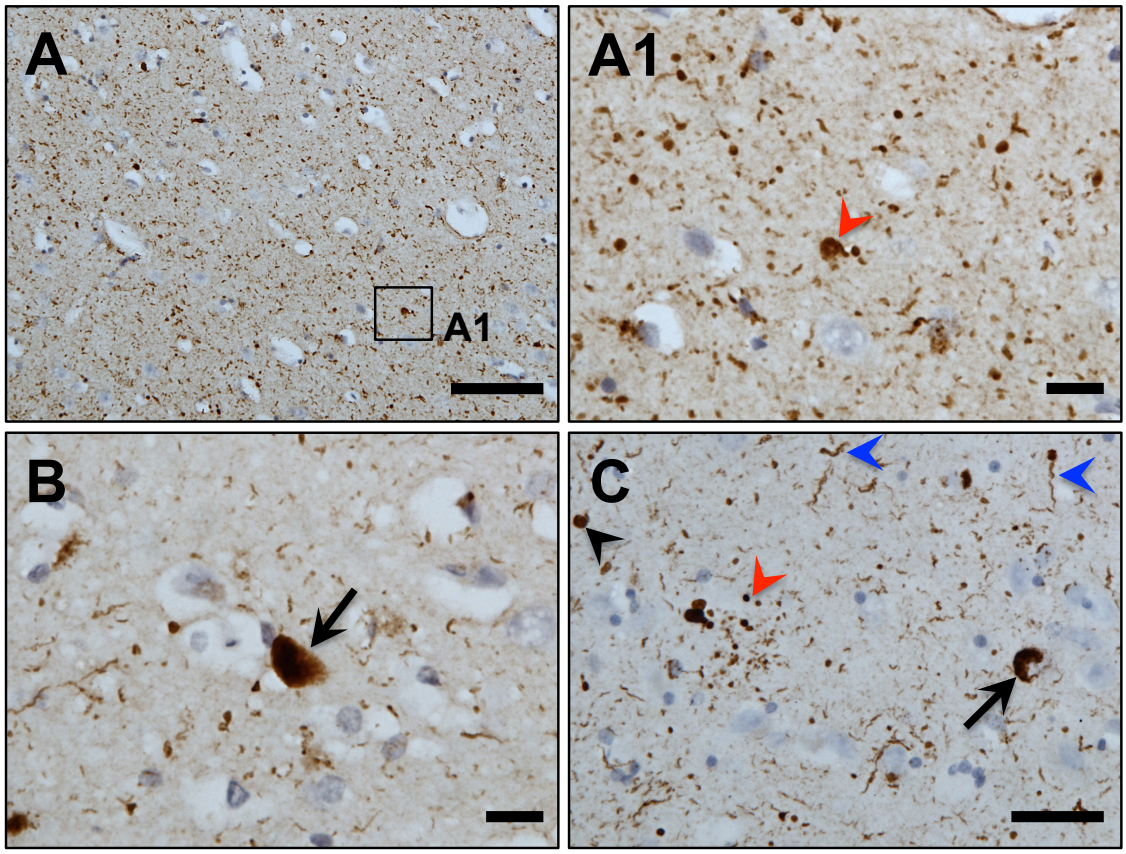

Figure 1.10. α-syn pathology: A) LB/LN in the thalamus of a DLB brain; classic LB with a pale hyaline eosinophilic core (A1, red arrowhead). B) cortical LB in temporal cortex (black arrow). C) reniform LB (black arrow), circular LB (black arrow head), LN with dot (red arrow head) and curvilinear (blue arrow head) morphologies. LB, Lewy bodies; LN, Lewy neurites; Immunohistochemistry; α-syn; Scale bars: A 100μm; A1, B 20μm; C 50μm.

DLB is the second most common age associated neurodegenerative dementia accounting for up to 26% of dementias (Ince, 2001). The core features of DLB, as opposed to other types of dementia, include cognitive fluctuations, visual hallucinations, Parkinsonism, REM sleep disorders, depression and neuroleptic sensitivity (McKeith et al., 2005). The brains of DLB patients may show widespread atrophy, similar to AD, or appear normal. Due to loss of pigmented neurons, the substantia nigra is usually pale and the locus coeruleus is usually depigmented. Histologically, DLB is characterized by severe LB and LN in the substantia nigra, locus coeruleus, hippocampus and neocortex, (Braak et al., 2003, McKeith et al., 2005).

PD has a prevalence of approximately 3% in the over 65 years. It is a progressive neurological movement disorder defined by both clinical extrapyramidal symptoms such as bradykinesia, resting tremor, rigidity, and postural instability (clinically referred to as Parkinsonism) and non-motor related

symptoms such as cognitive and neurobehavioural abnormalities (Dickson, 2012, Jankovic, 2008). The hallmark macroscopic pathological feature of PD is pallor of the substantia nigra and often locus coeruleus and histologically severe LB/LN are predominantly present in substantia nigra, locus coeruleus and dorsal motor nucleus of vagal nerve (Attems and Jellinger, 2013b). Furthermore, there is severe loss of pigmented neurons (45-66%) and dopaminergic (60-88%) neurons of the substantia nigra, particularly in striatal projections (Jellinger, 2012, Attems and Jellinger, 2013b, Damier et al., 1999).

DLB and PD are differentiated clinically by the predominance of extrapyramidal motor features of PD and dementia in DLB. However, in some patients there is an overlap in both features; for clinical classification, if dementia onset occurs within 12 months of parkinsonism features its is defined as DLB, if onset is after 12 months (although it is typically 10 years) it is defined as PDD (McKeith et al., 2005). Other than the age of onset there are no major differences between DLB and PDD in clinical variables including cognitive profile (Aarsland et al., 2003), neuropsychatric features (Ballard et al., 2002), sleep disorders (Boeve et al., 1998) and severity of parkinsonism (Aarsland et al., 2001). A definitive diagnosis of LBD is given *post mortem* via histological assessment of α-syn pathology. With disease progression α-syn pathology increase step-wise following a hierarchical pattern. Two different criteria are commonly used for the neuropathological diagnosis (these are described in more detail in section 2.3); Braak α-syn stages encompasses α-syn related pathology in 6 stages (Braak et al., 2003) and the Newcastle-McKeith criteria for LBD which distinguish between brainstem dominant, limbic and diffuse neocortical types (McKeith et al., 2005). This is used in conjunction with clinical information to give a definitive clinical-pathological diagnosis.

1.4.3 Tauopathies

Tauopathies are a class of neurodegenerative diseases associated with the pathological accumulation of HPT (Grundke-Iqbal et al., 1986) in neurons and glia cells. Alternative splices of *MAPT* gene yields 2 main species of tau referred to as 3R and 4R (Andreadis et al., 1992) that have preferential deposition in different tauopathies (Goedert et al., 1989). Tauopathies can also be classified as FTLD with tau (FTLD-tau) due to the high prevalence of cortical atrophy in the frontal and temporal lobes. For this study I will focus on

Corticobasal degeneration (CBD) and progressive supranuclear palsy (PSP) only.

CBD has a highly varied clinical presentation due to variation in focal cortical degeneration (Litvan et al., 2000), frequently seen in the frontal lobes (Kertesz et al., 2000). Classic presentation often referred to as corticobasal syndrome (CBS) shows marked asymmetrical atrophy of cortical gyri of the superior frontal and parietal parasagittal regions, and loss of pigmented neurons in the substantia nigra. Neuropathological hallmarks of CBS include the accumulation of hyperphosphorylated 4R tau isoform in the neuropil and distal segments of neurons and astrocytes of the cortex, DGM and brain stem. The astrocytic plaque is a specific hallmark lesion in CBD and is not present in other neurodegenerative diseases (Feany and Dickson, 1995, Komori et al., 1998). Swollen achromatic neurons are also frequently seen in affected cortical areas (Rebeiz et al., 1967).

The clinical presentation of PSP is commonly atypical Parkinsonism (Steele et al., 1964), with postural instability and gait failure (Williams et al., 2007) as well as dementia (Bigio et al., 1999). PSP is characterized by the accumulation of hyperphosphorylated 4R tau isoform. The distribution of tau determines the clinical presentation; some cases have severe brainstem involvement e.g. severe akinsia, while others have severe cortical involvement e.g. dementia, speech apraxia (Tsuboi et al., 2005). Core regions affected include basal ganglia, sub-thalamic nucleus, substania nigra (Hauw et al., 1994) and cerebellar atrophy (Tsuboi et al., 2003). Neuropathlogical hallmarks lesions include neuronal globose NFT, and tufted astrocytes, mainly in the motor cortex and corpus striatum, which are considered the characteristic lesion of PSP (Yamada et al., 1992). Neuronal loss and gliosis is marked in the substania nigra and subthalamic nucleus, in conjunction with many thread-like processes and coiled oligodendroglial bodies. In PSP, thread-like processes and coiled bodies are found together, whereas in CBD threads are in complete absence of coiled bodies, distinguishing between the two tauopathies (Dickson, 2009).

1.5 Cerebral vascular disease

Cerebral vascular disease (CVD) describes a group of disorders affecting the vascular system of the brain. The frequency and severity of CVD is associated with increasing age in both demented and non-demented individuals. Although the brain comprises only 2% of total body weight, cerebral blood flow makes up approximately 15% of cardiac input and 20% of total oxygen consumption, therefore, functional blood supply is critical for the physiological function and maintenance of cerebral tissues (Kalimo, 2005).

CVD is increasingly recognized as a cause of cognitive impairment and dementia, either alone or in conjunction with various other pathologies. Vascular cognitive impairment (VCI) describes a continuum of cognitive disorders ranging from mild cognitive impairment (MCI) to dementia as a result of CVD or injury (Jellinger, 2013). There is no generally accepted definition for VaD as it rather refers to a concept that implies severe impairment in multiple cognitive domains as a result of CVD (Ince, 2005). VaD is considered the second most common form of dementia after AD, although this is primarily based on clinical population-studies in which an accurate diagnosis is difficult due to overlapping clinical symptoms of neurodegenerative diseases. Autopsy series show that pure VaD, without other concomitant pathologies, is rather rare (12.3%) (Jellinger and Attems, 2010a).

The three most important vascular pathologies (VP) in the ageing human brain are atherosclerosis (AS), small-vessel disease (SVD) and CAA. AS is a degenerative disorder affecting large to medium sized cerebral arteries, most commonly the Circle of Willis (Beach et al., 2007) and the extra-cranial carotid arteries. Thickening of the *tunica intima* (innermost part of the vessel), splitting of the *lamina elastica interna* (outer elastic layer of the *tunica intima*), with subsequent accumulation of cholesterol-laden macrophages (foam cells) generates an atherosclerotic plaque (Stary, 2000, Stary et al., 1995, Stary et al., 1994) that eventually forms into cholesterol clefts and calcification (Figure 1.11 A). Mature atherosclerotic plaques may cause narrowing of the artery lumen, thereby reducing the blood supply for the supported region, and are prone to rupture causing subsequent thrombosis (vessel occlusion due to a blood clot at site of origin) or downstream thrombo-embolism (vessel occlusion from travelling thrombus) of a smaller vessel (Stary, 2000). The frequency and

severity of AS increases with ageing; a post mortem study found that 41% of 60-70 year olds and 76% of >81 years were found to have AS in the Circle of Willis (Larionov et al., 2006).

SVD itself encompasses three degenerative alterations of the vessels walls of smaller arteries and arterioles; 1) SVD-AS has a similar pathogenesis to AS affecting the small intracerebral and leptomeningeal arteries (200-800μm) forming small plaques known as microatheromas (Grinberg and Thal, 2010); 2) Lipohyalinosis affects the smaller arteries and arterioles (40-300μm) of the WM and DGM. Vessel walls exhibit asymmetric fibrosis/hyalinosis with foam cell infiltration as a result of blood-brain-barrier (BBB) breakdown implicating plasma protein leakage and hence fibroid necrosis (Grinberg and Thal, 2010); 3). Arteriolosclerosis is the concentric hyaline thickening of small arterioles (40-150μm) of the WM leading to stenosis of the blood vessel (Grinberg and Thal, 2010) (Figure 1.11 B-D). Usually SVD initially manifests in arteries and arterioles of the basal ganglia, spreading to WM arteries and eventually the brain stem, leaving cortical vessels relatively free (Thal et al., 2003). This study will focus only on SVD. Finally, CAA is characterized as deposits of Aβ in cerebral, leptomeningeal vessel walls and capillaries as previously described in section 1.4.1 (Figure 1.11 E).

Although AS, SVD and CAA are distinct entities studies have shown that they share risk factors, mainly arterial hypertension (Lammie et al., 1997, Lusis et al., 2004) and *APOE*ε4 allele (Yip et al., 2005, Thal et al., 2007). This is thought to account for similar morphological alterations e.g. AS, SVD-AS and similar pathological consequences e.g. BBB breakdown leading to plasma protein leakage in all 3 disease entities (Grinberg and Thal, 2010).

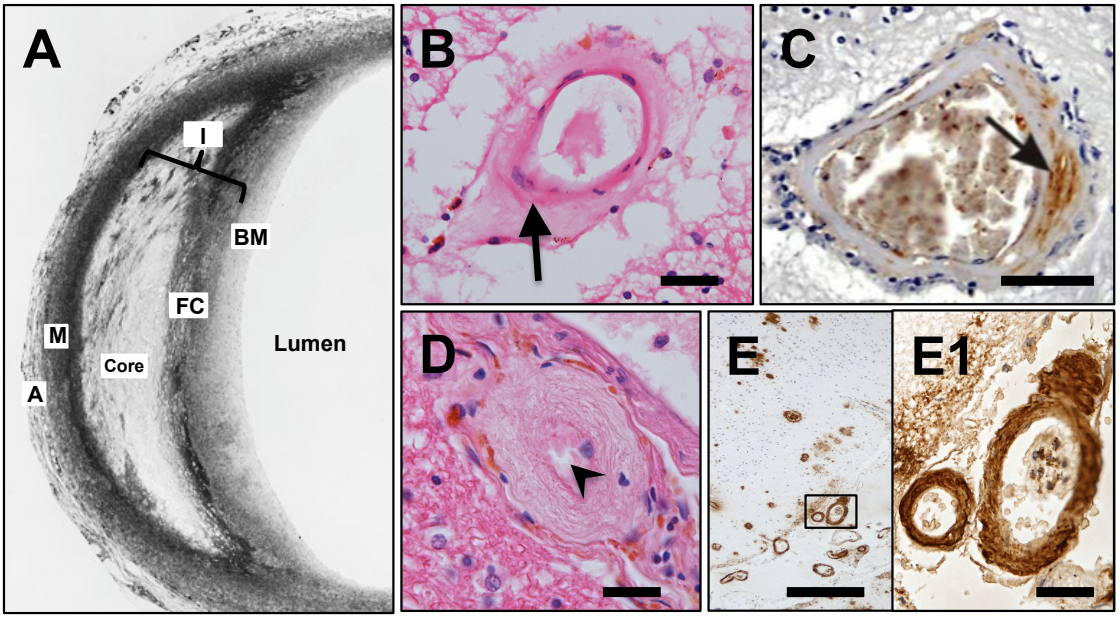

Figure 1.11. Cerebral vascular disease pathology. A) Photo-microimage of atherosclerotic plaque located in the *tunica intima* (I) (innermost layer below the *tunica adventitia* and *tunica media* (M)). Calcified material is located in the core (white area) above infiltrating foam cells (FC) above the basement membrane (BM). B) WM arteriole with asymmetric fibrosis (black arrow); C) WM artery exhibiting plasma protein A2M within the vessel wall. B, C) lipohyalinosis. D) WM arteriole exhibiting severe concentric fibrosis with almost complete occlusion of the vessel lumen (black arrowhead). E, E1) CAA in leptomeningeal arteries of the occipital lobe. Fixation/immunohistochemistry; A, fixation by pressure-perfusion with glutaraldehyde; B,D, H&E stain; C, A2M; E, E1, 4G8: Scale bars; Approximately x550 magnification on electron microscope (ref); B, D, E1 20µm; C 50µm; E 500µm. WM, white matter. Image A from (Stary et al., 1995), image C from (Grinberg and Thal, 2010).

Various cerebral vascular lesions (CVL) occur as a result of VP, varying in location and size according to the underlying vessel disorder (Figure 1.12). Cerebral infarction i.e. tissue necrosis due to insufficient blood supply, hemorrhage i.e. blood extravasation into the brain parenchyma and white matter lesions (WML) all result in damage and/or destruction of tissues leading to neurological and cognitive dysfunction and/or exacerbate other neuropathogies e.g. AD pathology (Grinberg and Thal, 2010). This study will focus on WML, which are discussed in detail in section 1.6.

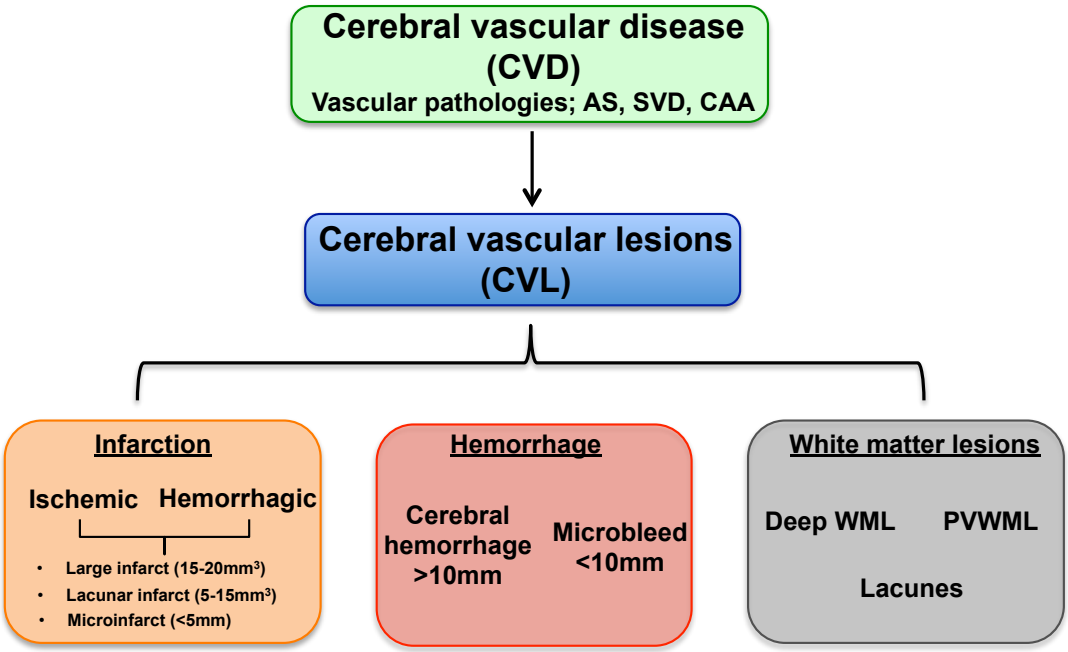

Figure 1.12. Diagram showing the various cerebral vascular lesions, as a consequence of cerebral vascular disease, in the ageing human brain. AS, atherosclerosis; SVD, small vessel disease; CAA, cerebral amyloid angiopathy; WML, white matter lesion; PVWML, periventricular white matter lesion.

Currently no validated consensus neuropathological criteria for VCI, VaD or VP are available, despite several attempts being put forward (Jellinger, 2008, Kalaria et al., 2004, Roman et al., 1993, Deramecourt et al., 2012). This is due to various reasons; i) VaD is not a single entity and CVL comprise of heterogenous changes with varying pathogenesis (Thal et al., 2012); ii) there are varying neuropathological terms for the same pathogenesis (Grinberg, 2013); iii) many cases contain mixed pathologies and with no general agreement of what level of vascular burden allows for cognitive decline it is difficult to determine if dementia is of vascular etiology; iv) current methods used may sometimes miss vascular changes as relatively small tissue sample are generally used (Grinberg, 2013). Current *post mortem* diagnosis relies on the identification of significant CVL in the absence of other changes that may explain cognitive decline (Hachinski et al., 2006, Kalaria et al., 2004). Pathologic studies have shown considerable differences in the prevalence of VaD ranging from 0.03% to 85.2%, indicating the lack of reliable data available due to the lack of consensus criteria (Jellinger, 2013). Hence, respective consensus criteria are urgently needed (Alafuzoff et al., 2012, Pantoni et al., 2006, Sachdev et al., 2014).

1.6 White matter lesions and hyperintensities

WML are synonymous with the radiological term ‘leukoaraiosis’ that was introduced over 20 years ago (Hachinski et al., 1987). Due to the rapid progress of neuroimaging methods, it became clear that diffuse density changes were apparent in the cerebral WM of both demented and non-demented brains. Leukoaraiosis is defined as bilateral, patchy or diffuse WM abnormalities i.e. low density changes on CT or white matter hyperintensities (WMH) on T2/FLAIR magnetic resonance imaging (MRI) that is commonly used (O'Sullivan, 2008).

Pathologically, these density changes are apparent in the deep WM as WML, characterized by enlarged perivascular spaces (EPVS) and rarefaction that is appreciated as WM pallor on histological slides stained with appropriate histochemical methods e.g. Luxol fast blue for myelin. WML also present with a decrease in axonal density, demyelination, complete axonal loss (Yamanouchi et al., 1989) and reactive gliosis but spare subcortical U-fibres (Debette and Markus, 2010, Gouw et al., 2011, Thal et al., 2012, van Swieten et al., 1991, Babikian and Ropper, 1987, Caplan and Schoene, 1978). Perivascular white matter lesions (PVWML) are evident as disruption to the ependymal lining, myelin pallor and astrogliosis within a 5-10mm zone adjacent to the ventricle. Radiologically, Perivascular white matter hyperintensities (PVWMH) are apparent as ‘caps’ around the frontal horns and as a ‘pencil-thin line’ or a ‘smooth halo’ around the sides of the lateral ventricles. Lacunes may also be present, defined histologically as small cavities in both the WM and DGM or round or ovoid subcortical cavities between 3-15 mm in diameter on MRI (Wardlaw et al., 2013), which are thought to result from occlusion of small perforating arteries (Grinberg and Thal, 2010).

Radiologically, WML are classified as i) single ‘punctate’ lesions <10mm, ii) ‘early confluent’ lesions that are 10-20mm in size linked by a ‘connecting bridge’, iii) finally ‘confluent’ lesions which are >20mm and show clear confluency between abnormalities. This is supported by the evidence of lesion progression; The Austrian Stroke Prevention Study (Schmidt et al., 2003) found no increase in WML volume in subjects with ‘punctate’ lesions at base-line to follow up in contrast to ‘early confluent’ and ‘confluent’ lesions which showed a rapid increase in volume in subsequent follow ups at 3 and 6 years. This indicates that ‘punctate’ lesions are of possible mixed origin and therefore less

harmful, whereas 'early confluent' and confluent' lesions are of ischemic origin and therefore progressive and more severe (Schmidt et al., 2011). Lacunes (>5mm) of the DGM are assessed based on the number of lesions i.e. 0, no lesions; 1, 1 lesion; 2, > 1 lesion; 3, confluent lesions.

It is widely accepted that SVD is the main cause of WML and lacunes in both demented and non-demented individuals (Gouw et al., 2011), affecting the long penetrating arteries and arterioles that branch from the pial vessel network on the surface of the brain that supply the cerebral WM. In the brains of asymptomatic patients vessel changes may be apparent but are thought to rarely progress past concentric hyaline thickening, hence leukoariosis is usually less severe when compared to the brains of demented individuals (Schmidt et al., 2011). Small vessel wall alterations are assumed to lead to disturbed arterial autoregulation with or without blood–brain barrier dysfunction (Schmidt et al., 2007) and promote progressive stenosis as well as occlusion leading to chronic hypoperfusion of surrounding tissues (Kalaria et al., 2004). Penetrating arteries from the pia mater do not arborise (Rowbotham and Little, 1965), consequently blood supply accommodates a cylindrical area of WM with very little collateral flow, therefore, SVD renders the entire area hypoxic resulting in diffuse areas of WM damage. Although, PVWML are thought to be of non-ischemic origin, as there is no evidence of SVD-related damage, their pathogenesis remains to be elucidated (Schmidt et al., 2011). Collectively, SVD and its associated neuropathological lesions i.e. EPVS, WML, lacunes, can be referred to as subcortical vascular pathology (SVP).

1.6.1 Clinical relevance of WML/WMH

Population-based studies have show the prevalence of WMH varies between 45-95% with prevalence increasing with age from >20% in the under 30 years up to 100% in 71-80 years (Christiansen et al., 1994, van Dijk et al., 2002). WMH are frequently seen in both the asymptomatic normally aged and demented individuals; asymptomatic individuals mostly exhibit PV 'caps' and 'punctate' lesions at a prevalence of 50% in 55 years and over and less frequently present with 'early confluent' or 'confluent' lesion at a rate of 20% in 75 years and over (Schmidt et al., 2011). In contrast, demented subjects show a much higher frequency and more severe WMH, regardless of the dementia type, with a clinical *in vivo* study showing frequency rates 85% in LBD, 89% in

AD (approx. 40% in neuropathological defined AD cases (O'Sullivan, 2008, Nagata et al., 2012)), and 96% in VaD (Barber et al., 1999). Therefore, WMH are a frequent co-morbidity that co-exists with neurodegenerative hallmark pathology.

There is ample evidence, in both community and hospital based cohorts of various ethnic groups, that WMH are associated with a wide range of cognitive deficits including cognitive impairment (Esiri et al., 1999, Kalaria et al., 2004, Smallwood et al., 2012, Vinters et al., 2000, Baune et al., 2009, Shenkin et al., 2005, Stenset et al., 2008, Zhou et al., 2008), cognitive decline (Koga et al., 2009), executive function deficits (Bracco et al., 2005), memory decline (Mungas et al., 2009) and decreased information processing speed (Prins et al., 2005, Sachdev et al., 2005). Furthermore, WMH are associated with increased disability such as gait disturbances, falls and bladder instability, and mood disturbances such as depression (O'Sullivan, 2008). In demented subjects, WMH have been shown to be significant predictor of all types of dementia with population studies showing a 3-fold increase in risk, especially in AD (Debette et al., 2010, Debette and Markus, 2010, Kuller et al., 2003, Prins et al., 2004). The Nun Study, a large longitudinal study of a relatively homogeneous cohort of nuns, showed that those with WML or lacunes had a higher prevalence of dementia compared to those without (Snowdon et al., 1997).

1.6.2 Current radiological and neuropathological assessment of WML/WMH

As well as *in vivo* MRI, imaging of *post mortem* fixed human brain slices has been a valuable complement to neuropathology for the past 25 years by providing three dimensions to histological specimens (Pfefferbaum et al., 2004). It is important to note that autolysis, temperature fluctuations and dehydration of tissue in the fixation process may cause significant shortening of relaxation times, especially in T2, although these have been shown to stabilize after 3-4 weeks fixation (Pfefferbaum et al., 2004, Shepherd et al., 2009).

Despite the understanding of the potential detrimental effects of tissue fixation and autolysis, currently there is very little data available comparing human *in-vivo* and *post mortem* imaging of WMH. The understanding and comparison of *ante* and *post mortem* imaging is required in order to establish what extent

tissue fixation alters the appearance of WMH and to validate that *post mortem* WMH correspond to *ante mortem* WMH. However, a longitudinal comparison study of *ante* and *post mortem* imaging in humans is very difficult to conduct as death is unpredictable and there may be a long delay between the final living MRI scan and autopsy. During this time there may be significant change/development of WML, which may make comparison unreliable. Fazekas and colleagues conducted a very brief comparison of 9 patients, with varying degrees of deep and PV WMH that underwent T2 MRI prior to death and had subsequent post mortem imaging of fixed brain slices. They revealed a correlation between *in-vivo* and *post mortem* MR images of larger deep WMH, however, small 'punctate' WMH were less well visualized in fixed specimens as were PVWML, thought to be due to air infiltration into the ventricular cavity (Fazekas et al., 1993). Furthermore, few studies have compared *ante* and *post mortem* volumetric measurements of human brain specimens. A single case study obtained 3D volumetric MRI imaging 48 hours after death, with the brain still encased in the skull, and subsequent 13 MRI scans over 70 days in formaldehyde, revealed deformities in the brain specimen due to extraction and global brain volume decrease of 8.1% (Schulz et al., 2011). Conversely, a recent comparative study of *in-vivo* and *post mortem* imaging in Wistar rats showed no significant changes in volumetric measurements of 22 anatomical regions (Oguz et al., 2013). In general, postmortem MRI of formalin fixed brain is considered a reliable method to obtain data on both the severity and also distribution of WM changes (Schmidt et al., 2011), although manual damage due to brain extraction, assessment of 'punctate' and PVWML and volumetric changes to the brain specimen should be taking into account when assessing *post mortem* images.

Several rating scales, for both *in vivo* and *post mortem* based on respective changes within PV and subcortical WM regions are in use for visual assessment of WMH (Scheltens et al., 1998). One of the strongest risk factors for WML is age (Schmidt et al., 1992); the age related white matter change scale (ARWMC) (Wahlund et al., 2001) is widely used to assess the subcortical WM based on lesion size and confluence. Lacunes are distinguishable from PVS as hyperintensities less than 3mm tend to be PVS (Longstreth et al., 1998).

The neuropathological *post mortem* diagnosis of SVP relies on the identification and grading of the associated specific vascular lesions based upon the examination of a limited number of histological slides containing selected frontal, parietal, temporal and occipital white matter as well as DGM. In contrast to MRI, no validated consensus neuropathological criteria for SVP (or specifically WML) are available despite several attempts being put forward (Jellinger, 2008, Kalaria et al., 2004, Roman et al., 1993, Deramecourt et al., 2012) and lack of neuropathological criteria is a hindrance in the investigation of SVP. Recently two scoring criteria for the assessment of SVD and associated WM and DGM pathologies have been proposed; Deramecourt and colleagues (Deramecourt et al., 2012) proposed a semi-quantitative approach that separately grades vessel wall fibrosis, PVS dilation, CAA, PV hemosiderin leakage and myelin density, while Smallwood and colleagues (Smallwood et al., 2012) proposed a more simple semi-quantitative approach that combines the grading of vessel wall fibrosis, PVS dilation and myelin density.

Numerous studies have directly compared both *in vivo* and *post mortem* MRI with histological findings to characterize the pathological substrates of WMH (Awad et al., 1986, Braffman et al., 1988, Bronge et al., 2002, Chimowitz et al., 1992, De Reuck et al., 2011, Englund et al., 1987, Fernando et al., 2004, Grafton et al., 1991, Marshall et al., 1988, Munoz et al., 1993, Revesz et al., 1989, Scarpelli et al., 1994, Smith et al., 2000, Yamamoto et al., 2009), confirming that different types of PVWMLH and WMH i.e. ‘punctate’, ‘early confluent’, confluent’ lesions, had specific pathological alterations. PVWMH histologically present as a discontinuation of the ependymal with mild/moderate subependymal gliosis accompanied by myelin loss and loosening of the fiber network. Histologically ‘punctate’ hyperintensities are composed of generally mild myelin loss confined to the area around enlarged PVS. ‘Early confluent’ hyperintensities reflect mild to moderate rarefaction of myelin accompanied by varying degree of axonal loss and astrogliosis, and ‘confluent’ hyperintensities consist of diffuse areas of complete tissue destruction inclusive of loss of myelin, axons and oligodendrocytes, reactive astrogliosis and intercellular edema (Bronge et al., 2002, Chimowitz et al., 1992, Fazekas et al., 1991, Fazekas et al., 1993, Munoz et al., 1993, Scarpelli et al., 1994).

1.6.3 Other types of WML pathogenesis

It has been suggested that axonal degeneration can occur as a secondary consequence of neurodegenerative pathology, resulting in the formation of WM changes; Leys *et al* observed more severe white matter changes in areas adjacent to cortical areas of high NFT in AD cases (Leys et al., 1991), and Professor Englund found that 42% of AD cases contained non-ischemic subcortical degeneration in the temporal lobes (Englund, 1998). More recently, the Oregon Brain Aging Study (OBAS), a community-dwelling imaging study in a 65 years and older population, found that a higher Braak NFT stage was associated with a greater WMH burden over time (Silbert et al., 2012).

Studies have suggested that axonal degeneration may precede neuronal death and occur independently (Coleman, 2013). Wallerian-like degeneration (WLD), or 'dying back' axonal degeneration, has been shown to occur in many neurodegenerative diseases (Coleman, 2013). Morphologically WLD is very similar to the experimental model of peripheral axonal degeneration 'Wallerian degeneration', but differs with regard to the triggering lesion; WLD is the result of insult and/or injury to the axon in the CNS, whereas, 'Wallerian degeneration' is initiated by cutting or crushing injury (Coleman, 2005, Stoll and Muller, 1999, Raff et al., 2002). WLD is the reactive retrograde demyelination and fragmentation of the axon from the distal end activating a proactive axonal death program resulting in the release of calcium-dependent protease calpain triggering cytoskeleton and membrane protein degradation (Mack et al., 2001, Coleman, 2005, Ma et al., 2013). A major activator of WLD in the brain is thought to be axonal transport dysfunction (Beirowski et al., 2010). Bidirectional trafficking of molecules and organelles is vital for metabolic reactions and blockage and/or transport failure can have detrimental effects on neuronal survival and aggregates of intra/extracellular proteins e.g. HPT and Aβ, are highly associated with impairment in axonal transport (Figure 1.13). *Post mortem* AD brains and brains of AD mouse model Tg-swAPP^{Prp} have been shown to exhibit excessive axonal swellings/ spheroids (a neuropathological hallmark of axonal transport dysfunction) (Stokin et al., 2005) and are associated with higher amounts of axonal demyelination (Howell et al., 2010) and axonal degeneration (Hilliard, 2009, Coleman, 2005, Stokin et al., 2005, Emre et al., 1992, Decressac et al., 2011).

Figure 1.13 Cartoon showing the proposed mechanisms in the development of axonal spheroids and WLD. A) a healthy neuron and axon with the proximal and distal ends. The accumulation of protein aggregates leads to impairment in axonal transport may result in focal blockages and accumulations of organelles and disorganized cytoskeleton in axon varicosities, preferentially at nodes of Ranvier (B). Swellings continuously increase in size, APP also accumulates and is used a immunohistochemical marker of axonal dysfunction. Swellings increase in size to form axonal spheroids. At this point the axon remains continuous (C). Eventually the block of axonal transport is sufficient to trigger WLD of the distal axon and the fragmentation of the axon and demyelination begins (D). Finally the entire distal axon undergoes fragmentation leaving a proximal axon stump or end bulb (E). WLD, Wallerian-like degeneration; AP, amyloid precursor protein. Image modified from Coleman et al., 2005.

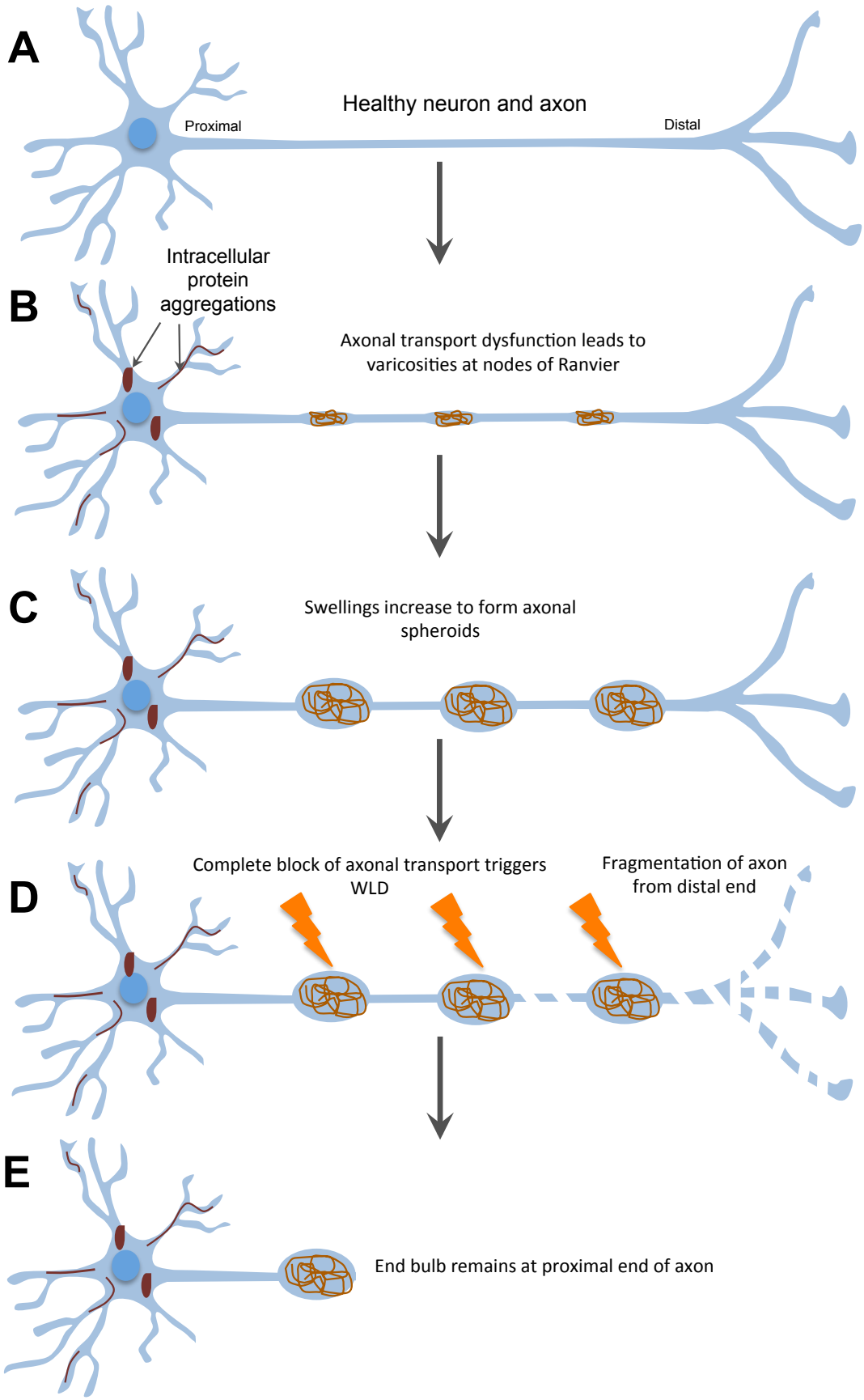
A
Healthy neuron and axon
Proximal
Distal
B
Intracellular protein aggregations
Axonal transport dysfunction leads to varicosities at nodes of Ranvier
C
Swellings increase to form axonal spheroids
D
Complete block of axonal transport triggers WLD
Fragmentation of axon from distal end
E
End bulb remains at proximal end of axon

Previous *in-vivo* investigations into the extent and spatial distribution of WMH have highlighted a posterior dominant location of WMH in AD cases (Gootjes et al., 2004, Lee et al., 2009, Lee et al., 2010, Leys et al., 1991, Meier et al., 2011, Portet et al., 2012, Tang et al., 2001, Yoshita et al., 2006) including WMH of the corpus callosum (CC) that are considered to be of non-ischemic origin (Moody et al., 1988). A cross-sectional comparison study of regional Fractional anisotropy (FA) values (a quantitative measure derived from diffusion tensor imaging (DTI) that reflects the microstructural intensity of the WM fibers) showed that AD patients have significantly lower FA values in the highly organized inter/intra-hemispheric fibers of the CC and superior longitudinal fasciculus (SLF) independent of vascular risk factors when compared to aged controls (Lee et al., 2009). The CC consists purely of inter/intra-hemispheric axonal fiber radiations that connect to all major cortical regions of the brain (Gazzaniga, 2000, Stricker et al., 2009, Esiri et al., 1990, Masliah et al., 1993). These fibers originate in primarily in pyramidal layers III and V (Nieuwenhuys, 1994, Gazzaniga, 2000) where neurons are specifically affected by AD pathology, especially HPT pathology (Giannakopoulos et al., 1998, Pearson et al., 1985, Lewis et al., 1987). The temporal-parietal cortices, which include the entorhinal cortex, are affected by HPT early and severely in AD (Braak and Braak, 1991) and the splenium of the CC has direct axonal connections in this region. Furthermore, FA values of the CC and parietal-temporal- occipital regions are significantly associated with the volume of corresponding cortical grey matter regions, suggesting that WM integrity is closely related to axonal fiber degeneration arising from primary grey matter injury (Lee et al., 2010) agreeing with previous neuropathological findings (Englund, 1998). Therefore, WMH in these regions, especially the splenium, might also be caused by cortical atrophy and/or WLD as a secondary consequence of neurodegenerative pathology.

However, SVD is still a major contributor to WMH; the inferior surface of the CC represents the terminal zone for penetrating arteries making it vulnerable to ischemic changes (Yoshita et al., 2006). DTI cross-sectional studies also revealed less organized strata (corona radiata and posterior thalamic radiations) and genu are at higher vascular damage risk compared to the splenium and SLF (Lee et al., 2009, Lee et al., 2010). However, a purely

vascular etiology would not explain the significant association of WMH with AD diagnosis (Yoshita et al., 2006) and the non-ischemic pathogenesis of posterior CC WMH (Moody et al., 1988).

It is currently not possible to draw exact conclusions regarding pathogenesis due to the homogeneity of WML on histological slides and WMH on MRI imaging. The inability to distinguish ischemic and non-ischemic WML/WMH may pose as a potential problem in future diagnosis and therapeutics i.e. patients with WMH may be diagnosed and treated for SVD when the pathogenesis may stem from associated cortical pathologies such as AD.

1.7 Ageing

Ageing is the strongest risk factor for dementia. Age-related decline in neuronal structure and function renders the brain vulnerable to pathological and vascular insults. Accumulation of HPT and Aβ pathology frequently occurs in normal aged individuals without compromising cognitive function (Braak and Braak, 1991, Ince, 2001, Thal et al., 2013, Jellinger and Attems, 2012) and is considered to represent asymptomatic/preclinical phase of AD (Thal et al., 2013, Hyman, 1998). A 15 year neuropathological study of 2292 *post mortem* brains found that overall 65% of non-demented cases had HPT pathology in the hippocampal region, 49% had Aβ pathology in the neocortex, 15% contained α-syn pathology and 49% had some form of VP (Alafuzoff, 2013). A large multi-center study found that of 109 non-demented cases only 13% of brains were considered free of pathology (Gibb, 1986). Concomitant morphological and functional decline of the cerebral vascular system including decreased cerebral blood flow (Chen et al., 2011), lower metabolic exchange of oxygen and glucose and compromised structural integrity of vasculature due to AS, SVD and CAA, is frequently seen in normal cerebral ageing (Grinberg and Thal, 2010). The increase of vascular changes, specifically SVD, is evident in the increased frequency of WML/WMH with ageing (de Groot et al., 2001, van Dijk et al., 2002); population-based studies have shown the prevalence of WML varies between 45-95% increasing from under 20% in the under 30 years to 100% in 71-80 years (Christiansen et al., 1994, van Dijk et al., 2002).

These pathophysiological changes, in conjunction with individual cognitive and brain reserves, eventually may lead to a compromise in cognitive and executive function, mild memory problems and gait disturbances normally associated with

old age (Schmidt et al., 2011). CR is thought to account for the differences between individual susceptibility to neurodegenerative changes and pathology i.e. why some people remain relatively cognitively sound and others may show a transition from preclinical/MCI to dementia when there is a similar BR and pathologic burden (Stern, 2012).

1.8 Cerebral multimorbidity

Multiple neurodegenerative pathologies can be found in brains of both demented and non-demented subjects (Alafuzoff, 2013, Attems and Jellinger, 2013a) and this finding coined the term cerebral multimorbidity. Since the prevalence of all distinct neurodegenerative pathologies increases with age, the prevalence of cerebral multimorbidity increases accordingly and *post mortem* autopsy studies have clearly shown that a single pathologies in the brains of 80 years and over is rather the exception (Jellinger and Attems, 2007, Jellinger and Attems, 2010b, Jellinger and Attems, 2010a, Kovacs et al., 2008). Distinct pathologies that are associated with a specific neurodegenerative disease, e.g. NFT/NT and Aβ with AD, are termed hallmark lesions/pathologies. However, as multimorbidity is highly prevalent distinct pathologies can no longer be strictly associated with a specific disease; e.g. LB pathology is the hallmark lesions of LBD but is frequently seen in the amygdala of AD brains, therefore, LB pathology is not exclusively seen in classical LBD. This principle may be applied to all major neuropathological lesions and it has become increasingly clear that the demented and non-demented ageing human brain is characterized by the presence of multiple pathologies rather than a single hallmark lesion for a particular neurodegenerative disease (Attems and Jellinger, 2013a).

A large consecutive autopsy study in Vienna (n=1500, mean age 83.3 ±6.0 years) has shown previously that of the 830 clinically diagnosed AD cases, 93.9% had neuropathologically confirmed AD pathology of which only 52% had no additional lesions. Of the remaining cases, 30.8% had additional pathologies consisting of CVL (22.1%), LB pathology (8.7%) and 2.4% were classified as MIX-type dementia (combination of definite AD and vascular encephalopathy) (Jellinger and Attems, 2007). Another study from 9 centers of the BrainNet Europe Consortium included neuropathological data of 3,303 clinically demented cases (1667, female; 1636, male; mean age, 74.14 ±12.07 years)

showed that 53.3% had mixed pathologies of which the most frequent additional lesions were AD pathology (89.6%), VP (52.6%), α-syn pathology (50%) and argyrophilic grain disease (11.4%; a common sporadic tauopathy (Saito et al., 2002)). The most frequent neurodegenerative disorders with additional pathologies were synucleinopathies (PD, 92%; LBD, 61%), followed by AGD (61%), AD (43%), PSP (22%), and CBD (21%) (Kovacs et al., 2008). The Rush Memory and Aging Project, a longitudinal community based clinico-pathological study consisting of 141 cases (57.4% female; mean age, 87.8 ±5.6 years), found that of the 56.7% were neuropathologically confirmed as AD of which 46.3% had no secondary pathologies. The remaining 53.75% had multiple pathologies consisting of AD with VP (58.1%), AD with α-syn pathology (27.9%) and AD with VP and α-syn pathology (9.3%) (Schneider et al., 2007). Finally, a comprehensive examination of 407 neuropathologically confirmed Parkinsonian disorder (inclusive of PD, DLB, PSP, multiple systems atrophy (MSA) and CBD) and controls found that of the PD cases (n =140) 38% had additional AD pathology, 9% had PSP inclusions, 25% AGD, 44% WML and 24% contain CAA and similar heterogeneity was seen for DLB, MSA and CBD cases (Dugger et al., 2014).

The prevalence of mixed pathologies also increases with age. A consecutive autopsy series of 1110 brains (64% female; mean age at death 83.3±5.6 years, range 60-103 years, 90% over age 70) found that AD with additional VP increased for a prevalence of 7.8% in the 7^{th} decade to 32.9% in the 10^{th} decade, in contrast to pure AD which increased from 32.2-45.1% between the 7^{th} and 9^{th} decade but the decreases to 39.2% in the 10^{th} decade (Jellinger and Attems, 2007). Multiple pathologies are also present in the non-demented aged human brain. A neuropathological study at Kuopio University Hospital of 2292 *post mortem* brains found that in 207 subjects (9%) AD and α-syn pathology was detected, and in 83 subjects (3.6%) AD, α-syn, and VP was detected (Alafuzoff, 2013).

From these *post mortem* studies of confirmed diagnosis it is apparent that approximately half of all neuropathologically diagnosed brains have multiple pathologies (Figure 1.14). The high prevalence of multiple pathologies potentially has two implications: i) Multiple pathologies may simply reflect the simultaneous presence of age-related pathologies of which one (or more) may

not be directly related to the primary neurodegenerative disorder e.g. VP is a frequent additional pathology in AD and the pathological burdens are considered independent of each other and reflect the concurrent increase of both pathologies with age, although, both are thought to contribute to cognitive impairment (Braak and Braak, 1996, Grinberg and Thal, 2010); ii) The pathologies may have a synergistic relationship between each other. It has been suggested that CVLs exert an influence on AD pathology and lower the threshold for dementia and therefore less AD pathology is required for the development of clinical dementia (Jellinger and Attems, 2003). Two previous neuropathological studies support this notion; Jellinger & Attems have shown that the prevalence of multiple pathologies increases with age (Jellinger and Attems, 2010b), and suggest additional pathologies may reduce the threshold for overt dementia (Jellinger and Attems, 2007). The Rush Memory and Aging Project concluded that patients with multiple pathologies had a 3-fold increase risk of developing dementia compared to those who only have a single pathology (Schneider et al., 2007). Furthermore, It has been shown that mixed AD-DLB cases (fulfill both AD and DLB neuropathological criteria) have accelerated cognitive decline and mortality compared to AD cases (Olichney et al., 1998), further supporting the idea that additional pathologies potentially reduce the threshold for dementia.

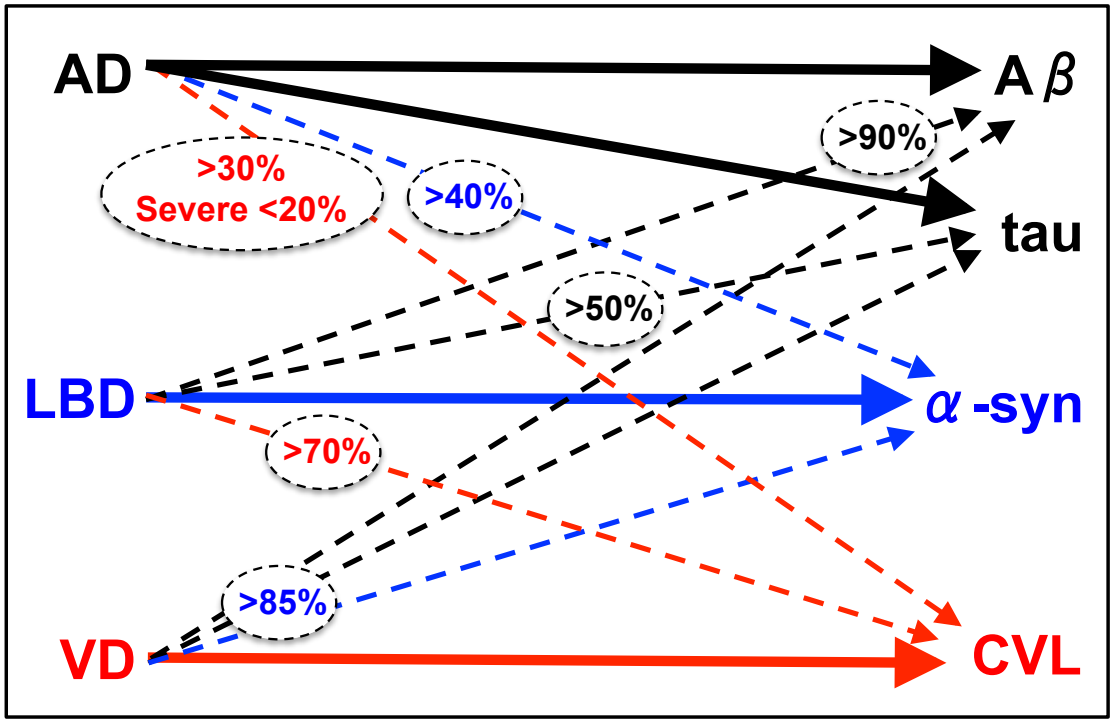

Figure 1.14. Schematic diagram of the multiple pathologies in the demented ageing human brain. Full arrows point towards the hallmark neuropathology of the respective disease while dotted arrows point towards neuropathological lesions that are frequently seen in addition to the main pathological hallmark lesions. Approximate percentages are encircled based on studies (Jellinger and Attems, 2007, Jellinger and Attems, 2008, Kovacs et al., 2008, Petrovitch et al., 2005, Uchikado et al., 2006)AD, Alzheimer's disease; LBD, Lewy body diseases; VaD, vascular dementia; Aβ, amyloid-β; α-syn, α-synuclein, CVL, cardiovascular lesions. Adapted from (Attems and Jellinger, 2013b).

In vitro studies have previously demonstrated that the co-incubation of tau and α-syn results in fibrillization and production of intraneuronal inclusions characteristic of neurodegenerative disease, suggesting their interactions can promote their fibrillization and drive the formation of pathological inclusions in human neurodegenerative diseases (Giasson et al., 2003). Clinton and colleagues have also suggested a mutual interaction of neurodegenerative pathologies (Clinton et al., 2010); they crossed 3xtg mice, that develop both tau and Aβ pathology (Oddo et al., 2003), with M83-h mice, which have a A53T mutation in the α-syn gene (Giasson et al., 2002) to produce 'DLB-AD' mice. At 12 months these mice exhibited significantly higher levels of soluble Aβ 1-40, soluble and insoluble Aβ 1-42, and insoluble tau than the 3xtg mice, and significantly higher amounts of α-syn than the M83-h mice. This evidence suggests *in vivo* interaction of tau, Aβ and α-syn promotes aggregation and accumulation of each other (Clinton et al., 2010). Nevertheless, direct human *in vivo* data is not yet available, and the exact pathological mechanisms and effects on cognitive integrity from multiple pathologies remain to be elucidated.

The investigation of concomitant pathologies in the ageing human brain is essential, especially for the development of new clinical diagnostic approaches and novel targeted therapies. An example of this is the co-morbidity of AD pathology and WML/WMH, seen in up to 40% of Alzheimer's disease (AD) cases (O'Sullivan, 2008, Nagata et al., 2012); WML/WMH are presumed to represent CVD, even though there are currently no standardized VP/WML criteria. However, with increasing evidence of WLD also causing demyelination and axonal degeneration (forming WML) in AD (Stokin et al., 2005, Coleman, 2005, Coleman, 2013, Emre et al., 1992, Hilliard, 2009), it is currently not possible to draw any reliable conclusions regarding the pathogenesis of WML in individual cases. Investigation into the relationship of AD and WML is clinically paramount as in most cases diagnosis is of CVD while in fact *in vivo* WMH may be caused by underlying AD-related pathologies and lead to incorrect patient therapy.

1.9 Neuropathological assessment

Currently, routine neuropathological assessment of the extent of neuropathological lesions is based on semi-quantitative scoring, usually on four-tiered scales i.e. 0, ‘absent’; 1, ‘sparse’; 2, ‘moderate’; 3, ‘severe’. For most common neuropathological hallmark lesions i.e. HPT, Aβ and α-syn pathologies, neuropathological criteria are available (Braak et al., 2006, Braak et al., 2003, McKeith et al., 2005, Thal et al., 2002b) which have frequently been standardized to ensure reproducibility for large-scale cohorts (Alafuzoff et al., 2008a, Alafuzoff et al., 2009a, Alafuzoff et al., 2009b).

While semi-quantitative assessment allows for the classification and staging of a neurodegenerative disorder it only provides a rough estimation of the amount of pathology present and it can be difficult to distinguish between adjacent grades. Data from studies carried out at the Institute for Ageing and Health indicate that the quantitative measure of area covered by immunopositivity for AT8 antibody for HPT in cases that were assigned the semi-quantitative score ‘severe’ differs by nearly 10-fold between cases, suggesting that semi-quantitative assessment is incapable of detecting subtle variations in the severity of neuropathological lesions across cases (Attems and Jellinger, 2013a). Moreover, semi-quantitative assessment is influenced by the subjective judgment of the assessor e.g. smaller lesions are more likely to be rated at a lower abundance class compared to larger lesions, and clustered lesions are more likely to be rated in a higher abundance class compared to evenly scattered pathology (Armstrong, 2003). Consequently, the main limitation of semi-quantitative assessment is the unconscious error of judgment and consequently low inter-rater-reliability (Armstrong, 2003), particularly when assessing ‘sparse’ and ‘moderate’ grades of pathology (Alafuzoff et al., 2008b).

On the other hand, quantitative measure of neuropathological lesions allows for more accurate and objective assessment. The use of quantitative methods has become an increasingly important aspect in neuropathology (Armstrong, 2000, Armstrong, 2003). Advances in image analysis systems enable microimages to be captured and enhanced on computers to highlight particular morphological features that can be quantified rapidly and objectively (Armstrong, 2003). Quantitative methods of neuropathological assessment have revealed new clinico-pathological correlations. As previously stated, the severity of Aβ

pathology, as assessed by semi-quantitative methods, does not correlate with clinical dementia (Delaere et al., 1990, Dickson et al., 1992). However, the 90+ Study, a prospective longitudinal population-based study of ageing and dementia, found that quantitative measures of neocortical Aβ pathology (measured as area covered by Aβ immunopositivity) did significantly correlate with the presence of clinical dementia (Robinson et al., 2011). Hence, quantitative assessment is capable of detecting subtle variations within pathology, which improves the evaluation of the impact of pathologies on clinical signs and symptoms. Indeed, in a large cohort study Murray and colleagues assessed hippocampal and entorhinal tau pathology quantitatively in 889 *post mortem* brains and discovered 3 subgroups of AD that differed in clinical presentation, age of onset, disease duration and rate of cognitive decline (Murray et al., 2011). Given that quantification of tau pathology alone in AD cases points towards a new clinico-pathological phenotype, it would seem helpful to pursue a more quantitative approach for the assessment of various neurodegenerative lesions to further reveal more phenotypes and investigate the impact of multimorbidity of the ageing human brain on clinical signs and symptoms.

However, major insights into cerebral multimorbidity can only be gained if large cohorts are assessed, and this can be hindered due to the time and financial constraints of histological assessment. Nevertheless, the Tissue MicroArray (TMA) has become a standard tool for tissue-based research during the last decade. TMAs consist of up to 1000 cylindrical tissue cores from different donor paraffin blocks relocated into one recipient block, allowing for efficient histopathological studies (Sjobeck et al., 2003). So far the TMA technique has predominantly been used in tumor studies (Kononen et al., 1998, Rao et al., 2013, Simon et al., 2001, Sipayya et al., 2012, Skacel et al., 2002) although TMA have been successfully used in investigating non-neoplastic intracranial disorders such as AD. Cortical tissue was successfully assessed by Kellner and colleagues (Kellner et al., 2009) in which a 576 sample TMA blocks of frontal, temporal and entorhinal cortex from 48 AD and 48 aged control cases were constructed and sections analyzed for immunopositive Aβ plaques. Likewise, Sjöbeck *et al.* (Sjobeck et al., 2003) applied the technique to assess the severity of pathological WM changes in 8 AD cases. Tissue sections cut from

this TMA paraffin block can be used to facilitate the quantification of multiple neuropathologies, at high throughput, on both a routine diagnostic and research basis. The array format is optimally suited for such kind of analysis as the defined diameter of the tissue samples allows for a highly standardized analysis of areas of exactly the same size and region (Simon, 2010).

Vascular pathology has also previously been quantified, commonly by the calculation of area fraction of pixels on digital images (Moody et al., 2004). The Sclerotic Index (SI) (Lammie et al., 1997, Low et al., 2007), which is calculated by a standard formula to evaluate the thickening of cerebral arteries/arterioles walls as a measure of SVD, can be used in conjunction with digital image acquisition and computer software analysis to generate a quantitative measure of SVD at high output (Craggs et al., 2013a, Craggs et al., 2013b, Yamamoto et al., 2009).

1.10 Aims

The main aim of this study was to improve the *post mortem* assessment of AD-related pathology and WML/WMH in the ageing human brain by the use of *post mortem* MRI and quantitative neuropathological assessment, and to investigate possible associations between AD pathology and WML.

My main research objectives were:

- To evaluate the feasibility of MRI of *post mortem* brain hemispheres as a mean of assessing SVP in demented and non-demented aged subjects (Chapter 3).

- To compare semi-quantitative and quantitative assessment of HPT and Aβ pathology and vascular fibrosis, as a measure of SVD, of the WM arteries/arterioles in demented and non-demented aged *post mortem* brains (Chapter 4).

- To explore a possible association of cortical AD-related pathology on white matter integrity in a cohort of AD and control human *post mortem* brains (Chapter 5).

- To further investigate the influence of AD-related pathology and SVD on white matter integrity. A combination of *post mortem* MRI-based WMH assessment, quantified cortical HPT and Aβ pathology using the TMA method and SI values of WM artery and arteriole fibrosis as measure of SVD (Chapter 6).

Chapter 2 - Materials and methods

2.1 Introduction

This chapter describes the histological diagnostic criteria used to diagnose various age related neurodegenerative diseases. It also outlines brain tissue processing and dissection, *post mortem* MRI protocol, TMA methodology, histological protocols, semi-quantitative and quantitative pathological assessment, and statistical analysis.

After autopsy all brains underwent standardized histological neuropathological assessment that yielded the neuropathological diagnosis. In clinico-pathological meetings neuropathological diagnoses were linked to clinical information to state the final clinico-pathological diagnosis for each cases.

2.2 Alzheimer's disease

AD is neuropathologically characterized by the presence of both HPT and Aβ depositions. With disease progression, the neuropathological lesions of AD increase step-wise following a hierarchical pattern, and several criteria are used to determine the neuropathological diagnosis.

2.2.1 Gross examination

Generally, gross examination of *post mortem* AD brains exhibited characteristic atrophy of the entorhinal cortex and hippocampus, as well as inferior temporal, superior frontal and middle frontal gyri (Halliday et al., 2003). Enlargement of the ventricles may have been visible, while the cerebellum remained unchanged.

2.2.2 Neurofibrillary tangles and neuropil threads

Braak neurofibrillary stages was used for neuropathological diagnosis to describe the progression of NFT/NT (Braak et al., 2006, Braak and Braak, 1991):

- Stages I/II, the 'transentorhinal/entorhinal stages': NFT/NT were present in the transentorhinal/entorhinal cellular pre-α and pri-α layer, forming distinct bands.

- Stages III/IV, the ‘limbic stages’: NFT/NT deposition extended into deeper layers of the entorhinal cortex, CA 3/4 of the hippocampus and occipito-temporal gyrus and insular cortex.
- Stages V/VI, the ‘isocortical stages’: NFT/NT deposition extended into the frontal, superolateral and occipital directions including the superior temporal gyrus and peristriate region extending into the Heschl’s gyrus and parastriate area.

2.2.3 Amyloid-beta plaques

AD diagnosis was also based on the distinct sequence of parenchymal Aβ depositions. Thal Aβ phases was used for neuropathological diagnosis to describe the progression of Aβ depositions (Thal et al., 2002):

- Phase 1: Small groups of diffuse Aβ deposits were visible in the frontal, parietal, temporal or occipital neocortex.
- Phase 2: Aβ deposition into progressed into the entorhinal cortex, CA1 of the hippocampus and insular cortex.
- Phase 3: Aβ deposition extended into the subcortical regions: caudate nucleus, putamen, thalamus, hypothalamus and basal fore brain. Continued progression of Aβ pathology into CA4 of the hippocampus.
- Phase 4: Aβ deposition extended into the brain stem including the medulla oblongata and substantia nigra.

  Phase 5: Aβ deposition extended further into the brain stem: pons, the pontine nuclei and locus coeruleus, and finally the cerebellum.

2.2.4 Age adjusted criteria of the Consortium to Establish a Registry for Alzheimer's Disease (CERAD)

Consortium to Establish a Registry for Alzheimer's Disease (CERAD), a neuropathology protocol for the *post mortem* assessment of dementia and control subjects based on age and semi-quantitative assessment of neuritic plaques in the middle frontal gyrus, superior/middle temporal gyrus and inferior parietal lobe, was used to state whether a cases has; A: "possible AD", B: "probable AD", C: "definite AD" and "normal brain" to indicate levels of diagnostic certainty (Mirra et al., 1991).

2.2.5 NIA-Alzheimer's Association guidelines

The NIA-Alzheimer's Association guidelines (Montine et al., 2012) combine Thal Aβ phases, Braak neurofibrillary tangle stages and CERAD guidelines. This criteria was used to state an 'ABC' score from the Aβ plaque score (Thal phases), Braak neurofibrillary stage and CERAD neuritic plaque score. Based on the ABC score the degree of "AD Neuropathological Change" (i.e. no, mild, moderate and severe) was stated regardless of presence or absence of clinical dementia (Table 1.1).

	Level of AD neuropathological change					
Thal phase	**A**	**B**			**C**	*CERAD*
		0-1	**2**	**3**		
0	**0**	**Not**	**Not**	**Not**	**0**	*neg*
1 or 2	**1**	**Low**	**Low**	**Low**	**0 or 1**	*neg or A*
1 or 2	**1**	**Low**	**Intermediate**	**Intermediate**	**2 or 3**	*B or C*
3	**2**	**Low**	**Intermediate**	**Intermediate**	**any C**	*neg or A-C*
4 or 5	**3**	**Low**	**Intermediate**	**Intermediate**	**0 or 1**	*neg or A*
4 or 5	**3**	**Low**	**Intermediate**	**High**	**2 or 3**	*B or C*
		Braak 0-II	*Braak II-V*	*Braak V-VI*		

Table 1.1. ABC criteria for the level of AD pathological change determined by Thal phase score (orange column), Braak neurofibrillary stage (green), and CERAD scores (blue column). Modified from (Attems and Jellinger, 2013).

2.3 Lewy body diseases

LBD included DLB, PD and PDD. The neuropathological diagnosis was based on the staging of α-syn pathology (LB and LN). Clinico-pathological diagnosis was based on the onset of clinical motor symptoms, cognitive decline and pathological criteria:

- Braak α-syn stages described α-syn related pathology, assuming α-syn depositions initiate in the medulla oblongata (stage 1) spreading gradually to the pons (stage 2), midbrain (stage 3), entorhinal cortex and hippocampus (stage 4) and finally the neocortex (stage 5 and 6) (Braak et al., 2003).
- Newcastle-McKeith criteria for LBD distinguished between brainstem dominant, limbic, and diffuse neocortical types, depending on the topographical localization of α-syn related pathology (McKeith et al., 2005).

2.4 Tauopathies

Tauopathies were neuropathologically characterised by the presence of 4R HPT pathology in neurons and neuroglia.

2.4.1 Corticobasal degeneration

CBD presented with marked asymmetrical atrophy of cortical gyri of the superior frontal and parietal parasagittal regions, with loss of pigmented neurons in the substantia nigra. Neuropathological hallmarks included the accumulation of 4R tau isoform in the neuropil and distal segments of astrocytes, presenting as so called astrocytic plaques, in the cortex, WM, DGM and brain stem and the presence of swollen achromatic neurons (Dickson et al., 2002) (Feany and Dickson, 1995).

2.4.2 Progressive supranuclear palsy

PSP presented with 4R tau pathology in core regions include basal ganglia, sub-thalamic nucleus, substania nigra (Hauw et al., 1994) and cerebellar atrophy (Dickson, 2009). Neuropathlogical hallmarks lesions included globose NFT and tufted astrocytes (4R tau in astrocytes), mainly in the motor cortex and corpus striatum.

2.5 Normal aged controls

Normally aged controls were selected on the basis of the absence of MCI, dementia and considerable neuropathological lesions including AD pathology (Braak stage <IV; CERAD, neg; NIA-AA: A, 0 or 1, B 0-2, C 0 or 1, low neuropathologic change) and LBD pathology (Braak α-syn stages < 4).

2.6 Subcortical cerebral white matter assessment

Subcortical WM and DGM pathology, collectively referred to as SVP, were assessed using a simple image matching four-tier scoring system. (Smallwood et al., 2012) (Figure 2.1).

- Score 0: normal appearing white or grey matter.
- Score 1: mild, slight pallor of the myelin stain and/or slight loosening of the parenchymal tissue of the DGM and/or mild dilation of the PVS.
- Score 2: moderate, marked loss of myelin and/or loosening of the parenchymal DGM tissue with a possible ‘bubble like’ appearance to the WM; marked widened PVS.

- Score 3: severe, Regions of almost complete loss of WM and severe loosening of DGM parenchymal tissue extending into cavitation and severely dilated PVS.

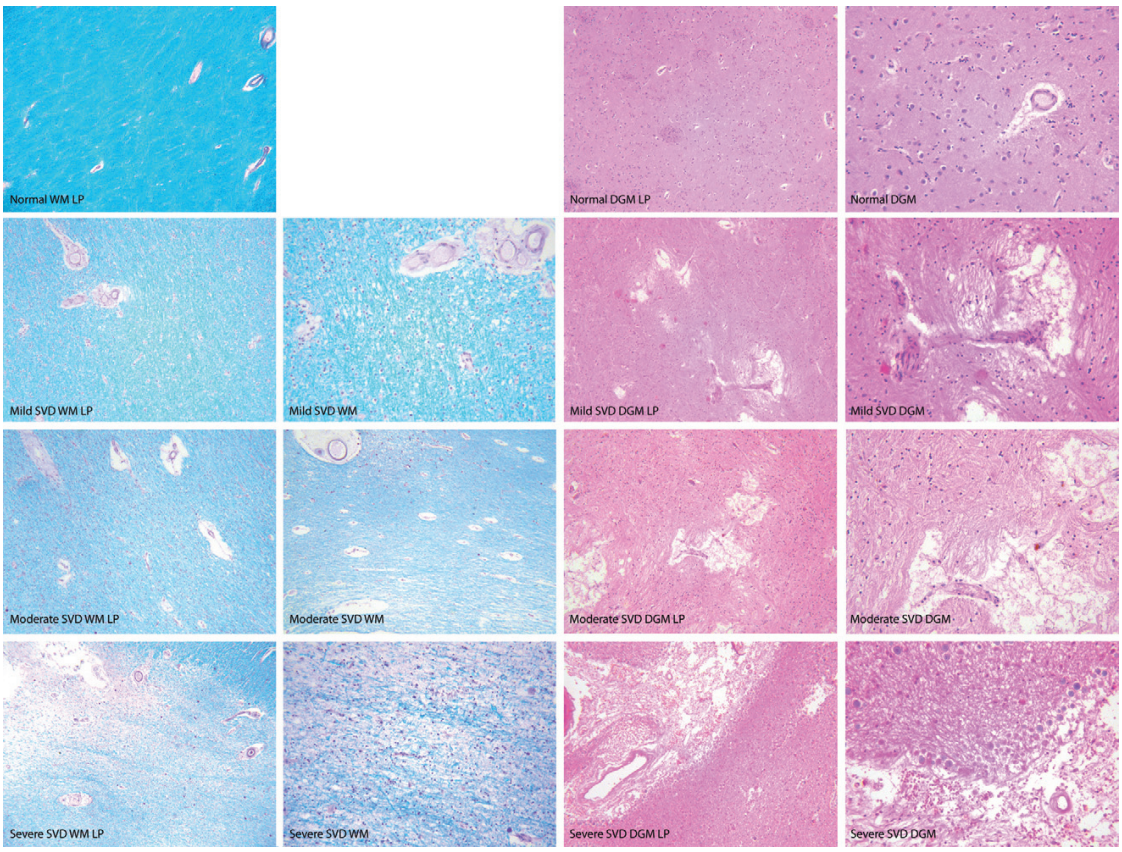

Figure 2.1. Semi-quantitative criteria used to asses SVP (Smallwood et al., 2012). Photomicrographs illustrating the histological appearance of subcortical WM stained with LFB (left 2 columns) and DGM stained with H&E (right 2 columns). Grade 0, normal; grade 1, mild pathology; grade 2, moderate pathology; grade 3, severe pathology.

2.7 Subject demographics

Case n	sex	age	Disease status	PMD (hours)	Braak stage	CERAD score	LB Braak	Included in cohorts in chapters
1	F	96	Normal Aged	95	3	0	0	3, 4, 6
2	M	77	Normal Aged	83	2	0	0	3, 4, 6
3	F	84	Normal Aged	46	6	3	0	3, 5
4	F	94	Normal Aged	82	2	0	0	3, 4, 5,6
5	F	98	Normal Aged	17	3	1	0	3, 4, 5
6	F	74	Normal Aged	40	3	0	1	3
7	F	81	Normal Aged	82	3	2	0	3, 6
8	F	70	Normal Aged	72	0	0	2	3, 4, 6
9	M	72	Normal Aged	39	1	0	0	3
10	F	89	Normal Aged	34	3	0	0	3, 6
11	F	78	Normal Aged	34	0	0	0	3, 6
12	F	95	Normal Aged	36	3	0	0	3, 4, 6
13	F	89	Normal Aged	49	3	0	3	3, 4, 6
14	M	72	Normal Aged	39	1	1	0	4, 5, 6
15	M	81	Normal Aged	43	2	0	0	6
16	M	73	Normal Aged	25	0	0	0	6
17	M	86	Normal Aged	50	4	2	0	6
18	F	97	Normal Aged	21	2	1	0	6
19	F	88	Normal Aged	22	3	0	0	3, 4, 6
20	F	86	AD	69	6	3	0	3, 4, 6
21	M	88	AD	84	6	3	0	3
22	F	93	AD	15	6	3	0	3, 4, 6
23	M	92	AD	59	6	3	0	3, 4, 6
24	M	78	AD	37	6	3	0	3, 4, 5, 6
25	F	86	AD	47	6	3	0	3, 4
26	M	85	AD	29	6	3	0	3, 4, 6
27	F	87	AD	54	6	3	0	3, 4, 5, 6
28	F	81	AD	73	5	3	0	3
29	F	81	AD	56	6	3	0	3, 6
30	M	90	AD	69	6	3	0	3, 4, 5, 6
31	F	75	AD	33	6	3	0	3, 4, 6
32	F	86	AD	5	6	3	0	3, 4, 6
33	F	89	AD	85	6	3	2	3, 4, 5, 6
34	F	90	AD	90	6	3	0	6
35	M	88	AD	22	6	3	0	6
36	F	79	AD	65	6	3	3	6
37	F	86	AD	51	6	3	0	6
38	M	89	AD	61	6	3	0	6
39	F	92	AD	74	6	3	0	6
40	M	80	AD	N/A	6	3	0	6
41	F	76	AD	37	6	3	0	6
42	M	91	AD	72	6	3	0	6
43	F	83	AD	52	6	3	0	6
44	M	76	AD	23	6	3	0	6
45	M	81	AD	41	6	3	0	6
46	M	72	DLB	89	3	0	6	3
47	M	78	DLB	34	6	3	6	3
48	M	77	DLB	46	3	0	6	3
49	F	81	DLB	44	4	2	6	3, 4
50	F	91	DLB	10	3	2	6	3, 4
51	F	73	DLB	99	3	0	6	3
52	M	81	DLB	81	3	2	6	3, 4
53	F	75	PDD	18	3	2	6	3, 4
54	M	68	CBD	9	2	0	0	3, 4
55	F	83	PSP	65	N/A	N/A	N/A	3, 4
56	M	90	PSP	N/A	2	0	0	3
57	M	78	PSP	53	N/A	N/A	N/A	3, 4

Table 2.2. Subject demographics of all 57 cases assessed. N, number; M, male; F, female; DLB, Dementia with Lewy bodies; AD, Alzheimer's disease; CBD, Cortiocobasal degeneration; PSP, Progressive supranuclear palsy; PDD, Parkinson's disease dementia; PMD, post mortem delay; N/A, not available.

2.8 Brain tissue

Brains were collected at autopsy and included in the Newcastle Brain Tissue Resource (NBTR) in accordance with Newcastle University ethics board and ethical approval awarded by The Joint Ethics Committee of Newcastle and North Tyneside Health Authority. After autopsy right hemispheres were immersion fixed in 4% buffered aqueous formaldehyde solution for 6 weeks.

2.9 *Post mortem* MRI

Fixed right hemispheres were removed from formalin solution and were subject to a 4.7 T MRI scanner (Bruker Medical, Ettlingen, Germany) following protocol stated in (McAleese et al., 2012): Bruker Biospec 47/60 VAS, (vertical, actively-shielded, the inner-bore width of 60 cm) fitted with a BGA-38-S gradient system (actively-shielded, the inner-bore width of 38 cm) and a birdcage RF coil with a working cross-section of 170 x 240 mm. A T2 -weighted pulse sequence was used: two spin echo images of effective echo time (TE) = 32/96ms, repetition time (TR) = 8200ms, with slice thickness of 2 mm and inplanar resolution of 1.0 x 0.78 mm. White matter hyperintensities (WMH) were rated by consensus between radioimaging experts Dr M. Firbank and Prof JT. O'Brien according to the Age-related white matter change scale (ARWMC) (Wahlund et al., 2001) (Figure 2.2).

- Score 0, absence of WMH
- Score 1, 'punctate' WMH (<10mm)
- Score 2, 'early confluent' WMH (<20mm)
- Score 3, 'confluent' WMH (>20mm)

Lacunes (>5mm) of the DGM are assessed based on the number of lesions i.e. 0, no lesions; 1, 1 lesion; 2, > 1 lesion; 3, confluent lesions (Bokura et al., 1998).

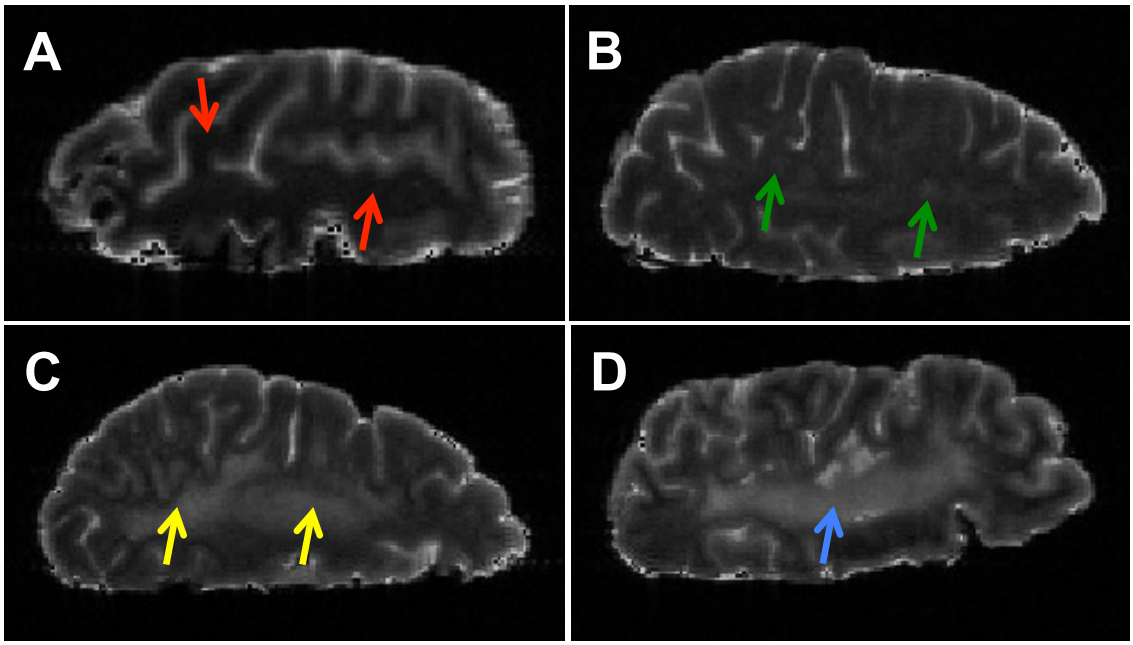

Figure 2.2. *Post mortem* MRI images showing WMH in the occipital lobe based on ARWMC criteria (Wahlund et al., 2001). A) grade 0, normal WM (red arrows); B) grade 1, punctate hyperintensities (green arrows); C) grade 2, early confluent hyperintentsities (yellow arrows); D) grade 3, confluent hyperintensities (blue arrow). Images taken on a T2-weighted 4.7 T scanner.

2.10 Dissection and sample regions

After *post mortem* MRI, hemispheres were dissected according to the Newcastle brain map (Figure 2.3) into approximately 25 coronal slabs at 7 mm intervals and further sub-dissection into tissue blocks A-L and R-AM, measuring from 4 cm^2 to 15 cm^2 and then paraffin embedded.

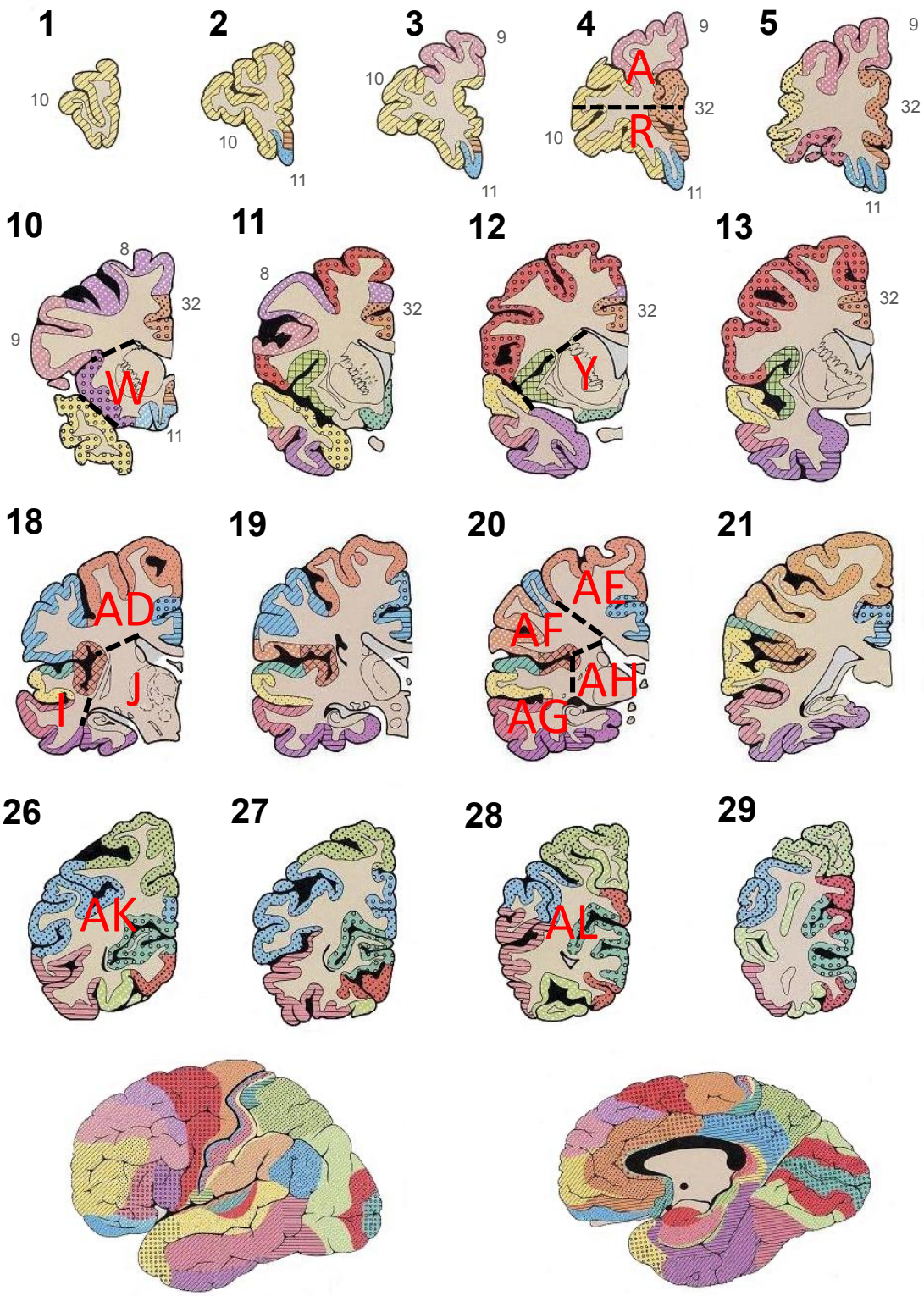
1
10
2
10
11
3
10
9
11
4
A
R
10
9
32
11
5
9
32
11
10
8
9
32
W
11
11
8
32
12
Y
32
13
32
18
AD
I
J
19
20
AE
AF
AH
AG
21
26
AK
27
28
AL
29

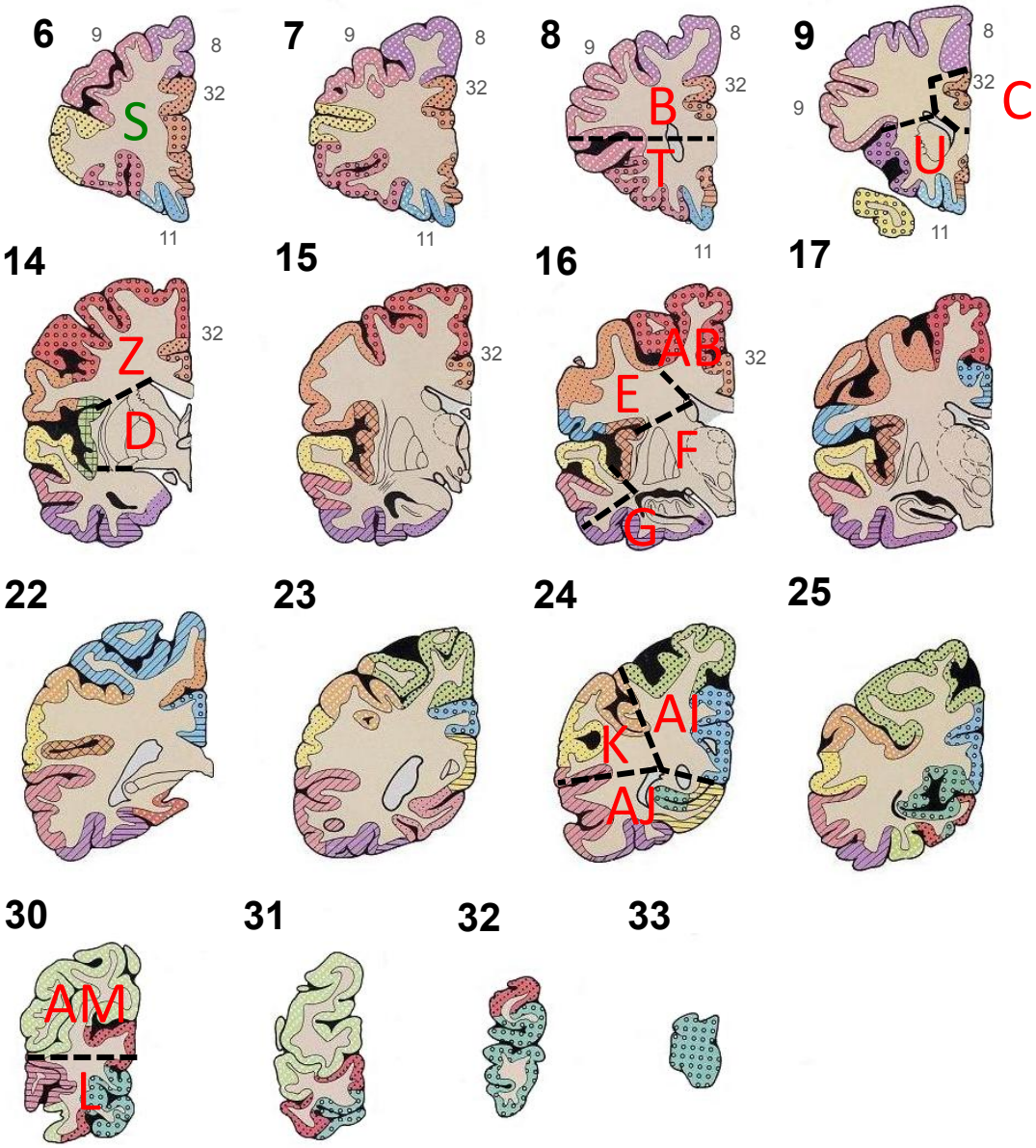

Figure 2.3. Newcastle brain map (Perry, 1993). Schematic representation of the coronal slices and sub-dissections used in this study. Black bold numbers indicate the coronal level; small grey numbers and colour coding indicate Brodmann areas; red letters indicate specific sub-dissections; dashed black line represent a sub-dissection line.

2.10.1 Frontal lobe

The frontal lobe represents up to two thirds of the human brain consisting of a pre-frontal cortex (involved in essential cognitive processes e.g. executive function, attention and reasoning) and a motor cortex (involved in sensory-motor transformations and action initiation) (Chayer and Freedman, 2001, Rizzolatti and Luppino, 2001). According to the Newcastle Brain map, frontal cortical and WM tissue included blocks A, B, S, T, U, Z, AD, AE, AF and/or Brodmann areas 9, 10, 8, 6, 4 and the lateral ventricle in coronal levels 1-21.

2.10.2 Temporal lobe

The temporal cortices comprise the medial temporal lobe (MTL), containing the hippocampus, entorhinal, perirhinal and parahippocampal cortices, and is responsible for the retention of declarative and long-term memories (Squire et al., 2004). Pathological hallmarks of AD include atrophy of the MTL (de Leeuw et al., 2006), especially hippocampal atrophy and thinning of the entorhinal cortex (Braak and Braak, 1996), and clinically loss of episodic memory. According to the Newcastle Brain map, temporal cortex and WM tissue are included in blocks I, G, AG, AJ and/or Brodmann areas 22/21/20 to 29 in coronal levels 11-24.

2.10.3 Parietal lobe

The parietal lobe is involved in a variety of cognitive functions including spatial information processing, somatic sensations and perception (Husain and Nachev, 2007), and is regarded as a polymodal area due to its high connectivity with the pre-frontal cortex and paralimbic cortex, including the hippocampus and parahippocampal gyrus (Rushworth et al., 2006). According to the Newcastle Brain map, parietal lobe cortex and WM tissue are included in blocks K, AI, AK and/or Brodmann areas 7/30 in coronal levels 23-27.

2.10.4 Occipital lobe

The occipital lobe is the visual processing center of the human brain. In AD, CAA is usually present and commonly and severely affects the occipital lobe (Attems et al., 2005, Tian et al., 2004). According to the Newcastle Brain map, occipital lobe cortex and WM tissue are included in blocks L, AL and/or in coronal levels 28-33.

2.10.5 Deep grey matter

The DGM is a collection of subcortical nuclei including the basal ganglia (comprised of the putamen, caudate and globus pallidus), substania nigra, sub-thalamic nucleus and thalamus. WM structures include the internal, external and extreme capsules. The DGM is directly connected to the cortex and has various roles in sensory-motor, limbic and cognitive information processing and relaying (Helms et al., 2009). According to the Newcastle Brain map, DGM is included in blocks W, Y, U, AH and coronal levels 11-19.

2.11 Tissue micro array

A TMA methodology was developed from 2011 to 2013 (McParland et al., 2014); 40 *post mortem* tissue samples from the pre-frontal cortex (block A), mid-frontal cortex (block B), cingulate (block C), DGM (blocks D, F) motor cortex (block E), entorhinal cortex (block G), temporal cortex (block I), parietal cortex (block K) and occipital cortex (block L) (Figure 2.4) Paraffin embedded blocks were incubated at 37°C for 1 hour to reduce chipping. All tissue samples were taken in numerical order using a Tissue-Tek Quick-Ray hand held punch with a 3mm diameter (Sakura, California, USA). The hand held punch tip was pushed into the tissue block at the specific location and removed along with the section of tissue. The tip of the punch was then placed into the correct empty hole of the pre-made TMA paraffin block (made from a pre-existing silicon mould supplied by the manufacturer) and the plunger pushed, depositing the tissue sample into the TMA hole (Figure 2.5 A-C).The complete TMA block was incubated at 37℃ and TMA silicon mold was heated to 60℃ for 1 hour. The TMA block was removed from the oven and ensured all tissue samples were firmly pushed into the wax and empty spaces were filled with molten wax. Molten wax was placed into the base of the silicone mold and the TMA block was placed punch down into the silicon mold, left for 5 minutes then incubated at 37℃ for 15 minutes (Figure 2.5 D).The block was left to fully cool before the silicone mold was removed and excess wax removed (Figure 2.5 E).

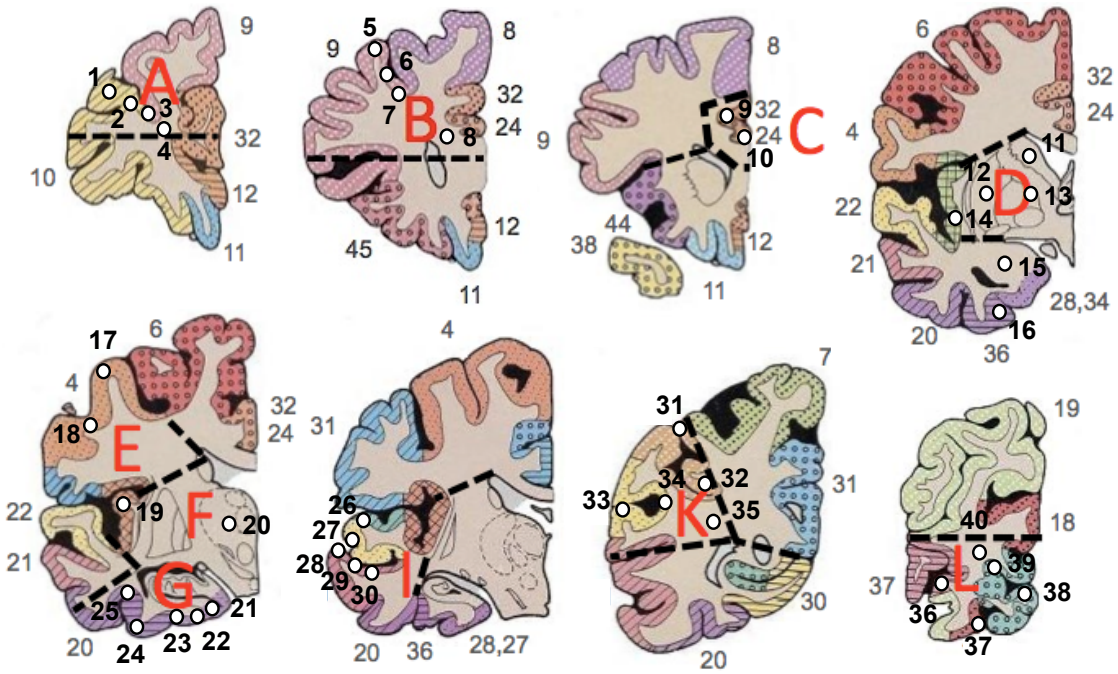

Figure 2.4. TMA sample map adapted from the Newcastle brain map (Perry, 1993). A schematic representation of blocks and sample areas used to create the TMA. White dots and bold black numbers indicate punch sample location and number; small grey numbers and colour coding indicate Brodmann areas; red letters indicate specific sub-dissection; dashed black line represent a sub-dissection line.

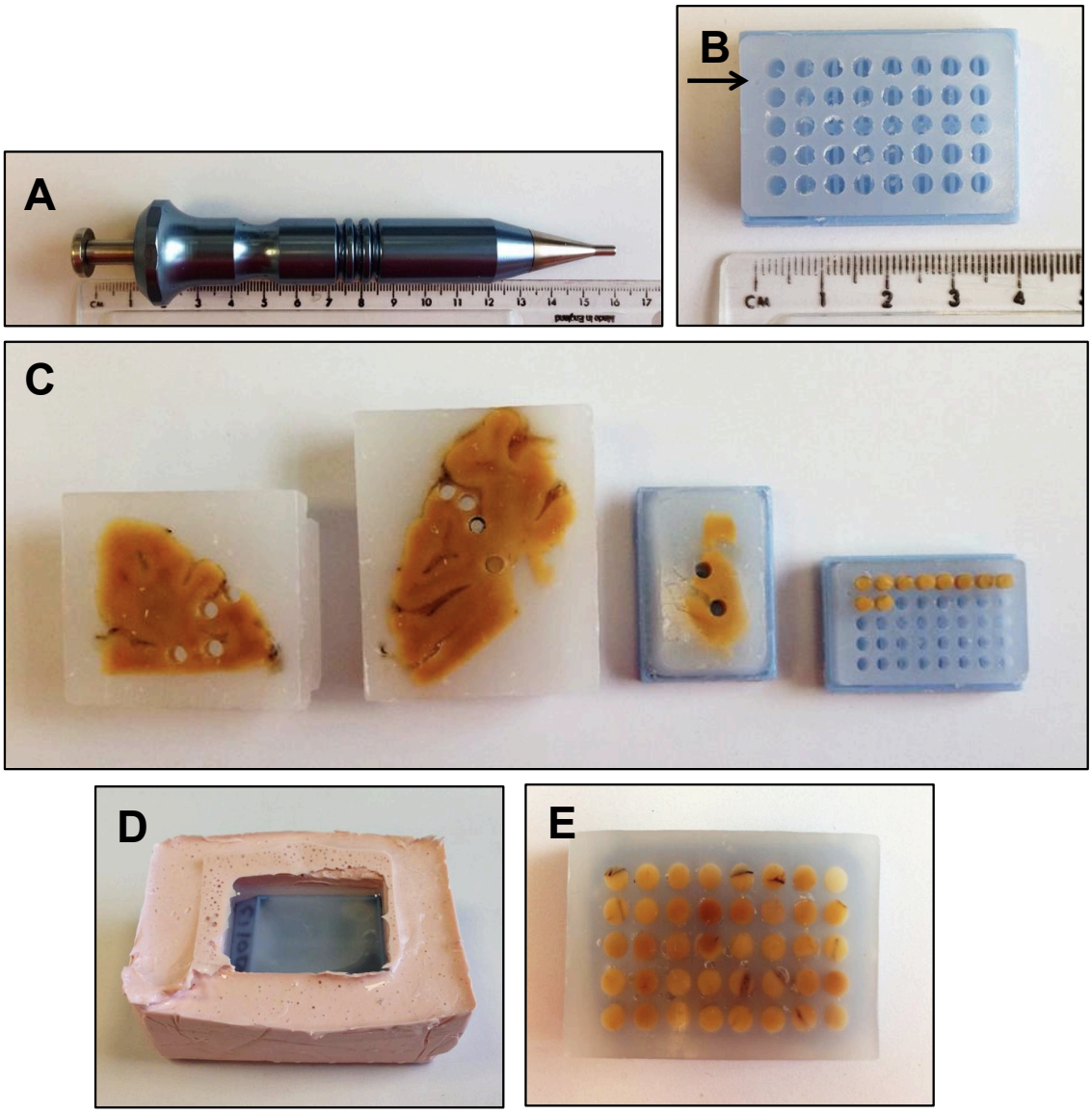

Figure 2.5 Tissue MicroArray. A) 3mm diameter Tissue-Tek Quick-Ray hand held punch; B) empty TMA paraffin block with 40 3mm holes, black arrow highlights a small hole that indicates the location of sample 1; C) Paraffin embedded tissue from blocks A, B and C with punch samples removed and placed into the TMA paraffin block; D) Completed TMA block placed into molten wax in a silicon mould; E) completed TMA block.

2.12 Histology

To aid the adhesion of tissue sections and glass slide, clean double frosted slides were immersed in acetone for 5 minutes, drained and placed in a 4% solution of 3 aminopropyl triethoxysilane (APES) in acetone for 5 minutes. Slides were drained, immersed in distilled water, dried at 45°C and stored until use. 6µm sections were cut from paraffin blocks using a rotary microtome (Shandon Finesse 325, Thermo Scientific), and sections mounted onto APES coated slides. Sections were dried at 37℃ for a minimum of 24 hours. Wax was melted at 60℃ for 1 hour and de-waxed in 2 10-minute changes in xylene.

2.12.1 Haematoxylin and eosin

Haematoxylin and eosin (H&E) staining was used to visualise brain parenchyma in the DGM for SVP assessment, and vessel walls in the WM for SI assessment. After dewaxing in xylene, sections were re-hydrated through decreasing concentrations of alcohols (100% 1, 100% 2, 95%, 70%, 50%) to water. Sections were then immersed in haematoxylin solution for 30 seconds, washed in tap water, then differentiated quickly in 1% acid alcohol, washed in again in water, placed into Scott's tap water substitute (ammonia water) until blue and rinsed in water. Sections were then couterstained in eosin for 15-30 seconds and washed well in water, dehydrated through increasing concentrations of alcohols (50%, 70%, 95%, 100% 1, 100% 2), into xylene and mounted with a cover slip and DPX.

2.12.2 Luxol Fast Blue

Luxol Fast Blue (LFB) is used to visualise myelinated axons, and was used when assessing SVP pathology in the WM. After dewaxing, sections were placed in 95% alcohol, and then incubated in preheated LFB solution at 60℃ for 1-2 hours. Sections were then washed in 95% alcohol and re-hydrated to water. Sections were differentiated in 1% lithum carbonate for 10-20 seconds and then further differentiated in 70% alcohol until grey and white matter is clearly distinguishable. Sections were counterstained in 0.1% cresyl fast violet (CFV) in 1% acetic acid for 10 minutes and washed well in water. Sections were checked for staining consistency before being dehydrated through increasing concentrations of alcohols, into xylene and mounted with a cover slip and DPX.

2.12.3 Standard procedure of single label immunohistochemistry (IHC)

Sections were dewaxed for 15 minutes in xylene and re-hydration through decreasing concentrations of alcohols to water. Antigen retrieval was performed depending on the primary antibody protocol (Table 2.3).

Primary antibody	Source (product code)	Target	Species	Primary antibody dilution (in TBS)	Anigen retrieval protocol
AT8	Thermo Scientific, Massachusetts, USA, (MN1020)	Phospho-PHF-tau pSer202+Thr205	Mouse monoclonal	1:4000	Sections were heated in 0.01M sodium citrate buffer (pH 6.0) in a microwave for 10 minutes
4G8	Sigma-Aldrich, Missouri, USA, (SIG-39220)	amyloid 17-24	Mouse monoclonal	1:15000	Sections were placed in 98-100% concentrated formic acid for 1 hour

Table 2.3 The primary antibodies, dilutions and antigen retrieval protocols used for single labelled immunohistochemistry.

Sections were left to cool, if required, and placed into distilled water, quenched in 3% hydrogen peroxide for 20 minutes and rinsed in water and then tris buffered saline (TBS) at pH 7.6. Menapath X-Cell HR polymer universal biotin-free detection kit (Menarini Diagnostics, California, USA) was used to identify mouse monoclonal antibodies. Primary antibodies at optimum dilution in TBS (Table 2.3) were applied to the sections and incubated at room temperature for 1 hour. Sections were thoroughly washed in 2 changes of TBS and a final wash of TBS with detergent Tween-20 (Tween). The universal probe applied and incubated at room temperature for 30 minutes and washed again as previous. Horseradish peroxidase-polymer (HRP) reagent was applied and incubated for 30 minutes. Sections underwent a wash of 3 changes of TBS and treated with 3,3‘- Diaminobenzadine (DAB), ratio 1 drop of DAB chromogen concentrate (approximately 32µl) per 1ml of DAB substrate, for 2-4 minutes until a brown stain was visible. Sections were rinsed well in tap water, counterstained lightly in haematoxylin to visualise cell nuclei, dehydrated through increasing concentrated alcohols to xylene and finally mounted with a cover slip and DPX.

2.13 Image analysis

2.13.1 Image capture

All analysis was carried out blind to neuropathological diagnosis. Digital images of WM, DGM, cortex, arteries and arterioles were captured using a Nikon Eclipse 90i microscope coupled with a Nikon DS-Fi1 camera and NIS-Elements AR3.2 software (Nikon, Surrey, UK). All images were white balanced and underwent background correction. During pathological analysis and capturing images the goniometer stage and magnification was adjusted and focused to incorporate the area of interest.

2.14 Semi-quantitative analysis

2.14.1 Subcortical vascular pathology

Analysis of SVP within the WM and DGM, as described in Chapter 3, was based on semi-quantitative assessment (Figure 2.1) of tissue from diagnostic blocks S, T, U, W, Y, U, Z, AD, AE, AF, AG, AH, AJ, AI, AK, AL and coronal levels 1-3, 5, 7, 9-13, 15, 17, 19, 21-23, 25, 27, 29 and 31-33. There was slight variation within hemispheric regions and Brodmann areas contained in each coronal level and availability within the individual cases. This was due to variation in hemispheric size, however, detailed notes from the neuropathologist enabled identification of WM and DGM regions (Table 2.4).

All blocks were examined before cutting to ensure adequate WM tissue was available. To reduce staining variation, one experienced technician produced the majority of the sections. 6μm tissue sections were cut and stained with H&E and LFB according to the protocols in sections 2.12.1 and 2.12.2. These sections are referred to as 'total' sections since they encompassed the entire WM. Diagnostic sections for blocks A, B, D, E, F, I, J, K and L were previously stained with H&E and LFB as part of the routine diagnostic assessment for the NBTR and referred to as 'diagnostic' sections. LFB sections for WM and H&E sections for DGM were viewed using Nikon Eclipse 90i microscope. The appropriate tissue and area was identified and assessed according to the SVD criteria. Scores were noted and a mean value was calculated for frontal, temporal, parietal-occipital and DGM separately for 'total' and 'diagnostic' scores per case. Parietal and occipital scores were combined to aid comparison to *post mortem* MRI scores.

Brain region	Total blocks and coronal levels	Diagnostic blocks
Frontal	S, T, U, Z, AD, AE, AF; CL: 1-3, 5, 7, 9-13, 15, 17, 19, 21	A, B, E
Temporal	AG, AJ; CL: 11, 13, 15, 17, 19, 21-23	I
Parietal	AI, AK; CL: 23, 25, 27	K
Occipital	AL; CL: 29, 31-33	L
DGM	W, Y, U, AH; CL: 11, 13, 15, 17, 19	D, F, J

Table 2.4. Table indicating the blocks and coronal levels used for the frontal, temporal, parietal, occipital regions and DGM for both 'total' and 'diagnostic' data sets. CL, coronal level.

2.14.2 Artery and arteriole fibrosis

Analysis of artery and arteriole vessel wall fibrosis, as described in Chapter 4, was based on semi-quantitative criteria from Esiri and colleagues (Esiri et al., 2011) (Figure 2.6). Previously H&E stained 6μm diagnostic sections from blocks A, B (frontal), I (temporal), K (parietal) and L (occipital) were used. Sections were viewed using Nikon Eclipse 90i microscope, the WM was identified and approximately eight >50μm arteries/arterioles were selected per section, depending on the amount of WM present. Vessels were given a vascular fibrosis score according to the criteria used by Esiri's group (Smallwood et al., 2012). Images of vessels were captured at x200 magnification with a Nikon DS-Fi1 camera and saved as a Jpeg image file for SI assessment (2.25.3). Scores were noted and a mean value was calculated for frontal, temporal, parietal, and occipital scores per case.

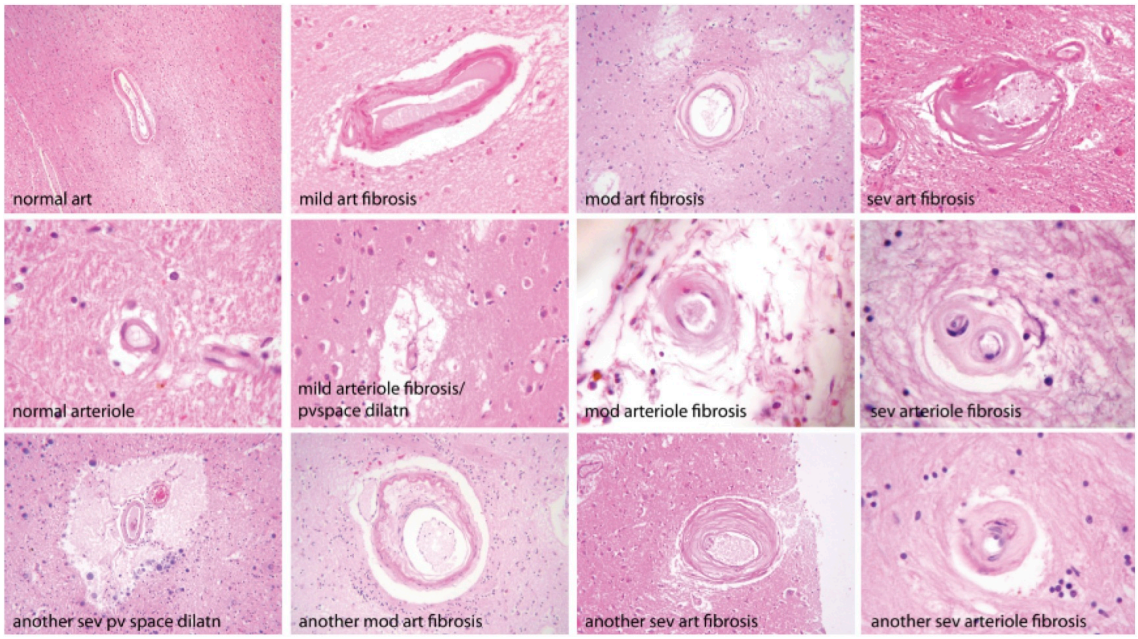

Figure 2.6. Semi-quantitative criteria used to asses arterial and arteriole wall fibrosis (Esiri et al., 2011). Photomicrographs illustrate the histological appearance of various grades of vascular fibrosis: grade 0, normal; grade 1, mild, grade 2, moderate; grade 3, severe vessel wall fibrosis. Histochemistry: H&E.

2.15 Quantitative analysis

2.15.1 Cortical pathology

Quantitative assessment of cortical pathology, as described in Chapters 4 and 5, was performed on 6µm tissue sections from blocks A, B, E, I, K, and L for AT8, and blocks A, I, K, and L for 4G8. Section underwent immunohistochemical staining for AT8 and 4G8, according to the protocols in sections 2.12 and 2.12.3. Of note, routine neuropathological protocol does not require 4G8 staining for blocks B and E as this is not required for diagnostic assessment.

Previous studies have shown that the density of neuropathological lesions i.e. HPT and Aβ, have been previously shown to be significantly higher in the sulci compared to the gyri crest (McParland et al., 2013, Gentleman et al., 1992).

For each stain, three separate sulci and gyri were assessed. Three was considered the most appropriate number of measurements as takes into consideration natural variation with in the sample and yields a reliable mean value, the vast majority of tissue samples contained three suci and gyri so it

was uniform for all sections and it enabled fast assessment of cases. Therefore, six measurements were taken per section (3 sulci, 3 gyri) from which the section mean value was calculated. Sulcal and gyral regions were identified and marked to aid stage adjustment (Figure 2.7 A). Sections were viewed using Nikon Eclipse 90i microscope, at illumination 3.9V, and the stage was guided to the tip of a gyrus and an x200 magnification 1x6 (0.41 x 1.67mm) image of cortical strip was captured (Figure 2.7 B-C). Using NIS-Elements AR3.2 software the pre-determined threshold for the specific stain was then applied to create a binary layer. Using automatic measurement the binary area fraction, defined as the ratio of the segmented/highlighted image area to the measured area, is counted (Figure 2.7 D). This was repeated on the other 2 sulci and gyri. Data was exported into a Microsoft Excel document. Binary area fraction counts are presented as values between 0-1; in order to express the percentage area of immunopositivity binary area fraction counts were multiplied by 100 to calculate a mean percentage areas of immunopositivity for each section. This enabled the mean percentage area calculation for frontal (A and B), temporal (I), parietal (section K), occipital (section L) cortices.

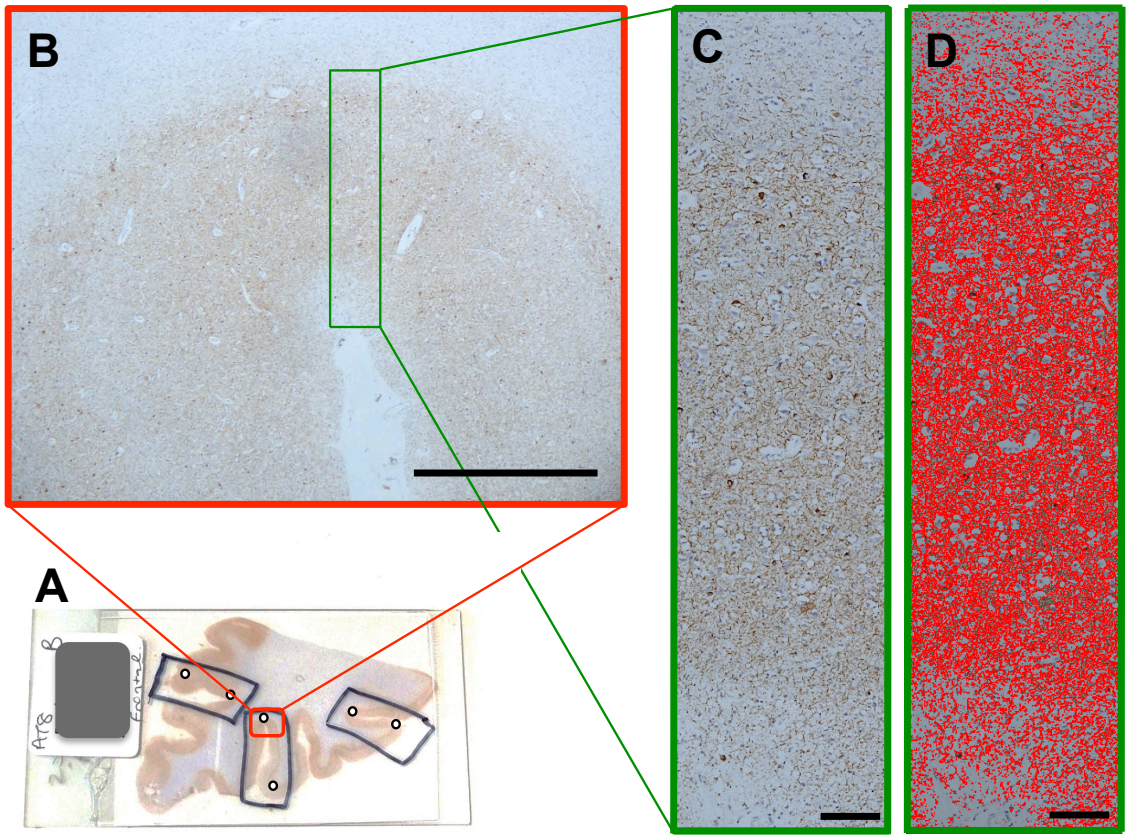

Figure 2.7. Quantification of cortical pathology. A) Section of frontal tissue with gyri and sulci labelled (black boxes), white dots indicate areas selected for cortical strip measurement; B) magnified image of a sulcus, green box indicates 1x6 capture area of cortical tissue; C) cortical strip with NFT/NT pathology; D) cortical strip with threshold. Immunohistochemistry AT8; scale bars: B, 500 μ m; C and D, 100 μ m.

2.15.2 TMA analysis

HPT and Aβ pathology were quantified in TMA sections, as described in Chapter 6. Paraffin TMA blocks were generated for each case according to the protocol in section 2.11. 6µm tissue sections were cut and mounted according to the protocol in section 2.12. Sections were carefully placed on the slide in the same orientation so the first tissue sample can be easily identified. Sections were then immunohistochemically stained with antibodies AT8 and 4G8 according to the protocol described in section 2.12.3 (Figure 2.8 A). Sections were viewed using a Nikon Eclipse 90i microscope, at illumination 3.9V, and the stage was guided to the tissue sample 1. At x40 magnification the center of the tissue sample is identified, magnification decreased to x20 magnification, focused and location recorded on a Macro that is programmed to take 2x3 (0.85

x 0.78mm) images (Figure 2.8 B). Magnification was then reduced to x40 and the stage moved to tissue sample number two and the process repeated for all 40 tissue samples. At the final sample the image was left in focus at x200 magnification and the Macro enabled starting the automatic capture of 2x3 images from sample one, continuing through all 40 tissue samples. Using NIS-Elements AR3.2 software a pre-determined threshold for the specific stain was then applied to all 40 photomicroimages, which were then measured as a binary area fraction (Figure 2.8 C). Data was exported into an Excel document and expressed as a percentage area of immunopositivity binary area fraction, as described in section 2.15.1. From these single punch measurements the mean percentage binary area fraction of immunopositivity for specific cortical regions (Table 2.5) was calculated.

Tissue sample number	Area	Brain region
1-3	Pre-frontal cortex	Frontal
5-7	Mid-frontal cortex	
17 + 18	Motor cortex	
21-25	Entorhinal cortex	Temporal
26-30	Temporal cortex	
31-34	Parietal cortex	Parietal
36-39	Occipital cortex	Occipital

Table 2.5. Table indicating the TMA tissue sample numbers and their specific areas used for the frontal, temporal, parietal, and occipital regions. Samples not included in the analysis were 4, 8. 15, 35 and 30 that consisted of white matter; 9 and 10 that consisted of cingulate, and 11-14 and 19-20 that consisted of deep grey matter.

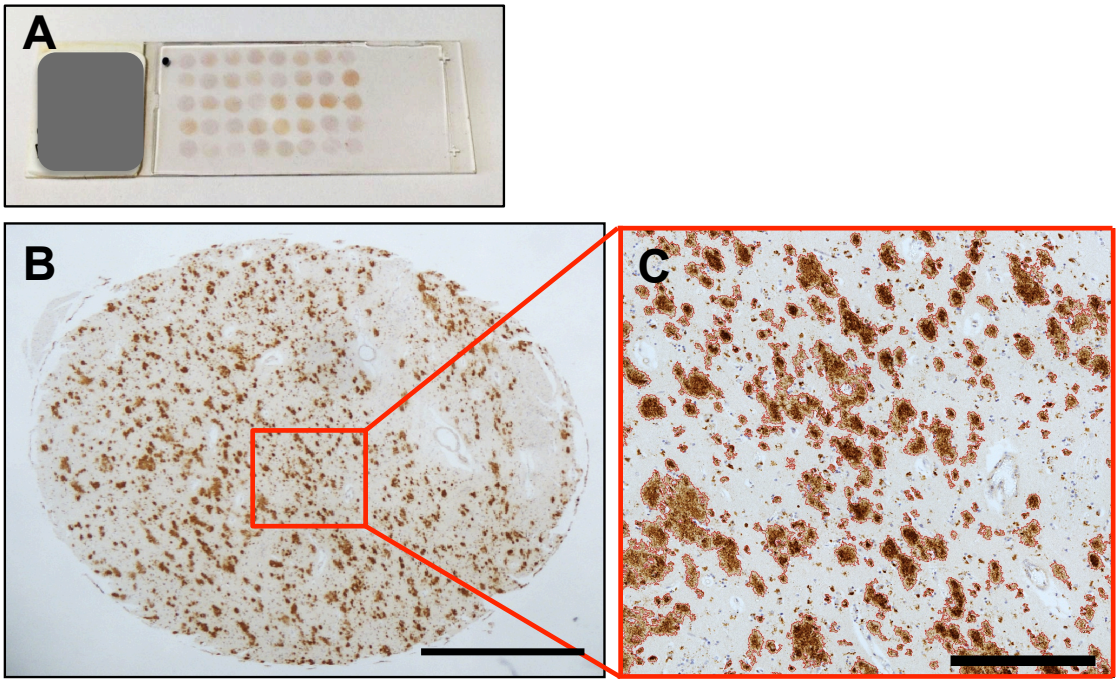

Figure 2.8. Quantification of TMA. A) TMA section. Black dot indicates sample 1; B) magnified image of TMA tissue sample, red box highlights area captured by 2x3 image at the center of the tissue sample; C) 2x3 image of A β pathology with threshold. Immunohistochemistry 4G8; scale bars: B, 500 μ m; C, 100 μ m.

2.15.3 Calculation of artery and arteriole Sclerotic Index

For the quantification of artery and arteriole fibrosis, as described in Chapters 4 and 6, the software program VasCalc was used to calculate the SI using photomicroimages of H&E sections (see: section 2.14.2). VasCalc was developed and previously used by Yamamoto (Yamamoto et al., 2009, Craggs et al., 2013, Yamamoto, 2011) (Full Visual Basic code for VasCalc can be found in appendix I (Yamamoto, 2011)). SI was developed by Lammie and colleagues (Lammie et al., 1997) and is used to evaluate the thickening of cerebral arteries and arterioles, as a measure of SVD and is calculated by standard formulae (Figure 2.9). For the study in Chapter 6 I modified the three-tiered SI criteria and included a 'moderate' value to keep all of our SVD pathology criteria on four-tiered scale. SI of normal vessels in this study was considered 0.2-0.29; SI value 0.3-0.39 represented mild SVD; SI value 0.4-0.49 represented moderate SVD; and SI values >0.5 represented severe SVD.

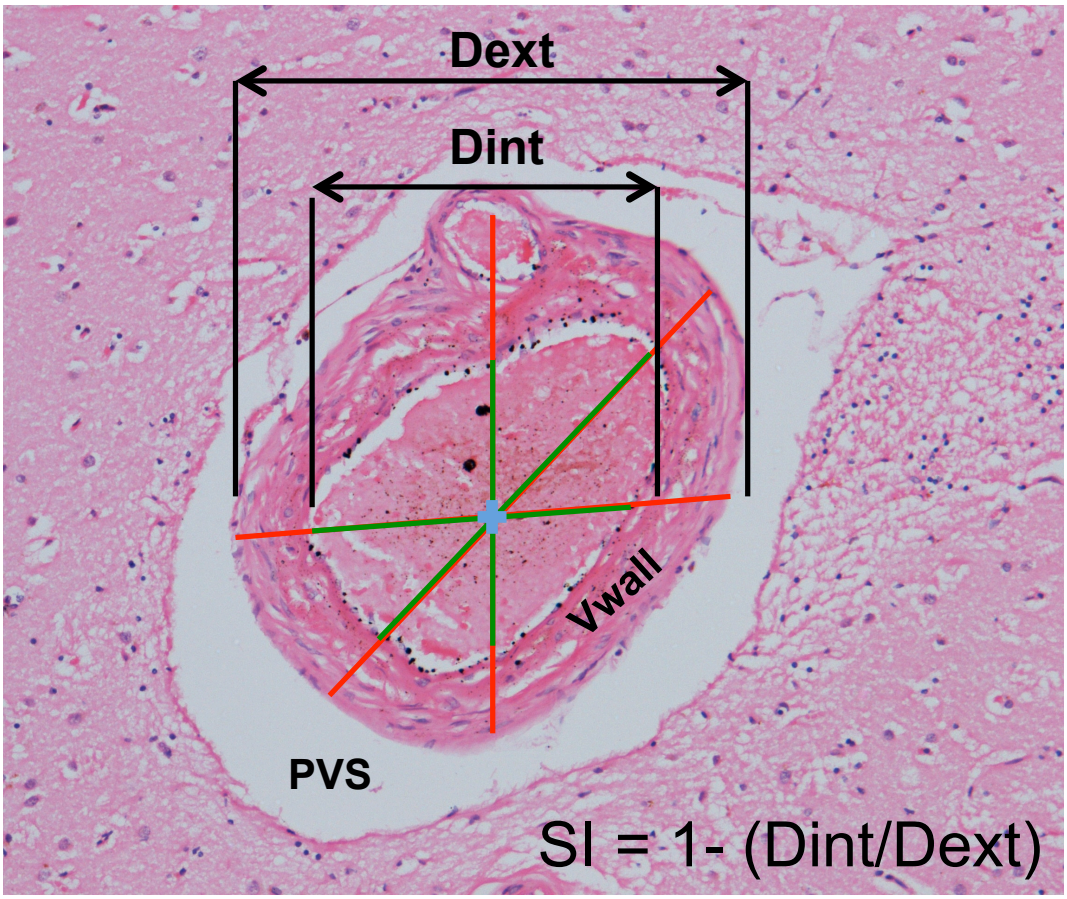

Figure 2.9. Definition of SI. Formulae used to calculate the SI value of the walls of arteries and arterioles. VasCalc software; Green lines indicate the 3 lines used to measure the internal diameter and red lines indicate the 3 lines used to measure the external diameter of the vessel wall. All 6 lines crossed the blue cross. Vwall, vessel wall; PVS, perivascular space; Dint, internal diameter; Dext, external diameter.

The protocol was identical for both studies described Chapters 4 and 6: 6µm tissue sections from blocks A, B, I, K and L were cut and stained with H&E according to the protocol in sections 2.12 and 2.12.1. Sections were viewed using Nikon Eclipse 90i microscope, the WM was identified and approximately eight >50µm arteries/arterioles were selected per section depending on the amount of WM present. Images were captured at x200 magnification with a Nikon DS-Fi1 camera and saved as a Jpeg image file. Jpeg files were loaded into VasCalc program and calibration settings based on the image magnification selected. 3 user-specific lines were used to measure the mean internal diameter (mDint) and mean external diameters (mDext). VasCalc then calculated the SI value and exported the data into a Word Excel document. An average SI score was calculated from the frontal (A and B), temporal (I), parietal (section K), occipital (section L), and a combined parietal-occipital WM SI values.

2.16 Statistical analysis

Statistical analyses were carried out using SPSS version 19. Data was checked for normal distribution using Kolmogorov-Smirnov test. All data was non-normally distributed.

To compare means non-parametric Kruskal-Wallis test was used. Linear Regression analysis was used to quantify how one variable related to another. Wilcoxon Rank sum and Mann-Whitney U tests were used to test for differences between groups. Spearman's rank correlation coefficient was calculated to find relationships between variables. Post hoc power calculations were generated using G*Power version 3.1.9.2 (Faul et al., 2009).

Chapter 3 - The use of MRI to assess white matter lesions in fixed *post mortem* brain hemispheres

3.1 Introduction

WMH, as seen on T2-weighted MRI, have a high prevalence within the population and are frequently seen in both demented and non-demented aged individuals (Schmidt et al., 2011b, Barber et al., 1999). WMH are associated with a plethora of physically disabilities (O'Sullivan, 2008) and cognitive deficits especially cognitive impairment (Esiri et al., 1999, Kalaria et al., 2004, Smallwood et al., 2012, Vinters et al., 2000, Baune et al., 2009, Shenkin et al., 2005, Stenset et al., 2008, Zhou et al., 2008). Importantly they are significantly associated with and increased risk of dementia and accelerated decline (Debette et al., 2010, Debette and Markus, 2010, Kuller et al., 2003, Prins et al., 2004, Snowdon et al., 1997) and are one of the most common co-pathologies in AD, seen in up to 40% of cases (O'Sullivan, 2008, Nagata et al., 2012, Schneider et al., 2007)

Pathologically, WMH appear as WML characterized by EPVS and WM rarefaction or lacunes in the DGM. It is generally assumed that in most cases WML result from ischemia caused by SVD (Grinberg and Thal, 2010). Collectively, SVD and associated lesions can be referred to as SVP, and definitive diagnosis relies on the *post mortem* identification and grading of the associated vascular and WML. However, there are currently 2 major difficulties in the histological assessment of SVP and WML:

1. No validated neuropathological consensus criteria for SVP or WML are available

2. Histological examination is based upon a limited number of histological slides containing selected frontal, parietal, temporal and occipital WM and DGM. A full histological assessment of all WM is deemed the best method of assessment but this rarely possible due to financial and time constraints.

In contrast, MRI has several validated rating scales for the visual assessment of WMH, that may be applied for both *in vivo* and *post mortem* MRI (Scheltens et al., 1998, Wahlund et al., 2001). Although there have been numerous studies comparing *in vivo* and *post mortem* MRI with histological findings (see section 1.6) (Figure 3.1), these studies focused on the identification of morphological substrates for respective MRI signals and did not investigate whether assessment scores reflected that of a neuropathological assessment. Therefore, it is not clear if *post mortem* MRI may routinely be used to complement *post mortem* examination for the assessment of SVP.

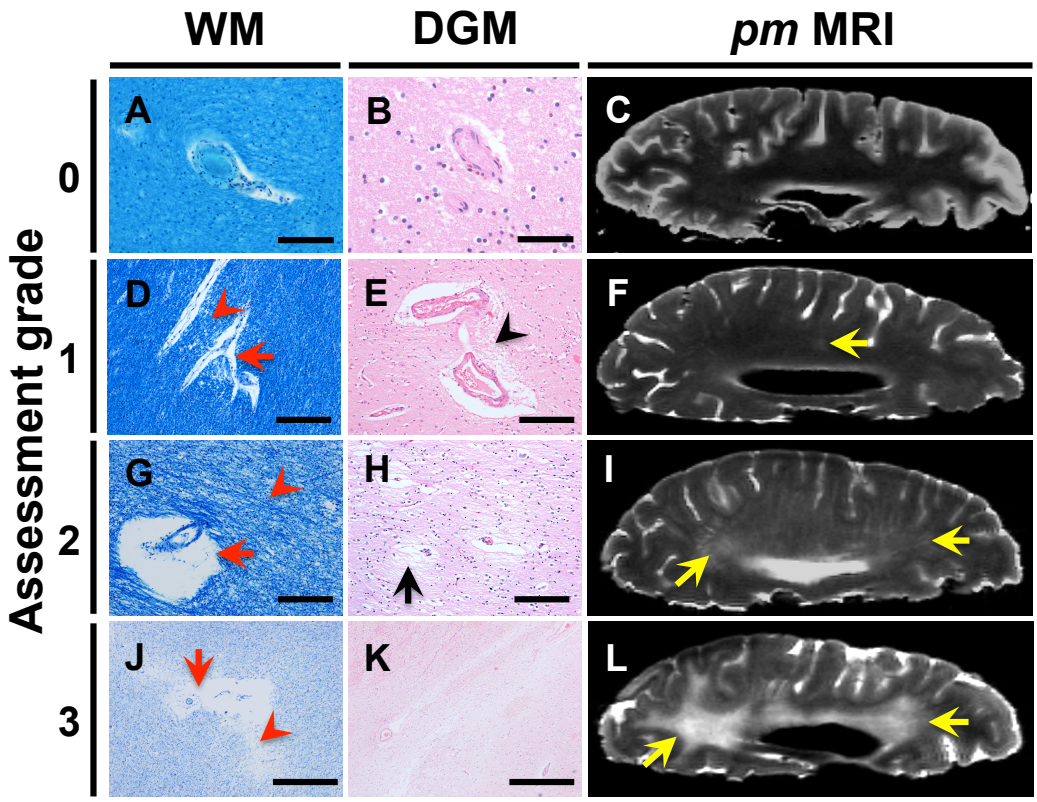

Figure 0.1 Micro-photoimages and corresponding *post mortem* T2-weighted MRI images showing SVP at various grades in the WM and DGM. Grade 0; normal myelin and PVS in WM (A), normal parenchyma DGM (B) and no hyperintensities present on MRI (C). Grade 1; mild myelin pallor (D, arrow head), mild dilation of PVS in WM (D, arrow), mild loosening of parenchyma in DGM (E, arrow), 'punctate' hyperintensities (F, arrow). Grade 2; moderate myelin pallor with a 'bubble-like' appearance (G, arrow head), moderate dilation of PVS in WM (G, arrow), moderate loosening of parenchyma in DGM (H, arrow), 'early confluent' hyperintensities (I, arrows). Grade 3; Severe myelin pallor with areas of cavitation (J, arrow head), severe dilation of PVS in WM (J, arrow), severe loosening of parenchyma in DGM, 'confluent' hyperintensities (L, arrows). WM, white matter; DGM, deep grey matter; PVS, perivascular space. Histochemistry; Luxol fast blue (A, D, G and J) and haematoxylin & eosin (B, E, H and K) and MRI images were taken with a T2-weighted vertical 4.7 T scanner, horizontal plane; frontal cortex, right hemisphere. Scale bars: A, 100 μm; B, 50 μm; D, E, G, H, 200 μm; J, H, 500 μm.

3.2 Aims

To evaluate the feasibility of MRI of *post mortem* brain hemispheres as a means of assessing SVP in demented and non-demented aged subjects.

3.3 Methods

3.3.1 Cohort

This study included clinico-pathologically confirmed non-demented aged controls and demented cases that included AD, DLB, PDD, CBD and PSP. This study compared scores from different pathological assessments; therefore case selection was not based on the neuropathological diagnosis (Table 3.1).

Case n	sex	age	Disease status	PMD (hours)	Braak stage	CERAD score	LB Braak
1	F	96	Normal Aged	95	3	0	0
2	M	77	Normal Aged	83	2	0	0
3	F	84	Normal Aged	46	2	0	0
4	F	94	Normal Aged	82	2	0	0
5	F	98	Normal Aged	17	3	1	0
6	F	74	Normal Aged	40	3	0	1
7	F	81	Normal Aged	82	3	2	0
8	F	70	Normal Aged	72	0	0	2
9	M	72	Normal Aged	39	1	0	0
10	F	89	Normal Aged	34	3	0	0
11	F	78	Normal Aged	34	0	0	0
12	F	95	Normal Aged	36	3	0	0
13	F	89	Normal Aged	49	3	0	3
19	F	88	Normal Aged	22	3	0	0
20	F	86	AD	69	6	3	0
21	M	88	AD	84	6	3	0
22	F	93	AD	15	6	3	0
23	M	92	AD	59	6	3	0
24	M	78	AD	37	6	3	0
25	F	86	AD	47	6	3	0
26	M	85	AD	29	6	3	0
27	F	87	AD	54	6	3	0
28	F	81	AD	73	5	3	0
29	M	81	AD	56	6	3	0
30	M	90	AD	69	6	3	0
31	F	75	AD	33	6	3	0
32	F	86	AD	5	6	3	0
33	F	89	AD	85	6	3	2
46	M	72	DLB	89	3	0	6
47	M	78	DLB	34	6	3	6
48	M	77	DLB	46	3	0	6
49	F	81	DLB	44	4	2	6
50	F	91	DLB	10	3	2	6
51	F	73	DLB	99	3	0	6
52	M	81	DLB	81	3	2	6
53	F	75	PDD	18	3	2	6
54	M	68	CBD	9	2	0	0
55	F	83	PSP	65	N/A	N/A	N/A
56	M	90	PSP	N/A	2	0	0
57	M	78	PSP	53	N/A	N/A	N/A

Table 3.1. Subject demographics. Case n refers to master demographic table 2.2. N, number; M, male; F, female; DLB, Dementia with Lewy bodies; AD, Alzheimer's disease; CBD, Cortiocobasal degeneration; PSP, Progressive supranuclear palsy; PDD, Parkinson's disease dementia; PMD, post mortem delay; N/A, not available.

3.3.2 MRI assessment

Formalin fixed *post mortem* right hemispheres underwent T2-weighted MRI and subsequently WMH were visually rated in frontal, parieto-occipital and temporal deep WM using the ARWMC scale (Wahlund et al., 2001), to generate ARWMC score. Lacunes >5mm of the DGM (Bokura et al., 1998), as described in section

2.9, were also assessed to generate a DGM-MRI score (Figure 3.2).

3.3.3 Neuropathological assessment

Paraffin embedded tissue was used for the histological assessment of SVP: For routine diagnostic histological assessment 6µm tissue sections were cut from diagnostic blocks and for extensive total histological assessment 6µm tissue sections were cut from total blocks and coronal levels shown in Table 2.4. Frontal, temporal, parieto-occipital sections were stained with LFB according to protocol in section 2.12.2, and DGM sections were stained with H&E according to protocol in section 2.12.1. SVP was rated using criteria from Esiri and colleagues (Smallwood et al., 2012), as stated in section 2.14.1, as this criteria was deemed more suitable for larger cohorts, to generate diagnostic WM score (WMs) and total WMs (Figure 3.2).

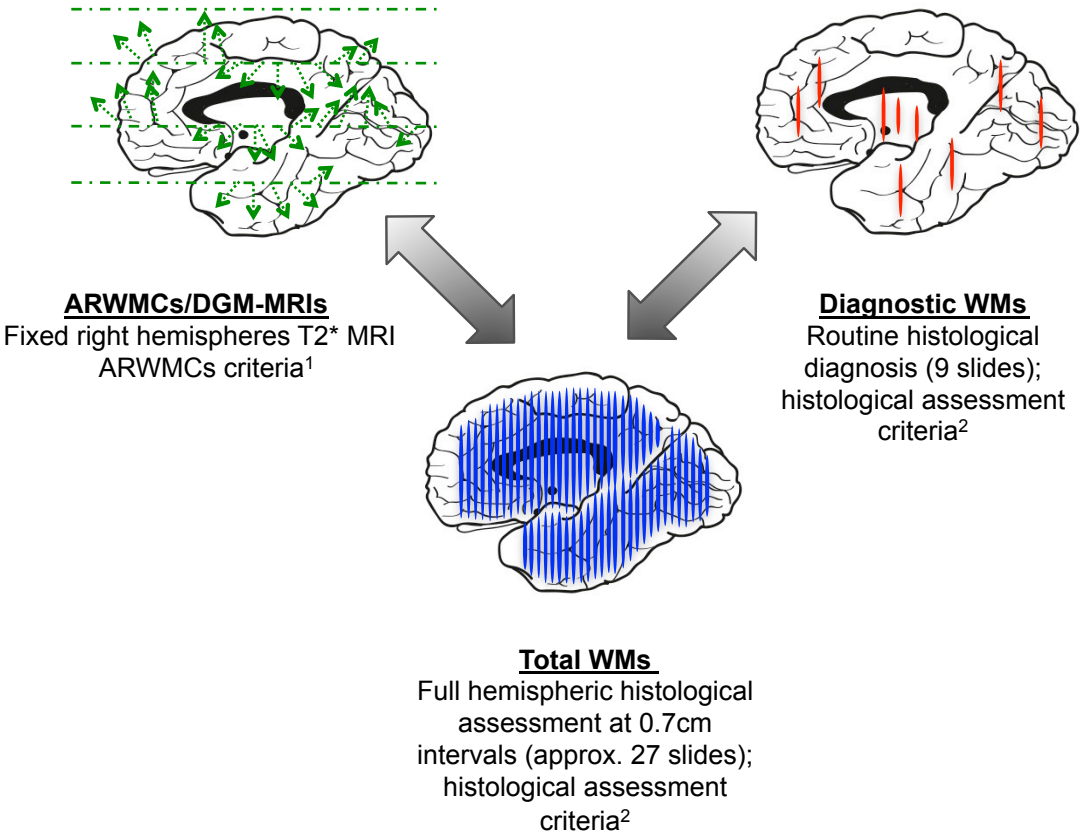

Figure 3.2. Schematic diagram indicating the 3 assessments per case. All brains undergo post mortem T2-weighted MRI and hyperintensities are scored. Dissected brains then underwent routine diagnostic scoring of WML and finally a total hemispheric histological assessment of WML, deemed as the best method of assessment. ARWMC/DGM-MRI scores and diagnostic scores are then compared to total scores. ARWMCs, Age-related white matter change score; DGM-MRIs, deep grey matter MRI score; WMs, white matter score. [1]Wahlund et al., 2001; [2]Smallwood et al., 2012.

3.3.4 Statistical analysis

Data were not normally distributed therefore nonparametric tests were employed; Spearman's rank correlation coefficient was used to correlate total and diagnostic WMs and ARWMC/DGM-MRI scores (ARWMCs/DGM-MRIs), as well as to correlate all scores with subject's age. Significant differences between total *vs.* diagnostic scores and between total score *vs.* ARWMCs/DGM-MRIs were determined using the Wilcoxon rank sum test. The Mann–Whitney *U-test* was employed to test for differences in all assessment scores in demented *vs*. non-demented subgroups and to test for an influence of *post mortem* delay on scores the Kruskall–Wallis test was used. The weighted kappa value was calculated to test for inter-rater reliability.

3.4 Results

One assessor (Kirsty E. McAleese) assessed both diagnostic and total slides to ensure consistency in scoring. To evaluate the reliability of the main assessor's scores, diagnostic scores were provided by four additional assessors (Dr. Jim Neal, Prof. David Mann, Prof. Margaret Esiri and Prof. Johannes Attems) in a subset of 12 cases and compared with the main assessor's scores. No significant differences were seen between all five scores and the weighted kappa value for inter-rater reliability was 0.64 ($P < 0.01$, SE: ± 0.19) indicating substantial agreement. All correlations remained statistically significant when controlling for *post mortem* delay.

3.4.1 White matter scores in frontal, parieto-occipital and temporal lobes

Mean total and diagnostic WM/DGMs and ARWMCs/DGM-MRIs for all individual cases are shown in Table 3.1.

Mean total WMs and ARWMC were highest in the parieto-occipital lobe (total WMs, mean: 1.55, SE:± 0.11; ARWMCs, mean: 1.9, SE: ± 0.14) followed by the frontal lobe (total WMs, mean: 1.47, SE: ± 0.09; ARWMCs, mean: 1.75, SE: ± 0.14). In contrast, mean diagnostic WMs in the frontal lobe were higher than the one observed in the parieto-occipital lobe (frontal, mean: 0.78, SE: ± 0.13; parieto-occipital, mean: 0.69, SE: ± 0.14). No significant differences in the scores between frontal and parieto-occipital lobes were seen. All scores were lowest in the temporal lobe (total WMs, mean: 1.4, SE: ± 0.09; diagnostic WMs, mean: 0.96, SE: ± 0.12; ARWMCs, mean: 0.93, SE: ± 0.15) and both diagnostic

WMs and ARWMCs were significantly lower in the temporal lobe compared with other lobes ($P < 0.01$). *Post mortem* delay had no statistically significant influence on any of the scores ($P > 0.05$).

				Frontal			Parieto-occipital			Temporal			Deep grey matter		
Case number	**Diag.**	**Sex**	**Age**	**TWMLs**	**DWMLs**	**ARWMCs**	**TWMLs**	**DWMLs**	**ARWMCs**	**TWMLs**	**DWMLs**	**ARWMCs**	**TDGMLs**	**DDMLs**	**DGM-MRIs**
1	C	F	96	1.44	2	2	2.3	2	2	2	2	1	2.5	2	0
2	C	M	77	1.55	0	1	1.5	1	1	1.83	N/A	0	1.5	0	0
3	C	F	94	2.8	1	3	3	0	3	3	N/A	2	2.75	1	2
4	C	F	89	1.45	2	3	1.11	2	2	1.17	1	0	1.5	1.5	0
5	C	F	74	0.64	1	2	0.67	0	3	0.57	1	0	1.2	0	1
6	C	F	84	1.26	0	2	1.36	0	2	1.29	0	1	0.75	0.5	0
7	C	F	70	1.28	0	1	1.12	1	2	1	1	1	1.67	0.5	0
8	C	F	81	1.29	2	1	1.25	0	1	1.38	1	0	1.67	0	1
9	C	M	72	0.87	0	1	0.67	0	2	0.63	1	0	0.5	0	0
10	C	F	89	1.75	1.3	2	1.4	1.5	2	1.5	1	2	1.56	1	0
11	C	F	78	0.82	0	2	0.9	0	1	1	0	1	1.2	0	0
12	C	F	95	0.75	1	2	0.8	1	3	0.38	0	1	1.17	1.5	1
13	C	F	98	1.78	1	2	1.85	0	3	1.33	1	1	1.29	0	1
14	C	F	88	2	0	2	2.14	0	1	1.6	1	0	1.89	0	1
Control mean (±SE)	-	M:F 2:12	84.6 (2.5)	1.41 (0.15)	0.81 (0.22)	1.86 (0.18)	1.43 (0.18)	0.61 (0.21)	2 (0.21)	1.33 (0.18)	0.83 (0.17)	0.71 (0.19)	1.51 (0.16)	0.57 (0.19)	0.5 (0.17)
15	AD	F	86	1.4	1	3	1.78	1	3	2	N/A	3	0.43	0.5	1
16	AD	M	88	0.7	0	0	1.4	0	3	0.67	1	0	0.64	0	1
17	AD	F	93	1.27	0	1	1.44	0	1	1.2	1	0	1.17	0	0
18	AD	M	92	1.94	1	1	2	1	2	2.33	2	1	1.76	0.5	0
19	AD	M	78	1.92	2	3	2.67	2	3	2.5	2	3	2.3	1	0
20	AD	F	86	1.67	2	1	1.4	0	0	1	N/A	0	1.22	0.5	0
21	AD	M	85	1.54	1	2	1.45	0	2	1.2	1	1	0.86	0	0
22	AD	M	81	2.13	0	2	1.86	0	2	1.83	1	0	1.33	1	0
23	AD	F	87	2.5	1	3	2.89	0	3	2.25	1	2	1.89	0.5	2
24	AD	M	90	2.31	3	3	2.62	3	3	1.89	2	3	1.56	1	0
25	AD	F	75	0.86	0	1	0.79	0	1	0.8	0	1	1.11	0	0
26	AD	F	86	2.25	0	3	1.9	0	1	1.25	1	1	1.5	0	0
27	AD	F	89	1.33	1	3	2.09	3	3	2.6	3	3	0.6	0.5	0
28	AD	F	81	2.6	1	3	2.88	1	3	2	1	2	2.2	0.5	1
AD mean (±SE)	-	M:F 6:8	85.5 (1.4)	1.74 (0.16)	0.93 (0.25)	2.07 (0.29)	1.94 (0.17)	0.79 (0.3)	2.14 (0.27)	1.68 (0.17)	1.33 (0.22)	1.43 (0.33)	1.33 (0.16)	0.43 (0.1)	0.36 (0.17)
29	DLB	M	72	1.38	0	1	1.5	0	0	1.22	2	0	0.91	0.5	0
30	DLB	M	78	1.47	0	1	1	0	1	1.14	1	1	0.93	0	1
31	DLB	M	77	0.86	0	2	1.42	2	2	1.4	1	1	1.1	0	1
32	DLB	F	81	2.08	0	1	2.29	1	2	2	2	1	1.4	0	0
33	PDD	F	75	1.21	0	1	1.38	0	1	1.25	1	0	1	0	0
34	DLB	F	91	1	2	2	1.38	1	3	0.5	1	1	0.67	0	1
35	DLB	F	73	0.73	1	1	0.57	1	1	0.5	0	0	1	0	0
36	DLB	M	81	0.64	1	2	0.7	1	2	1	1	1	0.82	0	0
LBD mean (±SE)	-	M:F 4:4	78.5 (2.1)	1.17 (0.17)	0.5 (0.27)	1.38 (0.18)	1.28 (0.19)	0.75 (0.25)	1.5 (0.33)	1.13 (0.23)	1.13 (0.23)	0.63 (0.18)	0.98 (0.08)	0.6 (0.6)	0.38 (0.18)
37	CBD	M	68	1.81	1	1	1.7	1	1	1.75	0	0	1.17	1	0
38	PSP	M	90	0.86	0	1	0.5	0	2	0.8	0	0	0.7	0	0
39	PSP	M	78	1.31	1	2	1.3	0	2	1.33	0	1	1.56	1	0
40	PSP	F	83	1.18	1	0	0.91	1	1	1	0	1	1.3	0.5	0
Tauopathies mean (±SE)	-	M:F 3:1	79.8 (4.6)	1.29 (0.2)	0.75 (0.25)	1 (0.41)	1.1 (0.26)	0.5 (0.29)	1.5 (0.29)	1.22 (0.21)	0	0.5 (0.29)	1.18 (0.18)	0.63 (0.24)	0
Total mean (±SE)	All	M:F 15:25	83.2 (1.2)	1.47 (0.09)	0.78 (0.13)	1.75 (0.14)	1.55 (0.11)	0.69 (0.14)	1.9 (0.14)	1.4 (0.09)	0.96 (0.12)	0.93 (0.15)	1.31 (0.09)	0.43 (0.08)	0.38 (0.09)

Table 3.2. Demographic characteristics, mean total scores, mean diagnostic scores, and mean ARMWC/DGM-MRI scores of 40 cases. Diag., clinicopathological diagnosis; TWMLs, total white matter lesion (histological) score; DWMLs, diagnostic white matter lesion (histological) score; ARWMCs, Age-related white matter change (MRI) score; TDGMLs, total grey matter lesion (histological) score; DDGMLs, diagnostic deep grey matter lesion (histological) score; DGM-MRIs, deep grey matter magnetic resonance imaging score; F, female; M, Male; C, control; AD, Alzheimer's disease; DLB, Dementia with Lewy bodies; PDD, Parkinson's disease dementia; LBD, Lewy bodies disease; CBD, corticobasal degeneration; PSP, progressive supranuclear palsy.

3.4.2 Total WMs vs. diagnostic WMs and ARWMCs/DGM-MRIs

Overall WM scores were calculated by adding all mean individual scores from the frontal, parieto-occipital and temporal lobes, with a maximum score of 9. When comparing overall scores no significant difference between overall total WMs (mean: 4.42, SE: ± 0.28) and overall ARWMCs (mean: 4.58, SE: ± 0.36) while overall diagnostic WMs were significantly lower (mean: 2.44, SE: ± 0.33) (Figure 3.3 A)

When restricting analysis to individual lobes, in both frontal and parieto-occipital lobes diagnostic WMs but not ARWMCs were significantly lower than total WMs ($P < 0.01$). In contrast, in the temporal lobe both diagnostic WMs and ARWMC were significantly lower than total WMs ($P < 0.01$) (Figure 3.3 B-D). Significant correlations between total WMs and ARWMCs were seen in the frontal (Rho 0.426, $P < 0.01$), parieto-occipital (Rho 0.455, $P < 0.01$) and temporal (Rho 0.498, $P < 0.01$) lobes. In addition, significant correlations were seen between total WMs and diagnostic WMs in the parieto-occipital (Rho 0.358, $P < 0.05$) and temporal (Rho 0.503, $P < 0.01$), but not in the frontal lobe respectively.

With respect to the DGM, a significant correlation was seen between total DGMs (mean: 1.31, SE: ± 0.09) and diagnostic DGMs (mean: 0.43, SE: ± 0.08; Rho 0.443, $P < 0.01$) but not between total DGMs and DGM-MRIs (mean: 0.38, SE: ± 0.09). However, both diagnostic DGMs and DGM-MRIs were significantly lower than total DGMs ($P < 0.001$) (Figure 3.3 E).

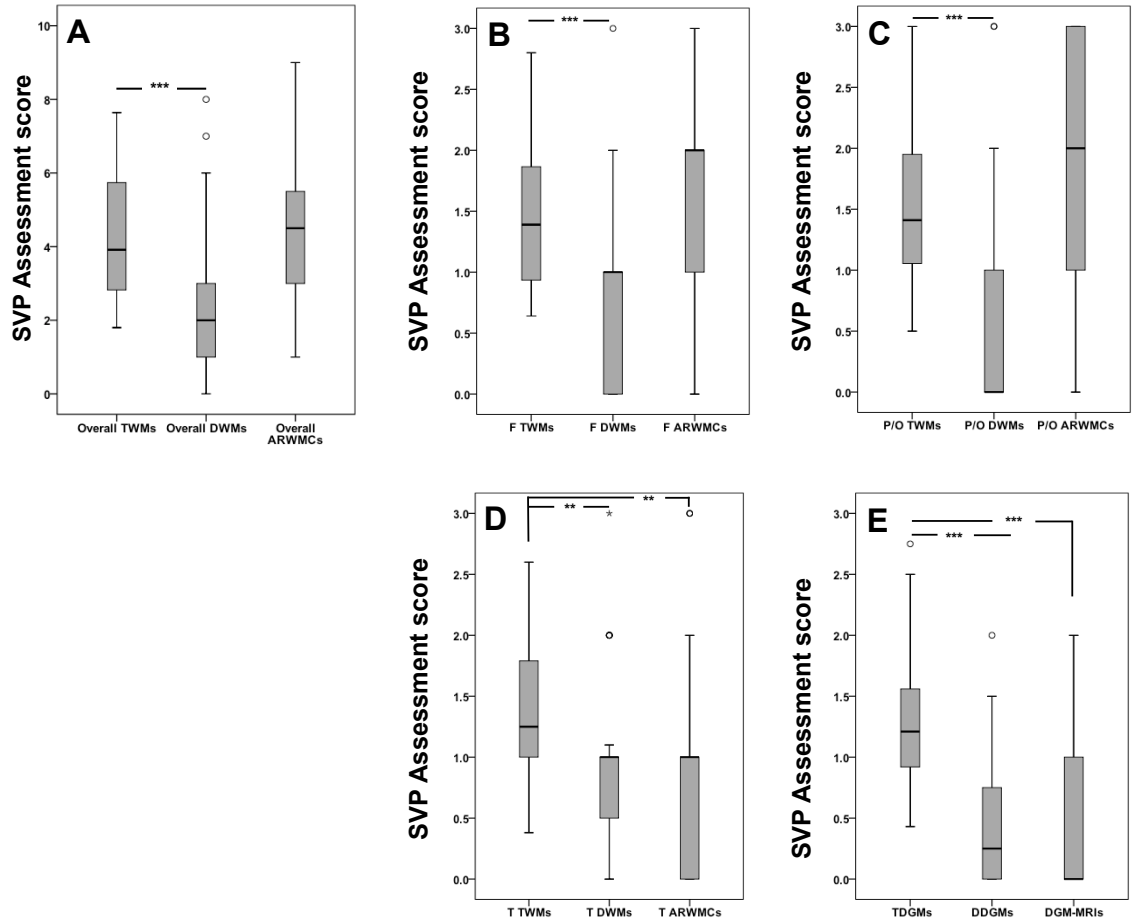

Figure 3.3 A) Mean overall TWMs are significantly higher than overall DWMs, while no significant differences are seen between overall ARWMCs and overall TWMs. B-E) Comparison between assessment scores in individual lobes. Mean TWMs are significantly higher than mean DWMs in all lobes (B, C and D) as are TDGMs compared with both DDGMs and DGM-MRIs (E). No significant differences are seen between TWMs and ARWMCs in both frontal (B) and parieto-occipital (C) lobes, while ARWMCs are significantly lower than TWMs in the temporal lobe (D). **P < 0.01; ***P < 0.001; rings, outliers; asterisks, extreme values. SVP, subcortical vascular pathology; F, frontal; P/O, parieto-occipital; T, temporal; TWMs, total white matter score; DWMs, diagnostic white matter score; TDGM, total deep grey matter; DDGMs, diagnostic deep grey matter score; ARWMCs, Age-related white matter change score; DGM-MRIs, deep grey matter MRI score.

3.4.3 Underrating of diagnostic WMs compared to total WMS and ARWMCs

Figure 3.4 illustrates how diagnostic WMs could have been scored lower than total WMS and ARWMCs.

3.4.4 Influence of SVP severity on assessment

In order to investigate if the severity of SVP i.e. aspects of SVD including PVS enlargement, myelin pallor, parenchymal loosening and lacunes, has an influence on the accuracy of either diagnostic WMs or ARWMCs in reflecting total WMs, the study group was classified into cases with (i) total WMs score 1-2; 'mild to moderate' and (ii) total WMs score 3; 'severe'. 'Mild to moderate' scores were combined to increase statistical power due to small case numbers in the 'mild' group and as the pathological difference between the two grades is slight compared to the 'severe' grade, it was deemed appropriate to combine the two grades. In the 'mild to moderate' subgroup a significant difference was seen in the temporal lobe ($P<0.01$), however, there were no significant differences between total WMs, diagnostic WMs and ARWMCs in the frontal and parieto-occipital lobes. In contrast, diagnostic WMs were significantly lower than total WMs scores in the frontal ($P<0.01$), parieto-occipital ($P<0.001$) and temporal ($P<0.01$) lobes. In the 'severe' subgroup neither diagnostic WMs nor ARWMCs differed significantly from total WMs (Figure 3.5)

3.4.5 Scoring methods and relationship with SVP severity, age and clinicopathological diagnosis

I investigated whether the method of assessment may influence results regarding the relation between the severity of SVP, age and clinicopathological diagnosis. The severity of SVP in the WM in all lobes significantly increased with age when using total WMs and ARWMCs (all $0.338 < Rho < 0.573$; frontal and parieto-occipital, $P < 0.01$; temporal, $P < 0.05$), while such a correlation was seen between age and diagnostic WMs in the frontal lobe only (Rho 0.478, $P < 0.01$). In contrast, diagnostic DGMs but not total DGMs or DGM-MRIs significantly increased with age (Rho 0.416, $P < 0.01$). All scores in WM and DGM were higher in the demented groups (AD, LBD, tauopathies) compared with non-demented (controls) (for mean values see Table 3.1), but these differences were not statistically significant.

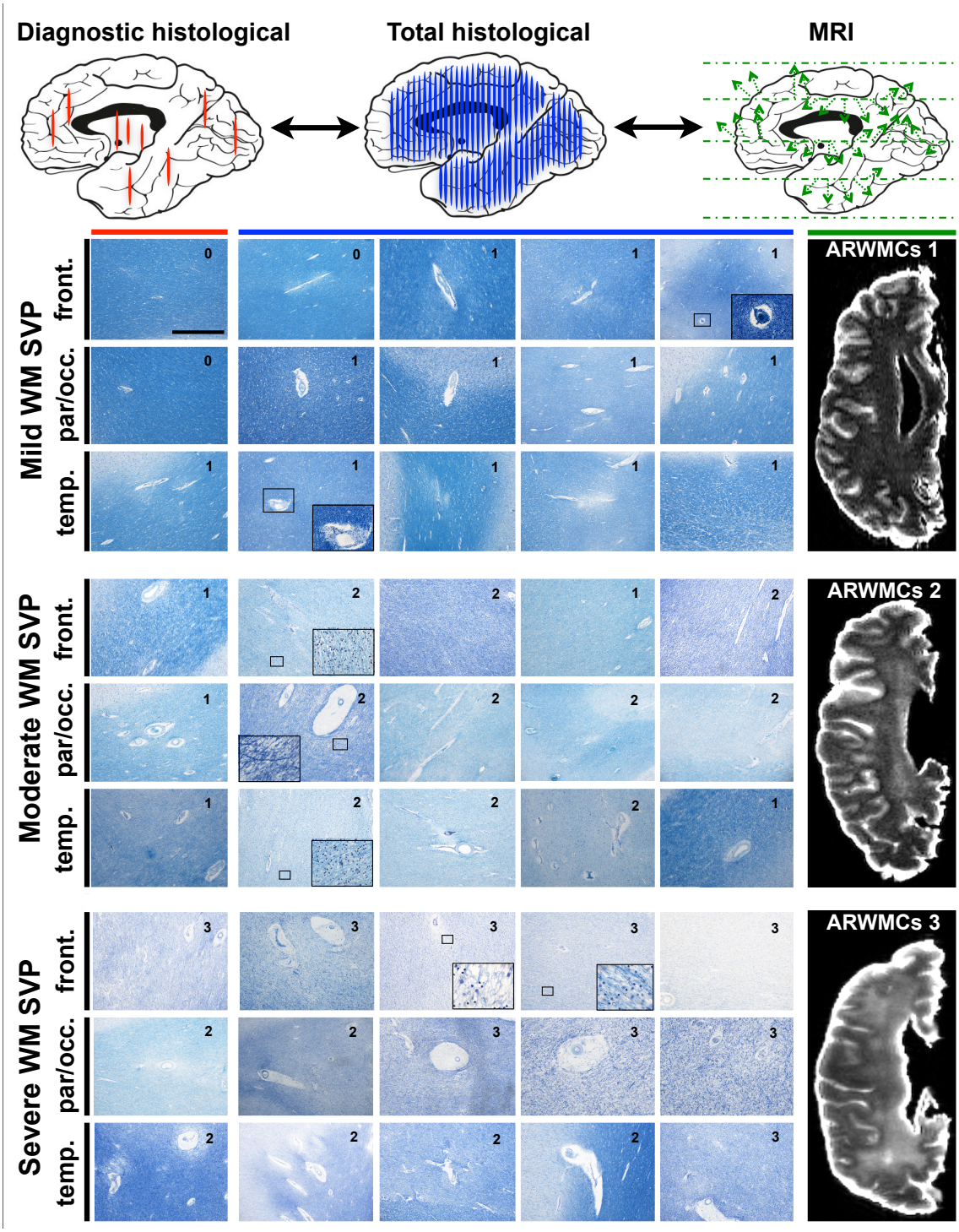
Diagnostic histological
Total histological
MRI
Mild WM SVP
front.
par/occ.
temp.
ARWMCs 1
Moderate WM SVP
front.
par/occ.
temp.
ARWMCs 2
Severe WM SVP
front.
par/occ.
temp.
ARWMCs 3

Figure 3.4. Examples of SVP the deep WM as seen by 3 methods of assessment illustrated as cartoons in the upper row. Red bar indicate columns containing photomicrographs from slides used for diagnostic, blue bars for TWMs and green bars indicate *post mortem* MRI images on a horizontal plane. Mild, moderate and severe subgroups were assigned based on TWMs; photomicrographs and MRI images were taken from one single case for each subgroup. Numbers in the right upper corner of individual photomicrographs indicate the assigned histological score for the pictured slide. Mild SVP of WM (grade 1); DWMs assign a score of 0 in frontal and parieto-occipital lobes, while TWMs indicate a score of 1 for most slides as does the ARWMCs: Moderate SVP of WM (grade 2):DWMs assign a score of 1 in frontal, parieto-occipital and temporal lobes, while TWMs indicate a score of 2 for most slides as does the ARWMCs: Severe SVP of WM (grade 3); a DWMs of 2 is given for parieto-occipital and temporal lobes a score of 3 is given to the majority of slides used for TWMs and are consistent with ARWMCs 3 on MRI images. Histochemistry, Luxol fast blue; scale bar, 1000 mm. WM SVP, white matter subcortical vascular pathology; front., frontal; par/occ, parieto-occipital; temp., temporal; TWMs, total white matter score; DWMs, diagnostic white matter score; ARWMCs, Age-related white matter change score.

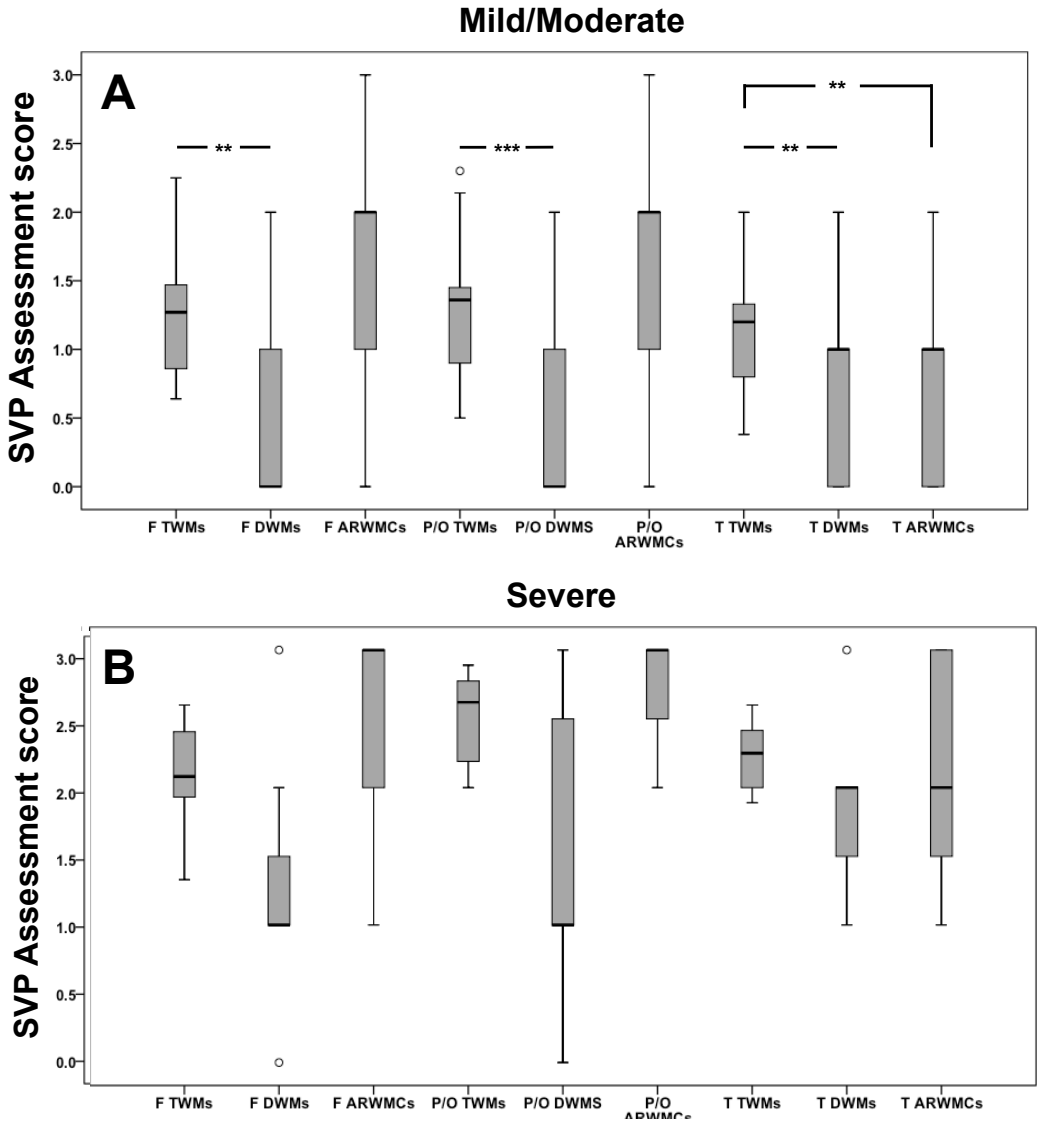

Figure 3.5 Comparison of assessment scores in subgroups with mild to moderate and with severe SVP. In the subgroup mild to moderate (A) DWMs are significant lower compared to TWMs in all lobes, in contrast to ARWMCs do not differ from TWMs in frontal and parieto-occipital lobe. On the other hand in the subgroup severe (B) no significant differences are seen between TWMs, DWMs and ARWMCs. **P < 0.01; ***P < 0.001; rings, outliers. SVP, subcortical vascular pathology; F, frontal; P/O, parieto-occipital; T, temporal; TWMs, total white matter score; DWMs, diagnostic white matter score; ARWMCs, Age-related white matter change score.

3.5 Discussion

3.5.1 MRI on post mortem brains reliably reflects WM SVP

MRI has been shown to detect WMH in *post mortem* brains (De Reuck et al., 2011, Fernando et al., 2004, Munoz et al., 1993), however, these studies focused on the identification of lesions and not whether assessment scores of visually rated MRI images reflected that of neuropathological assessments. This study has demonstrated that T2-weighted MRI, performed on whole fixed *post mortem* brain hemispheres reliably reflects the severity of SVP in the WM of frontal, parietal and occipital lobes as detailed as an extensive histological assessment of the entire WM at 7-mm intervals. In frontal, parietal and occipital lobes and the entire hemisphere no significant differences were seen between total histological WM scores and MRI-based ARWMCs.

3.5.2 Diagnostic histological assessment underrates SVP burden

This study indicated that, in the majority of cases, the severity of SVP is underestimated by diagnostic histological assessment. Diagnostic scores were significantly lower when compared to total histological scores in the frontal, parietal and occipital lobes. In the majority of cases the diagnostic score was 1 grade lower than the mean score of the total slides. This is most likely due to the limited number of slides assessed in diagnostic assessment compared to total histological assessment, which has been highlighted as a hindrance (Alafuzoff et al., 2012, Grinberg, 2013). Furthermore, diagnostic scores were also significantly lower than ARWMC scores; probably due to *post mortem* MRI assessing the entire hemisphere, consequently, less pathology is missed. Although, both total and diagnostic histological scores correlated with each other indicating that statistically the numeric difference between total and diagnostic histological scores remains consistent across cases.

However, when subdividing the study group into cases with either mild-moderate or severe SVP in the WM, based on total histological scores, no significant differences between total and diagnostic histological scores was observed in the severe subgroup. This finding suggests that in particular in the mild and moderate SVP cases the severity of SVP is frequently underestimated possibly due to; i) SVP pathology is more focal in mild/moderate cases and

could be missed if a limited number of slides are investigated; ii) SVP not being a single entity and comprising of heterogenous changes (Grinberg, 2013) of which not all were assessed; iii) variation in histochemical staining which could possible influence the scoring of myelin pallor. In the severe subgroup, SVP is seemingly easy to identify possibly due to the high degree of tissue destruction and therefore also a limited number of slides is sufficient to detect these lesions.

3.5.3 Post mortem MRI is not suitable for temporal lobe assessment

Despite the high accuracy of MRI-based ARWMCs in reflecting SVP in the frontal, parietal and occipital WM, ARWMCs and diagnostic histological scores were significantly lower than total histological scores in the temporal lobe.

There is no clear explanation for the low sensitivity of MRI in the temporal lobe, however, two possible explanations might be; i) the relatively small size of the temporal lobe compared to the other lobes possibly makes it difficult to accurately assess SVP on MRI images and pathology could be missed or misinterpreted as an anomaly due to indistinct cortical-WM borders; ii) a large proportion (35%) of our cohort were AD cases and one of the earliest and most pronounced changes in AD is MTL atrophy (Braak and Braak, 1991). MTL has long been associated as a diagnostic marker of AD and predictor of cognitive decline. Therefore, a substantial proportion of the cohort may have had severe atrophy within the temporal lobe making it difficult to gain an accurate MRI-based assessment. Although MTL atrophy is most severe in AD it is also not uncommon in non-demented elderly (Firbank et al., 2007, van der Flier et al., 2005, Visser et al., 1999). A recent MRI study by Cavallin and colleagues (Cavallin et al., 2012) investigating 544 healthy aged individuals enrolled in the Swedish National study on Ageing and Care, found that 95% of 66 years and over had some level of MTL atrophy, of which severity increased with age. Therefore, atrophy of the temporal lobe may have negatively influenced the accuracy of *post mortem* MRI-based assessment and findings should be interpreted with caution.

3.5.4 Post mortem MRI is not suitable for deep grey matter assessment

Similarly to the temporal lobe, in the DGM both diagnostic histological scores and DGM-MRI scores were significantly lower than total histological scores.

The low accuracy of MRI for the evaluation of lacunes in the DGM of *post mortem* brains is possibly due to the MRI criterion used. The main distinguishing factor between the morphologically similar lacunes and enlarged perivascular spaces (EPVS) (Awad et al., 1986, Chimowitz et al., 1992, Munoz et al., 1993) on MRI is size; only lesions larger than 5 mm (Bokura et al., 1998) were scored due to difficulty in reliably identifying smaller lacunes. Therefore, lacunes with a diameter below 5 mm, which are included and scored in histological assessment, are not scored in MRI assessment and may explain the lack of a statistically significant correlation between total DGMs and DGM-MRIs. Similarly to WM diagnostic histological assessment, limitations in slide number may explain the significantly lower diagnostic score compared to total scores. Previous studies that have compared MRI signals and pathological findings of lacunes to determine the morphological substrates for respective MRI signals (Bokura et al., 1998, Braffman et al., 1988, Matsusue et al., 2006, Pullicino et al., 1995, Revesz et al., 1989). Although the pathogenesis of lacunes still remains to be elucidated, their assumed origin is due to acute arteriole occlusion due to atherosclerosis or SVD. However, there is evidence suggesting that other more gradual pathomechanisms such as chronic hypoxia and blood-brain-barrier breakdown may also play a role in pathogenesis of lacunes (Wardlaw et al., 2003, Challa et al., 1990). Future MRI and histological studies are required to further investigate the pathogenesis and determine a more reliable MRI-based criterion for lacunes.

3.5.5 Statistical findings using post mortem MRI assessment are in agreement with previous studies

Using MRI-based assessment scores this study showed a correlation between age and severity of SVP in the WM and this finding is in agreement with previously published studies demonstrating an increase of SVP (including SVD and WML) with advancing age (Schmidt et al., 2007, Christiansen et al., 1994, de Groot et al., 2001, Grinberg and Thal, 2010, van Dijk et al., 2002). Therefore, I suggest that *post mortem* MRI-based assessment is a good indicator of SVP. Furthermore, total histological scores in the WM also correlated with age; although total histological assessment is unrealistic in a routine setting this indicates that *per se* the criteria used for the assessment of vessel pathology (Smallwood et al., 2012) are adequate for the histological assessment of SVP in

the WM.

In contrast, only diagnostic DGMs increased with age while both total DGM scores and DGM-MRIs failed to do so; total DGM histological scores were significantly higher than diagnostic DGM scores, most likely due to limitations in slide number, so it may be that the higher sensitivity of total DGM histological assessment might cause a ceiling effect that could explain the lack of a statistically significant correlation between total DGMs and age. The lack of correlation between DGM-MRI scores and age might be attributed to the low validity of *post mortem* MRI for the assessment of the DGM as discussed (see: section 3.5.4).

Multiple studies have demonstrated an association between SVP, dementia and Alzheimer's disease (Attems et al., 2008, Burton et al., 2006, Gootjes et al., 2004a, Gorelick et al., 2011, Meier et al., 2012, Thal et al., 2003). Unsurprisingly, all SVP scores were found to be higher in demented subjects compared to the non-demented ones, although differences were not significant. However, I assume that the size of the present study group is too small and the heterogeneity of the pathology too large to draw any conclusions regarding the association between SVP and dementia, especially a mixed cohort of dementias.

3.5.6 Future use of post mortem MRI for the assessment of SVP

It is becoming increasingly clear that the ageing brain is characterized by the presence of multiple pathologies and the prevalence of those increases with age (Jellinger and Attems, 2007, Jellinger and Attems, 2012, Kovacs et al., 2008, Alafuzoff, 2013, Attems and Jellinger, 2013a, Schneider et al., 2007, Jellinger and Attems, 2010b, Jellinger and Attems, 2010a). Therefore, neuropathological assessment of *post mortem* brains is required to demonstrate the wide variety of lesions with high accuracy in a large number of brains. With respect to the assessment of SVP an extensive histological assessment, as performed in the present study, inarguably constitutes the most accurate method. However, as this method would require approximately 30 histological slides per hemisphere it is practically and financially not feasible on the large scale needed to draw conclusions regarding the combined influence of multiple pathologies on the clinical phenotype from clinicopathological correlative

studies, or regarding pathogenic mechanisms from basic molecular research. In order to better understand the contribution of cerebrovascular pathology towards the clinical picture, these findings suggest that MRI-assessment scores of full hemispheres reliably reflect WM SVP scores as detailed as a full histological assessment. Therefore, *post mortem* MRI of fixed brain hemispheres can be used for the neuropathological assessment of WM SVP and *post mortem* MRI images should be rated according to the ARWMC (Wahlund et al., 2001). Of note, these findings do not suggest that MRI should replace histological assessment of the WM; histological assessment in a limited number of slides is paramount for interpretation of MRI findings due to the heterogeneity of SVP. Therefore, one histological slide containing prefrontal, frontal, parietal and occipital WM, respectively, should be neuropathologically assessed possibly using the criteria by Smallwood and colleagues (Smallwood et al., 2012) ideally with the addition of *post mortem* MRI. MRI-assessment failed to reliably reflect the actual amount of SVP in the temporal WM and DGM therefore these regions should be histologically assessed with the inclusion of additional histological slides.

3.5.7 Limitations of the study

A possible limitation in the study is that of variation in staining intensity. The study required the staining of over 2000 histological slides with basic stain LFB, which had to be stained in multiple batches. Although, the majority of staining was performed by one experienced biomedical technician to ensure minimal variation between batches this cannot be guaranteed and variation may have an influence on the histological scoring of myelin pallor.

Another confounding factor is the variation in coronal levels of at which sections were cut, especially in regards to the DGM. The DGM is made up of various nuclei and variation in coronal levels results in different nuclei being sectioned, however, lacunar infarcts are generally found in all major regions of the DGM (Jellinger, 2007, Roman et al., 2002) so potentially had very small influence on DGM scores.

As previously discussed *post mortem* MRI was not suitable for the assessment of SVP in the temporal lobe due to possible influence of MTL atrophy (section 3.5.3) and lacunes of the DGM (section 3.5.4). Another imitating factor due to

the MRI criterion is that it the parietal and occipital lobes are scored together (as stated by Wahlund et al., 2001). The exact reason for this is unclear but it may be due to:

I. The small size of the occipital lobe makes assessment difficult and reduces reliability of scoring.
II. The occipital lobe shares some vascular territory with the parietal lobe, and doesn't have clear lateral anatomical boundaries between it and the parietal lobe.
III. The ARWMC criterion is used in studies of all ages; in normal young people, the ventricles don't extend into the occipital lobe, whereas in older people ventricular enlargement is frequently seen and since white matter hyperintensities commonly occur in the periventricular region, it's more consistent to have a parieto-occipital region, rather than trying to somewhat arbitrarily decide if the WMH are in one or the other (Firbank, 2014).

In order to keep histological and MRI-based assessments consistent and comparable, histological parietal and occipital sores were combined to yield a parieto-occipital score. In future studies this should be addressed so that a more detailed insight into each separate lobe can be sought.

3.5.8 Conclusions

This study demonstrated that visual MRI-based assessment on fixed *post mortem* brains is a practical method that reliably reflects SVP in the frontal, parietal and occipital WM that is comparable with histological scores that were based on extensive histological assessment of the entire WM at 7-mm intervals. Therefore, *post mortem* MRI may be used assess white matter integrity for research purposes. These results also indicate that *post mortem* MRI is not helpful for the assessment of SVP in the DGM (at least in *post mortem* brains). *Post mortem* MRI may be used for the gross assessment of temporal white matter, but interpretation should be approached with caution with perhaps additional histological slides assessed.

Furthermore, current routine diagnostic histological assessment of SVP, using a limited number of slides, underrates the severity of SVP in the WM, therefore,

MRI on fixed *post mortem* brains should complement routine neuropathological diagnosis if a reliable evaluation of SVP of the WM is required.

Chapter 4 - Quantitative neuropathological assessment of cortical and vascular neurodegenerative lesions.

4.1 Introduction

The previous chapter described how MRI of fixed *post mortem* brains and the application of validated rating scales can improve and standardize the assessment of SVP. This chapter describes how quantification of cortical neuropathologies and SVD allows for a more accurate and objective measurements of pathological burden, which is required for the investigation of multiple pathologies in the ageing human brain.

4.1.1 Semi-quantitative vs. Quantitative

Standardized neuropathological criteria is available for the assessment of neurodegenerative hallmark pathologies i.e. NFT, NT, Aβ plaques and LB (Braak et al., 2006, Braak et al., 2003, McKeith et al., 2005, Thal et al., 2002b). Currently neuropathological assessment is based on semi-quantitative scoring, of which there are assigned grades of pathology, usually on a four-tiered scale i.e. 0, 'absent'; 1, 'sparse'; 2, 'moderate'; 3, 'severe', that allow for the classification and staging of neurodegenerative disorders. However, semi-quantitative assessment may be influenced by assessor bias and consequently high inter-rater-reliability (Armstrong, 2003), particularly when assessing 'sparse' and moderate' grades of pathology that can vary between cases (Alafuzoff et al., 2008b).

On the other hand, quantitative measure of neuropathological lesions allows for more accurate and objective assessment. The use of quantitative methods has become an increasingly important aspect in neuropathology due to technological advances in image analysis systems enabling valid quantification of pathological severity that is reproducible between raters (Armstrong, 2000, Armstrong, 2003, Armstrong et al., 2012). The use of semi-quantitative scoring creates a 'ceiling effect' were the range of data is constrained by the limits of the criteria i.e. the highest score is 'severe' although the amount of pathology within a 'severe' grade has been shown to differ by up to 100% (Attems and Jellinger, 2013a). No 'ceiling effect' is present in quantitative assessment as

cases are measured as continuous data. Furthermore, quantitative assessment, unlike semi-quantitative assessment, is capable of detecting subtle variations in the amount of pathology that is required when investigating the relationship of multiple pathologies in the human brain. The use of quantitative neuropathological assessment has revealed new findings about the impact of pathologies on the clinical status including limbic predominate and hippocampal sparing subtypes of AD (Murray et al., 2011a) and a previously undiscovered correlation between neocortical amyloid-β pathology the presence of clinical dementia (Robinson et al., 2011). VP has also previously been quantified. SI (Lammie et al., 1997, Low et al., 2007) can be used as a quantitative measure of SVD (Craggs et al., 2013a, Craggs et al., 2013b, Yamamoto et al., 2009) which has revealed differences in vascular degeneration in various types of hereditary SVD (Craggs et al., 2013a).

4.2 Aim

To compare semi-quantitative and quantitative assessment of HPT and Aβ pathology and vascular fibrosis, as a measure of SVD, of the WM arteries/arterioles in demented and non-demented aged *post mortem* brains.

4.3 Materials and methods

4.3.1 Case selection

For the evaluation of cortical pathologies 10 AD cases were selected from the cohort used for the investigations described in Chapter 3 (Table 3.1) mean age 84 ± 6.13 years, 50% female. All cases were neuropathological diagnosed as Braak stage VI; Thal Aβ phase 5; NIA-AA A3, B3, C2/3; high AD neuropathological change.

For the measurements of WM vessels 23 cases were randomly selected from the cohort used for the investigations described in Chapter 3 (Table 3.1) 9 non-demented and 15 demented individuals (7 AD, 3 DLB, 1 PDD, 2 PSP and 1 CBD); mean age 84.17 ± 8.4, 61% female (Table 4.1).

Case n	sex	age	Disease status	PMD (hours)	Braak stage	CERAD score	LB Braak	Pathological assessment
20	F	86	AD	69	6	3	0	Cortical
22	F	93	AD	15	6	3	0	Cortical
23	M	92	AD	59	6	3	0	Cortical
24	M	78	AD	37	6	3	0	Cortical
25	F	86	AD	47	6	3	0	Cortical
26	M	85	AD	29	6	3	0	Cortical
27	F	87	AD	54	6	3	0	Cortical
30	M	90	AD	69	6	3	0	Cortical
31	F	75	AD	33	6	3	0	Cortical
33	F	89	AD	85	6	3	2	Cortical
1	F	96	Normal Aged	95	3	0	0	Sclerotic Index
2	M	77	Normal Aged	83	2	0	0	Sclerotic Index
4	F	94	Normal Aged	82	2	0	0	Sclerotic Index
5	F	98	Normal Aged	17	3	1	0	Sclerotic Index
8	F	70	Normal Aged	72	0	0	2	Sclerotic Index
12	F	95	Normal Aged	36	3	0	0	Sclerotic Index
13	F	89	Normal Aged	49	3	0	3	Sclerotic Index
14	M	72	Normal Aged	39	1	1	0	Sclerotic Index
19	F	88	Normal Aged	22	3	0	0	Sclerotic Index
20	F	86	AD	69	6	3	0	Sclerotic Index
24	M	78	AD	37	6	3	0	Sclerotic Index
25	F	86	AD	47	6	3	0	Sclerotic Index
26	M	85	AD	29	6	3	0	Sclerotic Index
30	M	90	AD	69	6	3	0	Sclerotic Index
32	F	86	AD	5	6	3	0	Sclerotic Index
33	F	89	AD	85	6	3	2	Sclerotic Index
49	F	81	DLB	44	4	2	6	Sclerotic Index
50	F	91	DLB	10	3	2	6	Sclerotic Index
52	M	81	DLB	81	3	2	6	Sclerotic Index
53	F	75	PDD	18	3	2	6	Sclerotic Index
54	M	68	CBD	9	2	0	0	Sclerotic Index
55	F	83	PSP	65	N/A	N/A	N/A	Sclerotic Index
57	M	78	PSP	53	N/A	N/A	N/A	Sclerotic Index

Table 4.1. Subject demographics. Case n refers to master demographic Table 2.2. N, number; M, male; F, female; DLB, Dementia with Lewy bodies; AD, Alzheimer's disease; CBD, Cortiocobasal degeneration; PSP, Progressive supranuclear palsy; PDD, Parkinson's disease dementia; PMD, post mortem delay; N/A, not available.

4.3.2 Quantitative assessment of cortical pathology

In the AD cohort 6µm tissue sections from blocks A, B, E (frontal), I (temporal), K (parietal) and L (occipital) (see section 2.15.1) were stained with immunohistochemistry for HPT (AT8) and Aβ (4G8) according to protocol described in section 2.12.1.

On tissue sections three sulcal and three gyral cortical regions were identified. At x200 magnification photomicroimages of cortical strips were captured using a Nikon Eclipse 90i microscope coupled with NIS-Elements AR3.2 software. Percentage binary area fraction of immunopositivity (%BF) was calculated from three sulcal and three gyral measurements as described in section 2.15.1.

4.3.3 WM artery/arteriole fibrosis assessments

In the SVD cohort 6µm tissue sections from blocks A, B (frontal), I (temporal), K

(parietal) and L (occipital) were histologically stained with H&E according to protocol described in section 2.12.1.

Arteries and arterioles underwent semi-quantitative assessment using the criteria (Esiri et al., 2011) described in section 2.14.2. The same vessels had photomicroimages taken at x200 magnification using a Nikon Eclipse 90i microscope. SI was calculated using VasCal software program according to protocol in section 2.15.3. A mean value was calculated for frontal, temporal and parieto-occipital lobes (parietal and occipital scores were combined due to data being used in future studies that required a combined value). SI values were converted into a four-tiered scale, as shown in section 2.15.3, to allow Mann-Whitney U-test analysis between semi-quantitative and SI scores.

4.3.4 Statistical analysis

Data were not normally distributed therefore non-parametric tests were employed; significant differences between regional AT8 and 4G8 %BF and semi-quantitative SVD scores and SI scores were determined using the Mann–Whitney U-test and Spearman's correlation was employed to correlate semi-quantitative SVD scores and SI scores.

4.4 Results

4.4.1 Quantitative measurements of cortical pathology in Alzheimer's disease

AD cases were semi-quantitatively assessed as exhibiting 'severe' pathology in the neocortex i.e. Braak stage VI and Thal Aβ phase 5. The regional ranges of AT8 and 4G8 %BF are shown in Table 4.1.

Frontal, temporal, parietal and occipital AT8 and 4G8 immunopositivity values were plotted for each case to reveal the variations in the amount of pathology within the 'severe' grade (Figure 4.1). Overall AT8 %BF (mean 19.92 ± 14.98) was generally higher than overall 4G8 %BF (mean 14.25 ± 9.15), although this was not found to be significant. Scatter plots revealed that case 2 contained the highest and case 4 and 10 the lowest amounts of both AT8 and 4G8 % BF of all the cases.

AT8 %BF data points showed a large spread with the majority of data points concentrated between 3-45% immunopositivity. Upon observation, temporal AT8 % BF (mean 22.5 ± 18.22) was higher than frontal (mean 17.27 ± 12.38),

parietal (mean 16.9 ± 15.45) and occipital (mean 16.24 ± 13.24) cortices in 70% of cases. Mann-Whitney U-test confirmed that temporal AT8 % BF was significantly higher compared to frontal ($P<0.05$), parietal ($P<0.05$) and occipital ($P<0.05$). In the frontal, parietal and occipital lobes the AT8 %BF was more consistent with no significant differences between regions.

4G8 %BF data points exhibited a smaller spread than AT8 %BF with the majority of data points concentrated between 5-25% immunopositivity. Upon observation, frontal 4G8 %BF (mean 18.49 ± 14.36) was higher than temporal (mean 16.36 ± 10.45), parietal (mean 13.27 ± 8.12) and occipital (mean 12.01 ± 6.66) cortices in 60% of cases, although Mann-Whitney U-test found no significant differences between regions.

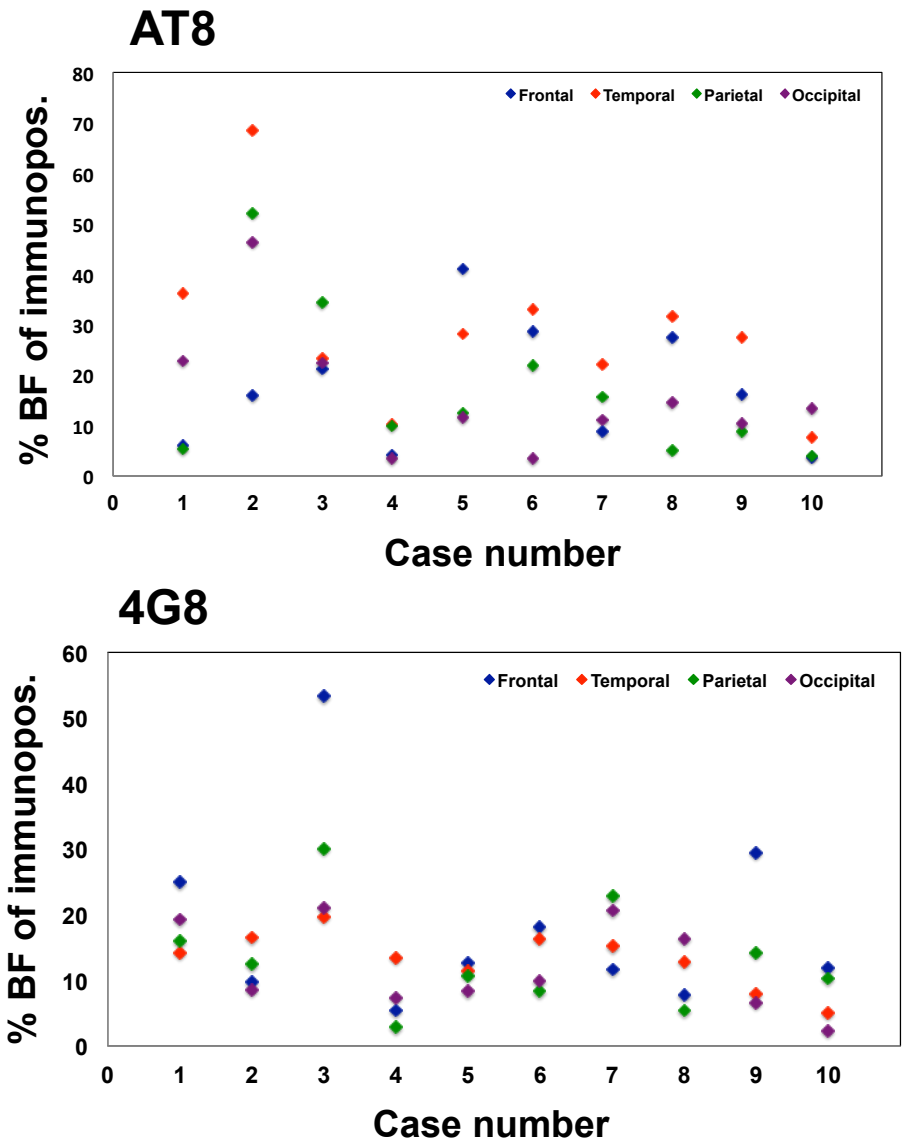

Figure 4.1. Scatter plots demonstrating the variation of AT8 and 4G8 %BF within the 'severe' semi-quantitative grade of 10 AD cases all neuropathological diagnosed as NIA-AA A3, B3, C2/3: % BF of immunopos., percentage binary area fraction of immunopositivity.

		Frontal	Temporal	Parietal	Occipital
AT8 (%)	Range	3.59 - 41.13	7.54 -68.38	3.98 - 52.13	3.44 - 46.38
	Mean	17.27	28.82	16.96	14.61
4G8 (%)	Range	5.41 - 53.23	4.95 - 19.75	2.8 - 29.96	2.33 - 20.95
	Mean	18.49	13.23	13.27	12.01

Table 4.2. Range and mean %BF values for AT8 and 4G8 in various brain regions of 10 AD cases.

4.4.2 Quantitative measurements of vascular fibrosis of WM arteries and arterioles

Quantified SI values were plotted against semi-quantitative SVD values to reveal the variation of pathology burden within each grade (Figure 4.2).

No significant correlation was seen between semi-quantitative SVD scores and SI scores in any region.

In frontal WM no vessels were semi-quantitatively graded as 0. Grade 1 mean SI value was 0.32 ± 0.044 with a range of 0.23-0.38, and grade 2 mean SI value was 0.37 ± 0.044 with a range of 0.32-0.42. Only one cases was graded 3 with an SI measurement of 0.36. In temporal WM no vessels were semi-quantitatively graded as 0 or 3. Grade 1 mean SI value was 0.31 ± 0.041 with a range of 0.23-0.4 and grade 2 mean SI value was 0.34 ± 0.035 with a range of 0.3-0.4. In pariteo-occipital WM no vessels were semi-quantitatively graded as 0 or 3. Grade 1 mean SI value was 0.34 ± 0.048 with a range of 0.24-0.43 and grade 2 mean SI value was 0.37 ± 0.056 with a range of 0.35-0.46.

Mann-Whitney U-test revealed SI values converted to a semi-quantitative scale were significantly lower than semi-quantitative values in the frontal ($P<0.01$), temporal ($P<0.01$) and parieto-occipital ($P<0.05$) regions.

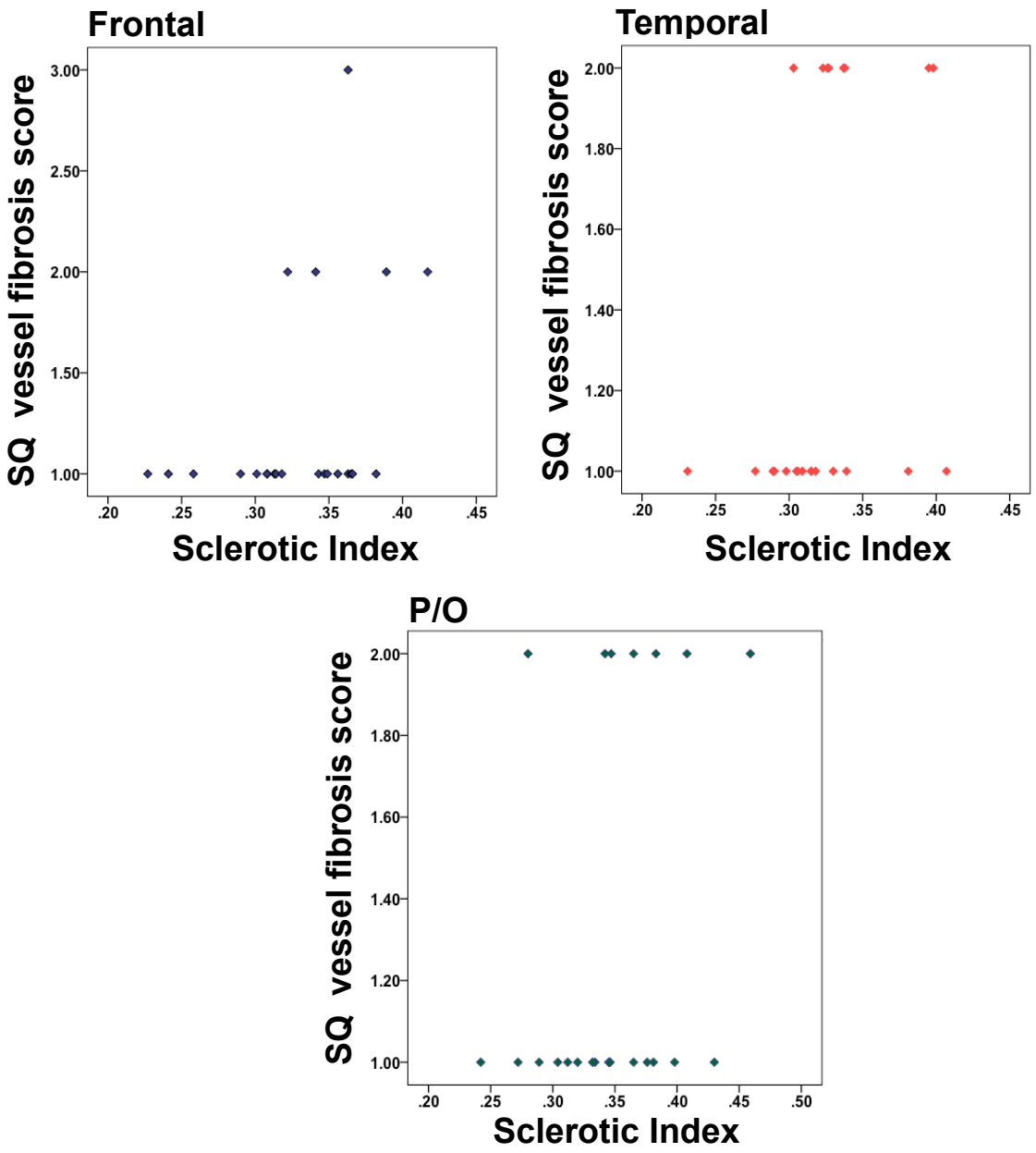

Figure 4.2. Scatter plots demonstrating the variation of SI values within semi-quantitative grades 0-3.

4.5 Discussion

4.5.1 Amounts of HPT differ within semi-quantitative 'severe' category

All AD cases were neuropathologically diagnosed as Braak stage VI and Thal Aβ phase 5 therefore exhibited 'severe' pathology in all neocortical regions i.e. frontal, temporal, parietal and occipital cortices.

Despite all cases presenting semi-quantitatively as 'severe' quantification of cortical HPT and Aβ revealed variations in pathology amount between cases in all regions e.g. case 4 exhibited overall 5.4% immunopositivity for HPT compared to 53.2% in case 3, agreeing with the work from Attems and Jellinger that found up a 100% difference in HPT between cases (Attems and Jellinger, 2013a). Although the differences in quantitative measurements are large they would not be appreciated (in the majority of cases) using the current semi-quantitative scoring method. Photomicroimages of AT8 immunohistochemistry (Figure 4.3) illustrates the differences in pathology amount between cases only detectable by quantitative assessment.

Additionally, HPT was found to be significantly higher in the temporal cortex compared to the frontal, parietal and occipital cortices. Although this is not unexpected as the temporal cortex is affected early and severely in AD (Braak and Braak, 1991) this difference would not have been seen without the use of quantitative measures.

Semi-quantitative scoring produces ordinal data, unlike quantitative assessment that yields continuous data which i) allow for the use of statistically powerful parametric tests, ii) remove the 'ceiling effect' as data is not constrained by the limits of the criteria. The combined use of quantitative neuropathology and more powerful statistics may help elucidate the impact of pathologies on the clinical syndrome. Two recent neuropathological studies have demonstrated the impact of quantitative neuropathology on neurodegenerative disease; Armstrong and colleagues (Armstrong et al., 2012) used quantitative assessment to characterize neuropathological lesions of FTLD with TDP43 pathology and revealed quantitative pathological differences in regional distributions, between familial and sporadic cases and different subtypes. Murray and colleagues (Murray et al., 2011a) quantitatively assessed HPT pathology in a large cohort of 889 post mortem brains and discovered subtypes of AD i.e. typical AD,

hippocampal sparing and limbic predominant, which differed in their clinical presentations, age of onset, disease duration and rate of cognitive decline.

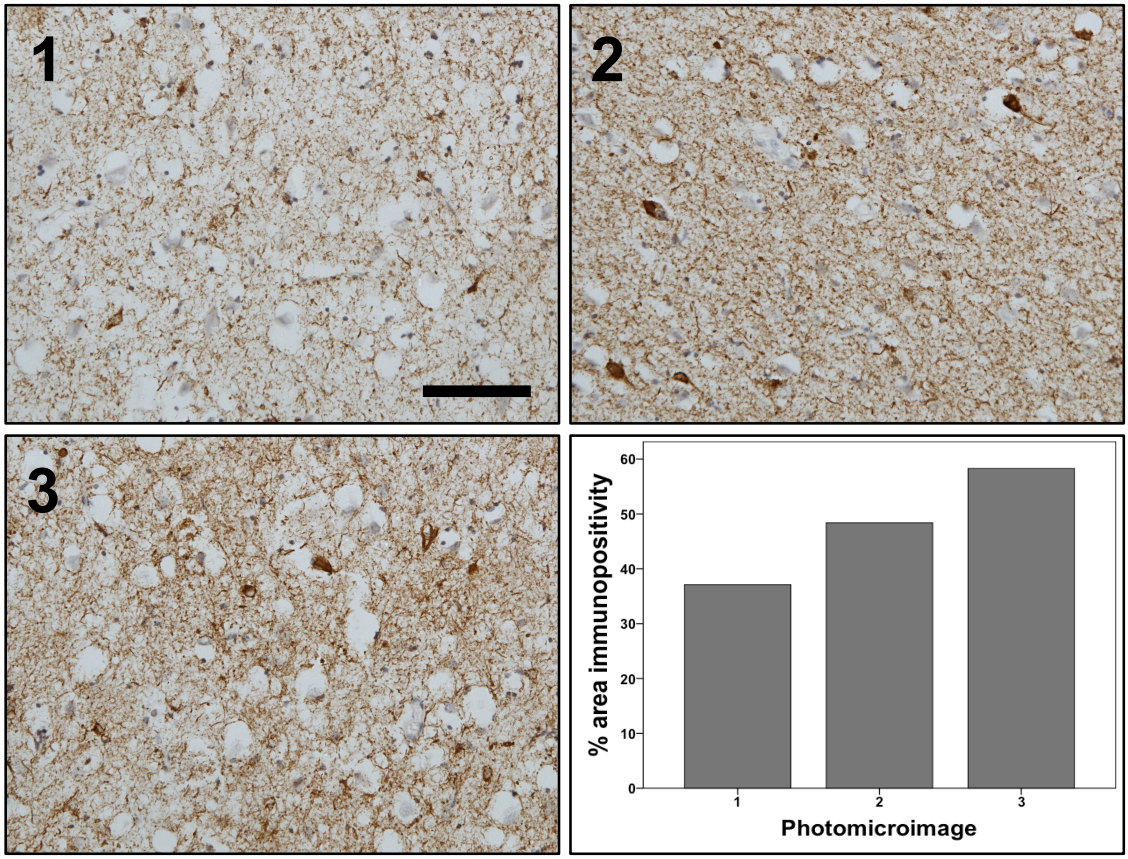

Figure 4.3. Example of quantitative assessment of HPT pathology on immunohistochemically stained slides. 1, 2 and 3 are photomicrographs of 3 separate temporal cortices. By standardized assessment all 3 would be graded as 'severe'. However, assessment of the total % area covered by immunohistochemically positive structures reveals considerable differences. These subtle differences can only be observed using a quantitative method of assessment. Immunohistochemistry; AT8; Scale bar, 50 μ m.

4.5.2 Severity of vessel wall fibrosis differs within each mild and moderate category of SVD severity

WM arteries and arterioles from 23 non-demented and demented brains underwent semi-quantitative assessment based on four-tiered scale criteria (Esiri et al., 2011) as well as quantitative assessment, using SI values (Lammie et al., 1997, Yamamoto et al., 2009) for vessel wall fibrosis as a measure of SVD. It is important to note that the SI measurement is exclusive for vessel wall thickness that is assumed to be the result of vascular fibrosis and/or hyalinosis, which is only one aspect of SVD. This measurement did not take into account the other important aspects of SVD including SMC loss, BBB and plasma

protein leakage. Additionally, a limitation of the cohort measured was that only one case was semi-quantitatively assessed as a grade 3, consequently, only one SI value for a grade 3 is unavailable. This may limit the ability to identify severe SVD as a cause of WMH when using SI assessment.

As semi-quantitative grades increased SI mean values also increased in all three regions, although no significant correlations were seen. Observation in the frontal lobe showed that there was general increasing of SI values in conjunction to increasing semi-quantitative grades. However, one cases was scored grade 3 ('severe') yet the SI measurement was lower than SI values in grades 1 and 2. Additionally, in the temporal and parieto-occipital WM large overlaps of SI values were observed between grades 1 and 2, with nearly all cases in each region overlapping. These observations indicate a lack of accuracy in semi-quantitative assessment. The overlaps of SI measurements within grades 1 and 2 may indicate widespread variation of pathology that can not be assessed by subjective methods. Fibrosis of the vessel walls is a chronic process with some vascular branches being affected more severely than others therefore, tissue section may exhibit varying degrees of pathology that range from 'absent' to 'severe'.

Converted SI values (<0.29 normal vessel; >0.3-<0.39 'mild'; >0.4-0.49 'moderate', >0.5 'severe' (Lammie et al., 1997)) were shown to be significantly lower than semi-quantitative scores. It is feasible that, due to variation of vascular fibrosis on the tissue section, the assessors may have been inadvertently influenced to score higher by the observation of severe degrees of vascular fibrosis. Whereas quantitative SI assessment measured the same vessels objectively, eliminating assessor bias.

Using quantitative assessment allows the identification of particular cases or sub-groups that have certain levels of pathology, which may have important phenotypical and/or clinical relevance. A recent study by Craggs and colleagues (Craggs et al., 2013a) used SI to investigate vascular changes of the frontal lobe and basal ganglia in familial and sporadic SVD disease cases and revealed quantitative pathological differences in vascular fibrosis between the different disease groups.

4.5.3 Quantification of MR images

This study also attempted to quantify *post mortem* T2 MR images. This was attempted using a software program called 'Sibyl' created by Dr M. Firbank, a

neuroimaging expert at Newcastle University. ‘Sibyl’ measures the percentage area of the WMH on each MR image slice based on pixel count with a subjective grey scale threshold set by the user. However, this assessment was unsuccessful due to poor resolution of the MR images making it very difficult to determine WMH and to distinguish between cortical and regional boarders and the process was very time consuming. The existing *post mortem* MR images were unable to be analyzed for WMH volume by existing software programs due the image acquisition that was used.

4.5.4 Limitations

The main limiting factor of this study was the relatively small cohort size, specifically regarding severe SVD cases, due to time constraints. The spread of quantitative data indicated that in future studies larger cohort sizes would be required to elucidate statistically significant findings, particularly when investigating numerous pathologies and their impacts.

4.6 Conclusions

By using digital quantitative neuropathological assessment this study revealed widespread variation in HPT and Aβ pathology and vascular fibrosis within a given semi-quantitative grade. Subtle differences in pathology amounts, that potentially have clinico-pathological relevance, are not appreciated using routine semi-quantitative scoring method and only detectable by quantitative assessment.

Chapter 5 - White matter hyperintensities of the parieto-occipital white matter are present in the absence of small vessel disease: potential association with cortical AD-related pathologies?

5.1 Introduction

The previous chapter described how quantitative measurement of cortical and vascular pathologies is a more accurate and objective measure of pathological burden as it can detect subtle variations in pathologies within a standard semi-quantitative grade.

During the assessment process of the studies described in Chapters 3 and 4 an observation was made when comparing semi-quantitative vessel scores with MRI-based ARWMC scores; a subgroup of eight control and AD brains contained ‘severe’ (grade 3) ARWMC scores in the parieto-occipital region but had ‘mild’ (grade 1) SVD scores (Figure 5.1). Due to the large difference in VP and ARWMC scores this suggested that SVD might not have been the primary cause of WMH in those cases.

5.1.1 Axonal degeneration secondary to neuronal loss

SVD plays a vital role in the pathogenesis of WML (Grinberg and Thal, 2010, Pantoni, 2010, Pantoni and Garcia, 1997), however, it has been suggested that axonal degeneration can result as a secondary consequence of degenerative neuronal and axonal loss associated with AD-related pathologies. Leys and colleagues (Leys et al., 1991) first described this in an AD case that presented with leukoaraiosis (with no predisposing risk factors e.g. hypertension, diabetes) but only mild hyaline thickening (presumably as a result of SVD) of the blood vessel walls. Furthermore, WM changes were more severe in the WM close to cortical areas with a high density of NFT, indicating leukoaraiosis may have been a secondary consequence of neuronal loss due NFT. Another neuropathological study by Professor Englund found that of 60 AD cases examined, 13 contained WM changes of the temporal lobes thought to be caused by Wallerian degeneration of the axon and not related to angiopathy (Englund, 1998). It is well established that the temporal cortex, which includes

the entorhinal cortex, parahippocampus and hippocampus, is affected by HPT pathology early and severely in AD (Braak and Braak, 1991) and less severely in up to 65% of non-demented aged individuals (Alafuzoff, 2013). Furthermore, multiple neurodegenerative pathologies can be found in brains of both demented and non-demented subjects (Alafuzoff, 2013, Attems and Jellinger, 2013a) with over 65% of LBD cases and over 85% of VaD cases exhibiting HPT pathology (Kovacs et al., 2008). Therefore, the effects of cortical HPT pathology on WM changes may not be exclusive to AD but also be present in other neurodegenerative disease groups and non-demented individuals.

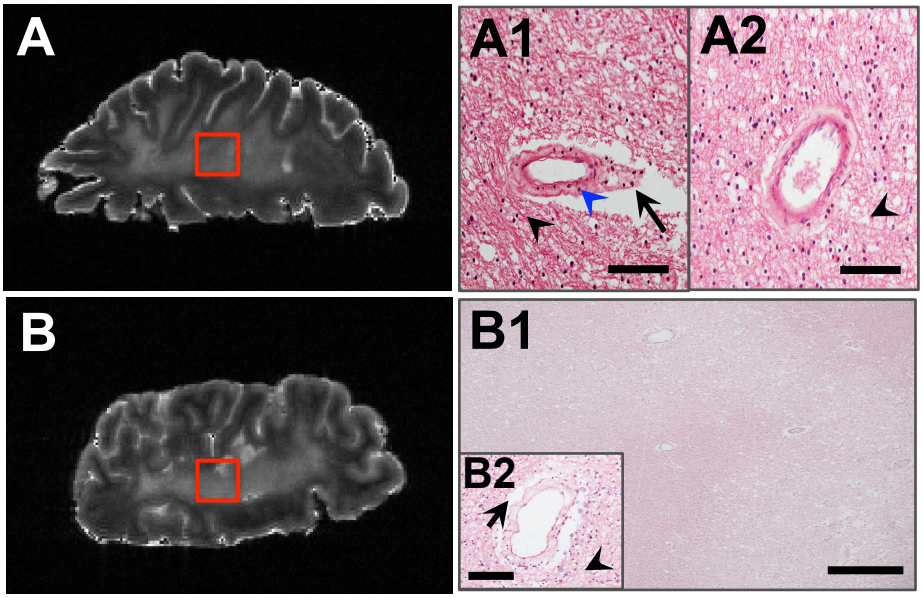

Figure 5.1. *Post mortem* MRI images of confluent WMH and with corresponding absent/mild fibrosis of vessel walls in occipital lobe in an aged control (A) and AD (B) brain. Red boxes indicate location of vessel microimages. A1) mild enlargement of the PVS (black arrow) with very mild fibrosis of the vessel walls (blue arrow head) WM has a 'bubble-like' appearance with severe loss of axons with individual fibres visible (black arrow head); A2) no PVS enlargement and normal arteriole walls, white matter has a 'bubble-like' appearance (black arrow head); B1) Widespread pallor of occipital WM; B2) mild enlargement of the PVS (black arrow) no fibrosis of the vessel walls, white severe loss of axons and individual axons visible (black arrow head); WMH, white matter hyperintensity; AD, Alzheimer's disease; PVS, perivascular space; WM, white matter. MRI images were taken with a T2-weighted vertical 4.7 T scanner, horizontal plane; occipital cortex, right hemisphere; Histochemistry; haematoxylin & eosin and. Scale bars: A1, B2, 50 μm; A2, 100 μm; B1, 500 μm.

5.2 Aims

I aimed to explore whether there is a possible association of cortical AD-related pathology on WM integrity in a cohort of AD and control human *post mortem* brains.

5.3 Methods

5.3.1 MRI assessment

All formalin fixed *post mortem* right hemispheres underwent T2-weighted MRI and subsequently WMH were visual rated in frontal, parieto-occipital and temporal deep WM using the ARWMC scale (Wahlund et al., 2001), to generate ARWMC score as described in section 2.9.

5.3.2 WM artery/arteriole fibrosis assessment

6μm tissue sections from blocks A, B (frontal), I (temporal), K (parietal) and L (occipital) were histologically stained with H&E according to protocol described in section 2.12.1, and were assessed using semi-quantitative criteria (Esiri et al., 2011) according to protocol described in section 2.14.2.

5.3.3 Case selection

MRI-based ARWMC (Wahlund et al., 2001) and WM artery/arteriole fibrosis (as a measure of SVD) criteria (Esiri et al., 2011) were both based on a four-tier semi-quantitative scale i.e. absent, mild, moderate, severe. Cases were selected on the basis of a difference of ≤ 1.5 between parieto-occipital ARWMC scores and parieto-occipital SVD scores. The study cohort consisted of 8 *post mortem* brains (4 aged controls, 4 AD), mean age 86.5 ± 8.42 years, 75% female.

5.3.4 Histology and IHC

6μm tissue sections from blocks A, B, E (frontal), I (temporal), K (parietal) and L (occipital) (see section 2.15.1) were stained with immunohistochemistry for HPT (AT8) and Aβ (4G8) according to the protocol described in section 2.12.3.

5.3.5 Quantitative assessment of cortical pathology

On tissue sections 3 sulcal and 3 gyral cortical regions were identified. At x200 magnification a photomicroimage of cortical strip was captured using a Nikon Eclipse 90i microscope coupled with NIS-Elements AR3.2 software and percentage binary area fraction of immunopositivity (%BF) per cortical stripe

was calculated as described in section 2.15.1. A mean value was calculated for the six measurements per section for frontal, temporal and parieto-occipital lobes.

5.3.6 Statistical analysis

Data were not normally distributed therefore non-parametric tests were employed; Spearman's rank correlation coefficient was used to correlate ARWMC scores with AT8 and 4G8 as well as to correlate all scores with subjects age. Significant differences between ARWMC scores, AT8 and 4G8 %BF for the frontal, temporal and parieto-occipital regions were determined using the Mann– Whitney U-test.

5.4 Results

Demographics of cases, ARWMC scores, artery/arteriolar fibrosis and quantitative measures of cortical pathology are shown in Table 5.1.

No significant correlation was seen between age and ARWMC scores. AT8 and 4G8 %BF did increase with age but this was not found to be significant.

							Frontal				Temporal				Parieto-occipital			
Case n	**Diag.**	**Sex**	**Age**	**PMD**	**Braak**	**CERAD**	**ARWMC**	**SVD**	**AT8 (% BF)**	**4G8 (% BF)**	**ARWMC**	**SVD**	**AT8 (% BF)**	**4G8 (% BF)**	**ARWMC**	**SVD**	**AT8 (% BF)**	**4G8 (% BF)**
3	C	F	84	46	3	0	1	3	0.03	2	1	3	0.21	3	3	1	0	0
4	C	F	94	82	2	0	3	1	0.18	0.09	2	0	3.8	0.02	3	1	0.21	0.03
5	C	F	98	17	3	1	2	0	0.19	7.2	1	0	3.4	6	2	0	0.82	5
14	C	M	72	39	1	1	2	1	0.02	2	1	1	2.2	2	3	1	0.04	1.2
24	AD	F	78	37	6	3	3	1	17	17.1	3	1	33	6.4	3	0.5	25.3	10.1
27	AD	F	87	54	6	3	3	0	22.7	6	2	1	24.2	5.6	3	1	7.8	4.8
30	AD	M	90	69	6	3	3	1	7.5	23.2	3	3	7.5	18	3	1.5	4.6	14
33	AD	F	89	85	6	3	3	1	9.1	12.4	3	2	17.4	7.4	3	1.5	17.2	7.1

Table 5.1. Diagnosis, sex, age, scores, AT8 and 4G8 %BF values of 8 cases. Case n refers to master demographic Table 2.2. ARMWC Diag., clinicopathological diagnosis; F, female; M, Male; C, control; AD, Alzheimer's disease; ARWMCs, Age-related white matter change (MRI) score; SVD, small vessel disease score; %BF, percentage binary area fraction

5.4.1 Distribution of HPT and Aβ between lobar regions

No significant difference was seen between frontal and parieto-occipital AT8 %BF. Temporal AT8 %BF was significantly higher than both frontal and parieto-occipital scores (both P< 0.05) (Figure 5.2 A). All AT8 %BF significantly correlated; frontal and temporal (P<0.01, Rho 0.929) frontal and parieto-occiptal (P<0.01, Rho 0.905) and temporal and parieto-occipital (P<0.01, Rho 0.952).

Frontal 4G8 %BF was significantly higher than temporal and parieto-occipital 4G8 %BF (both P<0.05). There was no significant difference seen between temporal and parieto-occipital 4G8 BF (Figure 5.2 B). All 4G8 %BF significantly correlated; frontal and temporal (P<0.01, Rho 0.976) frontal and parieto-occipital (P<0.01, Rho 0.976) and temporal and parieto-occipital (P<0.01, Rho 0.952).

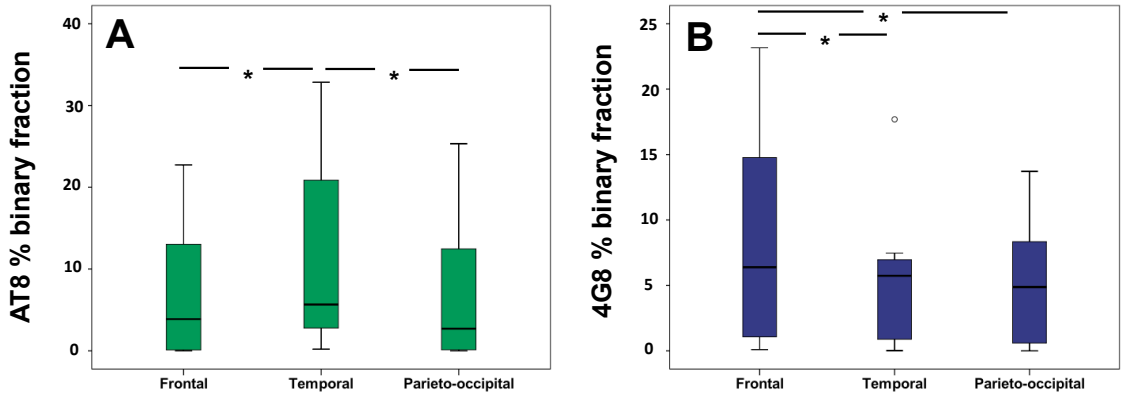

Figure 5.2. A) AT8 %BF was significantly higher in the temporal WM compared to the frontal and parieto-occipital white matter. B) 4G8 %BF was significantly higher in the frontal WM compared to the temporal and parieto-occipital white matter. *, P<0.05; ring, outlier; %BF, percentage binary area fraction.

5.4.2 Distribution of WMH between lobar regions

No significant differences were seen between frontal and parieto-occipital ARWMC scores. Temporal ARWMC scores were significantly lower than both frontal and parieto-occipital scores (both P< 0.05) (Figure 5.3). All ARWMC scores significantly correlated; frontal and temporal (P<0.01, Rho 0.899) frontal and parieto-occipital (P<0.05, Rho 0.800) and temporal and parieto-occipital (P<0.05, Rho 0.719). No significant differences were seen between regions.

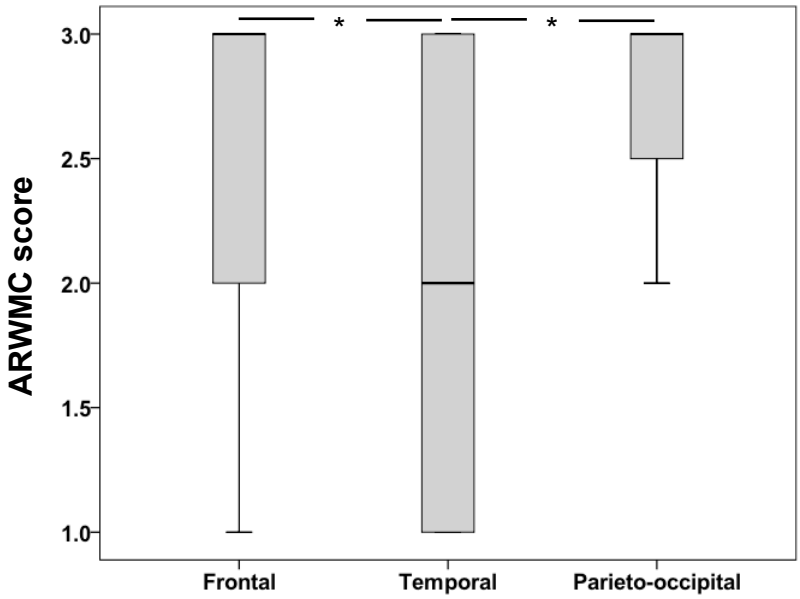

Figure 5.3. ARWMC scores were significantly lower in the temporal WM compared to the frontal and parieto-occipital white matter. *, P<0.05.

5.4.3 Association of WMH with HPT and Aβ

A positive R^2 value was seen in frontal, temporal and parieto-occipital regions, indicating an increase in AT8 and 4G8 %BF with increase ARWMC score (Figure 5.4 A-C). Frontal AT8 %BF significantly correlated with frontal ARWMC scores (P<0.05, Rho 0.729). Both temporal AT8 and 4G8 %BF significantly correlated with temporal ARWMC scores (P<0.01, Rho 0.849 and P<0.05, Rho 0.729 respectively). No significant correlations were seen between parieto-occipital AT8 and 4G8 %BF and ARWMC score (Figure 5.4 D).

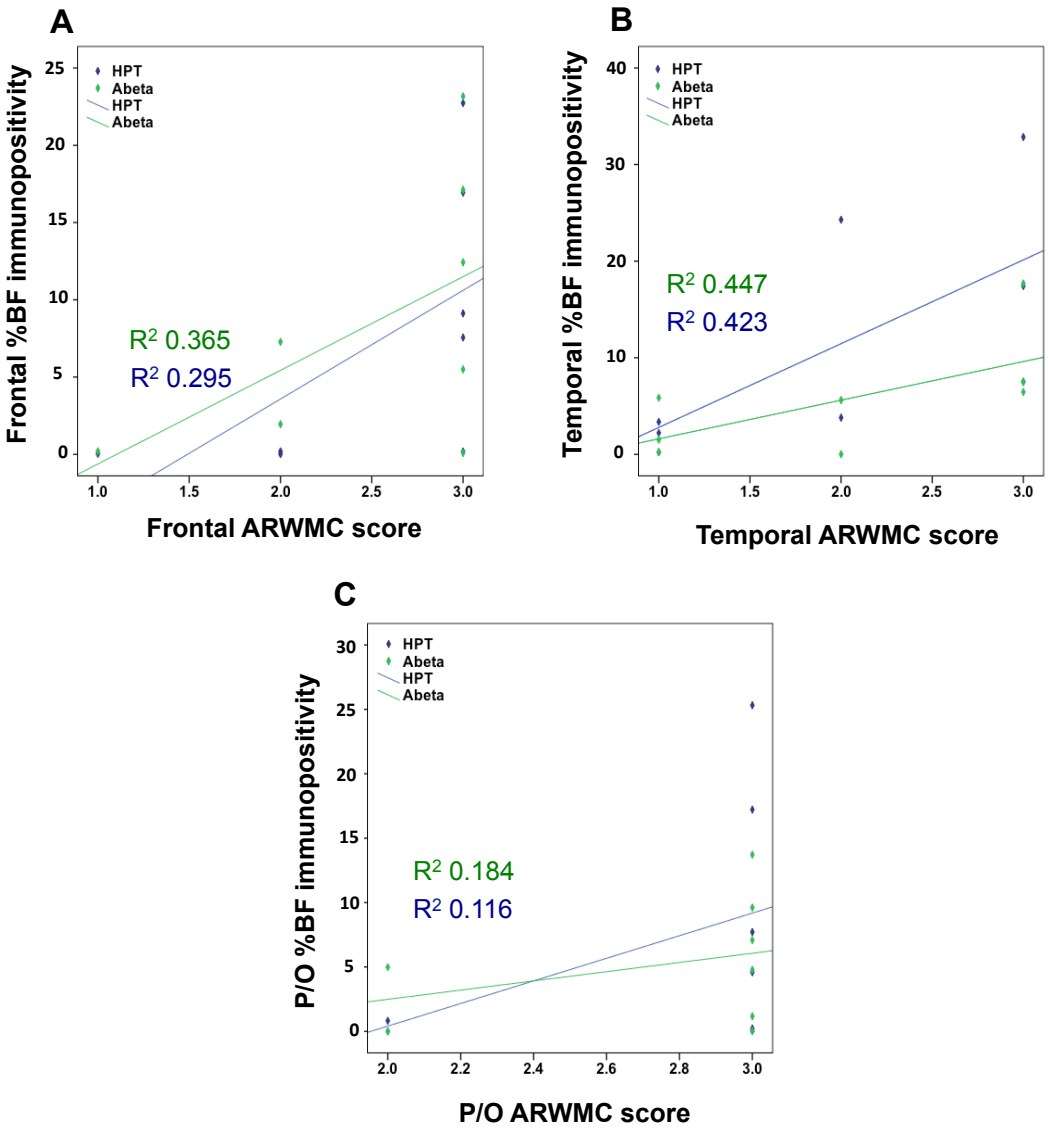

D	Frontal		Temporal		Parieto-occipital	
	AT8	**4G8**	**AT8**	**4G8**	**AT8**	**4G8**
ARWMC	0.04*	0.275	0.009**	0.04*	0.203	0.365
rho	0.729	0.44	0.84	0.729	0.504	0.378

Figure 5.4. Scatter graphs A-C show distribution of AT8 and 4G8 values in relation to ARWMC scores in the frontal (A), temporal (B) and P/O (C) WM. Table shows the correlations between ARWMC score with AT8 and 4G8 in frontal, temporal and parieto-occipital white matter. ARWMC represents individual lobar scores and AT8 and 4G8 are value of binary fraction; D) Significant correlation was seen between frontal ARWMC and AT8 %BF, and temporal ARWMC with both AT8 and 4G8. ARWMC, age related white matter change; %BF, % binary area fraction immunopositivity; WM, white matter; P/O, parieto-occipital; *, P<0.05; **, P<0.01.

5.5 Discussion

5.5.1 Distribution of HPT and Aβ

AT8 and 4G8 %BF was calculated as a quantitative measure of HPT and Aβ. Frontal, temporal and parieto-occipital AT8 and 4G8 %BF all significantly correlated with each other, indicating quantitative assessment is consistent in detecting changes within this cohort.

For the overall cohort temporal HPT was significantly higher than frontal and parieto-occipital HPT which follows the hierarchy pattern of NFT deposition (Braak and Braak, 1991). Specifically in the AD cohort this increase in temporal HPT is likely due to the temporal region being affected early and severely with HPT pathology in AD (Braak and Braak, 1991, Alafuzoff, 2013) and accumulated higher amounts of pathology over time. In normal aged individuals, accumulation of HPT frequently occurs without compromising cognitive function (Braak and Braak, 1991, Ince, 2001, Thal et al., 2013, Jellinger and Attems, 2012) but rarely surpasses Braak stage III confining pathology to the transentohinal/entorhinal and occipito-temporal gyrus (Braak and Braak, 1991).

Frontal Aβ was significantly higher than temporal and parieto-occipital Aβ. According to Thal Aβ phases, Aβ pathology is first seen in the neocortex with no specific preferential regional deposition (Thal et al., 2002b), therefore, the higher amount of Aβ the frontal cortex may be the result of variations between cases given the small cohort.

5.5.2 Parieto-occipital WMH were not significantly higher than other WM regions

Initial observation noted a large deviation between MRI- based ARWMC scores and SVD scores in the parieto-occipital region. Frontal, temporal and parieto-occipital ARWMC scores all significantly correlated with one another, indicating the MRI-based assessment is consistent in detecting changes within this cohort.

Parieto-occipital WMH scores were not significantly different to frontal WMH scores and temporal WMH were found to be significantly lower than both frontal and parieto-occipital regions. This was unexpected as previous studies have shown a higher burden of posterior hyperintensities in AD cases (Lee et al.,

2009, Lee et al., 2010, Leys et al., 1991, Yoshita et al., 2006), thought to be the results of degenerative processes associated with AD pathology, especially HPT, in the temporal cortex. However, since AD cases were Braak stage VI and Thal Aβ phase 5, they exhibit very high levels of pathology in all neocortical areas and potentially affect the integrity of WM in all areas. With regards to the temporal WMH, scores may be influenced by atrophy of the MTL, especially in the AD group (previously discussed section 3.5.3). Nevertheless, a very limited case number was used and a substantial increase in case number is required to further investigate the regional distribution of WMH.

5.5.3 WMH are associated with HPT and Aβ

No significant correlation was seen between parieto-occipital HPT and Aβ with ARWMC scores. Lack of correlations in this region may be attributed to the case selection that was based on parietal-occipital ARWMC scores. Six (75%) of the cases had a parieto-occipital ARWMC grade of 3 and the remain two (25%) were scored as a grade 2, therefore, lack of correlation may be due to a ceiling effect created by ARWMC scores.

HPT significantly correlated with WMH in the frontal and temporal WM and between WMH and Aβ in the temporal WM indicating that as the amount of cortical pathology increases so does WMH severity in both AD and non-demented healthy aged. Previous *post mortem* studies have observed an association of higher cortical HPT and degenerative axonal loss, resulting in WML, in the temporal lobe (Leys et al., 1991, Englund, 1998) signifying potential axonal loss as secondary consequence of neuronal drop out. Furthermore, MTL atrophy is commonly seen in both AD and (to a lesser extent) the normally aged (Cavallin et al., 2012) thought to be due to neuronal loss as a result of HPT pathology seen in both AD and non-demented brains (Braak and Braak, 1991, Alafuzoff, 2013).

Although neuronal loss was not measured, neuropathological studies suggest that the number of neurons in the cerebral cortices remains stable in the normal ageing process (Terry et al., 1987, Pakkenberg and Gundersen, 1997). A study by Freeman and colleagues (Freeman et al., 2008) investigated neuronal density in a small cohort of non-demented *post mortem* brains with an age range of 56-103 years, and found that temporal neuronal density did not change

throughout ageing, however, there was an increase in cortical thinning with age and suggested decrease in cerebral volume was attributed to neuronal shrinkage and loss of dendritic and axonal architecture. Furthermore, Pakkenberg and colleagues found only a 10% loss of neurons while there was up to 45% loss of axons in normal ageing (Pakkenberg and Gundersen, 1997). In AD there is a much greater rate of neuronal loss that differs between individuals. However, there may be other pathomechanisms attributed to axonal loss in the normal aged and AD brains. WLD, the reactive retrograde demyelination and fragmentation of the axon, has been shown to occur in many neurodegenerative diseases and can occur independent of neuronal loss (Coleman, 2013). A major trigger of WLD is thought to be axonal transport dysfunction (Beirowski et al., 2010) as a result of pathological forms of HPT and Aβ (Kamal et al., 2001, LaPointe et al., 2009, Patrick et al., 1999, Salehi et al., 2006, Seitz et al., 2002). One could speculate that in regions of high cortical pathology, such as the temporal lobe, cortical pathologies, especially intracellular HPT, may be involved in the activation of WLD and therefore attributed to axonal loss and the generation of WMH as demonstrated in our significant correlations between our quantified cortical pathologies and WMH.

Given the limited size of the present study cohort and no inclusive measurement of SVD, no conclusion can be drawn on the pathomechanisms of the WMH.

5.5.4 Limitations

A major limitation in this study was the cohort consisting of only eight cases. In order to elucidate the potential effect of cortical pathologies on WM larger cohorts are required to allow separate analyses for different disease groups. However, this was a pilot study and included all cases that were available that exhibited high WMH and low SVD scores.

This study did not quantitatively measure SVD pathology; therefore I could not investigate the influence of SVD and compare it to my findings.

Case selection was based on the differences between parietal-occipital WMH and SVD scores only and did not take into consideration WMH and SVD scores of the frontal and parieto-occipital regions. Furthermore, the SVD scores that were used in the selection of cases was based on a semi-quantified scale, and

as previously discussed in Chapter 4, this is not the most accurate and reliable measure of pathology. Some SVD scores were less than 1 (on a 4 tiered-sale); this is possible although quite rare as even non-demented normally age still exhibit some mild degree of SVD (Grinberg and Thal, 2010). Additionally, with the increasing understanding of cerebral multimorbidity (Alafuzoff, 2013, Attems and Jellinger, 2013a) it is essential to understand the combined effects of various pathologies, therefore, in future studies SVD and its influence will have to be taken into account.

5.6 Conclusion

This study showed a significant correlation between cortical HPT and Aβ pathology with WMH severity in the temporal lobe and HPT with WMH severity in the frontal lobe. Further investigation is required to elucidate a potential secondary influence of neocortical pathologies on axonal degeneration and the possible interaction with SVD.

Chapter 6 - The influence of cortical AD-related pathologies and SVD on white matter integrity

6.1 Introduction

The previous chapter described a correlation between cortical HPT and Aβ pathology with WMH severity in the temporal lobe and HPT with WMH severity in the frontal lobe, suggesting neocortical pathology might have an influence on WM integrity. Using quantitative neuropathological assessments in a larger cohort, this study further investigates the influence of AD-related pathologies on WM integrity also taking into account the influence of SVD.

6.1.1 Potential role of HPT and Aβ in the formation of white matter lesions

There is mounting data indicating that pathological forms of HPT and Aβ, found in both AD and normal aged individuals, may be a principal trigger of WLD via deregulation of axonal transport, an essential process for the maintenance and physiological function of neurons (Kamal et al., 2001, LaPointe et al., 2009, Patrick et al., 1999, Salehi et al., 2006, Seitz et al., 2002, Beirowski et al., 2010, Calkins et al., 2011, Coleman, 2005, Coleman, 2013, Stokin et al., 2005). Transgenic mice that overexpress wild-type (wt) or mutant APP (Salehi et al., 2006, Stokin et al., 2005) and tau (Ishihara et al., 1999, Zhang et al., 2004) have been shown to exhibit axonal transport deficits and axonal swellings (early events in WLD) that proceed the deposition of HPT and Aβ pathology, suggesting that axonal transport deficits, and possible secondary axonal degeneration, are an early event in neurodegenerative disease.

6.1.2 Tissue MicroArray

Accurate digital assessment at high output is required to gain insight into how HPT and Aβ may influence WM integrity. Quantitative analysis using standard diagnostic histological assessment on limited slides is not sufficient and increasing slide numbers is impracticable. However, the TMA has become a standard tool for tissue-based research consisting of numerous cylindrical tissue cores from different donor paraffin blocks relocated into one recipient block, allowing for efficient histopathological studies. The array format is

optimally suited for quantitative analysis as defined diameters of the tissue samples allows for a highly standardized analysis of areas of exactly the same size and region (Simon, 2010) that can be quantitatively assessed at high throughput.

6.2 Aims

I aimed to further investigate the possible influence of AD-related pathology and SVD on white matter integrity using a combination of *post mortem* MRI-based WMH assessment, quantified cortical HPT and Aβ pathology using the TMA methodology and SI values of WM artery and arteriole fibrosis as measure of SVD.

6.3 Methods

6.3.1 Case selection

The study cohort consisted of 38 post mortem brains (15 aged controls, 23 AD) (Table 6.1). All cases had undergone post mortem MRI as described in section 6.3.2.

6.3.2 MRI assessment

Formalin fixed *post mortem* right hemispheres underwent T2-weighted MRI and subsequently WMH were visual rated in frontal, parieto-occipital and temporal deep WM using the ARWMC scale (Wahlund et al., 2001), to generate ARWMC score as described in section 2.9.

6.3.3 Tissue MicroArray

An in-house TMA methodology was developed from 2011-2012 (McParland et al., 2014b) as described in section 2.11. For cost effectiveness and efficient sectioning of tissue TMA blocks were composed of paraffin. The silicon mould used to hold and embedded the TMA paraffin block was also made in-house to specific fit the TMA block.

Case n	sex	age	Disease status	PMD (hours)	Braak stage	CERAD score
1	F	96	Normal Aged	95	3	0
2	M	77	Normal Aged	83	2	0
4	F	94	Normal Aged	82	2	0
7	F	81	Normal Aged	82	3	2
8	F	70	Normal Aged	72	0	0
10	F	89	Normal Aged	34	3	0
11	F	78	Normal Aged	34	0	0
12	F	95	Normal Aged	36	3	0
13	F	89	Normal Aged	49	3	0
14	M	72	Normal Aged	39	1	1
15	M	81	Normal Aged	43	2	0
16	M	73	Normal Aged	25	0	0
17	M	86	Normal Aged	50	4	2
18	F	97	Normal Aged	21	2	1
19	F	88	Normal Aged	22	3	0
20	F	86	AD	69	6	3
22	F	93	AD	15	6	3
23	M	92	AD	59	6	3
24	M	78	AD	37	6	3
26	M	85	AD	29	6	3
27	F	87	AD	54	6	3
29	F	81	AD	56	6	3
30	M	90	AD	69	6	3
31	F	75	AD	33	6	3
32	F	86	AD	5	6	3
33	F	89	AD	85	6	3
34	F	90	AD	90	6	3
35	M	88	AD	22	6	3
36	F	79	AD	65	6	3
37	F	86	AD	51	6	3
38	M	89	AD	61	6	3
39	F	92	AD	74	6	3
40	M	80	AD	N/A	6	3
41	F	76	AD	37	6	3
42	M	91	AD	72	6	3
43	F	83	AD	52	6	3
44	M	76	AD	23	6	3
45	M	81	AD	41	6	3

Table 6.1. Subject demographics. Case n refers to master demographic Table 2.2. N, number; M, male; F, female; AD, Alzheimer's disease; PMD, post mortem delay; N/A, not available.

6.3.4 Histology and IHC

Tissue sections from TMA paraffin blocks were stained with immunohistochemistry for HPT (AT8) and Aβ (4G8) according to protocol described in section 2.12.3.

Tissue sections from diagnostic blocks from frontal, temporal, parietal and occipital WM were stained with H&E according to protocol described in section 2.12.1.

6.3.5 Quantitative assessment of cortical pathology

TMA tissue sections were assessed at x200 magnification using a Nikon Eclipse 90i microscope coupled with NIS-Elements AR3.2 software to calculate percentage mean binary area fraction of immunopositivity (%BF) per tissue punch as described in section 2.15.1. A mean value was calculated for frontal, temporal and parieto-occipital lobes.

6.3.6 Sclerotic Index

Photomicroimages of H&E stained sections containing approximately 8 WM arteries/arterioles were taken at x200 magnification using a Nikon Eclipse 90i microscope. SI was calculated using VasCalc software program according to protocol in section 2.15.3. A mean value was calculated for frontal, temporal and parieto-occipital lobes.

6.3.7 Statistical analysis

To compare means of AT8 and 4G8 %BF, SI values and ARWMC scores, non-parametric Kruskal-Wallis test was used. The Mann– Whitney *U-test* was employed to test for significant differences in AT8 and 4G8 %BF, SI values and ARWMC scores within AD and controls groups. Spearman's rank correlation coefficient was used to correlate ARWMC, AT8, 4G8 and SI values as well as to correlate all scores with subject's age. Linear Regression with stepwise analysis was used to investigate the influence of AT8 and 4G8 %BF, SI values and PMD on ARWMC scores. Power calculations for AT8 and 4G8 %BF and SI were generated using G*Power version 3.1.9.2 (Faul et al., 2009).

6.4 Results

As previously discussed *post mortem* MRI values for the parietal and occipital lobes are stated as a combined score for the parieto-occipital region (Firbank, 2014). By contrast, cortical and VP is quantified separately for each region, therefore, parietal, occipital and parieto-occipital pathological scores were statistically compared.

6.4.1 Associations of WMH with age and PMD

Demographics of cases used in the study are shown in Table 6.1. No significant influence was seen between PMD and WMH scores.

In the control cohort, spearman's rank correlations coefficient revealed a significant correlation between age and WMH severity ($P<0.05$) and age and AT8 % BF ($P<0.05$). No significant correlation was seen between age with SI values or 4G8 %BF. In contrast, the AD cohort showed no significant correlation between age with WMH severity, SI values, and AT8 or 4G8 %BF. All AD cases were Braak stage 6 and had significantly higher amounts of AT8 and 4G8 %BF ($P<0.01$) compared to controls.

	AD	Controls	P value
Case n	23	15	-
Age (years ± S.E)	84.2 (5.7)	84.4 (9.12)	0.869
Sex M:F	10:13	6:9	-
PMD (hours)	49.95 (22.9)	51.13 (25)	0.926
MMSE	5.5 (7.2)	28 (4.23)	0.000
Braak NFT stage	6.00	2 (1.3)	0.000
ARWMC	2.3 (0.91)	1.33 (0.67)	0.047
AT8 (BF %)	19 (10.6)	0.6 (4.7)	0.000
4G8 (BF %)	10.6 (6.6)	0.5 (4.3)	0.000
SI	0.38 (0.07)	0.35 (0.07)	0.38

Table 6.2. Demographic characteristics of 38 cases. AD, Alzheimer's disease; C, control; F, female; M, Male; PMD, post mortem delay; MMSE, mini mental scale examination; NFT, neurofibrillary tangle; ARWMCs, Age-related white matter change (MRI) score; SI, Sclerotic Index.

6.4.2 Significant differences between AD and control cohorts

No significant differences were found between AD and controls for age, PMD and SI. In contrast MMSE scores ($P<0.01$), Braak NFT stage ($P<0.01$), MRI-based ARWMC scores ($P<0.05$), AT8 and 4G8 % BF (both $P<0.01$), were significantly higher in the AD cases compared to controls.

6.4.3 Regional severity of WMH between disease groups

AD temporal ARWMC scores were significantly higher than control temporal ARWMC scores ($P<0.05$), however, no significant differences were seen in any other regions.

With respect to the control group, spearman's rank correlations coefficient revealed a significant correlation between frontal ARWMC scores and frontal AT8 %BF (Rho 0.652, $P<0.01$) and 4G8 %BF (Rho 0.705, $P<0.01$) (Figure 6.1 A). In the temporal lobe significant correlations were seen between ARWMC scores and SI values (Rho 0.560, $P<0.05$) (Figure 6.1 B). No significant correlations were seen in the parieto-occipital region between ARWMC scores with any pathology (Figure 6.1 C). The summation of all regional scores generated a mean overall hemispheric value and here significant correlations between ARWMC scores and 4G8 %BF (Rho 0.535, $P<0.05$) was seen (Figure 6.1 D). No significant correlation was seen in any region or overall between ARWMC scores and SI value.

With respect to the AD group no significant correlations were seen between ARWMC scores and SI values and AT8 and 4G8 % immunopositivity in any region or as an overall hemispheric score (Figure 6.2). To allow for a broader range of scores and to identify the influence of higher amounts of AT8 and 4G8 on WM in the AD group all both AD and controls were combined. In the full cohort a significant correlation was seen between ARWMC scores with AT8 % immunopositivity and 4G8 % immunopositivity in the frontal (Rho 0.333, $P<0.05$; Rho 0.331, $P<0.05$), temporal (Rho 0.485, $P<0.01$; Rho 0.424, $P<0.01$), parieto-occiptal lobes (Rho 0.370, $P<0.05$; Rho 0.329, $P<0.05$), and as an overall hemisphere (Rho 0.373, $P<0.05$; Rho 0.445, $P<0.01$) (Figure 6.3 A-D).

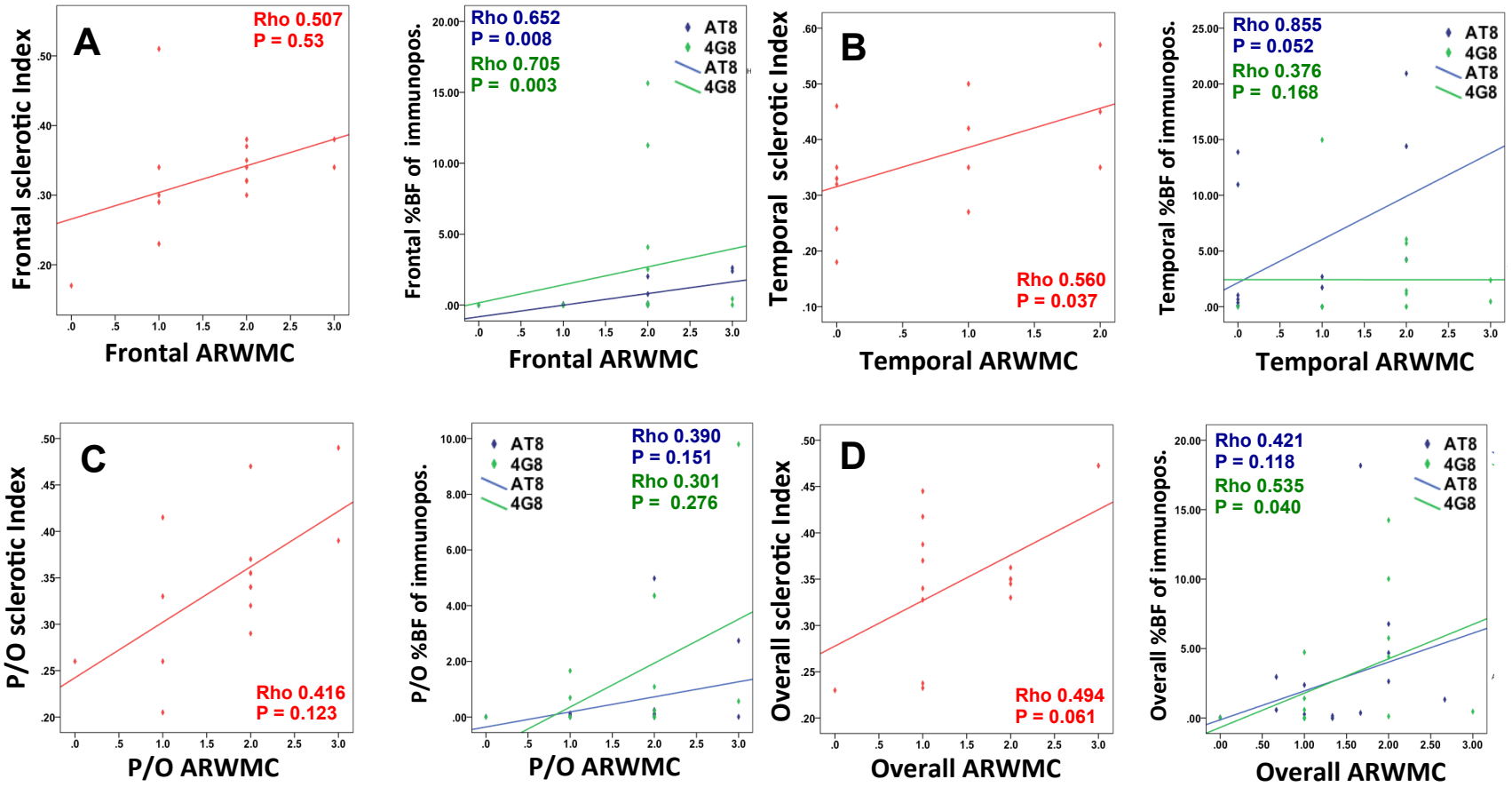
A
Rho 0.507
P = 0.53
Frontal sclerotic Index
Frontal ARWMC
Rho 0.652
P = 0.008
Rho 0.705
P = 0.003
AT8
4G8
AT8
4G8
Frontal %BF of immunopos.
Frontal ARWMC
B
Rho 0.560
P = 0.037
Temporal sclerotic Index
Temporal ARWMC
Rho 0.855
P = 0.052
Rho 0.376
P = 0.168
AT8
4G8
AT8
4G8
Temporal %BF of immunopos.
Temporal ARWMC
C
Rho 0.416
P = 0.123
P/O sclerotic Index
P/O ARWMC
AT8
4G8
AT8
4G8
Rho 0.390
P = 0.151
Rho 0.301
P = 0.276
P/O %BF of immunopos.
P/O ARWMC
D
Rho 0.494
P = 0.061
Overall sclerotic Index
Overall ARWMC
Rho 0.421
P = 0.118
Rho 0.535
P = 0.040
AT8
4G8
AT8
4G8
Overall %BF of immunopos.
Overall ARWMC

Figure 6.1. Scatter plots showing various correlations between MRI-based ARWMC scores with SI values and AT8 and 4G8 % immunopositivity in the frontal (A), temporal (B), parieto-occipital (C) lobes and overall hemispheric (D) of the control cohort. ARWMC, Age related white matter change; %BF of immunopos., percentage binary area fraction of immunopositivity; P/O, parieto-occipital

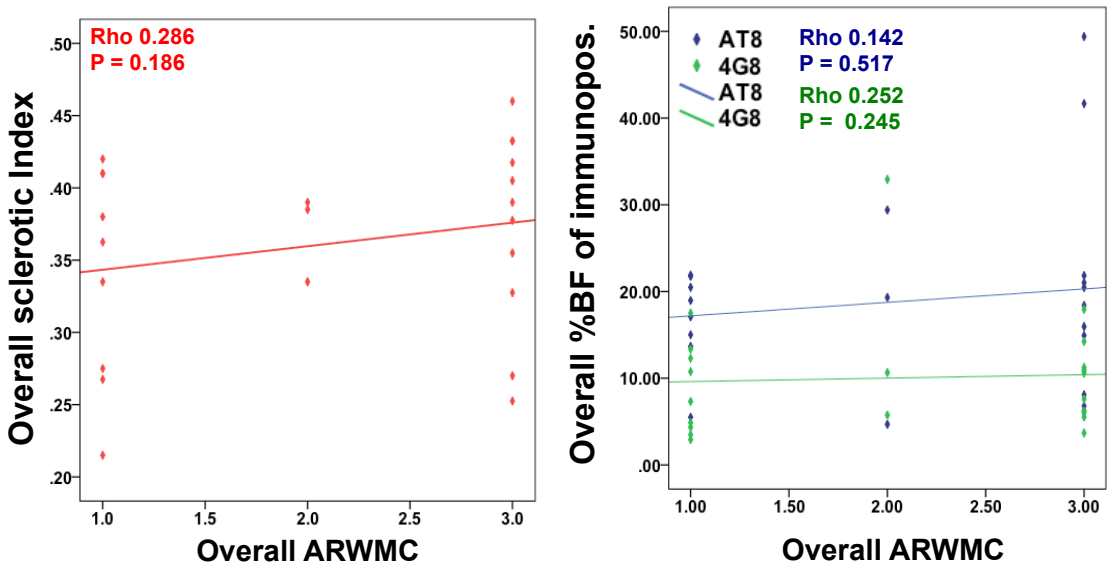

Figure 6.2. No significant correlations were seen in the AD cohort between MRI-based ARWMC scores with SI values and AT8 and 4G8 % immunopositivity. Scatter graphs exhibit overall hemispheric data for AD cohort. ARWMC, Age related white matter change; % BF Immunopos., percentage binary area fraction of immunopositivity

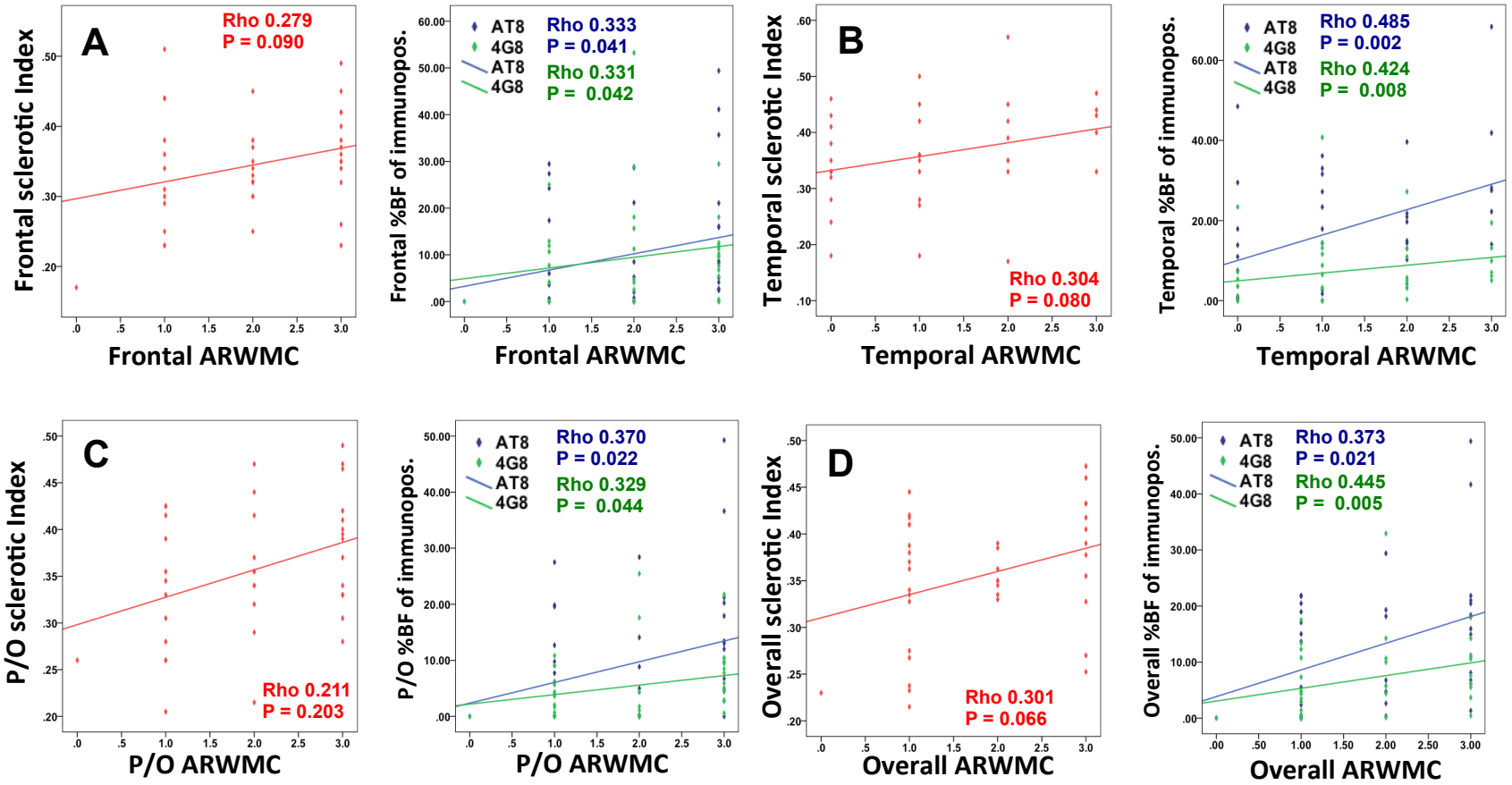
A
Rho 0.279
P = 0.090
Frontal sclerotic Index
Frontal ARWMC
AT8
4G8
AT8
4G8
Rho 0.333
P = 0.041
Rho 0.331
P = 0.042
Frontal %BF of immunopos.
Frontal ARWMC
B
Rho 0.304
P = 0.080
Temporal sclerotic Index
Temporal ARWMC
AT8
4G8
AT8
4G8
Rho 0.485
P = 0.002
Rho 0.424
P = 0.008
Temporal %BF of immunopos.
Temporal ARWMC
C
Rho 0.211
P = 0.203
P/O sclerotic Index
P/O ARWMC
AT8
4G8
AT8
4G8
Rho 0.370
P = 0.022
Rho 0.329
P = 0.044
P/O %BF of immunopos.
P/O ARWMC
D
Rho 0.301
P = 0.066
Overall sclerotic Index
Overall ARWMC
AT8
4G8
AT8
4G8
Rho 0.373
P = 0.021
Rho 0.445
P = 0.005
Overall %BF of immunopos.
Overall ARWMC

Figure 6.3. Overall cohort correlations between MRI-based ARWMC scores with SI values and AT8 and 4G8 % immunopositivity in the frontal (A), temporal (B), parieto-occipital (C) lobes and overall hemispheric (D). ARWMC, Age related white matter change; %BF of immunopos., percentage binary area fraction of immunopositivity; P/O, parieto-occipital

Finally, I investigated whether SI, AT8 and 4G8 %BF had a significant relationship with WMH severity in a connecting region in the full cohort. A significant correlation was also seen between temporal ARWMC scores and frontal AT8 %BF (Rho 0.458, $P<0.01$) and 4G8 %BF (Rho 0.475, $P<0.01$) (Figure 6.4 A). A significant correlation was revealed between parieto-occipital ARWMC scores with frontal AT8 %BF (Rho 0.336, $P<0.05$) and frontal 4G8 %BF (Rho 0.403, $P<0.05$) (Figure 6.4 B). Interestingly, a reciprocal significant correlation was seen between frontal ARWMC scores and parieto-occiptal AT8 %BF (Rho 0.366, $P<0.05$) and parieto-occipital 4G8 %BF (Rho 0.338, $P<0.05$) (Figure 6.4 C). Finally, significant correlations were seen between temporal ARWMC scores and parieto-occiptal AT8 %BF (Rho 0.472, $P<0.01$) and parieto-occipital 4G8 %BF (Rho 0.515, $P<0.01$) (Figure 6.4 D). No significant correlations were seen between temporal lobe AT8 or 4G8 %BF with frontal or parieto-occiptal ARWMC scores.

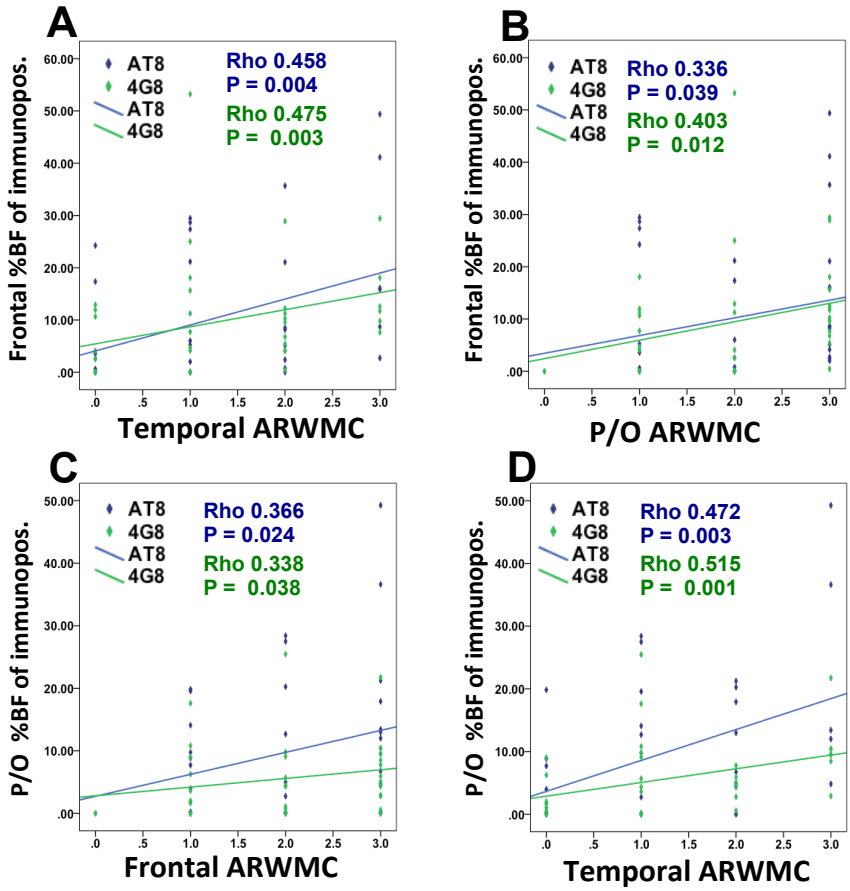

Figure 6.4. Scatter graphs exhibit overall hemispheric data for the overall combined cohort. Significant correlations between MRI-based ARWMC scores with SI values and AT8 and 4G8 % immunopositivity values from other cortical regions. ARWMC, Age related white matter change; %BF of immunopos., percentage binary area fraction of immunopositivity; P/O, parieto-occipital.

6.4.4 Influence of SVD, HPT and Aβ on WMH severity

Multiple linear regression was employed to explore the influence of AT8 and 4G8 %BF and SI values on WMH score and to determine which of the three pathologies has the strongest association and is best predictor of WMH score.

With respect to the control cohort AT8 %BF was revealed to be a significant predictor of ARWMC score in the frontal ($P<0.01$) and temporal ($P<0.05$) lobes, and 4G8 %BF was found to be a significant predictor in the parieto-occipital lobe ($P<0.05$). For the overall hemisphere both AT8 %BF ($P<0.01$) and SI ($P<0.05$) were significantly associated and deemed a predictor of ARWMC score. SI was found to be a significant predictor of ARWMC score in the temporal ($P<0.05$) and parieto-occipital ($P<0.01$) lobes.

In the AD cohort there were no significant influence between ARWMC with AT8 and 4G8 %BF or SI values.

For the overall cohort, AT8 %BF was a significant predictor of ARWMC severity in the fontal ($P<0.01$), temporal ($P<0.001$) and parietal lobe ($P<0.01$). For the overall hemisphere, both AT8 %BF ($P<0.05$) and SI ($P<0.05$) was a significant predictor of ARWMC score. Aβ had no significant influence in any region on ARWMC score. SI was found to be a significant predictor of ARWMC score in the parieto-occipital lobe ($P<0.05$).

Using the entire cohort, I investigated the influence of cortical and VP on ARWMC scores in connecting lobes. Frontal AT8 %BF values were a significant predictor of temporal ARWMC score ($P<0.01$), with no significant influence of frontal pathologies on parieto-occipital ARWMC scores. A significant influence was also seen between temporal AT8 %BF and frontal ARWMC score ($P<0.05$), with no significant influence of temporal pathology values on parieto-occipital ARWMC scores. Finally, parietal AT8 %BF values were a significant predictor of frontal ARWMC score ($P<0.05$) and both parietal and occipital AT8 % immunopositivity were a significant predictor of temporal ARWMC scores. No significant influence was found with SI values.

6.4.5 Power calculations

Due to the significant difference in AT8 and 4G8 values and no significant difference in SI between the AD and control groups a power calculation was conducted to investigate whether the study was sufficiently powered to detect differences between groups. Cohen's d is defined as the sum of the difference between the two means, divided by their standard deviation. This was used to calculate the effect size using the highest standard deviations for AT8, 4G8 and SI. Power analysis for AT8 and 4G8 yielded $\alpha=0.99$ and for SI $\alpha=0.24$. At the standard 0.8 threshold used by convention (Coolican, 2013) the required study case number for HPT and Aβ was 8 and SVD was 600.

6.5 Discussion

The cohort used in this study was limited to a total of 38 brains due the requirement of *post mortem* MRI, therefore, post hoc power calculations were employed to test for adequate statistical power. Considering the very small P values and large differences in AT8 and 4G8 values between AD and controls, $\alpha=0.99$ suggesting that the study methodology is sufficiently powered to detect differences. This was not unexpected given the severe difference in cortical pathology between AD and controls, therefore a case number as small as 8 per

group may have been used. Estimates for SVD power suggest that the present cohort was too small to detect differences between the experimental groups as α=0.24, and case number of approximately 600 was required per group. The large case requirement maybe due to a limitation of the case selection for this study that consisted primarily of SVD grade 1 and 2 cases an only one grade 3 measurement, therefore, there is very little difference to detect within the cases resulting in a small Cohen D's value. It may also indicate; i) there is no significant difference to detect between the two groups, which was further confirmed by the Kruskal-Wallis test; ii) the methodology used is unable to detect differences (further discussed in section 6.5.6).

6.5.1 AD cases exhibited more severe WMH in the temporal lobe compared to controls

This study showed that AD brains contained more severe WMH than non-demented control brains in agreement with previous studies (Brickman, 2013a, Kalaria, 2000, Rezek et al., 1987, Scheltens et al., 1992, Nagata et al., 2012, O'Sullivan, 2008, Polvikoski et al., 2010). The AD group exhibited more severe temporal WMH compared to controls, however, there was no significant difference in the severity of parieto-occipital WMH between AD and controls. Higher burden of posterior WMH in AD cases has been shown numerous times (Gootjes et al., 2004a, Lee et al., 2009, Lee et al., 2010, Leys et al., 1991, Yoshita et al., 2006) and has been shown to be specific predictor to AD (Brickman et al., 2012). Hyperintensities in these regions are thought to be the result of degenerative processes associated with AD pathology, especially HPT in the temporal cortex. However, it was unexpected not to find an increase in parieto-occipital WMH in the AD group as studies have shown a greater burden of hyperintensites in the splenium of the CC (Teipel et al., 1999, Di Paola et al., 2010, Yoshita et al., 2006) located in the medial parietal lobe. This study was unable to investigate the influence of various pathologies on the CC, as it is currently not included in the *post mortem* MRI assessment but is an important area for future investigation. Previous studies have shown that the increased hyperintensity burden seen in the posterior of AD brains may be attributed to non-ischemic axonal loss (Moody et al., 1988) in the splenium. CC fibers are heavily connected to the temporal and parietal regions originating from pyramidal layers III and V neurons (Nieuwenhuys, 1994, Gazzaniga, 2000) which are specifically vulnerable by AD pathology, especially HPT

(Giannakopoulos et al., 1998, Pearson et al., 1985, Lewis et al., 1987, Braak and Braak, 1991), therefore, it is highly likely and expected to be affected in the AD process (Yoshita et al., 2006).

6.5.2 No significant increase in SVD in the AD group despite significantly higher WMH

Despite the significant higher WMH in the AD cohort, no significant difference was seen in SVD, consequently, SVD may not be the only cause of WMH within these groups as suggested in the studies described in Chapter 5. SVD significantly correlated with WMH severity in the temporal lobe of controls only. However, SVD was shown to have an influence on and is a significant predictor of WMH severity, respectively, in temporal and parieto-occipital lobes of controls and for the parieto-occipital lobe and overall hemisphere of the full cohort. It was unexpected to find no significant differences in SVD mscores between the two groups as SVD is assumed to be the main factor in the pathogenesis of WML (Grinberg and Thal, 2010, Pantoni, 2010, Pantoni and Garcia, 1997) and SVD has been shown to be lower in non-demented compared to demented individuals (Schmidt et al., 2011b). If SVD were the main pathogenic factor in the formation of WML/WMH an increase in SVD in parallel with increasing WMH severity would be expected. Although, a recent extensive study by Craggs and colleagues (Craggs et al., 2013a) measured WM SVD using SI in a familial and sporadic SVD disease cases and observed that the level of fibrosis in the sporadic SVD group were not always significantly higher than in control group. Therefore, it is possible that only a subtle increase in vascular fibrosis is required and SVD at mild to moderate grades has a much bigger chronic effect the previously thought indicating severe graded pathology is not always required to instigate severe WML/WMH. This could explain why there was no significant increase of SVD but it still had an influence on WM changes. In order to fully understand the impact of SVD on WMH more detailed histological investigations are warranted.

On the other hand, the vascular measurements included in this study were very limited, inclusive of only vascular fibrosis as a measure of assumed SVD, and only SVD as a vascular measure. There is growing evidence of an association between CAA and the formation of WMH (Gurol et al., 2006, Holland et al., 2008, Smith et al., 2004, Viswanathan et al., 2008). As well as accumulation of Aβ in the vessel walls, CAA is characterized by SMC loss, vessel wall

thickening, luminal narrowing and concentric splitting (Viswanathan and Greenberg, 2011), which can result in disturbed arterial autoregulation that may reduce cerebral perfusion in the penetrating arteries leading to hypoxia, and there for ischemic events, downstream in the WM. Studies have suggested that advanced CAA is associated with higher burdens of WML compared to normal aged controls or patients with just AD (Gurol et al., 2006), and that CAA-related WM is associated with cognitive impairment (Smith et al., 2004, Viswanathan et al., 2008). In this study only vessel wall thickness was quantitatively assessed as a measure of SVD, but it is also a hallmark of CAA. Assessment of CAA was not included in this study due to time constraints, therefore, the possible influence of CAA on WM integrity, especially in the AD group, cannot be ruled out and should be taking into consideration when drawing conclusions on WMH pathogenesis. Furthermore, mechanisms for cerebral ischemia are not just limited to the brain parenchyma. Orthostatic hypotension, a fall in blood pressure when a subject assumes a standing position, may play a role in the development of WMH (Ballard et al., 2000, Colloby et al., 2011, Richardson et al., 2009, Soennesyn et al., 2012). Animal models have demonstrated ischemic WMH as a result of decreases in blood pressure (Pantoni and Garcia, 1997), and an association between the severity of orthostatic systolic blood pressure decrease and WMH volume was previously shown in late-life depression patients (Ballard et al., 2000). Furthermore, thromboembolism results in cerebral vascular occlusion due to a migrating blood clot, which frequently originate in the atrium of the heart as a consequence of atrial fibrillation and ischemic heart disease (Force, 1986), resulting in cerebral infarction. Finally, agonal hypoxia as result of prolonged agonal state has been shown to have an influence on *post mortem* tissue integrity (Monoranu et al., 2009) and, thus, may account for the higher amount of WMH in relation to the amount of SVD. Nevertheless, this study did not take into consideration or account for cardiovascular risk factor or medical history, but these factors should be included in future studies.

6.5.3 Neocortical AD-related pathologies may be a major contributor to WML/WMH pathogenesis in both the normal aged and AD

The control group showed a significant correlation with HPT and Aβ in the frontal lobe and overall hemispheric Aβ significantly correlated with WMH, not with SVD. No conclusions could be drawn from the statistical findings of the AD

cohort; although quantitative assessment yields continuous data that can detect the subtle variations within Braak stage IV and Thal stage 5, it is likely that the cohort was not big enough to draw any statistical conclusions due to the large data spread.

All cases were combined to expose the potential influence of higher amounts of pathology in the AD group. This revealed significant correlations between WMH severity with both HPT and Aβ in all cortical regions and as an overall hemisphere. This was not surprising as WMH were significantly more severe in the AD group and AD cases exhibit a considerable higher amount of cortical pathology compared to controls.

The most noteworthy findings were from the linear regression; HPT was shown to be a significant predictor in the frontal and temporal lobe of controls, and all cortical areas in the full cohort. Overall, both HPT and SVD were predictors of WMH but HPT was statistically strongest. Aβ was also found to be a predictor of WMH score in the parieto-occipital lobe of controls. Of all 3 pathologies investigated, HPT was the most significant predictor of WMH score over the entire cohort. These findings are in agreement with numerous other studies indicating a potential link between HPT pathology and the pathogenesis of WML/WMH. Leys and colleagues observed more severe white matter changes in areas adjacent to cortical areas of high NFT in AD cases (Leys et al., 1991), and Professor Englund found that 42% of AD cases contained non-ischemic subcortical degeneration in the temporal lobes (Englund, 1998). More recently, the Oregon Brain Aging Study (OBAS), a community-dwelling study accessing WMH in 65 years and older, found a greater rate of WMH burden accumulation over time was associated with higher Braak NFT stage, suggestive of a WML formation as a secondary effect to neocortical pathology (Silbert et al., 2012). A neuropathological study at Newcastle University in the oldest old also showed a significant association of higher amounts of frontal WMH with higher NFT Braak stage (Polvikoski et al., 2010). Finally, a DTI based study measured WM diffusion anisotropy in a mouse model of human tauopathy (rTg4510) and controls at various stages of ageing (2.5, 4.5 and 8 months). At 8 months the rTg4510 mice had lower fractional anisotropy (FA) values (reflecting the microstructural integrity of the WM fibers) compared to control mice, suggesting a role of tau pathology in reducing WM integrity (Sahara et al., 2014).

6.5.4 WLD may influence WM integrity in connecting lobes

It is well established that cortical regions and corresponding WM do not work in isolation but are interconnected anatomically in a precise and unique manner by a series of fiber networks facilitating the formation of neural network necessary for core cerebral processes e.g. memory, attention and language. This study also investigated whether cortical and vascular pathologies have an influence on WM changes outside of their regional boundaries.

With respect to the full cohort, frontal HPT significantly correlated with both temporal and parieto-occipital WMH scores, as did parieto-occipital HPT with frontal WMH scores. Furthermore, significant correlations were seen between frontal Aβ and temporal WMH scores and parieto-occipital Aβ and temporal WMH scores. No correlation were seen with temporal lobe pathology, which was unexpected, however it may be because the temporal lobe harbors the highest burden of HPT and Aβ no statistical significance could be found. Linear regression revealed that HPT was a highly significant predictor of WMH score in various connections (Figure 6.5) with no significant influence of SVD. Consequently this study determined that cortical pathology in one region is a potential influencing factor for WM change in another. Association fibers bi-directionally link various cerebral regions of the same hemisphere, specifically long association fibers bundles connect cortex to cortex (Schmahmann and Pandya, 2006). Interestingly, long association fibers arise from pyramidal layers II and III (Nieuwenhuys, 1994) and these neurons are known to be selectively affected by AD pathology especially HPT (Giannakopoulos et al., 1998). The directional influence of HPT seen in this study corresponds to the four main long association bundles; the superior longitudinal fasciculus (SLF) is made up of three sections (horizontal, superior and vertical) projecting from the frontal lobe to the most lateral region of the temporal lobe with a characteristic C-shaped trajectory (Martino et al., 2011, Wakana et al., 2004); the inferior longitudinal fasciculus (ILF) which projects mostly between the occipital lobes and the posterior temporal regions; middle longitudinal fasciculus (MLF) linking the inferior parietal to superior temporal (Schmahmann and Pandya, 2006); and finally the uncinate fasciculus (UF) that connects the limbic regions, including the parahippocampal and entorhinal areas, to the frontal lobe (Wakana et al., 2004) (Figure 6.5). Previous DTI studies have shown abnormalities of the WM

in MCI and early AD patients in the UF and SLF (Masdeu et al., 2012) and a Norwegian longitudinal study compared regional WM changes in MCI patients with pathogenic and non-pathogenic levels of cerebral spinal fluid (CSF) tau and found the MCI group with pathogenic levels of CSF tau had specific WM changes in the SLF and ILF (Amlien et al., 2013). One may speculate that cortical HPT pathology has a selective effect on these fiber bundles, possible due to their origins that might potentially trigger WLD of the axons. However, a detailed histological assessment is required to identify specific fibers types and investigate specific axonal loss in these bundles.

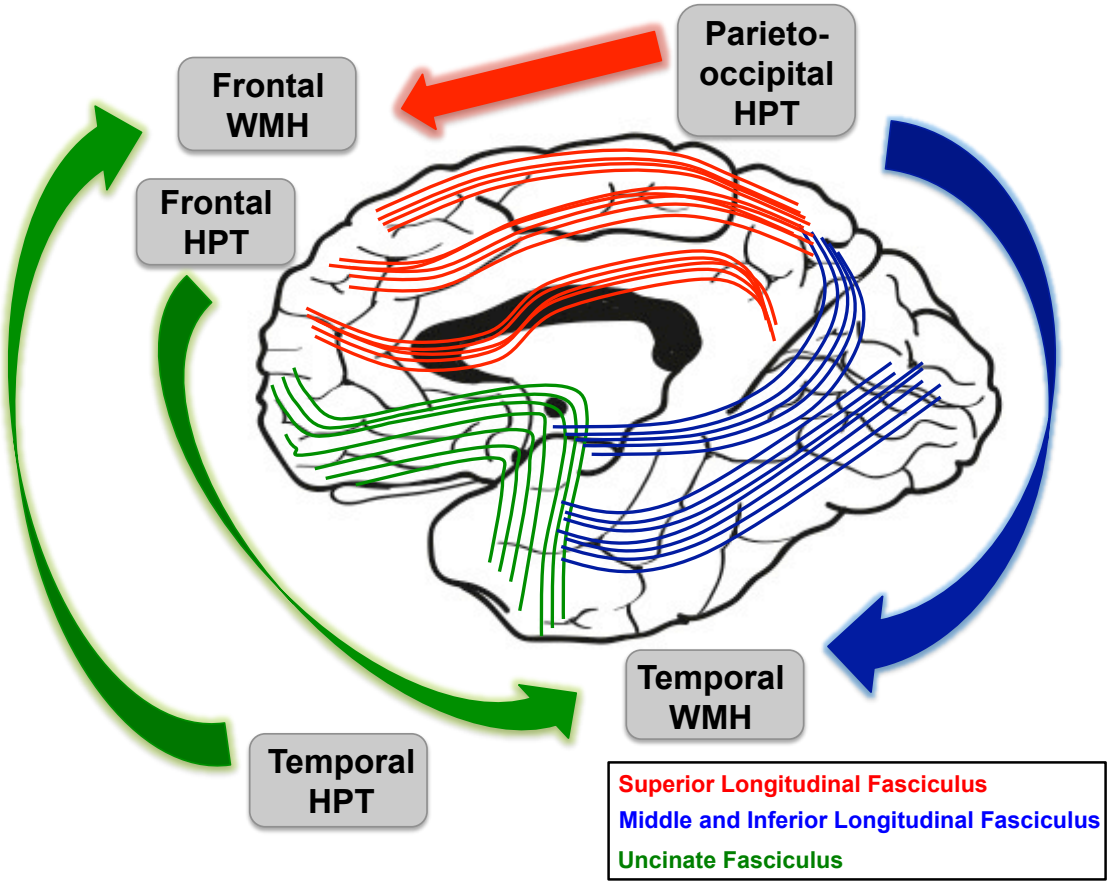

Figure 6.5. Influence of HPT on long association fiber bundles. Data from this study indicated a strong influence of HPT pathology on WM integrity in regions connected by long association fibers. Frontal HPT influenced and temporal WMH score and vice versa with temporal HPT influencing frontal WMH score which may involve the uncinate fasciculus. Parieto-occipital HPT was shown to influence frontal WMH scores indicative of the superior longitudinal fasciculus. Parieto-occipital HPT also has an influence on temporal WMH scores, which may involve the middle and/or inferior longitudinal fasciculus. Arrows indicate the direction of influence. WMH, white matter hyperintensity score; HPT, hyperphosphorylated tau.

6.5.5 Potential involvement of HPT in the triggering of WLD

Although there are numerous studies associating HPT to WML/WMH the exact pathomechanism is still to be elucidated. It has been suggested that HPT accumulation triggers axonal transport failure via various interactions seen in various *in vitro* studies. As previously discussed, tau is an intracellular microtuble-bound protein found in neuronal processes (Ittner et al., 2010) and, in addition to the neuronal soma, APP, Aβ and probably APP-processing enzymes β and γ-secretase have been shown to also reside in axons and dendrites (Lazarov et al., 2002, Wirths et al., 2006). Evidence suggests that physiological tau permits the accumulation of Aβ oligomers (Calkins et al.,

2011, Ittner et al., 2010) and disruption of glycogen synthase kinase 3β (GSK-3β), which in turn disrupts mitochondrial life cycle and mobility, thereby impairing axonal transport. Both changes were found to be tau dependent (Llorens-Martin et al., 2011); decreasing tau prevented Aβ-induced defects in axonal transport in an *in vitro model* of wild type hippocampal neurons (Vossel et al., 2010).

Axonal transport dysfunction has been suggested to activate WLD. Pharmacological studies have indicated that several neurological disorders share the final pathway of Wallerian degeneration, which comprises of extracellular calcium influx, activating the ubiquitous calcium-dependent cysteine protease calpain to degrade the cytoskeleton of the axon (Schlaepfer, 1977, Schlaepf.Ww, 1974) (Figure 6.6). The trigger of calcium influx differs between disorders; in neurodegenerative disorders of the CNS abnormal protein aggregates i.e. HPT and Aβ oligomers directly (via disruption of GSK-3β) and indirectly (via disrupt axonal transport dysfunction) impair mitochondria. Impaired mitochondria leads to a decrease in ATP subsequently activating a cascade of events that reduce ATPase activities and various ion pumps and exchangers in the axon eventually leading to an increase in intra-axonal calcium and activation of calpain (Ikegami and Koike, 2003, Coleman, 2005), resulting in the retrograde degeneration of the axon. WLD, as a secondary consequence of abnormal protein aggregation, may therefore account for the disproportionate loss of axons compared to neurons in both the normal aged and diseased (Freeman et al., 2008, Marner et al., 2003, Pakkenberg and Gundersen, 1997).

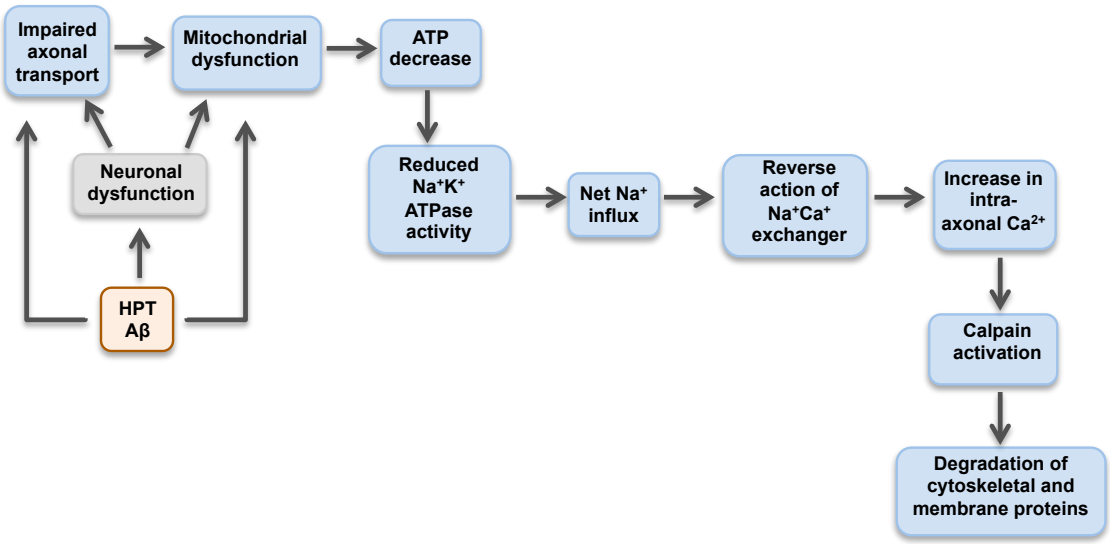

Figure 6.6. Proposed pathway of WLD. It is proposed the accumulation of HPT and A β directly and indirectly leads to neuronal dysfunction, impaired axonal transport from the neuronal soma and mitochondria dysfunction which trigger known mechanisms of axon degeneration via calpain-mediated degradation of axonal cytoskeleton proteins.

6.5.6 Pathogenesis of WML/WMH is likely to be a combination of ischemia and degenerative axonal loss

Although linear regression revealed HPT influences the progression of WMH, it also showed that (in the overall cohort) SVD was also significant predictor of hemispheric WMH score. Two previous studies are in agreement with this finding; Yoshita and colleagues investigated the extent and distribution of WMH using MRI mapping in a cohort of controls, MCI and AD and concluded that spatial differences of hyperintensities between groups may result from the additive effects of vascular and degenerative injury (Yoshita et al., 2006). An additive relationship is a conceivable concept given the very low burden of SVD found in this study, and perhaps it is the addition of neurodegenerative axonal loss that is driving greater WM changes in some cases. Furthermore, a study by Erton-Lyons and colleagues combining longitudinal WMH accumulation data with neuropathological assessment correlates (including NFT Braak stages, myelin pallor, and cardiovascular pathologies i.e. atherosclerosis) from the OBAS cohort, found strong association of both atherosclerosis and NFT Braak score with WMH accumulation over 1 year (Erten-Lyons et al., 2013).

Ischemia may also play a role in the activation of WLD; chronic ischemia is thought to play a key role demyelination that in turn raises the energy demand of the axon (Stys, 1998) potentially exacerbating the decrease in axonal ATP. Furthermore, ischemic injury leads to an increase in intra-axonal calcium via calcium release from intra-cellular stores and blocking of this intracellular release has been show to be axonal protective (Ouardouz et al., 2003).

Cerebral multimorbidity is highly prevalent with multiple neurodegenerative pathologies frequently seen in brains of both demented and non-demented subjects (Alafuzoff, 2013, Attems and Jellinger, 2013a). One of the most common co-pathologies is AD-related and vascular pathology, seen in approximately a third of all neuropathologically confirmed AD cases (Jellinger and Attems, 2007(Ince, 2001, Schneider et al., 2007). Is it likely that the formation of WML/WMH both degenerative and ischemic mechanisms are involved, conceivably in an additive or synergistic relationship, with varying degrees between individuals and disease status.

6.5.7 Limitations

The cohort was limited to 38 cases due to the requirement of *post mortem* MRI, (added to the NBTR diagnostic protocol in 2009) and neuropathological diagnosis.

This study did not histologically investigate axonal loss, axonal fragmentation, demyelination or ischemic markers; it was simple a preliminary study to investigate any potential influence of cortical pathologies and SVD. Therefore all suggested pathogenesis of WML/WMH such as WLD are all proposed mechanism and cannot be confirmed or validated with out future investigations.

It is importantly to note the study did not include neuronal density. Cortical thickness, as a measure of atrophy, was attempted on *post mortem* MRI but was unsuccessful due to indistinct cortical-white matter boarders. Due to time constraints and the TMA methodology not allowing for an accurate measure, neuropathological assessment of neuronal density was not carried. However, due to the interesting findings this will be a vital addition and a control variable in linear regression analysis when investigating the influence of various pathologies.

Although the TMA allows for fast and accurate quantitative assessment of

cortical pathologies it was not without its limitations;

I. Approximately 20% of TMA blocks had single missing punches due to lack of tissue in the diagnostic block. Although AT8 and 4G8 measurements were average values, it still may have influenced scores for some cases.
II. Immunohistochemisty was performed in as few batches as possible to ensure minimal variation in staining intensity. However, staining intensity did vary slightly between cases, which meant imaging thresholds were slightly altered to highlight all pathology and potentially involving subjective bias.
III. Damage to the tissue sections e.g. tears, and anatomical features such as vessels, white matter and space between sulci had to be manually selected and removed from quantitative measurement as not to influence the pathology density. Due to human error it is possible not all anomalies were discovered and removed.

Power calculations estimated 600 per group to detect difference in SVD. A possible reason for this may be failure of the SI methodology to detect difference between groups. SI is a quantitative measure of vessel wall fibrosis which represents the severity of SVD (Lammie et al., 1997) which is assumed to be the main cause of chronic hypoxia and ischemia resulting in WML/WMH (Grinberg and Thal, 2010), therefore, this study assumed SI is representative of all types of vascular pathologies that may lead to ischemic-type WM damage. Although SVD is highly related, other vascular pathologies have also been associated with WML/WMH that where not assessed for; WM changes have been increasing recognized as a feature of sporadic CAA with or without AD with proximal Aβ deposits in penetrating arteries leading to vessel wall destruction, although it is unknown whether deposits alone without atherosclerotic changes are sufficient to cause WML (Greenberg et al., 2004).
One of the main limiting factors of the SI methodology is the ‘diluting’ of SI values i.e. is the mean value a true representation of the degree of vascular pathology. In a given section approximately 8 arteries/arterioles were assessed, however, it may be that only one particular area/vascular branch has higher amounts of pathology but these values will be averaged with the remaining un-affected vessels making it very difficult to see subtle difference between groups.

In future studies, SI should be confined to specific regions of interest e.g. in and around the WML boundary so that an accurate measure of lesion-related vascular pathology can be taken, and combined with additional markers and measurements of ischemic damage and vascular pathologies e.g. plasma protein leakage, SMC loss and microglia activation.

6.6 Conclusion

This study has demonstrated that quantitatively assessed HPT, Aβ and SVD are associated with WM integrity as measured by *post mortem* MRI, suggesting that these pathologies play a role in the pathogenesis of WML. The severity of all three pathologies was found to influence WMH score in a given region in both non-demented normal aged and AD brains. However, HPT was the most significant predictor of WMH score over the entire cohort not SVD that has long been associated with WMH pathogenesis. Furthermore, HPT had a strong influence on WM integrity in regions connected by long association fibers indicating hyperintensities along these fibers may have a different pathogenic mechanism compared to other fibers in the brain. It is presumed HPT triggers WLD in degenerative axonal loss but this remains to be elucidated with an extensive neuropathological investigation. Is it likely that the formation of WML/WMH involve both degenerative and ischemic mechanisms, conceivably in an additive or synergistic relationship, with varying degrees between individuals and disease status.

Chapter 7 – Discussion

7.1 Introduction

The main aim of this study was to improve the *post mortem* assessment of AD-related pathology and WML/WMH in the ageing human brain by the use of *post mortem* MRI and quantitative neuropathological assessment, and to investigate possible associations between AD pathology and WML. The presence of both AD pathology and WML/WMH is one of the most common co-pathologies in the ageing human brain; seen in up to 40% of Alzheimer's disease (AD) cases (O'Sullivan, 2008, Nagata et al., 2012, Schneider et al., 2007) it has been suggested these pathologies have a synergistic relationship with CVL exerting an influence on AD pathology and potentially lower the threshold for dementia (Jellinger and Attems, 2003, Jellinger and Attems, 2007, Schneider et al., 2007).

However, there are two difficulties when investigating CVL and AD-related pathologies. Firstly, due to the lack of standardized histological criteria accurate assessment of SVP is difficult, therefore, the study described in Chapter 3 investigated the use of *post mortem* MRI as a tool in the assessment of WMH, as a reflection of SVP. Secondly, current neuropathological assessment of cortical pathologies is based on subjective-based a semi-quantitative criterion that is based on the grading of pathological amounts not precise measurements. Consequently, the study described in Chapter 4 investigated the use of quantitative neuropathological assessment of AD-related cortical pathology and vascular fibrosis, as a reflection of SVD. A chance observation in the analysis of studies described in Chapter 3 and 4 lead to the discovery of an association of HPT with WMH severity (Chapter 5), in contrast to the widely presumed notion that WML/WMH are the result of CVD. This study was extended, expanding the use of quantitative neuropathological assessment via introduction of the TMA and SI to investigate the influence of cortical pathologies on WM integrity (Chapter 6). The key findings of this study are listed below and discussed in the following subsections:

- MRI-based assessment on fixed *post mortem* brains is a practical method that reliably reflects WML in the frontal, parietal and occipital WM

comparable with an extensive histological assessment at 7-mm intervals.
    - *Post mortem* MRI is not useful for the assessment of lacunes in the DGM
    - *Post mortem* MRI may be used for the gross assessment of temporal WM; interpretation should be inclusive of MTL atrophy
- Current routine diagnostic histological assessment of SVP underrates severity in the WM.
- Digital quantification of 'severe' cortical HPT and Aβ pathology in AD brains revealed variations in pathological burden in all neocortical regions.
- Quantitative neuropathological assessment in AD brains revealed HPT pathology was significantly higher in the temporal cortex compared to the frontal, parietal and occipital cortices.
- Sclerotic Index measurements of vascular fibrosis revealed disparities in pathological burden within semi-quantitative grades of 'mild' and 'moderate' pathology.
- WMH were significantly higher in AD brains compared to normal aged controls.
- No significant difference was seen in SVD between AD and normal aged controls brains.
- HPT, Aβ pathology and SVD had a significant influence on WMH severity in both non-demented normal aged and AD brains.
    - Of all three pathologies, HPT was the most significant predictor of WMH score
- HPT had a significant influence on WMH severity in regions connected by long association fibers

7.2 *Post mortem* MRI

This study established that visual MRI-based assessment on fixed *post mortem* brains is a practical method that reliably reflects SVP i.e. WML, EPVS, in the frontal, parietal and occipital WM, comparable with an extensive histological assessment of the entire WM at 7-mm intervals. Furthermore, this study also confirmed that current routine diagnostic histological assessment of SVP underrates the severity of SVP in the WM, likely due to the limited number of slides assessed. Given the current lack of validated neuropathological

consensus criteria, this study concludes that *post mortem* MRI assessment may be used to assess WM integrity in research and complement diagnostic neuropathological diagnosis. Numerous previous studies have directly compared both *in vivo* and *post mortem* MRI with histological findings to gain a better understanding of the underlying pathological substrates of WMH i.e. 'punctate' hyperintensities correspond to EPVS (Chimowitz et al., 1992, Fazekas et al., 1991) and 'early confluent' and 'confluent' WMH are dependent upon a pathological continuum of myelin and axonal loss (Bronge et al., 2002, Fazekas et al., 1993). Although these studies were specific in their investigation of associations of particular pathologies and hyperintensities, this is the first study to evaluate whether *post mortem* MRI as a reliable method of gross WMH assessment. Of note, this study can make no conclusions on the pathogenesis of WML. Although the study compared radiological images to histological findings, neuropathological criteria assessed perivascular enlargement, demyelination and parenchyma tissue loss that are consequences of a pathogenic process that is assumed to be SVD.

Future improvements to *post mortem* MRI may include the introduction of DTI that detects anisotropy-related alterations of tissue that reflect the coherence of directionally of water diffusion. Various measures of water diffusion can reveal specific information about axonal integrity and the myelin sheath such as demyelination, axonal swelling and fragmentation (Gold et al., 2012). Studies have shown that DTI is feasible in *post mortem* brain tissue (Englund et al., 2004, Gouw et al., 2008, Larsson et al., 2004) and WM changes are more extensively visible on DTI compared to conventional T2-weighted MRI (Larsson et al., 2004). *Post mortem* DTI WM assessment would be a valuable addition to WMH assessment especially when specific types of axonal pathologies are required for future studies such as the elaborating of findings from the study described in Chapter 6.

7.3 Use of quantitative neuropathological assessment

One of the main areas of this thesis was to evaluate the use of digital quantitative neuropathological assessment in order to accurately measure and detect subtle differences in pathology amount that cannot be appreciated using semi-quantitative scoring. The study in Chapter 4 revealed widespread variation and overlap of quantitatively measured cortical HPT and Aβ pathology and

vascular fibrosis within a given semi-quantitative grade. These findings indicated a lack of accuracy and possible influence of assessor bias in semi-quantitative assessment concluding quantitative assessment is a better means of measuring pathological burden. The main hindrance of quantitative assessment was the requirement of large cohort numbers required to gain statistical power. The use of the TMA (Kellner et al., 2009, Sjobeck et al., 2003) was introduced in the final study (Chapter 6); the array format is optimally suited for standardized quantitative analysis at high output (Simon, 2010) which allowed an increase in case numbers and areas assessed. TMA assessment was deemed successful and is to be continually used in future studies.

Quantitative measurements of pathological burden may play a key role in future clinico-pathological studies as it allows the identification cases and/or sub-groups containing a specific level of pathology. Murray and colleagues (Murray et al., 2011b) conducted a large quantitative neuropathological study on 889 cases of confirmed AD (Braak stage IV/V). NFT were quantitatively counted in the hippocampus (CA1 and subiculum) and three association cortices (middle frontal, inferior parietal and superior temporal). Three distinct subtypes of AD were determined: i) 75% of cases were classified as typical AD; ii) 11% of cases were classed as hippocampal sparing that exhibited higher NFT in cortical areas and lower NFT in hippocampal areas when compared to typical AD cases. These cases also had a younger age of death (average 72 ± 10 years) and a higher proportion of them were men; iii) 14% of cases were classified as limbic predominant that exhibited higher NFT in the hippocampus and lower NFT in cortical areas when compared to typical AD cases. These cases were older (average 86 ± 6 years) and a higher proportion of them were women. Identification of clinic-pathological subtypes through quantitative neuropathological assessment could have major implications when designing clinical, genetic and therapeutic studies in AD.

7.4 Influence of cortical pathologies on white matter integrity

Using a combination of *post mortem* MRI WMH assessment and quantitative assessment, subsequent studies investigated associations between cortical and vascular pathologies and WM integrity in a cohort of normal aged controls and AD brains. The study in Chapter 5 showed a significant correlation between quantified temporal HPT and Aβ pathology with WMH severity in cases that

exhibited moderate/severe WMH but absent/mild SVD, that is widely assumed to cause WML (Grinberg and Thal, 2010, Pantoni, 2010, Pantoni and Garcia, 1997). This indicated that SVD might not have been the primary cause of the WMH in some cases due to the large difference in SVD grade and WMH score. This investigation was extended in a larger cohort with the addition of TMA and SI (Chapter 6). The main findings are discussed in more detail below.

7.4.1 Hyperintensities of the deep WM are potential caused by a combination of HPT and SVD

AD brains were found to contain significantly more severe WMH, both overall and in the temporal region, compared to non-demented control brains in agreement with previous studies (Brickman, 2013b, Kalaria, 2000, Rezek et al., 1987, Scheltens et al., 1992). However, no significant difference was seen in SI between the two groups; If SVD were the main pathogenic factor in the formation of WML/WMH an increase in SVD in parallel with increasing WMH severity would be expected. However, it is important to note that the SI measurement is exclusive for vessel wall thickness that is only one aspect of SVD. This measurement is limited and did not take into account the other important aspects of SVD including. For a comprehensive assessment all aspects of SVD need to be assessed including loss of SMC from the vessel wall, plasma protein leakage and BBB, which can be assessed on *post mortem* tissue sections using specific immunohistochemical antibodies and quantitatively assessed using NIS-Elements software. Furthermore, SVD was the only vascular pathology assessed and there is growing evidence of an association between CAA and the formation of WMH (Gurol et al., 2006, Holland et al., 2008, Smith et al., 2004, Viswanathan et al., 2008). As well as the accumulation of Aβ in the vessel walls, CAA is also characterized by vessel wall thickening and luminal narrowing (Viswanathan and Greenberg, 2011), therefore, since assessment of CAA was not included in this study, I was unable to distinguish the possible influence of CAA on WM integrity. It is also important to note that possible causes of ischemic damage outside of the brain e.g. orthostatic hypotension, agonal state and thromboembolism, may also have played a factor in WM integrity, and would not have affected the histological characteristics of the small vessels that were assessed. Therefore, in future studies it is important to include and control for cardiovascular risk factor,

medical history and agonal state.

Interestingly of all 3 pathologies (HPT, Aβ and vascular fibrosis as a measure of SVD) investigated, HPT was the most significant predictor of WMH score in all cortical regions. Both HPT and SVD were predictors of WMH in the total overall WM. These outcomes agree with previous findings that WMH are the product of a combination of both neurodegenerative and vascular pathologies; Yoshita and colleagues concluded that spatial differences of hyperintensities between groups may result from the additive effects of degenerative and vascular injury (Yoshita et al., 2006), and a recent combined neuropathological and radiological study found strong association of both atherosclerosis and NFT Braak score with WMH accumulation over 1 year (Erten-Lyons et al., 2013).

7.4.2 Association fiber bundle connections

This study also determined that AD-related cortical pathology in one region is a potential influencing factor for WM changes outside of their regional boundaries. HPT was a highly significant predictor of WMH scores; significant associations were seen between frontal HPT and temporal WMH score, temporal HPT and frontal WMH score and parieto-occipital HPT with both frontal and temporal WMH scores. No significant influence of SVD was found which one could speculate indicates a possible has a selective effect of HPT, and therefore, a different pathogenic mechanism may be occurring. Cerebral regions of the same hemisphere are bi-directionally linked via long association fibers bundles connect cortex to cortex (Schmahmann and Pandya, 2006). The directional influence of HPT corresponded to the four main long association bundles, including the superior-, middle-, and inferior longitudinal fasciculus and the uncinate fasciculus, that originate from pyramidal neurons in layers II and III (Nieuwenhuys, 1994) that are selectively affected by HPT (Giannakopoulos et al., 1998). A cross-sectional comparison study of DTI regional fractional anisotropy FA values (reflects the microstructural integrity of the WM fibers) demonstrated that independent of vascular risk factors AD patients have significantly lower FA values in the highly organized inter/intra-hemispheric fibers of the CC and SLF compared to MCI and aged controls (Lee et al., 2009). A second DTI-based study compared microstructure integrity of axons in the superior and inferior longitudinal fasciculus 16 AD patients and 14 aged controls and found significantly lower FA values in AD patients compared to aged

controls, especially in the ILF, indicative of a decrease in axonal integrity (Stricker et al., 2009).

7.4.3 Possible patho-mechanisms connecting degenerative pathologies and CVL to WM changes

WLD was discussed in detail in Chapter 6 (section 6.5.5) as a potential patho-mechanism that associates AD-related pathology and WM integrity. The formation of WML/WMH likely involves both degenerative and ischemic mechanisms, however, the exact patho-mechanism that connects the two remains to be elucidated and the determination of how the two are related remains critical.

The most likely scenario is the formation of WML/WMH involves both degenerative and ischemic mechanisms, as AD-related and vascular pathology are one of the most common co-pathologies (Jellinger and Attems, 2007(Ince, 2001, Schneider et al., 2007), conceivably in an additive or synergistic relationship, with varying degrees between individuals and disease status. A previous study showed that spatial differences of hyperintensities between controls, MCI and AD subjects might result from the additive effects of vascular and degenerative injury (Yoshita et al., 2006), a conceivable concept given the very low burden of SVD found in this study, and perhaps it is the addition of neurodegenerative axonal loss that is driving greater WM changes in some cases. Furthermore, a combined neuropathological and radiological study found strong association of both atherosclerosis and NFT Braak score with WMH accumulation over 1 year (Erten-Lyons et al., 2013). The findings in Chapter 6 revealed both HPT and SVD had a significant influence on overall hemispheric WMH score.

A second scenario could be that WMH distribution reflects HPT and Aβ pathology, with WMH being the result of degenerative mechanisms i.e. WLD and axonal degeneration secondary to neuronal death. The findings in the final study numerous associations between AD-related pathology and WMH in all cortical regions independent of SVD. HPT and Aβ pathology are abundant in all neocortical regions of AD brains and highly exhibited in the transentorhinal/entorhinal region in the non-demented aged brain (Braak and Braak, 1991) and therefore, might account for the vast distribution of WMH in all WM regions. In demented subjects, WMH have been shown to be significant

predictor of all types of dementia with population studies showing a 3-fold increase in risk, especially in AD (Debette et al., 2010, Debette and Markus, 2010, Kuller et al., 2003, Prins et al., 2004). The Nun Study, a large longitudinal study of a relatively homogeneous cohort of nuns, showed that those with WML or lacunes had a higher prevalence of dementia compared to those without (Snowdon et al., 1997). Therefore, one may speculate that WMH may be a indicator of underlying neurodegenerative pathology. However, although this study found no strong association with SVD there are copious amounts of evidence indicating a pathogenic link between CVL and ischemia with WMH pathogenesis in the ageing human brain (Grinberg and Thal, 2010).

A third explanation could be that WML/WMH are independent of AD-pathology and represent ischemic damage as a result of hypoperfusion, hypertension and/or metabolic syndromes, e.g. diabetes, which numerous studies have shown (Alosco et al., 2013a, Alosco et al., 2013b, Brickman, 2013a, Brickman et al., 2010, Jefferson et al., 2007, Portet et al., 2012). Gootjes and colleagues (Gootjes et al., 2004b) found similar regional distribution of WMH between AD, VaD and non-demented controls that is indicative of a common vascular pathogenic factor between diseased patients and controls. However, similar to this study, Gootjes and colleagues showed very little association with SVD and WMH and no significant increase was seen in SVD severity between AD and controls, despite a significantly high level of WMH in the AD cohort, therefore a potential secondary mechanism (possibly a degenerative mechanism) may have also played a role in the formation of WMH in the AD cohort. Polvikoski and colleagues investigated the degenerative and vascular process involved in late-onset AD in the Vantaa 85+ population based cohort and concluded that *post mortem* WMH in the frontal WM were associated with NFT Braak stage but as a surrogate of SVD (Polvikoski et al., 2010). However, my final study found very little association with SVD and WMH score in contrast to a vast array of studies. Interestingly, a recent neuropathological study by Craggs and colleagues (Craggs et al., 2013a) extensively measured WM SVD using SI in a familial and sporadic SVD disease cases. The group observed that the level of fibrosis in the sporadic SVD group was not always significantly higher than the control group. This suggests that only a subtle increase in vascular fibrosis may be required i.e. ‘mild’/‘moderate’ grades of pathology, to instigate WML/WMH, possibly indicating severe graded pathology is not always required and that

SVD has a greater chronic effect the previously thought. This may explain why in my study the AD group had higher WMH scores without significantly higher SVD scores; the AD group did exhibit slightly higher SI measurements, therefore, the subtle increase may have been enough to cause more severe WMH. Further in depth histological assessments are required to clarify this.

7.4.4 Future implications

Future studies are required to further elucidate the different patho-physiological mechanisms that may underlie WM damage in the ageing brain. This may lead to the identification of defined patterns of WMH on MRI that are associated with specific pathological mechanisms e.g. posterior dominate WMH in AD (Lee et al., 2009, Lee et al., 2010). A better understanding of these processes in conjunction with future biomarkers may aid clinical decision making in terms of deciding whether WMH are related to underlying vascular pathology, as currently assumed, or a primary cortical neurodegenerative process such as AD or a combination of both, to ensure that patients receive earlier detection and intervention, the most appropriate diagnosis and therapeutics.

7.5 General strengths and limitations

All cases used in this study have undergone *post mortem* WMH assessment, fully neuropathological diagnosis and quantitative neuropathological assessment as part of routine protocol at the NBTR. It is this unique combination of methodologies that has made it possible to deduce relationships between WML/WMH and pathological features on a large number of cases. All subjects were recruited, assessed and all tissue was processed under the same conditions at the NBTR, allowing for reliable comparison between subjects.

Regarding the human tissue there are general limitations; i) immediately after death tissue begins autolysis so PMD must be as short as possible. Although no statistical influence was found in this study the use of PMD as a measure of autolysis is limited as it does not take into account important factors such as temperature i.e. room temperature compared to refrigerated storage and tissue pH, which will influence tissue degradation. Therefore, as with all *post mortem* studies, findings, especially WMH scores, should be carefully considered to ensure they are not reflecting artifacts of *post mortem* interval; ii) fixation of tissues can affect the reliability of *post mortem* MRI due to the dehydration of

the tissue, however, this has been shown to be restored after 3-4 weeks fixation time which all brains underwent (Pfefferbaum et al., 2004, Shepherd et al., 2009); iii) after autopsy, brains are dissected into left and right hemispheres with only the right hemisphere undergoing fixation and hence assessment. The use of one hemisphere for the assessment of SVP in the WM has been shown not significantly influence scores due to the uniform structure (Fazekas et al., 1991). Finally, as with all *post-mortem* studies, the possibility that tissue morphology was affected during tissue processing cannot be rule out. However, all cases in this study were treated and analyzed the same way, therefore all groups should have been equally affected allowing valid comparisons to be made.

Quantification of *post mortem* T2 MR images was attempted using software program 'Sibyl' that measures the percentage area of the WMH on each MR image slice based on pixel count with a subjective grey scale threshold set by the user. However, this assessment was unsuccessful due to time constraints and poor resolution of the MR images, and due the image acquisition that was used the existing *post mortem* MR images were unable to be analyzed for WMH volume by existing software programs. Therefore, all *post mortem* MRI measurements remained semi-quantitative. Quantification of WMH would have allowed for a more accurate and objective global and regional measure which may have revealed more specific regional and local WM changes. However, in order for this to be incorporated into future studies the MRI protocol needs to be changed to allow for volumetric WMH analysis at the time of acquisition, which is both more labour intensive and a financial burden.

7.5.1 Additional factors

Since the start of this study minor changes have to be incorporated to the TMA methodology used in the study described in Chapter 6 for use in future studies; quantitative measurement for this study was performed at x200 magnification that would only allow capture of large image acquisitions at 2x3 covering only one third of the tissue punch, increasing the risk of inter-rater variability. Modifications have included reducing the magnification to x100 to allow for a 3x3 image acquisition and thus, a larger area of the tissue punch to be covered. No changes were made to the methodology during this study but would be incorporated into future investigations. Furthermore, the number of cardiovascular risk factors i.e. hypertension, diabetes etc., and treatments i.e.

antihypertensive, antidepressants, anti-inflammatories, may have also impacted on brain mechanisms contributing to pathological changes. Although assessment of these variables was beyond the scope of my PhD and will be controlled for in future studies, the detailed information available from the NBTR cohort allows the influence of these factors to be investigated.

7.6 Future directions

The Alzheimer's Society has recently confirmed funding for a three-year research project beginning August 2014 that aims to further elucidate the influence of AD-related and vascular pathology on WM integrity. The study will continually use *post mortem* MRI for WMH assessment and TMA, and SI for quantitative neuropathological assessment with the addition of extensive histological investigations detailed in the short-term studies.

7.6.1 Short-term studies

It is vital to distinguish between WML that are primarily associated with neurodegenerative mechanisms i.e. WLD and neuronal loss, and those associated with CVL i.e. SVD

- Measuring neuronal and axonal loss and determining levels of axonal transport dysfunction markers and activation levels of various calcium-dependent proteases involved in neuronal WLD may determine WML that are primarily associated with degenerative axonal loss.
- WML primarily associated with ischemic damage should be evaluated via assessment of ischemic damage markers, hypoxia markers, vessel morphology and BBB alterations and other vascular pathologies e.g. CAA.
- The integrity of neuroglia is vital for cerebral homeostasis, myelin production development, and regulation of neurovascular units, therefore, loss of mature and precursor oligodendrocytes, astrogliosis and activation of microglia should also be evaluated to determine if there are any distinguishable differences between degenerative and ischemic lesions.

7.6.2 Medium and long-term studies

- Once specific patho-physiological mechanisms and morphological differences of degenerative and ischemic WML are determined these

findings can be compared with in-vivo MRI imaging, preferentially DTI. This will give a better understanding of these processes in a clinical setting, helping to determine whether WMH are related to underlying vascular pathology or a primary cortical neurodegenerative process such as AD or a combination of both and ensure that patients receive the most appropriate treatment.

- Clinico-pathological associations should be investigated to identify any specific clinical characteristics within sub-groups exhibiting degenerative, ischemic or both WML.
- Ideally, transgenic mouse models of normal ageing, AD, SVD and mixed AD-SVD will undergo a combined imaging and neuropathological longitudinal study to assess the underlying pathogenic mechanisms of WML development.

7.7 Conclusion

The projected aimed to improve the *post mortem* assessment of WML/WMH and neuropathological lesions and investigate the co-morbidity of AD-related pathology and WML/WMH. This project showed that MRI-based assessment on fixed *post mortem* brains is a practical method that reliably reflects WML in the deep WM and may be used in research and diagnostic neuropathological assessment of WM integrity.

Digital quantitative neuropathological assessment revealed widespread variation in HPT and Aβ pathology and vascular fibrosis within a given semi-quantitative grade and detected subtle differences in the amount of pathology, that are not appreciated using the current semi-quantitative scoring methods.

Investigation into the association of AD-related and vascular pathologies with WMH revealed HPT and Aβ pathology, and SVD had a significant influence on WMH severity in both non-demented normal aged and AD brains, although HPT was the strongest predictor. Extensive histological and radiological studies are required to further elucidate the different patho-physiological mechanisms that may underlie WM damage in the ageing brain. These studies may lead to the identification of defined patterns of WMH on MRI that are associated with specific diseases to ensure patients receive the most appropriate diagnosis and therapeutics.

References

AARSLAND, D., BALLARD, C., MCKEITH, I., PERRY, R. H. & LARSEN, J. P. 2001. Comparison of extrapyramidal signs in dementia with Lewy bodies and Parkinson's disease. *J Neuropsychiatry Clin Neurosci,* 13**,** 374-9.

AARSLAND, D., LITVAN, I., SALMON, D., GALASKO, D., WENTZEL-LARSEN, T. & LARSEN, J. P. 2003. Performance on the dementia rating scale in Parkinson's disease with dementia and dementia with Lewy bodies: comparison with progressive supranuclear palsy and Alzheimer's disease. *J Neurol Neurosurg Psychiatry,* 74**,** 1215-20.

AID 2009. World Alzheimer Report. London.

AID 2010. World Alzheimer Report: The Global economic impact of Dementia.

AID 2013. World Alzheimer Report: Journey of Caring

AN ANALYSIS OF LONG-TERM CARE FOR DEMENTIA. London.

ALAFUZOFF, I. 2013. Alzheimer's disease-related lesions. *J Alzheimers Dis,* 33 Suppl 1**,** S173-9.

ALAFUZOFF, I., ARZBERGER, T., AL-SARRAJ, S., BODI, I., BOGDANOVIC, N., BRAAK, H., BUGIANI, O., DEL-TREDICI, K., FERRER, I., GELPI, E., GIACCONE, G., GRAEBER, M. B., INCE, P., KAMPHORST, W., KING, A., KORKOLOPOULOU, P., KOVACS, G. G., LARIONOV, S., MEYRONET, D., MONORANU, C., PARCHI, P., PATSOURIS, E., ROGGENDORF, W., SEILHEAN, D., TAGLIAVINI, F., STADELMANN, C., STREICHENBERGER, N., THAL, D. R., WHARTON, S. B. & KRETZSCHMAR, H. 2008a. Staging of neurofibrillary pathology in Alzheimer's disease: a study of the BrainNet Europe Consortium. *Brain Pathol,* 18**,** 484-96.

ALAFUZOFF, I., ARZBERGER, T., AL-SARRAJ, S., BODI, I., BOGDANOVIC, N., BRAAK, H., BUGIANI, O., DEL-TREDICI, K., FERRER, I., GELPI, E., GIACCONE, G., GRAEBER, M. B., INCE, P., KAMPHORST, W., KING, A., KORKOLOPOULOU, P., KOVÁCS, G. G., LARIONOV, S., MEYRONET, D., MONORANU, C., PARCHI, P., PATSOURIS, E., ROGGENDORF, W., SEILHEAN, D., TAGLIAVINI, F., STADELMANN, C., STREICHENBERGER, N., THAL, D. R., WHARTON, S. B. & KRETZSCHMAR, H. 2008b. Staging of Neurofibrillary Pathology in Alzheimer's Disease: A Study of the BrainNet Europe Consortium. *Brain Pathology,* 18**,** 484-496.

ALAFUZOFF, I., GELPI, E., AL-SARRAJ, S., ARZBERGER, T., ATTEMS, J., BODI, I., BOGDANOVIC, N., BUDKA, H., BUGIANI, O., ENGLUND, E., FERRER, I., GENTLEMAN, S., GIACCONE, G., GRAEBER, M. B., HORTOBAGYI, T., HOFTBERGER, R., IRONSIDE, J. W., JELLINGER, K., KAVANTZAS, N., KING, A., KORKOLOPOULOU, P., KOVACS, G. G., MEYRONET, D., MONORANU, C., PARCHI, P., PATSOURIS, E., ROGGENDORF, W., ROZEMULLER, A., SEILHEAN, D., STREICHENBERGER, N., THAL, D. R., WHARTON, S. B. & KRETZSCHMAR, H. 2012. The need to unify neuropathological assessments of vascular alterations in the ageing brain: Multicentre survey by the BrainNet Europe consortium. *Exp Gerontol,* 47**,** 825-33.

ALAFUZOFF, I., INCE, P. G., ARZBERGER, T., AL-SARRAJ, S., BELL, J., BODI, I., BOGDANOVIC, N., BUGIANI, O., FERRER, I., GELPI, E., GENTLEMAN, S., GIACCONE, G., IRONSIDE, J. W., KAVANTZAS, N., KING, A., KORKOLOPOULOU, P., KOVACS, G. G., MEYRONET, D., MONORANU, C., PARCHI, P., PARKKINEN, L., PATSOURIS, E.,

ROGGENDORF, W., ROZEMULLER, A., STADELMANN-NESSLER, C., STREICHENBERGER, N., THAL, D. R. & KRETZSCHMAR, H. 2009a. Staging/typing of Lewy body related alpha-synuclein pathology: a study of the BrainNet Europe Consortium. *Acta Neuropathol,* 117**,** 635-52.

ALAFUZOFF, I., THAL, D. R., ARZBERGER, T., BOGDANOVIC, N., AL-SARRAJ, S., BODI, I., BOLUDA, S., BUGIANI, O., DUYCKAERTS, C., GELPI, E., GENTLEMAN, S., GIACCONE, G., GRAEBER, M., HORTOBAGYI, T., HOFTBERGER, R., INCE, P., IRONSIDE, J. W., KAVANTZAS, N., KING, A., KORKOLOPOULOU, P., KOVACS, G. G., MEYRONET, D., MONORANU, C., NILSSON, T., PARCHI, P., PATSOURIS, E., PIKKARAINEN, M., REVESZ, T., ROZEMULLER, A., SEILHEAN, D., SCHULZ-SCHAEFFER, W., STREICHENBERGER, N., WHARTON, S. B. & KRETZSCHMAR, H. 2009b. Assessment of beta-amyloid deposits in human brain: a study of the BrainNet Europe Consortium. *Acta Neuropathol,* 117**,** 309-20.

ALOSCO, M. L., BRICKMAN, A. M., SPITZNAGEL, M. B., GARCIA, S. L. & NARKHEDE, A. 2013a. Cerebral perfusion is associated with white matter hyperintensities in older adults with heart failure. *Congest Heart Fail.***,** 29-34.

ALOSCO, M. L., BRICKMAN, A. M., SPITZNAGEL, M. B., GRIFFITH, E. Y., NARKHEDE, A., RAZ, N., COHEN, R., SWEET, L. H., HUGHES, J., ROSNECK, J. & GUNSTAD, J. 2013b. Independent and interactive effects of blood pressure and cardiac function on brain volume and white matter hyperintensities in heart failure. *Journal of the American Society of Hypertension,* 7**,** 336-343.

ALVAREZ, A., MUNOZ, J. P. & MACCIONI, R. B. 2001. A Cdk5-p35 stable complex is involved in the beta-amyloid-induced deregulation of Cdk5 activity in hippocampal neurons. *Exp Cell Res,* 264**,** 266-74.

ALVAREZ, A., TORO, R., CACERES, A. & MACCIONI, R. B. 1999. Inhibition of tau phosphorylating protein kinase cdk5 prevents beta-amyloid-induced neuronal death. *FEBS Lett,* 459**,** 421-6.

ALZHEIMER, A. 1907. Uber eine eigenartige Erkrankung der Hirnrinde. *Allg Z Psychiat Psych Gerichtl. Med.,***,** 146-148.

AMLIEN, I. K., FJELL, A. M., WALHOVD, K. B., SELNES, P., STENSET, V., GRAMBAITE, R., BJORNERUD, A., DUE-TONNESSEN, P., SKINNINGSRUD, A., GJERSTAD, L., REINVANG, I. & FLADBY, T. 2013. Mild cognitive impairment: cerebrospinal fluid tau biomarker pathologic levels and longitudinal changes in white matter integrity. *Radiology,* 266**,** 295-303.

ANDERSON, J. P., WALKER, D. E., GOLDSTEIN, J. M., DE LAAT, R., BANDUCCI, K., CACCAVELLO, R. J., BARBOUR, R., HUANG, J., KLING, K., LEE, M., DIEP, L., KEIM, P. S., SHEN, X., CHATAWAY, T., SCHLOSSMACHER, M. G., SEUBERT, P., SCHENK, D., SINHA, S., GAI, W. P. & CHILCOTE, T. J. 2006. Phosphorylation of Ser-129 is the dominant pathological modification of alpha-synuclein in familial and sporadic Lewy body disease. *J Biol Chem,* 281**,** 29739-52.

ANDREADIS, A., BROWN, W. M. & KOSIK, K. S. 1992. Structure and novel exons of the human tau gene. *Biochemistry,* 31**,** 10626-33.

APAYDIN, H., AHLSKOG, J. E., PARISI, J. E., BOEVE, B. F. & DICKSON, D. W. 2002. Parkinson disease neuropathology: later-developing dementia and loss of the levodopa response. *Arch Neurol,* 59**,** 102-12.

ARENDS, Y. M., DUYCKAERTS, C., ROZEMULLER, J. M., EIKELENBOOM, P. & HAUW, J. J. 2000. Microglia, amyloid and dementia in alzheimer disease. A correlative study. *Neurobiol Aging,* 21**,** 39-47.

ARMSTRONG, R. A. 2000. Analysis of spatial patterns in histological sections of brain tissue using a method based on regression. *J Neurosci Methods,* 95**,** 39-45.

ARMSTRONG, R. A. 2003. Quantifying the pathology of neurodegenerative disorders: quantitative measurements, sampling strategies and data analysis. *Histopathology,* 42**,** 521-9.

ARMSTRONG, R. A., CARTER, D. & CAIRNS, N. J. 2012. A quantitative study of the neuropathology of 32 sporadic and familial cases of frontotemporal lobar degeneration with TDP-43 proteinopathy (FTLD-TDP). *Neuropathol Appl Neurobiol,* 38**,** 25-38.

ATTEMS, J. & JELLINGER, K. 2013a. Neuropathological correlates of cerebral multimorbidity. *Curr Alzheimer Res,* 10**,** 569-77.

ATTEMS, J. & JELLINGER, K. 2013b. Neuropathology. *Oxford Textbook of old age psychiatry* Oxford University Press.

ATTEMS, J. & JELLINGER, K. A. 2004. Only cerebral capillary amyloid angiopathy correlates with Alzheimer pathology--a pilot study. *Acta Neuropathol,* 107**,** 83-90.

ATTEMS, J. & JELLINGER, K. A. 2006. Hippocampal sclerosis in Alzheimer disease and other dementias. *Neurology,* 66**,** 775.

ATTEMS, J., JELLINGER, K. A. & LINTNER, F. 2005a. Alzheimer's disease pathology influences severity and topographical distribution of cerebral amyloid angiopathy. *Acta Neuropathol,* 110**,** 222-31.

ATTEMS, J., KONIG, C., HUBER, M., LINTNER, F. & JELLINGER, K. A. 2005b. Cause of death in demented and non-demented elderly inpatients; an autopsy study of 308 cases. *J Alzheimers Dis,* 8**,** 57-62.

ATTEMS, J., LAUDA, F. & JELLINGER, K. A. 2008. Unexpectedly low prevalence of intracerebral hemorrhages in sporadic cerebral amyloid angiopathy: an autopsy study. *J Neurol,* 255**,** 70-6.

ATTEMS, J., LINTNER, F. & JELLINGER, K. A. 2005c. Olfactory involvement in aging and Alzheimer's disease: an autopsy study. *J Alzheimers Dis,* 7**,** 149-57; discussion 173-80.

ATTEMS, J., THOMAS, A. & JELLINGER, K. 2012. Correlations between cortical and subcortical tau pathology. *Neuropathol Appl Neurobiol,* 38**,** 582-90.

AWAD, I. A., JOHNSON, P. C., SPETZLER, R. F. & HODAK, J. A. 1986. Incidental subcortical lesions identified on magnetic resonance imaging in the elderly. II. Postmortem pathological correlations. *Stroke,* 17**,** 1090-7.

BABIKIAN, V. & ROPPER, A. H. 1987. Binswanger's disease: a review. *Stroke,* 18**,** 2-12.

BALL, M. J. 1977. Neuronal loss, neurofibrillary tangles and granulovacuolar degeneration in the hippocampus with ageing and dementia. A quantitative study. *Acta Neuropathol,* 37**,** 111-8.

BALL, M. J. & LO, P. 1977. Granulovacuolar degeneration in the ageing brain and in dementia. *J Neuropathol Exp Neurol,* 36**,** 474-87.

BALLARD, C. G., AARSLAND, D., MCKEITH, I., O'BRIEN, J., GRAY, A., CORMACK, F., BURN, D., CASSIDY, T., STARFELDT, R., LARSEN, J. P., BROWN, R. & TOVEE, M. 2002. Fluctuations in attention: PD dementia vs DLB with parkinsonism. *Neurology,* 59**,** 1714-20.

BALLARD, C., O'BRIEN, J., BARBER, B., SCHELTENS, P., SHAW, F., MCKEITH, I. & KENNY, R. A. 2000. Neurocardiovascular instability, hypotensive episodes, and MRI lesions in neurodegenerative dementia. *Ann N Y Acad Sci,* 903**,** 442-5.

BARBER, R., SCHELTENS, P., GHOLKAR, A., BALLARD, C., MCKEITH, I., INCE, P., PERRY, R. & O'BRIEN, J. 1999. White matter lesions on magnetic resonance imaging in dementia with Lewy bodies, Alzheimer's disease, vascular dementia, and normal aging. *J Neurol Neurosurg Psychiatry,* 67**,** 66-72.

BARKER, R., WELLINGTON, D., ESIRI, M. M. & LOVE, S. 2013. Assessing white matter ischemic damage in dementia patients by measurement of myelin proteins. *J Cereb Blood Flow Metab*.

BARULLI, D. & STERN, Y. 2013. Efficiency, capacity, compensation, maintenance, plasticity: emerging concepts in cognitive reserve. *Trends Cogn Sci,* 17**,** 502-9.

BAUNE, B. T., ROESLER, A., KNECHT, S. & BERGER, K. 2009. Single and combined effects of cerebral white matter lesions and lacunar infarctions on cognitive function in an elderly population. *J Gerontol A Biol Sci Med Sci,* 64**,** 118-24.

BEACH, T. G., WILSON, J. R., SUE, L. I., NEWELL, A., POSTON, M., CISNEROS, R., PANDYA, Y., ESH, C., CONNOR, D. J., SABBAGH, M., WALKER, D. G. & ROHER, A. E. 2007. Circle of Willis atherosclerosis: association with Alzheimer's disease, neuritic plaques and neurofibrillary tangles. *Acta Neuropathol,* 113**,** 13-21.

BEIROWSKI, B., NOGRADI, A., BABETTO, E., GARCIA-ALIAS, G. & COLEMAN, M. P. 2010. Mechanisms of axonal spheroid formation in central nervous system Wallerian degeneration. *J Neuropathol Exp Neurol,* 69**,** 455-72.

BERTRAND, E., LECHOWICZ, W., SZPAK, G. M., LEWANDOWSKA, E., DYMECKI, J. & WIERZBA-BOBROWICZ, T. 2004. Limbic neuropathology in idiopathic Parkinson's disease with concomitant dementia. *Folia Neuropathol,* 42**,** 141-50.

BIGIO, E. H., BROWN, D. F. & WHITE, C. L., 3RD 1999. Progressive supranuclear palsy with dementia: cortical pathology. *J Neuropathol Exp Neurol,* 58**,** 359-64.

BOEVE, B. F., SILBER, M. H., FERMAN, T. J., KOKMEN, E., SMITH, G. E., IVNIK, R. J., PARISI, J. E., OLSON, E. J. & PETERSEN, R. C. 1998. REM sleep behavior disorder and degenerative dementia: an association likely reflecting Lewy body disease. *Neurology,* 51**,** 363-70.

BOKURA, H., KOBAYASHI, S. & YAMAGUCHI, S. 1998. Distinguishing silent lacunar infarction from enlarged Virchow-Robin spaces: a magnetic resonance imaging and pathological study. *J Neurol,* 245**,** 116-22.

BRAAK, H., ALAFUZOFF, I., ARZBERGER, T., KRETZSCHMAR, H. & DEL TREDICI, K. 2006. Staging of Alzheimer disease-associated neurofibrillary pathology using paraffin sections and immunocytochemistry. *Acta Neuropathol,* 112**,** 389-404.

BRAAK, H. & BRAAK, E. 1988. Neuropil threads occur in dendrites of tangle-bearing nerve cells. *Neuropathol Appl Neurobiol,* 14**,** 39-44.

BRAAK, H. & BRAAK, E. 1991. Neuropathological stageing of Alzheimer-related changes. *Acta Neuropathol,* 82**,** 239-59.

BRAAK, H. & BRAAK, E. 1996. Evolution of the neuropathology of Alzheimer's disease. *Acta Neurol Scand Suppl,* 165**,** 3-12.

BRAAK, H. & DEL TREDICI, K. 2011. The pathological process underlying Alzheimer's disease in individuals under thirty. *Acta Neuropathol,* 121**,** 171-81.

BRAAK, H., DEL TREDICI, K., RUB, U., DE VOS, R. A., JANSEN STEUR, E. N. & BRAAK, E. 2003. Staging of brain pathology related to sporadic Parkinson's disease. *Neurobiol Aging,* 24**,** 197-211.

BRACCO, L., PICCINI, C., MORETTI, M., MASCALCHI, M., SFORZA, A., NACMIAS, B., CELLINI, E., BAGNOLI, S. & SORBI, S. 2005. Alzheimer's disease: role of size and location of white matter changes in determining cognitive deficits. *Dement Geriatr Cogn Disord,* 20**,** 358-66.

BRAFFMAN, B. H., ZIMMERMAN, R. A., TROJANOWSKI, J. Q., GONATAS, N. K., HICKEY, W. F. & SCHLAEPFER, W. W. 1988. Brain MR: pathologic correlation with gross and histopathology. 1. Lacunar infarction and Virchow-Robin spaces. *AJR Am J Roentgenol,* 151**,** 551-8.

BRICKMAN, A. M. 2013a. Contemplating Alzheimer's disease and the contribution of white matter hyperintensities. *Curr Neurol Neurosci Rep,* 13**,** 415.

BRICKMAN, A. M. 2013b. Contemplating Alzheimer's Disease and the Contribution of White Matter Hyperintensities. *Curr Neurol Neurosci Rep,* 13.

BRICKMAN, A. M., PROVENZANO, F. A., MURASKIN, J., MANLY, J. J., BLUM, S., APA, Z., STERN, Y., BROWN, T. R., LUCHSINGER, J. A. & MAYEUX, R. 2012. Regional white matter hyperintensity volume, not hippocampal atrophy, predicts incident Alzheimer disease in the community. *Arch Neurol,* 69**,** 1621-7.

BRICKMAN, A. M., REITZ, C., LUCHSINGER, J. A., MANLY, J. J., SCHUPF, N., MURASKIN, J., DECARLI, C., BROWN, T. R. & MAYEUX, R. 2010. Long-term Blood Pressure Fluctuation and Cerebrovascular Disease in an Elderly Cohort. *Arch Neurol,* 67**,** 564-569.

BRION, J. P., FLAMENT-DURAND, J. & DUSTIN, P. 1986. Alzheimer's disease and tau proteins. *Lancet,* 2**,** 1098.

BRONGE, L., BOGDANOVIC, N. & WAHLUND, L. O. 2002. Postmortem MRI and histopathology of white matter changes in Alzheimer brains. A quantitative, comparative study. *Dement Geriatr Cogn Disord,* 13**,** 205-12.

BURKE, R. E., DAUER, W. T. & VONSATTEL, J. P. 2008. A critical evaluation of the Braak staging scheme for Parkinson's disease. *Ann Neurol,* 64**,** 485-91.

BURTON, E. J., MCKEITH, I. G., BURN, D. J., FIRBANK, M. J. & O'BRIEN, J. T. 2006. Progression of white matter hyperintensities in Alzheimer disease, dementia with lewy bodies, and Parkinson disease dementia: a comparison with normal aging. *Am J Geriatr Psychiatry,* 14**,** 842-9.

CALKINS, M. J., MANCZAK, M., MAO, P., SHIRENDEB, U. & REDDY, P. H. 2011. Impaired mitochondrial biogenesis, defective axonal transport of mitochondria, abnormal mitochondrial dynamics and synaptic degeneration in a mouse model of Alzheimer's disease. *Hum Mol Genet,* 20**,** 4515-29.

CAPLAN, L. R. & SCHOENE, W. C. 1978. Clinical features of subcortical arteriosclerotic encephalopathy (Binswanger disease). *Neurology,* 28**,** 1206-15.

CAVALLIN, L., BRONGE, L., ZHANG, Y., OKSENGARD, A. R., WAHLUND, L. O., FRATIGLIONI, L. & AXELSSON, R. 2012. Comparison between

visual assessment of MTA and hippocampal volumes in an elderly, non-demented population. *Acta Radiol,* 53**,** 573-9.
CHABRIAT, H., JOUTEL, A., DICHGANS, M., TOURNIER-LASSERVE, E. & BOUSSER, M. G. 2009. Cadasil. *Lancet Neurol,* 8**,** 643-53.
CHALLA, V. R., BELL, M. A. & MOODY, D. M. 1990. A combined hematoxylin-eosin, alkaline phosphatase and high-resolution microradiographic study of lacunes. *Clin Neuropathol,* 9**,** 196-204.
CHALMERS, K., LOVE, S., INCE, E., ESIRI, M., ATTEMS, J., JELLINGER, K., YAMADA, M., MCCARRON, M., JOACHIM, C., FROSCH, M. P., MANN, D. M., NICOLL, J. & THAL, D. M. K., P. 2009. Validation of International consensus criteria for the assessment of cerebral amyloid angiopathing in post-mortem brain. *6th International conference on Vascular Dementia.* Barcelona, Spain.
CHANDRA, S., GALLARDO, G., FERNANDEZ-CHACON, R., SCHLUTER, O. M. & SUDHOF, T. C. 2005. Alpha-synuclein cooperates with CSPalpha in preventing neurodegeneration. *Cell,* 123**,** 383-96.
CHAYER, C. & FREEDMAN, M. 2001. Frontal lobe functions. *Curr Neurol Neurosci Rep,* 1**,** 547-52.
CHEN, J. J., ROSAS, H. D. & SALAT, D. H. 2011. Age-associated reductions in cerebral blood flow are independent from regional atrophy. *Neuroimage,* 55**,** 468-78.
CHIMOWITZ, M. I., ESTES, M. L., FURLAN, A. J. & AWAD, I. A. 1992. Further observations on the pathology of subcortical lesions identified on magnetic resonance imaging. *Arch Neurol,* 49**,** 747-52.
CHRISTIANSEN, P., LARSSON, H. B., THOMSEN, C., WIESLANDER, S. B. & HENRIKSEN, O. 1994. Age dependent white matter lesions and brain volume changes in healthy volunteers. *Acta Radiol,* 35**,** 117-22.
CITRON, M., DIEHL, T. S., GORDON, G., BIERE, A. L., SEUBERT, P. & SELKOE, D. J. 1996. Evidence that the 42- and 40-amino acid forms of amyloid beta protein are generated from the beta-amyloid precursor protein by different protease activities. *Proc Natl Acad Sci U S A,* 93**,** 13170-5.
CLINTON, L. K., BLURTON-JONES, M., MYCZEK, K., TROJANOWSKI, J. Q. & LAFERLA, F. M. 2010. Synergistic Interactions between Abeta, tau, and alpha-synuclein: acceleration of neuropathology and cognitive decline. *J Neurosci,* 30**,** 7281-9.
COLEMAN, M. 2005. Axon degeneration mechanisms: commonality amid diversity. *Nat Rev Neurosci,* 6**,** 889-98.
COLEMAN, M. P. 2013. The challenges of axon survival: Introduction to the special issue on axonal degeneration. *Exp Neurol,* 246**,** 1-5.
COLLOBY, S. J., VASUDEV, A., O'BRIEN, J. T., FIRBANK, M. J., PARRY, S. W. & THOMAS, A. J. 2011. Relationship of orthostatic blood pressure to white matter hyperintensities and subcortical volumes in late-life depression. *Br J Psychiatry,* 199**,** 404-10.
COLOSIMO, C., HUGHES, A. J., KILFORD, L. & LEES, A. J. 2003. Lewy body cortical involvement may not always predict dementia in Parkinson's disease. *J Neurol Neurosurg Psychiatry,* 74**,** 852-6.
COOLICAN, H. 2013. *Research methods and statistics in psycology,* New York, USA, Routledge.
CRAGGS, L. J., HAGEL, C., KUHLENBAEUMER, G., BORJESSON-HANSON, A., ANDERSEN, O., VIITANEN, M., KALIMO, H., MCLEAN, C. A., SLADE, J. Y., HALL, R. A., OAKLEY, A. E., YAMAMOTO, Y.,

DERAMECOURT, V. & KALARIA, R. N. 2013a. Quantitative vascular pathology and phenotyping familial and sporadic cerebral small vessel diseases. *Brain Pathol,* 23**,** 547-57.

CRAGGS, L. J., YAMAMOTO, Y., IHARA, M., FENWICK, R., BURKE, M., OAKLEY, A. E., ROEBER, S., DUERING, M., KRETZSCHMAR, H. & KALARIA, R. N. 2013b. White matter pathology and disconnection in the frontal lobe in CADASIL. *Neuropathol Appl Neurobiol*.

CRAS, P., SMITH, M. A., RICHEY, P. L., SIEDLAK, S. L., MULVIHILL, P. & PERRY, G. 1995. Extracellular neurofibrillary tangles reflect neuronal loss and provide further evidence of extensive protein cross-linking in Alzheimer disease. *Acta Neuropathol,* 89**,** 291-5.

DAMIER, P., HIRSCH, E. C., AGID, Y. & GRAYBIEL, A. M. 1999. The substantia nigra of the human brain. II. Patterns of loss of dopamine-containing neurons in Parkinson's disease. *Brain,* 122 (Pt 8)**,** 1437-48.

DE FELICE, F. G., WU, D., LAMBERT, M. P., FERNANDEZ, S. J., VELASCO, P. T., LACOR, P. N., BIGIO, E. H., JERECIC, J., ACTON, P. J., SHUGHRUE, P. J., CHEN-DODSON, E., KINNEY, G. G. & KLEIN, W. L. 2008. Alzheimer's disease-type neuronal tau hyperphosphorylation induced by A beta oligomers. *Neurobiol Aging,* 29**,** 1334-47.

DE GROOT, J. C., DE LEEUW, F. E., OUDKERK, M., HOFMAN, A., JOLLES, J. & BRETELER, M. M. 2001. Cerebral white matter lesions and subjective cognitive dysfunction: the Rotterdam Scan Study. *Neurology,* 56**,** 1539-45.

DE LEEUW, F. E., KORF, E., BARKHOF, F. & SCHELTENS, P. 2006. White matter lesions are associated with progression of medial temporal lobe atrophy in Alzheimer disease. *Stroke,* 37**,** 2248-52.

DE REUCK, J., AUGER, F., CORDONNIER, C., DERAMECOURT, V., DURIEUX, N., PASQUIER, F., BORDET, R., MAURAGE, C. A. & LEYS, D. 2011. Comparison of 7.0-T T(2)*-magnetic resonance imaging of cerebral bleeds in post-mortem brain sections of Alzheimer patients with their neuropathological correlates. *Cerebrovasc Dis,* 31**,** 511-7.

DEANE, R., SAGARE, A., HAMM, K., PARISI, M., LANE, S., FINN, M. B., HOLTZMAN, D. M. & ZLOKOVIC, B. V. 2008. apoE isoform-specific disruption of amyloid beta peptide clearance from mouse brain. *J Clin Invest,* 118**,** 4002-13.

DEBETTE, S., BEISER, A., DECARLI, C., AU, R., HIMALI, J. J., KELLY-HAYES, M., ROMERO, J. R., KASE, C. S., WOLF, P. A. & SESHADRI, S. 2010. Association of MRI markers of vascular brain injury with incident stroke, mild cognitive impairment, dementia, and mortality: the Framingham Offspring Study. *Stroke,* 41**,** 600-6.

DEBETTE, S. & MARKUS, H. S. 2010. The clinical importance of white matter hyperintensities on brain magnetic resonance imaging: systematic review and meta-analysis. *BMJ,* 341**,** c3666.

DECRESSAC, M., ULUSOY, A., MATTSSON, B., GEORGIEVSKA, B., ROMERO-RAMOS, M., KIRIK, D. & BJORKLUND, A. 2011. GDNF fails to exert neuroprotection in a rat alpha-synuclein model of Parkinson's disease. *Brain,* 134**,** 2302-11.

DELAERE, P., DUYCKAERTS, C., MASTERS, C., BEYREUTHER, K., PIETTE, F. & HAUW, J. J. 1990. Large amounts of neocortical beta A4 deposits without neuritic plaques nor tangles in a psychometrically assessed, non-demented person. *Neurosci Lett,* 116**,** 87-93.

DENG, W., YUE, Q., ROSENBERG, P. A., VOLPE, J. J. & JENSEN, F. E. 2006. Oligodendrocyte excitotoxicity determined by local glutamate accumulation and mitochondrial function. *J Neurochem,* 98**,** 213-22.

DERAMECOURT, V., SLADE, J. Y., OAKLEY, A. E., PERRY, R. H., INCE, P. G., MAURAGE, C. A. & KALARIA, R. N. 2012. Staging and natural history of cerebrovascular pathology in dementia. *Neurology,* 78**,** 1043-50.

DI PAOLA, M., SPALLETTA, G. & CALTAGIRONE, C. 2010. In vivo structural neuroanatomy of corpus callosum in Alzheimer's disease and mild cognitive impairment using different MRI techniques: a review. *J Alzheimers Dis,* 20**,** 67-95.

DICKSON, D. W. 2009. Neuropathology of non-Alzheimer degenerative disorders. *Int J Clin Exp Pathol,* 3**,** 1-23.

DICKSON, D. W. 2012. Parkinson's disease and parkinsonism: neuropathology. *Cold Spring Harb Perspect Med,* 2.

DICKSON, D. W., BERGERON, C., CHIN, S. S., DUYCKAERTS, C., HOROUPIAN, D., IKEDA, K., JELLINGER, K., LANTOS, P. L., LIPPA, C. F., MIRRA, S. S., TABATON, M., VONSATTEL, J. P., WAKABAYASHI, K. & LITVAN, I. 2002. Office of Rare Diseases neuropathologic criteria for corticobasal degeneration. *J Neuropathol Exp Neurol,* 61**,** 935-46.

DICKSON, D. W., CRYSTAL, H. A., MATTIACE, L. A., MASUR, D. M., BLAU, A. D., DAVIES, P., YEN, S. H. & ARONSON, M. K. 1992. Identification of normal and pathological aging in prospectively studied nondemented elderly humans. *Neurobiol Aging,* 13**,** 179-89.

DUGGER, B. N., ADLER, C. H., SHILL, H. A., CAVINESS, J., JACOBSON, S., DRIVER-DUNCKLEY, E. & BEACH, T. G. 2014. Concomitant pathologies among a spectrum of parkinsonian disorders. *Parkinsonism Relat Disord*.

DUYCKAERTS, C., DELATOUR, B. & POTIER, M. C. 2009. Classification and basic pathology of Alzheimer disease. *Acta Neuropathol,* 118**,** 5-36.

DUYCKAERTS, C. & HAUW, J. J. 1997. Prevalence, incidence and duration of Braak's stages in the general population: can we know? *Neurobiol Aging,* 18**,** 362-9; discussion 389-92.

DUYCKAERTS, C., HAUW, J. J., BASTENAIRE, F., PIETTE, F., POULAIN, C., RAINSARD, V., JAVOY-AGID, F. & BERTHAUX, P. 1986. Laminar distribution of neocortical senile plaques in senile dementia of the Alzheimer type. *Acta Neuropathol,* 70**,** 249-56.

EMRE, M., GEULA, C., RANSIL, B. J. & MESULAM, M. M. 1992. The acute neurotoxicity and effects upon cholinergic axons of intracerebrally injected beta-amyloid in the rat brain. *Neurobiol Aging,* 13**,** 553-9.

ENGLUND, E. 1998. Neuropathology of white matter changes in Alzheimer's disease and vascular dementia. *Dement Geriatr Cogn Disord,* 9 Suppl 1**,** 6-12.

ENGLUND, E., BRUN, A. & PERSSON, B. 1987. Correlations between histopathologic white matter changes and proton MR relaxation times in dementia. *Alzheimer Dis Assoc Disord,* 1**,** 156-70.

ENGLUND, E., SJOBECK, M., BROCKSTEDT, S., LATT, J. & LARSSON, E. M. 2004. Diffusion tensor MRI post mortem demonstrated cerebral white matter pathology. *J Neurol,* 251**,** 350-2.

ERTEN-LYONS, D., WOLTJER, R., KAYE, J., MATTEK, N., DODGE, H. H., GREEN, S., TRAN, H., HOWIESON, D. B., WILD, K. & SILBERT, L. C.

2013. Neuropathologic basis of white matter hyperintensity accumulation with advanced age. *Neurology,* 81**,** 977-83.

ESIRI, M., ATTEMS, J., BODI, I., DERAMEOURT, V., HORTOBAGYI, T., JOACHIM, C., KALARIA, R. N., KING, A., MANN, D. M., MORRIS, J. H., NEAL, J., OULHAJ, A. & AL-SARRAJ, S. 2011. The semi-quantitative assessment of subcortical small vessel disease pathology in elderly subjects: an initiative from the UK BD collaboration. *Neuropathol Appl Neurobiol,* 37**,** 1.

ESIRI, M. M., NAGY, Z., SMITH, M. Z., BARNETSON, L. & SMITH, A. D. 1999. Cerebrovascular disease and threshold for dementia in the early stages of Alzheimer's disease. *Lancet,* 354**,** 919-20.

ESIRI, M. M., PEARSON, R. C., STEELE, J. E., BOWEN, D. M. & POWELL, T. P. 1990. A quantitative study of the neurofibrillary tangles and the choline acetyltransferase activity in the cerebral cortex and the amygdala in Alzheimer's disease. *J Neurol Neurosurg Psychiatry,* 53**,** 161-5.

FAUL, F., ERDFELDER, E., BUCHNER, A. & LANG, A. E. 2009. Statistical power analyses using G*Power 3.1: Tests for correlation and regression analyses. *Behaviour Research Methods,* 41**,** 1149-1160.

FAZEKAS, F., KLEINERT, R., OFFENBACHER, H., PAYER, F., SCHMIDT, R., KLEINERT, G., RADNER, H. & LECHNER, H. 1991. The morphologic correlate of incidental punctate white matter hyperintensities on MR images. *AJNR Am J Neuroradiol,* 12**,** 915-21.

FAZEKAS, F., KLEINERT, R., OFFENBACHER, H., SCHMIDT, R., KLEINERT, G., PAYER, F., RADNER, H. & LECHNER, H. 1993. Pathologic correlates of incidental MRI white matter signal hyperintensities. *Neurology,* 43**,** 1683-9.

FEANY, M. B. & DICKSON, D. W. 1995. Widespread cytoskeletal pathology characterizes corticobasal degeneration. *Am J Pathol,* 146**,** 1388-96.

FEIN, J. A., SOKOLOW, S., MILLER, C. A., VINTERS, H. V., YANG, F., COLE, G. M. & GYLYS, K. H. 2008. Co-localization of amyloid beta and tau pathology in Alzheimer's disease synaptosomes. *Am J Pathol,* 172**,** 1683-92.

FERNANDO, M. S., O'BRIEN, J. T., PERRY, R. H., ENGLISH, P., FORSTER, G., MCMEEKIN, W., SLADE, J. Y., GOLKHAR, A., MATTHEWS, F. E., BARBER, R., KALARIA, R. N. & INCE, P. G. 2004. Comparison of the pathology of cerebral white matter with post-mortem magnetic resonance imaging (MRI) in the elderly brain. *Neuropathol Appl Neurobiol,* 30**,** 385-95.

FIRBANK, M. 2014. *RE: Personal communication; post mortem MRI-based visual assessment standards.*

FIRBANK, M. J., BURTON, E. J., BARBER, R., STEPHENS, S., KENNY, R. A., BALLARD, C., KALARIA, R. N. & O'BRIEN, J. T. 2007. Medial temporal atrophy rather than white matter hyperintensities predict cognitive decline in stroke survivors. *Neurobiol Aging,* 28**,** 1664-9.

FORCE, CET. 1986. Cardiogenic brain embolism. Cerebral Embolism Task Force. *Arch Neurol,* 43**,** 71-84.

FREEMAN, S. H., KANDEL, R., CRUZ, L., ROZKALNE, A., NEWELL, K., FROSCH, M. P., HEDLEY-WHYTE, E. T., LOCASCIO, J. J., LIPSITZ, L. A. & HYMAN, B. T. 2008. Preservation of neuronal number despite age-related cortical brain atrophy in elderly subjects without Alzheimer disease. *J Neuropathol Exp Neurol,* 67**,** 1205-12.

G8UK 2013. G8 dementia summit declaration. London, UK.

GALVIN, J. E., LEE, V. M. & TROJANOWSKI, J. Q. 2001. Synucleinopathies: clinical and pathological implications. *Arch Neurol,* 58**,** 186-90.
GARCIA-SIERRA, F., MONDRAGON-RODRIGUEZ, S. & BASURTO-ISLAS, G. 2008. Truncation of tau protein and its pathological significance in Alzheimer's disease. *J Alzheimers Dis,* 14**,** 401-9.
GAZZANIGA, M. S. 2000. Cerebral specialization and interhemispheric communication: does the corpus callosum enable the human condition? *Brain,* 123 (Pt 7)**,** 1293-326.
GENTLEMAN, S. M., ALLSOP, D., BRUTON, C. J., JAGOE, R., POLAK, J. M. & ROBERTS, G. W. 1992. Quantitative differences in the deposition of beta A4 protein in the sulci and gyri of frontal and temporal isocortex in Alzheimer's disease. *Neurosci Lett,* 136**,** 27-30.
GIANNAKOPOULOS, P., HERRMANN, F. R., BUSSIERE, T., BOURAS, C., KOVARI, E., PERL, D. P., MORRISON, J. H., GOLD, G. & HOF, P. R. 2003. Tangle and neuron numbers, but not amyloid load, predict cognitive status in Alzheimer's disease. *Neurology,* 60**,** 1495-500.
GIANNAKOPOULOS, P., HOF, P. R. & BOURAS, C. 1998. Selective vulnerability of neocortical association areas in Alzheimer's disease. *Microsc Res Tech,* 43**,** 16-23.
GIASSON, B. I., DUDA, J. E., MURRAY, I. V., CHEN, Q., SOUZA, J. M., HURTIG, H. I., ISCHIROPOULOS, H., TROJANOWSKI, J. Q. & LEE, V. M. 2000. Oxidative damage linked to neurodegeneration by selective alpha-synuclein nitration in synucleinopathy lesions. *Science,* 290**,** 985-9.
GIASSON, B. I., DUDA, J. E., QUINN, S. M., ZHANG, B., TROJANOWSKI, J. Q. & LEE, V. M. 2002. Neuronal alpha-synucleinopathy with severe movement disorder in mice expressing A53T human alpha-synuclein. *Neuron,* 34**,** 521-33.
GIASSON, B. I., FORMAN, M. S., HIGUCHI, M., GOLBE, L. I., GRAVES, C. L., KOTZBAUER, P. T., TROJANOWSKI, J. Q. & LEE, V. M. 2003. Initiation and synergistic fibrillization of tau and alpha-synuclein. *Science,* 300**,** 636-40.
GIBB, W. R. 1986. Idiopathic Parkinson's disease and the Lewy body disorders. *Neuropathol Appl Neurobiol,* 12**,** 223-34.
GLENNER, G. G. & WONG, C. W. 1984. Alzheimer's disease: initial report of the purification and characterization of a novel cerebrovascular amyloid protein. *Biochem Biophys Res Commun,* 120**,** 885-90.
GOEDERT, M. 2001. Alpha-synuclein and neurodegenerative diseases. *Nat Rev Neurosci,* 2**,** 492-501.
GOEDERT, M., SPILLANTINI, M. G., POTIER, M. C., ULRICH, J. & CROWTHER, R. A. 1989. Cloning and sequencing of the cDNA encoding an isoform of microtubule-associated protein tau containing four tandem repeats: differential expression of tau protein mRNAs in human brain. *EMBO J,* 8**,** 393-9.
GOLD, B. T., JOHNSON, N. F., POWELL, D. K. & SMITH, C. D. 2012. White matter integrity and vulnerability to Alzheimer's disease: preliminary findings and future directions. *Biochim Biophys Acta,* 1822**,** 416-22.
GOMEZ-ISLA, T., HOLLISTER, R., WEST, H., MUI, S., GROWDON, J. H., PETERSEN, R. C., PARISI, J. E. & HYMAN, B. T. 1997. Neuronal loss correlates with but exceeds neurofibrillary tangles in Alzheimer's disease. *Ann Neurol,* 41**,** 17-24.

GONG, C. X., LIU, F., GRUNDKE-IQBAL, I. & IQBAL, K. 2005. Post-translational modifications of tau protein in Alzheimer's disease. *J Neural Transm,* 112**,** 813-38.

GOOTJES, L., TEIPEL, S. J., ZEBUHR, Y., SCHWARZ, R., LEINSINGER, G., SCHELTENS, P., MOLLER, H. J. & HAMPEL, H. 2004a. Regional distribution of white matter hyperintensities in vascular dementia, Alzheimer's disease and healthy aging. *Dement Geriatr Cogn Disord,* 18**,** 180-8.

GOOTJES, L., TEIPEL, S. J., ZEBUHR, Y., SCHWARZ, R., LEINSINGER, G., SCHELTENS, P., MOLLER, H. J. & HAMPEL, H. 2004b. Regional distribution of white matter hyperintensities in vascular dementia, Alzheimer's disease and healthy aging. *Dement Geriatr Cogn Disord,* 18**,** 180-188.

GORELICK, P. B., SCUTERI, A., BLACK, S. E., DECARLI, C., GREENBERG, S. M., IADECOLA, C., LAUNER, L. J., LAURENT, S., LOPEZ, O. L., NYENHUIS, D., PETERSEN, R. C., SCHNEIDER, J. A., TZOURIO, C., ARNETT, D. K., BENNETT, D. A., CHUI, H. C., HIGASHIDA, R. T., LINDQUIST, R., NILSSON, P. M., ROMAN, G. C., SELLKE, F. W. & SESHADRI, S. 2011. Vascular contributions to cognitive impairment and dementia: a statement for healthcare professionals from the american heart association/american stroke association. *Stroke,* 42**,** 2672-713.

GOUW, A. A., SEEWANN, A., VAN DER FLIER, W. M., BARKHOF, F., ROZEMULLER, A. M., SCHELTENS, P. & GEURTS, J. J. 2011. Heterogeneity of small vessel disease: a systematic review of MRI and histopathology correlations. *J Neurol Neurosurg Psychiatry,* 82**,** 126-35.

GOUW, A. A., SEEWANN, A., VRENKEN, H., VAN DER FLIER, W. M., ROZEMULLER, J. M., BARKHOF, F., SCHELTENS, P. & GEURTS, J. J. 2008. Heterogeneity of white matter hyperintensities in Alzheimer's disease: post-mortem quantitative MRI and neuropathology. *Brain,* 131**,** 3286-98.

GRAFTON, S. T., SUMI, S. M., STIMAC, G. K., ALVORD, E. C., JR., SHAW, C. M. & NOCHLIN, D. 1991. Comparison of postmortem magnetic resonance imaging and neuropathologic findings in the cerebral white matter. *Arch Neurol,* 48**,** 293-8.

GREENBERG, S. M., GUROL, M. E., ROSAND, J. & SMITH, E. E. 2004. Amyloid angiopathy-related vascular cognitive impairment. *Stroke,* 35**,** 2616-9.

GRINBERG, L. T. Neuropathological assessment of vascular lesions: pitfalls and challenges. ICVD, 2013 Athens, Greece.

GRINBERG, L. T. & THAL, D. R. 2010. Vascular pathology in the aged human brain. *Acta Neuropathol,* 119**,** 277-90.

GRUNDKE-IQBAL, I., IQBAL, K., QUINLAN, M., TUNG, Y. C., ZAIDI, M. S. & WISNIEWSKI, H. M. 1986. Microtubule-associated protein tau. A component of Alzheimer paired helical filaments. *J Biol Chem,* 261**,** 6084-9.

GUNTERT, A., DOBELI, H. & BOHRMANN, B. 2006. High sensitivity analysis of amyloid-beta peptide composition in amyloid deposits from human and PS2APP mouse brain. *Neuroscience,* 143**,** 461-75.

GUROL, M. E., IRIZARRY, M. C., SMITH, E. E., RAJU, S., DIAZ-ARRASTIA, R., BOTTIGLIERI, T., ROSAND, J., GROWDON, J. H. & GREENBERG, S. M. 2006. Plasma beta-amyloid and white matter lesions in AD, MCI, and cerebral amyloid angiopathy. *Neurology,* 66**,** 23-9.

HACHINSKI, V., IADECOLA, C., PETERSEN, R. C., BRETELER, M. M., NYENHUIS, D. L., BLACK, S. E., POWERS, W. J., DECARLI, C., MERINO, J. G., KALARIA, R. N., VINTERS, H. V., HOLTZMAN, D. M., ROSENBERG, G. A., WALLIN, A., DICHGANS, M., MARLER, J. R. & LEBLANC, G. G. 2006. National Institute of Neurological Disorders and Stroke-Canadian Stroke Network vascular cognitive impairment harmonization standards. *Stroke,* 37**,** 2220-41.

HACHINSKI, V. C., POTTER, P. & MERSKEY, H. 1987. Leuko-araiosis. *Arch Neurol,* 44**,** 21-3.

HALLIDAY, G. M., DOUBLE, K. L., MACDONALD, V. & KRIL, J. J. 2003. Identifying severely atrophic cortical subregions in Alzheimer's disease. *Neurobiol Aging,* 24**,** 797-806.

HARDY, J. 2002. Testing times for the "amyloid cascade hypothesis". *Neurobiol Aging,* 23**,** 1073-4.

HARDY, J. & SELKOE, D. J. 2002. The amyloid hypothesis of Alzheimer's disease: progress and problems on the road to therapeutics. *Science,* 297**,** 353-6.

HARDY, J. A. & HIGGINS, G. A. 1992. Alzheimer's disease: the amyloid cascade hypothesis. *Science,* 256**,** 184-5.

HAUW, J. J., DANIEL, S. E., DICKSON, D., HOROUPIAN, D. S., JELLINGER, K., LANTOS, P. L., MCKEE, A., TABATON, M. & LITVAN, I. 1994. Preliminary NINDS neuropathologic criteria for Steele-Richardson-Olszewski syndrome (progressive supranuclear palsy). *Neurology,* 44**,** 2015-9.

HELMS, G., DRAGANSKI, B., FRACKOWIAK, R., ASHBURNER, J. & WEISKOPF, N. 2009. Improved segmentation of deep brain grey matter structures using magnetization transfer (MT) parameter maps. *Neuroimage,* 47**,** 194-8.

HILLIARD, M. A. 2009. Axonal degeneration and regeneration: a mechanistic tug-of-war. *J Neurochem,* 108**,** 23-32.

HOLLAND, C. M., SMITH, E. E., CSAPO, I., GUROL, M. E., BRYLKA, D. A., KILLIANY, R. J., BLACKER, D., ALBERT, M. S., GUTTMANN, C. R. & GREENBERG, S. M. 2008. Spatial distribution of white-matter hyperintensities in Alzheimer disease, cerebral amyloid angiopathy, and healthy aging. *Stroke,* 39**,** 1127-33.

HOWELL, O. W., RUNDLE, J. L., GARG, A., KOMADA, M., BROPHY, P. J. & REYNOLDS, R. 2010. Activated microglia mediate axoglial disruption that contributes to axonal injury in multiple sclerosis. *J Neuropathol Exp Neurol,* 69**,** 1017-33.

HUSAIN, M. & NACHEV, P. 2007. Space and the parietal cortex. *Trends Cogn Sci,* 11**,** 30-6.

HUTTON, M., LENDON, C. L., RIZZU, P., BAKER, M., FROELICH, S., HOULDEN, H., PICKERING-BROWN, S., CHAKRAVERTY, S., ISAACS, A., GROVER, A., HACKETT, J., ADAMSON, J., LINCOLN, S., DICKSON, D., DAVIES, P., PETERSEN, R. C., STEVENS, M., DE GRAAFF, E., WAUTERS, E., VAN BAREN, J., HILLEBRAND, M., JOOSSE, M., KWON, J. M., NOWOTNY, P., CHE, L. K., NORTON, J., MORRIS, J. C., REED, L. A., TROJANOWSKI, J., BASUN, H., LANNFELT, L., NEYSTAT, M., FAHN, S., DARK, F., TANNENBERG, T., DODD, P. R., HAYWARD, N., KWOK, J. B., SCHOFIELD, P. R., ANDREADIS, A., SNOWDEN, J., CRAUFURD, D., NEARY, D., OWEN,

F., OOSTRA, B. A., HARDY, J., GOATE, A., VAN SWIETEN, J., MANN, D., LYNCH, T. & HEUTINK, P. 1998. Association of missense and 5'-splice-site mutations in tau with the inherited dementia FTDP-17. *Nature,* 393**,** 702-5.

HYMAN, B. T. 1998. New neuropathological criteria for Alzheimer disease. *Arch Neurol,* 55**,** 1174-6.

IKEGAMI, K. & KOIKE, T. 2003. Non-apoptotic neurite degeneration in apoptotic neuronal death: Pivotal role of mitochondrial function in neurites. *Neuroscience,* 122**,** 617-626.

INCE, P. G. 2001. Pathological correlates of late-onset dementia in a multicentre, community-based population in England and Wales. Neuropathology Group of the Medical Research Council Cognitive Function and Ageing Study (MRC CFAS). *Lancet,* 357**,** 169-75.

INCE, P. G. 2005. Acquired forms of Vascular Dementia. *In:* KALIMO, H. (ed.) *Pathology and genetics: Cerebrovascular Diseases.* Sweden: International Society of Neuropathology.

IQBAL, K., GRUNDKE-IQBAL, I., ZAIDI, T., MERZ, P. A., WEN, G. Y., SHAIKH, S. S., WISNIEWSKI, H. M., ALAFUZOFF, I. & WINBLAD, B. 1986. Defective brain microtubule assembly in Alzheimer's disease. *Lancet,* 2**,** 421-6.

ISHIHARA, T., HONG, M., ZHANG, B., NAKAGAWA, Y., LEE, M. K., TROJANOWSKI, J. Q. & LEE, V. M. 1999. Age-dependent emergence and progression of a tauopathy in transgenic mice overexpressing the shortest human tau isoform. *Neuron,* 24**,** 751-62.

ITTNER, L. M. & GOTZ, J. 2011. Amyloid-beta and tau--a toxic pas de deux in Alzheimer's disease. *Nat Rev Neurosci,* 12**,** 65-72.

ITTNER, L. M., KE, Y. D., DELERUE, F., BI, M., GLADBACH, A., VAN EERSEL, J., WOLFING, H., CHIENG, B. C., CHRISTIE, M. J., NAPIER, I. A., ECKERT, A., STAUFENBIEL, M., HARDEMAN, E. & GOTZ, J. 2010. Dendritic function of tau mediates amyloid-beta toxicity in Alzheimer's disease mouse models. *Cell,* 142**,** 387-97.

JANKOVIC, J. 2008. Parkinson's disease: clinical features and diagnosis. *J Neurol Neurosurg Psychiatry,* 79**,** 368-76.

JEFFERIES, K. & ARGRAWAL, N. 2009. Early-onset dementia. *Adv Psychiatr Treat,* 15**,** 380-388.

JEFFERSON, A. L., TATE, D. F., POPPAS, A., BRICKMAN, A. M., PAUL, R. H., GUNSTAD, J. & COHEN, R. A. 2007. Lower cardiac output is associated with greater white matter hyperintensities in older adults with cardiovascular disease. *J Am Geriatr Soc,* 55**,** 1044-1048.

JELLINGER, K. A. 2007. The enigma of vascular cognitive disorder and vascular dementia. *Acta Neuropathol,* 113**,** 349-88.

JELLINGER, K. A. 2008. Morphologic diagnosis of "vascular dementia" - a critical update. *J Neurol Sci,* 270**,** 1-12.

JELLINGER, K. A. 2009. A critical evaluation of current staging of alpha-synuclein pathology in Lewy body disorders. *Biochim Biophys Acta,* 1792**,** 730-40.

JELLINGER, K. A. 2010. Basic mechanisms of neurodegeneration: a critical update. *J Cell Mol Med,* 14**,** 457-87.

JELLINGER, K. A. 2012. Neuropathology of sporadic Parkinson's disease: evaluation and changes of concepts. *Mov Disord,* 27**,** 8-30.

JELLINGER, K. A. 2013. Pathology and pathogenesis of vascular cognitive impairment-a critical update. *Front Aging Neurosci,* 5**,** 17.

JELLINGER, K. A. & ATTEMS, J. 2003. Incidence of cerebrovascular lesions in Alzheimer's disease: a postmortem study. *Acta Neuropathol,* 105**,** 14-7.
JELLINGER, K. A. & ATTEMS, J. 2007. Neuropathological evaluation of mixed dementia. *J Neurol Sci,* 257**,** 80-7.
JELLINGER, K. A. & ATTEMS, J. 2008. Prevalence and impact of vascular and Alzheimer pathologies in Lewy body disease. *Acta Neuropathol,* 115**,** 427-36.
JELLINGER, K. A. & ATTEMS, J. 2010a. Prevalence and pathology of vascular dementia in the oldest-old. *J Alzheimers Dis,* 21**,** 1283-93.
JELLINGER, K. A. & ATTEMS, J. 2010b. Prevalence of dementia disorders in the oldest-old: an autopsy study. *Acta Neuropathol,* 119**,** 421-33.
JELLINGER, K. A. & ATTEMS, J. 2012. Neuropathology and general autopsy findings in nondemented aged subjects. *Clin Neuropathol,* 31**,** 87-98.
KALARIA, R. N. 2000. The role of cerebral ischemia in Alzheimer's disease. *Neurobiol Aging,* 21**,** 321-30.
KALARIA, R. N., KENNY, R. A., BALLARD, C. G., PERRY, R., INCE, P. & POLVIKOSKI, T. 2004. Towards defining the neuropathological substrates of vascular dementia. *J Neurol Sci,* 226**,** 75-80.
KALIMO, H. 2005. *Pathology and genetics: Cerebrovascular Diseases,* Basel, Switerland, Internation Society of Neuropathology.
KAMAL, A., ALMENAR-QUERALT, A., LEBLANC, J. F., ROBERTS, E. A. & GOLDSTEIN, L. S. 2001. Kinesin-mediated axonal transport of a membrane compartment containing beta-secretase and presenilin-1 requires APP. *Nature,* 414**,** 643-8.
KARRAN, E., MERCKEN, M. & DE STROOPER, B. 2011. The amyloid cascade hypothesis for Alzheimer's disease: an appraisal for the development of therapeutics. *Nat Rev Drug Discov,* 10**,** 698-712.
KELLNER, A., MATSCHKE, J., BERNREUTHER, C., MOCH, H., FERRER, I. & GLATZEL, M. 2009. Autoantibodies against beta-amyloid are common in Alzheimer's disease and help control plaque burden. *Ann Neurol,* 65**,** 24-31.
KERTESZ, A., MARTINEZ-LAGE, P., DAVIDSON, W. & MUNOZ, D. G. 2000. The corticobasal degeneration syndrome overlaps progressive aphasia and frontotemporal dementia. *Neurology,* 55**,** 1368-75.
KILINC, D., PEYRIN, J. M., SOUBEYRE, V., MAGNIFICO, S., SAIAS, L., VIOVY, J. L. & BRUGG, B. 2011. Wallerian-like degeneration of central neurons after synchronized and geometrically registered mass axotomy in a three-compartmental microfluidic chip. *Neurotox Res,* 19**,** 149-61.
KOGA, H., TAKASHIMA, Y., MURAKAWA, R., UCHINO, A., YUZURIHA, T. & YAO, H. 2009. Cognitive consequences of multiple lacunes and leukoaraiosis as vascular cognitive impairment in community-dwelling elderly individuals. *J Stroke Cerebrovasc Dis,* 18**,** 32-7.
KOMORI, T., ARAI, N., ODA, M., NAKAYAMA, H., MORI, H., YAGISHITA, S., TAKAHASHI, T., AMANO, N., MURAYAMA, S., MURAKAMI, S., SHIBATA, N., KOBAYASHI, M., SASAKI, S. & IWATA, M. 1998. Astrocytic plaques and tufts of abnormal fibers do not coexist in corticobasal degeneration and progressive supranuclear palsy. *Acta Neuropathol,* 96**,** 401-8.
KONONEN, J., BUBENDORF, L., KALLIONIEMI, A., BARLUND, M., SCHRAML, P., LEIGHTON, S., TORHORST, J., MIHATSCH, M. J., SAUTER, G. & KALLIONIEMI, O. P. 1998. Tissue microarrays for high-throughput molecular profiling of tumor specimens. *Nat Med,* 4**,** 844-7.

KOVACS, G. G., ALAFUZOFF, I., AL-SARRAJ, S., ARZBERGER, T., BOGDANOVIC, N., CAPELLARI, S., FERRER, I., GELPI, E., KOVARI, V., KRETZSCHMAR, H., NAGY, Z., PARCHI, P., SEILHEAN, D., SOININEN, H., TROAKES, C. & BUDKA, H. 2008. Mixed brain pathologies in dementia: the BrainNet Europe consortium experience. *Dement Geriatr Cogn Disord,* 26**,** 343-50.

KSIEZAK-REDING, H., LIU, W. K. & YEN, S. H. 1992. Phosphate analysis and dephosphorylation of modified tau associated with paired helical filaments. *Brain Res,* 597**,** 209-19.

KULLER, L. H., LOPEZ, O. L., NEWMAN, A., BEAUCHAMP, N. J., BURKE, G., DULBERG, C., FITZPATRICK, A., FRIED, L. & HAAN, M. N. 2003. Risk factors for dementia in the cardiovascular health cognition study. *Neuroepidemiology,* 22**,** 13-22.

LAKEY, L. 2012. Dementia 2012: A national challenge.

LAMMIE, G. A., BRANNAN, F., SLATTERY, J. & WARLOW, C. 1997. Nonhypertensive cerebral small-vessel disease. An autopsy study. *Stroke,* 28**,** 2222-9.

LAPOINTE, N. E., MORFINI, G., PIGINO, G., GAISINA, I. N., KOZIKOWSKI, A. P., BINDER, L. I. & BRADY, S. T. 2009. The amino terminus of tau inhibits kinesin-dependent axonal transport: implications for filament toxicity. *J Neurosci Res,* 87**,** 440-51.

LARIONOV, S., DEDECK, O., BIRKENMEIER, G., ORANTES, M., GHEBREMEDHIN, E. & THAL, D. R. 2006. The intronic deletion polymorphism of the Alpha2- macroglobulin gene modulates the severity and extent of atherosclerosis in the circle of Willis. *Neuropathol Appl Neurobiol,* 32**,** 451-4.

LARSSON, E. M., ENGLUND, E., SJOBECK, M., LATT, J. & BROCKSTEDT, S. 2004. MRI with diffusion tensor imaging post-mortem at 3.0 T in a patient with frontotemporal dementia. *Dement Geriatr Cogn Disord,* 17**,** 316-9.

LAZAROV, O., LEE, M., PETERSON, D. A. & SISODIA, S. S. 2002. Evidence that synaptically released beta-amyloid accumulates as extracellular deposits in the hippocampus of transgenic mice. *J Neurosci,* 22**,** 9785-93.

LEE, D. Y., FLETCHER, E., MARTINEZ, O., ORTEGA, M., ZOZULYA, N., KIM, J., TRAN, J., BUONOCORE, M., CARMICHAEL, O. & DECARLI, C. 2009. Regional pattern of white matter microstructural changes in normal aging, MCI, and AD. *Neurology,* 73**,** 1722-8.

LEE, D. Y., FLETCHER, E., MARTINEZ, O., ZOZULYA, N., KIM, J., TRAN, J., BUONOCORE, M., CARMICHAEL, O. & DECARLI, C. 2010. Vascular and degenerative processes differentially affect regional interhemispheric connections in normal aging, mild cognitive impairment, and Alzheimer disease. *Stroke,* 41**,** 1791-7.

LEWIS, D. A., CAMPBELL, M. J. & MORRISON, J. H. 1987. Laminar and regional distributions of neurofibrillary tangles and neuritic plaques in Alzheimer's disease: a quantitative study of visual and auditory cortices. *Journal of NeuroSci,* 7**,** 1799-1808.

LEYS, D., PRUVO, J. P., PARENT, M., VERMERSCH, P., SOETAERT, G., STEINLING, M., DELACOURTE, A., DEFOSSEZ, A., RAPOPORT, A., CLARISSE, J. & ET AL. 1991. Could Wallerian degeneration contribute to "leuko-araiosis" in subjects free of any vascular disorder? *J Neurol Neurosurg Psychiatry,* 54**,** 46-50.

LINDWALL, G. & COLE, R. D. 1984. Phosphorylation affects the ability of tau protein to promote microtubule assembly. *J Biol Chem,* 259**,** 5301-5.

LITVAN, I., GRIMES, D. A. & LANG, A. E. 2000. Phenotypes and prognosis: clinicopathologic studies of corticobasal degeneration. *Adv Neurol,* 82**,** 183-96.

LLORENS-MARTIN, M., LOPEZ-DOMENECH, G., SORIANO, E. & AVILA, J. 2011. GSK3beta is involved in the relief of mitochondria pausing in a Tau-dependent manner. *Plos One,* 6**,** e27686.

LOCKHART, A., LAMB, J. R., OSREDKAR, T., SUE, L. I., JOYCE, J. N., YE, L., LIBRI, V., LEPPERT, D. & BEACH, T. G. 2007. PIB is a non-specific imaging marker of amyloid-beta (Abeta) peptide-related cerebral amyloidosis. *Brain,* 130**,** 2607-15.

LONGSTRETH, W. T., JR., BERNICK, C., MANOLIO, T. A., BRYAN, N., JUNGREIS, C. A. & PRICE, T. R. 1998. Lacunar infarcts defined by magnetic resonance imaging of 3660 elderly people: the Cardiovascular Health Study. *Arch Neurol,* 55**,** 1217-25.

LOW, W. C., JUNNA, M., BORJESSON-HANSON, A., MORRIS, C. M., MOSS, T. H., STEVENS, D. L., ST CLAIR, D., MIZUNO, T., ZHANG, W. W., MYKKANEN, K., WAHLSTROM, J., ANDERSEN, O., KALIMO, H., VIITANEN, M. & KALARIA, R. N. 2007. Hereditary multi-infarct dementia of the Swedish type is a novel disorder different from NOTCH3 causing CADASIL. *Brain,* 130**,** 357-67.

LUSIS, A. J., MAR, R. & PAJUKANTA, P. 2004. Genetics of atherosclerosis. *Annu Rev Genomics Hum Genet,* 5**,** 189-218.

MA, M., FERGUSON, T. A., SCHOCH, K. M., LI, J., QIAN, Y., SHOFER, F. S., SAATMAN, K. E. & NEUMAR, R. W. 2013. Calpains mediate axonal cytoskeleton disintegration during Wallerian degeneration. *Neurobiol Dis,* 56**,** 34-46.

MACCIONI, R. B. & CAMBIAZO, V. 1995. Role of microtubule-associated proteins in the control of microtubule assembly. *Physiol Rev,* 75**,** 835-64.

MACCIONI, R. B., MUNOZ, J. P. & BARBEITO, L. 2001. The molecular bases of Alzheimer's disease and other neurodegenerative disorders. *Arch Med Res,* 32**,** 367-81.

MACK, T. G., REINER, M., BEIROWSKI, B., MI, W., EMANUELLI, M., WAGNER, D., THOMSON, D., GILLINGWATER, T., COURT, F., CONFORTI, L., FERNANDO, F. S., TARLTON, A., ANDRESSEN, C., ADDICKS, K., MAGNI, G., RIBCHESTER, R. R., PERRY, V. H. & COLEMAN, M. P. 2001. Wallerian degeneration of injured axons and synapses is delayed by a Ube4b/Nmnat chimeric gene. *Nat Neurosci,* 4**,** 1199-206.

MAHLEY, R. W. 1988. Apolipoprotein E: cholesterol transport protein with expanding role in cell biology. *Science,* 240**,** 622-30.

MANDELKOW, E. M., BIERNAT, J., DREWES, G., GUSTKE, N., TRINCZEK, B. & MANDELKOW, E. 1995. Tau domains, phosphorylation, and interactions with microtubules. *Neurobiol Aging,* 16**,** 355-62; discussion 362-3.

MARNER, L., NYENGAARD, J. R., TANG, Y. & PAKKENBERG, B. 2003. Marked loss of myelinated nerve fibers in the human brain with age. *J Comp Neurol,* 462**,** 144-52.

MARSHALL, V. G., BRADLEY, W. G., JR., MARSHALL, C. E., BHOOPAT, T. & RHODES, R. H. 1988. Deep white matter infarction: correlation of MR imaging and histopathologic findings. *Radiology,* 167**,** 517-22.

MARTINO, J., DE WITT HAMER, P. C., VERGANI, F., BROGNA, C., DE LUCAS, E. M., VAZQUEZ-BARQUERO, A., GARCIA-PORRERO, J. A. & DUFFAU, H. 2011. Cortex-sparing fiber dissection: an improved method for the study of white matter anatomy in the human brain. *J Anat,* 219**,** 531-41.

MASDEU, J. C., KREISL, W. C. & BERMAN, K. F. 2012. The neurobiology of Alzheimer disease defined by neuroimaging. *Curr Opin Neurol,* 25**,** 410-20.

MASLIAH, E., MILLER, A. & TERRY, R. D. 1993. The synaptic organization of the neocortex in Alzheimer's disease. *Med Hypotheses,* 41**,** 334-40.

MATSUSUE, E., SUGIHARA, S., FUJII, S., OHAMA, E., KINOSHITA, T. & OGAWA, T. 2006. White matter changes in elderly people: MR-pathologic correlations. *Magn Reson Med Sci,* 5**,** 99-104.

MAYEUX, R. & STERN, Y. 2012. Epidemiology of Alzheimer disease. *Cold Spring Harb Perspect Med,* 2.

MAZUR-KOLECKA, B., DICKSON, D. & FRACKOWIAK, J. 2006. Induction of vascular amyloidosis-beta by oxidative stress depends on APOE genotype. *Neurobiol Aging,* 27**,** 804-14.

MCALEESE, K. E., FIRBANK, M., HUNTER, D., SUN, L., HALL, R., NEAL, J. W., MANN, D. M., ESIRI, M., JELLINGER, K. A., O'BRIEN, J. T. & ATTEMS, J. 2012. Magnetic resonance imaging of fixed post mortem brains reliably reflects subcortical vascular pathology of frontal, parietal and occipital white matter. *Neuropathol Appl Neurobiol*.

MCKEITH, I. G., DICKSON, D. W., LOWE, J., EMRE, M., O'BRIEN, J. T., FELDMAN, H., CUMMINGS, J., DUDA, J. E., LIPPA, C., PERRY, E. K., AARSLAND, D., ARAI, H., BALLARD, C. G., BOEVE, B., BURN, D. J., COSTA, D., DEL SER, T., DUBOIS, B., GALASKO, D., GAUTHIER, S., GOETZ, C. G., GOMEZ-TORTOSA, E., HALLIDAY, G., HANSEN, L. A., HARDY, J., IWATSUBO, T., KALARIA, R. N., KAUFER, D., KENNY, R. A., KORCZYN, A., KOSAKA, K., LEE, V. M., LEES, A., LITVAN, I., LONDOS, E., LOPEZ, O. L., MINOSHIMA, S., MIZUNO, Y., MOLINA, J. A., MUKAETOVA-LADINSKA, E. B., PASQUIER, F., PERRY, R. H., SCHULZ, J. B., TROJANOWSKI, J. Q. & YAMADA, M. 2005. Diagnosis and management of dementia with Lewy bodies: third report of the DLB Consortium. *Neurology,* 65**,** 1863-72.

MCPARLAND, P., MCALEESE, K. E., WALKER, L., JOHNSON, M. & ATTEMS, J. 2014a. Quantitative-tissue microarray in neuropathology. *In Prep*.

MCPARLAND, S., MCALEESE, K. E., WALKER, L., JOHNSON, M., FIELDER, E., KNOWLES, I. & ATTEMS, J. 2013. Tissue Microarray in the quantification of hyper-phosphorylated tau, amyloid-beta and alpha-synuclein. *114th British Neuropathological Society meeting.* London, UK.

MCPARLAND, S., THOMAS, A. & ATTEMS, J. 2014b. Cingulate and parietal Lewy pathology are asscoaited with neuropyschiatric features of dementia with Lewy bodies. *In:* MALEK, M. A. (ed.) *115th Meeting of British Neuropathological Society.* London, UK: Wiley Blackwell.

MEIER, I. B., MANLY, J., PROVENZANO, F. A., HECTOR, J., WASSERMAN, B. T. & LOUIE, K. 2011. White matter predictors of cognitive functioning. *Annual meeting of International Neuropsychological Society.* Boston, MA.

MEIER, I. B., MANLY, J. J., PROVENZANO, F. A., LOUIE, K. S., WASSERMAN, B. T., GRIFFITH, E. Y., HECTOR, J. T., ALLOCCO, E. &

BRICKMAN, A. M. 2012. White matter predictors of cognitive functioning in older adults. *J Int Neuropsychol Soc,* 18**,** 414-27.

METCALFE, M. J. & FIGUEIREDO-PEREIRA, M. E. 2010. Relationship between tau pathology and neuroinflammation in Alzheimer's disease. *Mt Sinai J Med,* 77**,** 50-8.

MIRRA, S. S., HEYMAN, A., MCKEEL, D., SUMI, S. M., CRAIN, B. J., BROWNLEE, L. M., VOGEL, F. S., HUGHES, J. P., VAN BELLE, G. & BERG, L. 1991. The Consortium to Establish a Registry for Alzheimer's Disease (CERAD). Part II. Standardization of the neuropathologic assessment of Alzheimer's disease. *Neurology,* 41**,** 479-86.

MONORANU, C. M., APFELBACHER, M., GRUNBLATT, E., PUPPE, B., ALAFUZOFF, I., FERRER, I., AL-SARAJ, S., KEYVANI, K., SCHMITT, A., FALKAI, P., SCHITTENHELM, J., HALLIDAY, G., KRIL, J., HARPER, C., MCLEAN, C., RIEDERER, P. & ROGGENDORF, W. 2009. pH measurement as quality control on human post mortem brain tissue: a study of the BrainNet Europe consortium. *Neuropathol Appl Neurobiol,* 35**,** 329-37.

MONTINE, T. J., PHELPS, C. H., BEACH, T. G., BIGIO, E. H., CAIRNS, N. J., DICKSON, D. W., DUYCKAERTS, C., FROSCH, M. P., MASLIAH, E., MIRRA, S. S., NELSON, P. T., SCHNEIDER, J. A., THAL, D. R., TROJANOWSKI, J. Q., VINTERS, H. V. & HYMAN, B. T. 2012. National Institute on Aging-Alzheimer's Association guidelines for the neuropathologic assessment of Alzheimer's disease: a practical approach. *Acta Neuropathol,* 123**,** 1-11.

MOODY, D. M., BELL, M. A. & CHALLA, V. R. 1988. The corpus callosum, a unique white-matter tract: anatomic features that may explain sparing in Binswanger disease and resistance to flow of fluid masses. *AJNR Am J Neuroradiol,* 9**,** 1051-9.

MOODY, D. M., THORE, C. R., ANSTROM, J. A., CHALLA, V. R., LANGEFELD, C. D. & BROWN, W. R. 2004. Quantification of afferent vessels shows reduced brain vascular density in subjects with leukoaraiosis. *Radiology,* 233**,** 883-90.

MUNGAS, D., REED, B. R., FARIAS, S. T. & DECARLI, C. 2009. Age and education effects on relationships of cognitive test scores with brain structure in demographically diverse older persons. *Psychol Aging,* 24**,** 116-28.

MUNOZ, D. G. & FERRER, I. 2008. Neuropathology of hereditary forms of frontotemporal dementia and parkinsonism. *Handb Clin Neurol,* 89**,** 393-414.

MUNOZ, D. G., HASTAK, S. M., HARPER, B., LEE, D. & HACHINSKI, V. C. 1993. Pathologic correlates of increased signals of the centrum ovale on magnetic resonance imaging. *Arch Neurol,* 50**,** 492-7.

MURRAY, M. E., GRAFF-RADFORD, N. R., ROSS, O. A., PETERSEN, R. C., DUARA, R. & DICKSON, D. W. 2011a. Neuropathologically defined subtypes of Alzheimer's disease with distinct clinical characteristics: a retrospective study. *The Lancet Neurology,* 10**,** 785-796.

MURRAY, M. E., GRAFF-RADFORD, N. R., ROSS, O. A., PETERSEN, R. C., DUARA, R. & DICKSON, D. W. 2011b. Neuropathologically defined subtypes of Alzheimer's disease with distinct clinical characteristics: a retrospective study. *Lancet Neurol,* 10**,** 785-96.

NAGATA, K., TAKANO, D., YAMAZAKI, T., MAEDA, T., SATOH, Y., NAKASE, T. & IKEDA, Y. 2012. Cerebrovascular lesions in elderly Japanese patients with Alzheimer's disease. *J Neurol Sci,* 322**,** 87-91.

NAKAMURA, K., NEMANI, V. M., AZARBAL, F., SKIBINSKI, G., LEVY, J. M., EGAMI, K., MUNISHKINA, L., ZHANG, J., GARDNER, B., WAKABAYASHI, J., SESAKI, H., CHENG, Y., FINKBEINER, S., NUSSBAUM, R. L., MASLIAH, E. & EDWARDS, R. H. 2011. Direct membrane association drives mitochondrial fission by the Parkinson disease-associated protein alpha-synuclein. *J Biol Chem,* 286**,** 20710-26.

NASLUND, J., SCHIERHORN, A., HELLMAN, U., LANNFELT, L., ROSES, A. D., TJERNBERG, L. O., SILBERRING, J., GANDY, S. E., WINBLAD, B., GREENGARD, P. & ET AL. 1994. Relative abundance of Alzheimer A beta amyloid peptide variants in Alzheimer disease and normal aging. *Proc Natl Acad Sci U S A,* 91**,** 8378-82.

NELSON, P. T., SCHMITT, F. A., LIN, Y., ABNER, E. L., JICHA, G. A., PATEL, E., THOMASON, P. C., NELTNER, J. H., SMITH, C. D., SANTACRUZ, K. S., SONNEN, J. A., POON, L. W., GEARING, M., GREEN, R. C., WOODARD, J. L., VAN ELDIK, L. J. & KRYSCIO, R. J. 2011. Hippocampal sclerosis in advanced age: clinical and pathological features. *Brain,* 134**,** 1506-18.

NELSON, P. T., SMITH, C. D., ABNER, E. L., WILFRED, B. J., WANG, W. X., NELTNER, J. H., BAKER, M., FARDO, D. W., KRYSCIO, R. J., SCHEFF, S. W., JICHA, G. A., JELLINGER, K. A., VAN ELDIK, L. J. & SCHMITT, F. A. 2013. Hippocampal sclerosis of aging, a prevalent and high-morbidity brain disease. *Acta Neuropathol,* 126**,** 161-77.

NIEUWENHUYS, R. 1994. The neocortex. An overview of its evolutionary development, structural organization and synaptology. *Anat Embryol (Berl),* 190**,** 307-37.

NOWRANGI, M. A., RAO, V. & LYKETSOS, C. G. 2011. Epidemiology, assessment, and treatment of dementia. *Psychiatr Clin North Am,* 34**,** 275-94, vii.

OGUZ, I., YAXLEY, R., BUDIN, F., HOOGSTOEL, M., LEE, J., MALBIE, E., LIU, W., CREWS, F.T. 2013. Comparison of magnetic resonance imaging in live vs. post mortem rat brains. *Plos One*, 8:e71027.

O'SULLIVAN, M. 2008. Leukoaraiosis. *Pract Neurol,* 8**,** 26-38.

ODDO, S., CACCAMO, A., SHEPHERD, J. D., MURPHY, M. P., GOLDE, T. E., KAYED, R., METHERATE, R., MATTSON, M. P., AKBARI, Y. & LAFERLA, F. M. 2003. Triple-transgenic model of Alzheimer's disease with plaques and tangles: intracellular Abeta and synaptic dysfunction. *Neuron,* 39**,** 409-21.

OLICHNEY, J. M., GALASKO, D., SALMON, D. P., HOFSTETTER, C. R., HANSEN, L. A., KATZMAN, R. & THAL, L. J. 1998. Cognitive decline is faster in Lewy body variant than in Alzheimer's disease. *Neurology,* 51**,** 351-7.

OLSHANSKY, S. J. 1985. Pursuing longevity: delay vs elimination of degenerative diseases. *Am J Public Health,* 75**,** 754-7.

OUARDOUZ, M., NIKOLAEVA, M. A., CODERRE, E., ZAMPONI, G. W., MCRORY, J. E., TRAPP, B. D., YIN, X. H., WANG, W. L., WOULFE, J. & STYS, P. K. 2003. Depolarization-induced Ca2+ release in ischemic spinal cord white matter involves L-type Ca2+ channel activation of ryanodine receptors. *Neuron,* 40**,** 53-63.

PAIK, S. R., SHIN, H. J. & LEE, J. H. 2000. Metal-catalyzed oxidation of alpha-synuclein in the presence of Copper(II) and hydrogen peroxide. *Arch Biochem Biophys,* 378**,** 269-77.

PAKKENBERG, B. & GUNDERSEN, H. J. 1997. Neocortical neuron number in humans: effect of sex and age. *J Comp Neurol,* 384**,** 312-20.

PANTONI, L. 2010. Cerebral small vessel disease: from pathogenesis and clinical characteristics to therapeutic challenges. *Lancet Neurol,* 9**,** 689-701.

PANTONI, L. & GARCIA, J. H. 1997. Pathogenesis of leukoaraiosis: a review. *Stroke,* 28**,** 652-9.

PANTONI, L., SARTI, C., ALAFUZOFF, I., JELLINGER, K., MUNOZ, D. G., OGATA, J. & PALUMBO, V. 2006. Postmortem examination of vascular lesions in cognitive impairment: a survey among neuropathological services. *Stroke,* 37**,** 1005-9.

PARKKINEN, L., PIRTTILA, T. & ALAFUZOFF, I. 2008. Applicability of current staging/categorization of alpha-synuclein pathology and their clinical relevance. *Acta Neuropathol,* 115**,** 399-407.

PATRICK, G. N., ZUKERBERG, L., NIKOLIC, M., DE LA MONTE, S., DIKKES, P. & TSAI, L. H. 1999. Conversion of p35 to p25 deregulates Cdk5 activity and promotes neurodegeneration. *Nature,* 402**,** 615-22.

PAXINOU, E., CHEN, Q., WEISSE, M., GIASSON, B. I., NORRIS, E. H., RUETER, S. M., TROJANOWSKI, J. Q., LEE, V. M. & ISCHIROPOULOS, H. 2001. Induction of alpha-synuclein aggregation by intracellular nitrative insult. *J Neurosci,* 21**,** 8053-61.

PEARSON, R. C., ESIRI, M. M., HIORNS, R. W., WILCOCK, G. K. & POWELL, T. P. 1985. Anatomical correlates of the distribution of the pathological changes in the neocortex in Alzheimer disease. *Proc Natl Acad Sci U S A,* 82**,** 4531-4.

PERNECZKY, R., ALEXOPOULOS, P., WAGENPFEIL, S., BICKEL, H. & KURZ, A. 2012. Head circumference, apolipoprotein E genotype and cognition in the Bavarian School Sisters Study. *Eur Psychiatry,* 27**,** 219-22.

PERRY, R. O. A. 1993. Coronal map of Brodmann areas in the human brain. London: Wolfe.

PETROVITCH, H., ROSS, G. W., STEINHORN, S. C., ABBOTT, R. D., MARKESBERY, W., DAVIS, D., NELSON, J., HARDMAN, J., MASAKI, K., VOGT, M. R., LAUNER, L. & WHITE, L. R. 2005. AD lesions and infarcts in demented and non-demented Japanese-American men. *Ann Neurol,* 57**,** 98-103.

PFEFFERBAUM, A., SULLIVAN, E. V., ADALSTEINSSON, E., GARRICK, T. & HARPER, C. 2004. Postmortem MR imaging of formalin-fixed human brain. *Neuroimage,* 21**,** 1585-95.

POLVIKOSKI, T. M., VAN STRAATEN, E. C., BARKHOF, F., SULKAVA, R., ARONEN, H. J., NIINISTO, L., OINAS, M., SCHELTENS, P., ERKINJUNTTI, T. & KALARIA, R. N. 2010. Frontal lobe white matter hyperintensities and neurofibrillary pathology in the oldest old. *Neurology,* 75**,** 2071-8.

PORTET, F., BRICKMAN, A. M., STERN, Y., SCARMEAS, N., MURASKIN, J. & PROVENZANO, F. A. 2012. Metabolic syndrome and localization of white matter hyperintensities in the elderly population. *Alzheimers Dement,* 5 Suppl**,** 88-95.

PRINS, N. D., VAN DIJK, E. J., DEN HEIJER, T., VERMEER, S. E., JOLLES, J., KOUDSTAAL, P. J., HOFMAN, A. & BRETELER, M. M. 2005. Cerebral small-vessel disease and decline in information processing speed, executive function and memory. *Brain,* 128**,** 2034-41.

PRINS, N. D., VAN DIJK, E. J., DEN HEIJER, T., VERMEER, S. E., KOUDSTAAL, P. J., OUDKERK, M., HOFMAN, A. & BRETELER, M. M. 2004. Cerebral white matter lesions and the risk of dementia. *Arch Neurol,* 61**,** 1531-4.

PULLICINO, P. M., MILLER, L. L., ALEXANDROV, A. V. & OSTROW, P. T. 1995. Infraputaminal 'lacunes'. Clinical and pathological correlations. *Stroke,* 26**,** 1598-602.

PUZZO, D., PRIVITERA, L., LEZNIK, E., FA, M., STANISZEWSKI, A., PALMERI, A. & ARANCIO, O. 2008. Picomolar amyloid-beta positively modulates synaptic plasticity and memory in hippocampus. *J Neurosci,* 28**,** 14537-45.

RAFF, M. C., WHITMORE, A. V. & FINN, J. T. 2002. Axonal self-destruction and neurodegeneration. *Science,* 296**,** 868-71.

RAO, P., LAHAT, G., ARNOLD, C., GAVINO, A. C., LAHAT, S., HORNICK, J. L., LEV, D. & LAZAR, A. J. 2013. Angiosarcoma: a tissue microarray study with diagnostic implications. *Am J Dermatopathol,* 35**,** 432-7.

RAPOPORT, M., DAWSON, H. N., BINDER, L. I., VITEK, M. P. & FERREIRA, A. 2002. Tau is essential to beta -amyloid-induced neurotoxicity. *Proc Natl Acad Sci U S A,* 99**,** 6364-9.

REBEIZ, J. J., KOLODNY, E. H. & RICHARDSON, E. P., JR. 1967. Corticodentatonigral degeneration with neuronal achromasia: a progressive disorder of late adult life. *Trans Am Neurol Assoc,* 92**,** 23-6.

REITZ, C., BRAYNE, C. & MAYEUX, R. 2011. Epidemiology of Alzheimer disease. *Nat Rev Neurol,* 7**,** 137-52.

REVESZ, T., HAWKINS, C. P., DU BOULAY, E. P., BARNARD, R. O. & MCDONALD, W. I. 1989. Pathological findings correlated with magnetic resonance imaging in subcortical arteriosclerotic encephalopathy (Binswanger's disease). *J Neurol Neurosurg Psychiatry,* 52**,** 1337-44.

REZEK, D. L., MORRIS, J. C., FULLING, K. H. & GADO, M. H. 1987. Periventricular white matter lucencies in senile dementia of the Alzheimer type and in normal aging. *Neurology,* 37**,** 1365-8.

RICHARDSON, J., KERR, S. R., SHAW, F., KENNY, R. A., O'BRIEN, J. T. & THOMAS, A. J. 2009. A study of orthostatic hypotension in late-life depression. *Am J Geriatr Psychiatry,* 17**,** 996-9.

RIZZOLATTI, G. & LUPPINO, G. 2001. The cortical motor system. *Neuron,* 31**,** 889-901.

ROBINSON, J. L., GESER, F., CORRADA, M. M., BERLAU, D. J., ARNOLD, S. E., LEE, V. M., KAWAS, C. H. & TROJANOWSKI, J. Q. 2011. Neocortical and hippocampal amyloid-beta and tau measures associate with dementia in the oldest-old. *Brain,* 134**,** 3708-15.

ROMAN, G. C., ERKINJUNTTI, T., WALLIN, A., PANTONI, L. & CHUI, H. C. 2002. Subcortical ischaemic vascular dementia. *Lancet Neurol,* 1**,** 426-36.

ROMAN, G. C., TATEMICHI, T. K., ERKINJUNTTI, T., CUMMINGS, J. L., MASDEU, J. C., GARCIA, J. H., AMADUCCI, L., ORGOGOZO, J. M., BRUN, A., HOFMAN, A. & ET AL. 1993. Vascular dementia: diagnostic criteria for research studies. Report of the NINDS-AIREN International Workshop. *Neurology,* 43**,** 250-60.

ROSSLER, M., ZARSKI, R., BOHL, J. & OHM, T. G. 2002. Stage-dependent and sector-specific neuronal loss in hippocampus during Alzheimer's disease. *Acta Neuropathol,* 103**,** 363-9.

ROWBOTHAM, G. F. & LITTLE, E. 1965. A New Concept of the Circulation and the Circulations of the Brain. The Discovery of Surface Arteriovenous Shunts. *Br J Surg,* 52**,** 539-42.

RUSHWORTH, M. F., BEHRENS, T. E. & JOHANSEN-BERG, H. 2006. Connection patterns distinguish 3 regions of human parietal cortex. *Cereb Cortex,* 16**,** 1418-30.

SACHDEV, P., KALARIA, R., O'BRIEN, J., SKOOG, I., ALLADI, S., BLACK, S. E., BLACKER, D., BLAZER, D. G., CHEN, C., CHUI, H., GANGULI, M., JELLINGER, K., JESTE, D. V., PASQUIER, F., PAULSEN, J., PRINS, N., ROCKWOOD, K., ROMAN, G. & SCHELTENS, P. 2014. Diagnostic Criteria for Vascular Cognitive Disorders: A VASCOG Statement. *Alzheimer Dis Assoc Disord*.

SACHDEV, P. S., WEN, W., CHRISTENSEN, H. & JORM, A. F. 2005. White matter hyperintensities are related to physical disability and poor motor function. *J Neurol Neurosurg Psychiatry,* 76**,** 362-7.

SAHARA, N., PEREZ, P. D., LIN, W. L., DICKSON, D. W., REN, Y., ZENG, H., LEWIS, J. & FEBO, M. 2014. Age-related decline in white matter integrity in a mouse model of tauopathy: an in vivo diffusion tensor magnetic resonance imaging study. *Neurobiol Aging,* 35**,** 1364-74.

SAITO, Y., KAWASHIMA, A., RUBERU, N. N., FUJIWARA, H., KOYAMA, S., SAWABE, M., ARAI, T., NAGURA, H., YAMANOUCHI, H., HASEGAWA, M., IWATSUBO, T. & MURAYAMA, S. 2003. Accumulation of phosphorylated alpha-synuclein in aging human brain. *J Neuropathol Exp Neurol,* 62**,** 644-54.

SAITO, Y., YAMAZAKI, M., KANAZAWA, I. & MURAYAMA, S. 2002. Severe involvement of the ambient gyrus in a case of dementia with argyrophilic grain disease. *J Neurol Sci,* 196**,** 71-5.

SALEHI, A., DELCROIX, J. D., BELICHENKO, P. V., ZHAN, K., WU, C., VALLETTA, J. S., TAKIMOTO-KIMURA, R., KLESCHEVNIKOV, A. M., SAMBAMURTI, K., CHUNG, P. P., XIA, W., VILLAR, A., CAMPBELL, W. A., KULNANE, L. S., NIXON, R. A., LAMB, B. T., EPSTEIN, C. J., STOKIN, G. B., GOLDSTEIN, L. S. & MOBLEY, W. C. 2006. Increased App expression in a mouse model of Down's syndrome disrupts NGF transport and causes cholinergic neuron degeneration. *Neuron,* 51**,** 29-42.

SCARPELLI, M., SALVOLINI, U., DIAMANTI, L., MONTIRONI, R., CHIAROMONI, L. & MARICOTTI, M. 1994. MRI and pathological examination of post-mortem brains: the problem of white matter high signal areas. *Neuroradiology,* 36**,** 393-8.

SCHELTENS, P., BARKHOF, F., VALK, J., ALGRA, P. R., VAN DER HOOP, R. G., NAUTA, J. & WOLTERS, E. C. 1992. White matter lesions on magnetic resonance imaging in clinically diagnosed Alzheimer's disease. Evidence for heterogeneity. *Brain,* 115 (Pt 3)**,** 735-48.

SCHELTENS, P., ERKINJUNTI, T., LEYS, D., WAHLUND, L. O., INZITARI, D., DEL SER, T., PASQUIER, F., BARKHOF, F., MANTYLA, R., BOWLER, J., WALLIN, A., GHIKA, J., FAZEKAS, F. & PANTONI, L. 1998. White matter changes on CT and MRI: an overview of visual rating scales. European Task Force on Age-Related White Matter Changes. *Eur Neurol,* 39**,** 80-9.

SCHLAEPF.WW 1974. Calcium-Induced Degeneration of Axoplasm in Isolated Segments of Rat Peripheral-Nerve. *Brain Res,* 69**,** 203-215.
SCHLAEPFER, W. W. 1977. Structural Alterations of Peripheral-Nerve Induced by Calcium Ionophore A23187. *Brain Res,* 136**,** 1-9.
SCHMAHMANN, J. D. & PANDYA, D. N. 2006. *Fiber pathways of the brain,* New York, USA, Oxford University Press.
SCHMIDT, R., ENZINGER, C., ROPELE, S., SCHMIDT, H. & FAZEKAS, F. 2003. Progression of cerebral white matter lesions: 6-year results of the Austrian Stroke Prevention Study. *Lancet,* 361**,** 2046-8.
SCHMIDT, R., FAZEKAS, F., KLEINERT, G., OFFENBACHER, H., GINDL, K., PAYER, F., FREIDL, W., NIEDERKORN, K. & LECHNER, H. 1992. Magnetic resonance imaging signal hyperintensities in the deep and subcortical white matter. A comparative study between stroke patients and normal volunteers. *Arch Neurol,* 49**,** 825-7.
SCHMIDT, R., GRAZER, A., ENZINGER, C., ROPELE, S., HOMAYOON, N., PLUTA-FUERST, A., SCHWINGENSCHUH, P., KATSCHNIG, P., CAVALIERI, M., SCHMIDT, H., LANGKAMMER, C., EBNER, F. & FAZEKAS, F. 2011a. MRI-detected white matter lesions: do they really matter? *J Neural Transm,* 118**,** 673-81.
SCHMIDT, R., PETROVIC, K., ROPELE, S., ENZINGER, C. & FAZEKAS, F. 2007. Progression of leukoaraiosis and cognition. *Stroke,* 38**,** 2619-25.
SCHMIDT, R., SCHMIDT, H., HAYBAECK, J., LOITFELDER, M., WEIS, S., CAVALIERI, M., SEILER, S., ENZINGER, C., ROPELE, S., ERKINJUNTTI, T., PANTONI, L., SCHELTENS, P., FAZEKAS, F. & JELLINGER, K. 2011b. Heterogeneity in age-related white matter changes. *Acta Neuropathol,* 122**,** 171-85.
SCHNEIDER, J. A., ARVANITAKIS, Z., BANG, W. & BENNETT, D. A. 2007. Mixed brain pathologies account for most dementia cases in community-dwelling older persons. *Neurology,* 69**,** 2197-204.
SCHULZ, G., CROOIJMANS, H.J., GERMANN, M., SCHEFFLER, K., MULLER-GERL, M, MULLER, B. 2011. Three-dimensional strain fields in human brain resultin.g from formalin fixation. *J Neurosci Methods* 202:17-27.
SEITZ, A., KOJIMA, H., OIWA, K., MANDELKOW, E. M., SONG, Y. H. & MANDELKOW, E. 2002. Single-molecule investigation of the interference between kinesin, tau and MAP2c. *EMBO J,* 21**,** 4896-905.
SELKOE, D. J. 2008. Biochemistry and molecular biology of amyloid beta-protein and the mechanism of Alzheimer's disease. *Handb Clin Neurol,* 89**,** 245-60.
SHAHANI, N. & BRANDT, R. 2002. Functions and malfunctions of the tau proteins. *Cell Mol Life Sci,* 59**,** 1668-80.
SHENKIN, S. D., BASTIN, M. E., MACGILLIVRAY, T. J., DEARY, I. J., STARR, J. M., RIVERS, C. S. & WARDLAW, J. M. 2005. Cognitive correlates of cerebral white matter lesions and water diffusion tensor parameters in community-dwelling older people. *Cerebrovasc Dis,* 20**,** 310-8.
SHEPHERD, T. M., THELWALL, P. E., STANISZ, G. J. & BLACKBAND, S. J. 2009. Aldehyde fixative solutions alter the water relaxation and diffusion properties of nervous tissue. *Magn Reson Med,* 62**,** 26-34.
SILBERT, L. C., DODGE, H. H., PERKINS, L. G., SHERBAKOV, L., LAHNA, D., ERTEN-LYONS, D., WOLTJER, R., SHINTO, L. & KAYE, J. A. 2012. Trajectory of white matter hyperintensity burden preceding mild cognitive impairment. *Neurology,* 79**,** 741-7.

SIMON, R. 2010. Applications of tissue microarray technology. *Methods Mol Biol,* 664**,** 1-16.

SIMON, R., RICHTER, J., WAGNER, U., FIJAN, A., BRUDERER, J., SCHMID, U., ACKERMANN, D., MAURER, R., ALUND, G., KNONAGEL, H., RIST, M., WILBER, K., ANABITARTE, M., HERING, F., HARDMEIER, T., SCHONENBERGER, A., FLURY, R., JAGER, P., FEHR, J. L., SCHRAML, P., MOCH, H., MIHATSCH, M. J., GASSER, T. & SAUTER, G. 2001. High-throughput tissue microarray analysis of 3p25 (RAF1) and 8p12 (FGFR1) copy number alterations in urinary bladder cancer. *Cancer Res,* 61**,** 4514-9.

SIPAYYA, V., SHARMA, I., SHARMA, K. C. & SINGH, A. 2012. Immunohistochemical expression of IDH1 in gliomas: a tissue microarray-based approach. *J Cancer Res Ther,* 8**,** 598-601.

SJOBECK, M., HAGLUND, M., PERSSON, A., STURESSON, K. & ENGLUND, E. 2003. Brain tissue microarrays in dementia research: white matter microvascular pathology in Alzheimer's disease. *Neuropathology,* 23**,** 290-5.

SKACEL, M., SKILTON, B., PETTAY, J. D. & TUBBS, R. R. 2002. Tissue microarrays: a powerful tool for high-throughput analysis of clinical specimens: a review of the method with validation data. *Appl Immunohistochem Mol Morphol,* 10**,** 1-6.

SKOVRONSKY, D. M., LEE, V. M. & TROJANOWSKI, J. Q. 2006. Neurodegenerative diseases: new concepts of pathogenesis and their therapeutic implications. *Annu Rev Pathol,* 1**,** 151-70.

SMALLWOOD, A., OULHAJ, A., JOACHIM, C., CHRISTIE, S., SLOAN, C., SMITH, A. D. & ESIRI, M. 2012. Cerebral subcortical small vessel disease and its relation to cognition in elderly subjects: a pathological study in the Oxford Project to Investigate Memory and Ageing (OPTIMA) cohort. *Neuropathol Appl Neurobiol,* 38**,** 337-43.

SMITH, C. D., SNOWDON, D. & MARKESBERY, W. R. 2000. Periventricular white matter hyperintensities on MRI: correlation with neuropathologic findings. *J Neuroimaging,* 10**,** 13-6.

SMITH, E. E., GUROL, M. E., ENG, J. A., ENGEL, C. R., NGUYEN, T. N., ROSAND, J. & GREENBERG, S. M. 2004. White matter lesions, cognition, and recurrent hemorrhage in lobar intracerebral hemorrhage. *Neurology,* 63**,** 1606-12.

SNOWDON, D. A., GREINER, L. H., MORTIMER, J. A., RILEY, K. P., GREINER, P. A. & MARKESBERY, W. R. 1997. Brain infarction and the clinical expression of Alzheimer disease. The Nun Study. *JAMA,* 277**,** 813-7.

SOENNESYN, H., NILSEN, D. W., OPPEDAL, K., GREVE, O. J., BEYER, M. K. & AARSLAND, D. 2012. Relationship between orthostatic hypotension and white matter hyperintensity load in older patients with mild dementia. *Plos One,* 7**,** e52196.

SOSA-ORTIZ, A. L., ACOSTA-CASTILLO, I. & PRINCE, M. J. 2012. Epidemiology of dementias and Alzheimer's disease. *Arch Med Res,* 43**,** 600-8.

SPILLANTINI, M. G., SCHMIDT, M. L., LEE, V. M., TROJANOWSKI, J. Q., JAKES, R. & GOEDERT, M. 1997. Alpha-synuclein in Lewy bodies. *Nature,* 388**,** 839-40.

SQUIRE, L. R., STARK, C. E. & CLARK, R. E. 2004. The medial temporal lobe. *Annu Rev Neurosci,* 27**,** 279-306.

STARY, H. C. 2000. Natural history and histological classification of atherosclerotic lesions: an update. *Arterioscler Thromb Vasc Biol,* 20**,** 1177-8.

STARY, H. C., CHANDLER, A. B., DINSMORE, R. E., FUSTER, V., GLAGOV, S., INSULL, W., JR., ROSENFELD, M. E., SCHWARTZ, C. J., WAGNER, W. D. & WISSLER, R. W. 1995. A definition of advanced types of atherosclerotic lesions and a histological classification of atherosclerosis. A report from the Committee on Vascular Lesions of the Council on Arteriosclerosis, American Heart Association. *Arterioscler Thromb Vasc Biol,* 15**,** 1512-31.

STARY, H. C., CHANDLER, A. B., GLAGOV, S., GUYTON, J. R., INSULL, W., JR., ROSENFELD, M. E., SCHAFFER, S. A., SCHWARTZ, C. J., WAGNER, W. D. & WISSLER, R. W. 1994. A definition of initial, fatty streak, and intermediate lesions of atherosclerosis. A report from the Committee on Vascular Lesions of the Council on Arteriosclerosis, American Heart Association. *Arterioscler Thromb,* 14**,** 840-56.

STEELE, J. C., RICHARDSON, J. C. & OLSZEWSKI, J. 1964. Progressive Supranuclear Palsy. A Heterogeneous Degeneration Involving the Brain Stem, Basal Ganglia and Cerebellum with Vertical Gaze and Pseudobulbar Palsy, Nuchal Dystonia and Dementia. *Arch Neurol,* 10**,** 333-59.

STENSET, V., HOFOSS, D., BERSTAD, A. E., NEGAARD, A., GJERSTAD, L. & FLADBY, T. 2008. White matter lesion subtypes and cognitive deficits in patients with memory impairment. *Dement Geriatr Cogn Disord,* 26**,** 424-31.

STERN, Y. 2002. What is cognitive reserve? Theory and research application of the reserve concept. *J Int Neuropsychol Soc,* 8**,** 448-60.

STERN, Y. 2012. Cognitive reserve in ageing and Alzheimer's disease. *Lancet Neurol,* 11**,** 1006-12.

STOKIN, G. B., LILLO, C., FALZONE, T. L., BRUSCH, R. G., ROCKENSTEIN, E., MOUNT, S. L., RAMAN, R., DAVIES, P., MASLIAH, E., WILLIAMS, D. S. & GOLDSTEIN, L. S. 2005. Axonopathy and transport deficits early in the pathogenesis of Alzheimer's disease. *Science,* 307**,** 1282-8.

STOLL, G. & MULLER, H. W. 1999. Nerve injury, axonal degeneration and neural regeneration: basic insights. *Brain Pathol,* 9**,** 313-25.

STRICKER, N. H., SCHWEINSBURG, B. C., DELANO-WOOD, L., WIERENGA, C. E., BANGEN, K. J., HAALAND, K. Y., FRANK, L. R., SALMON, D. P. & BONDI, M. W. 2009. Decreased white matter integrity in late-myelinating fiber pathways in Alzheimer's disease supports retrogenesis. *Neuroimage,* 45**,** 10-6.

STYS, P. K. 1998. Anoxic and ischemic injury of myelinated axons in CNS white matter: From mechanistic concepts to therapeutics. *Journal of Cerebral Blood Flow and Metabolism,* 18**,** 2-25.

SUCHY, Y., KRAYBILL, M. L. & FRANCHOW, E. 2011. Instrumental activities of daily living among community-dwelling older adults: discrepancies between self-report and performance are mediated by cognitive reserve. *J Clin Exp Neuropsychol,* 33**,** 92-100.

TANG, M. X., CROSS, P., ANDREWS, H., JACOBS, D. M., SMALL, S., BELL, K., MERCHANT, C., LANTIGUA, R., COSTA, R., STERN, Y. & MAYEUX, R. 2001. Incidence of AD in African-Americans, Caribbean Hispanics, and Caucasians in northern Manhattan. *Neurology,* 56**,** 49-56.

TEIPEL, S. J., HAMPEL, H., PIETRINI, P., ALEXANDER, G. E., HORWITZ, B., DALEY, E., MOLLER, H. J., SCHAPIRO, M. B. & RAPOPORT, S. I. 1999. Region-specific corpus callosum atrophy correlates with the regional pattern of cortical glucose metabolism in Alzheimer disease. *Arch Neurol,* 56**,** 467-73.

TERRY, R. D., DETERESA, R. & HANSEN, L. A. 1987. Neocortical cell counts in normal human adult aging. *Ann Neurol,* 21**,** 530-9.

THAL, D. R., DEL TREDICI, K., LUDOLPH, A. C., HOOZEMANS, J. J., ROZEMULLER, A. J., BRAAK, H. & KNIPPSCHILD, U. 2011. Stages of granulovacuolar degeneration: their relation to Alzheimer's disease and chronic stress response. *Acta Neuropathol,* 122**,** 577-89.

THAL, D. R., GHEBREMEDHIN, E., ORANTES, M. & WIESTLER, O. D. 2003. Vascular pathology in Alzheimer disease: correlation of cerebral amyloid angiopathy and arteriosclerosis/lipohyalinosis with cognitive decline. *J Neuropathol Exp Neurol,* 62**,** 1287-301.

THAL, D. R., GHEBREMEDHIN, E., RUB, U., YAMAGUCHI, H., DEL TREDICI, K. & BRAAK, H. 2002a. Two types of sporadic cerebral amyloid angiopathy. *J Neuropathol Exp Neurol,* 61**,** 282-93.

THAL, D. R., GRINBERG, L. T. & ATTEMS, J. 2012. Vascular dementia: different forms of vessel disorders contribute to the development of dementia in the elderly brain. *Exp Gerontol,* 47**,** 816-24.

THAL, D. R., LARIONOV, S., ABRAMOWSKI, D., WIEDERHOLD, K. H., VAN DOOREN, T., YAMAGUCHI, H., HAASS, C., VAN LEUVEN, F., STAUFENBIEL, M. & CAPETILLO-ZARATE, E. 2007. Occurrence and co-localization of amyloid beta-protein and apolipoprotein E in perivascular drainage channels of wild-type and APP-transgenic mice. *Neurobiol Aging,* 28**,** 1221-30.

THAL, D. R., RUB, U., ORANTES, M. & BRAAK, H. 2002b. Phases of A beta-deposition in the human brain and its relevance for the development of AD. *Neurology,* 58**,** 1791-800.

THAL, D. R., VON ARNIM, C., GRIFFIN, W. S., YAMAGUCHI, H., MRAK, R. E., ATTEMS, J. & UPADHAYA, A. R. 2013. Pathology of clinical and preclinical Alzheimer's disease. *Eur Arch Psychiatry Clin Neurosci,* 263 Suppl 2**,** S137-45.

THIES, W. & BLEILER, L. 2013. 2013 Alzheimer's disease facts and figures. *Alzheimers Dement,* 9**,** 208-45.

TIAN, J., SHI, J. & MANN, D. M. 2004. Cerebral amyloid angiopathy and dementia. *Panminerva Med,* 46**,** 253-64.

TSUBOI, Y., JOSEPHS, K. A., BOEVE, B. F., LITVAN, I., CASELLI, R. J., CAVINESS, J. N., UITTI, R. J., BOTT, A. D. & DICKSON, D. W. 2005. Increased tau burden in the cortices of progressive supranuclear palsy presenting with corticobasal syndrome. *Mov Disord,* 20**,** 982-8.

TSUBOI, Y., SLOWINSKI, J., JOSEPHS, K. A., HONER, W. G., WSZOLEK, Z. K. & DICKSON, D. W. 2003. Atrophy of superior cerebellar peduncle in progressive supranuclear palsy. *Neurology,* 60**,** 1766-9.

TYLER, S. J., DAWBARN, D., WILCOCK, G. K. & ALLEN, S. J. 2002. alpha- and beta-secretase: profound changes in Alzheimer's disease. *Biochem Biophys Res Commun,* 299**,** 373-6.

UCHIKADO, H., LIN, W. L., DELUCIA, M. W. & DICKSON, D. W. 2006. Alzheimer disease with amygdala Lewy bodies: a distinct form of alpha-synucleinopathy. *J Neuropathol Exp Neurol,* 65**,** 685-97.

UVERSKY, V. N., LI, J. & FINK, A. L. 2001. Evidence for a partially folded intermediate in alpha-synuclein fibril formation. *J Biol Chem,* 276**,** 10737-44.

VAN DER FLIER, W. M., VAN DER VLIES, A. E., WEVERLING-RIJNSBURGER, A. W., DE BOER, N. L., ADMIRAAL-BEHLOUL, F., BOLLEN, E. L., WESTENDORP, R. G., VAN BUCHEM, M. A. & MIDDELKOOP, H. A. 2005. MRI measures and progression of cognitive decline in nondemented elderly attending a memory clinic. *Int J Geriatr Psychiatry,* 20**,** 1060-6.

VAN DIJK, E. J., PRINS, N. D., VERMEER, S. E., KOUDSTAAL, P. J. & BRETELER, M. M. 2002. Frequency of white matter lesions and silent lacunar infarcts. *J Neural Transm Suppl***,** 25-39.

VAN SWIETEN, J. C., VAN DEN HOUT, J. H., VAN KETEL, B. A., HIJDRA, A., WOKKE, J. H. & VAN GIJN, J. 1991. Periventricular lesions in the white matter on magnetic resonance imaging in the elderly. A morphometric correlation with arteriolosclerosis and dilated perivascular spaces. *Brain,* 114 (Pt 2)**,** 761-74.

VINTERS, H. V. 1987. Cerebral amyloid angiopathy. A critical review. *Stroke,* 18**,** 311-24.

VINTERS, H. V., ELLIS, W. G., ZAROW, C., ZAIAS, B. W., JAGUST, W. J., MACK, W. J. & CHUI, H. C. 2000. Neuropathologic substrates of ischemic vascular dementia. *J Neuropathol Exp Neurol,* 59**,** 931-45.

VISSER, P. J., SCHELTENS, P., VERHEY, F. R., SCHMAND, B., LAUNER, L. J., JOLLES, J. & JONKER, C. 1999. Medial temporal lobe atrophy and memory dysfunction as predictors for dementia in subjects with mild cognitive impairment. *J Neurol,* 246**,** 477-85.

VISWANATHAN, A. & GREENBERG, S. M. 2011. Cerebral amyloid angiopathy in the elderly. *Ann Neurol,* 70**,** 871-80.

VISWANATHAN, A., PATEL, P., RAHMAN, R., NANDIGAM, R. N., KINNECOM, C., BRACOUD, L., ROSAND, J., CHABRIAT, H., GREENBERG, S. M. & SMITH, E. E. 2008. Tissue microstructural changes are independently associated with cognitive impairment in cerebral amyloid angiopathy. *Stroke,* 39**,** 1988-92.

VOSSEL, K. A., ZHANG, K., BRODBECK, J., DAUB, A. C., SHARMA, P., FINKBEINER, S., CUI, B. & MUCKE, L. 2010. Tau reduction prevents Abeta-induced defects in axonal transport. *Science,* 330**,** 198.

WAHLUND, L. O., BARKHOF, F., FAZEKAS, F., BRONGE, L., AUGUSTIN, M., SJOGREN, M., WALLIN, A., ADER, H., LEYS, D., PANTONI, L., PASQUIER, F., ERKINJUNTTI, T. & SCHELTENS, P. 2001. A new rating scale for age-related white matter changes applicable to MRI and CT. *Stroke,* 32**,** 1318-22.

WAKANA, S., JIANG, H., NAGAE-POETSCHER, L. M., VAN ZIJL, P. C. & MORI, S. 2004. Fiber tract-based atlas of human white matter anatomy. *Radiology,* 230**,** 77-87.

WANG, J. Z., GRUNDKE-IQBAL, I. & IQBAL, K. 2007. Kinases and phosphatases and tau sites involved in Alzheimer neurofibrillary degeneration. *Eur J Neurosci,* 25**,** 59-68.

WARDLAW, J. M., SANDERCOCK, P. A., DENNIS, M. S. & STARR, J. 2003. Is breakdown of the blood-brain barrier responsible for lacunar stroke, leukoaraiosis, and dementia? *Stroke,* 34**,** 806-12.

WARDLAW, J. M., SMITH, E. E., BIESSELS, G. J., CORDONNIER, C., FAZEKAS, F., FRAYNE, R., LINDLEY, R. I., O'BRIEN, J. T., BARKHOF,

F., BENAVENTE, O. R., BLACK, S. E., BRAYNE, C., BRETELER, M., CHABRIAT, H., DECARLI, C., DE LEEUW, F. E., DOUBAL, F., DUERING, M., FOX, N. C., GREENBERG, S., HACHINSKI, V., KILIMANN, I., MOK, V., OOSTENBRUGGE, R., PANTONI, L., SPECK, O., STEPHAN, B. C., TEIPEL, S., VISWANATHAN, A., WERRING, D., CHEN, C., SMITH, C., VAN BUCHEM, M., NORRVING, B., GORELICK, P. B. & DICHGANS, M. 2013. Neuroimaging standards for research into small vessel disease and its contribution to ageing and neurodegeneration. *Lancet Neurol,* 12**,** 822-38.

WAXMAN, E. A. & GIASSON, B. I. 2009. Molecular mechanisms of alpha-synuclein neurodegeneration. *Biochim Biophys Acta,* 1792**,** 616-24.

WELLER, R. O., DJUANDA, E., YOW, H. Y. & CARARE, R. O. 2009. Lymphatic drainage of the brain and the pathophysiology of neurological disease. *Acta Neuropathol,* 117**,** 1-14.

WHITWELL, J. L. 2010. The protective role of brain size in Alzheimer's disease. *Expert Rev Neurother,* 10**,** 1799-801.

WILLIAMS, D. R., HOLTON, J. L., STRAND, K., REVESZ, T. & LEES, A. J. 2007. Pure akinesia with gait freezing: a third clinical phenotype of progressive supranuclear palsy. *Mov Disord,* 22**,** 2235-41.

WINNER, B., JAPPELLI, R., MAJI, S. K., DESPLATS, P. A., BOYER, L., AIGNER, S., HETZER, C., LOHER, T., VILAR, M., CAMPIONI, S., TZITZILONIS, C., SORAGNI, A., JESSBERGER, S., MIRA, H., CONSIGLIO, A., PHAM, E., MASLIAH, E., GAGE, F. H. & RIEK, R. 2011. In vivo demonstration that alpha-synuclein oligomers are toxic. *Proc Natl Acad Sci U S A,* 108**,** 4194-9.

WIRTHS, O., WEIS, J., SZCZYGIELSKI, J., MULTHAUP, G. & BAYER, T. A. 2006. Axonopathy in an APP/PS1 transgenic mouse model of Alzheimer's disease. *Acta Neuropathol,* 111**,** 312-9.

YAMADA, T., MCGEER, P. L. & MCGEER, E. G. 1992. Appearance of paired nucleated, Tau-positive glia in patients with progressive supranuclear palsy brain tissue. *Neurosci Lett,* 135**,** 99-102.

YAMAMOTO, Y. 2011. *Characterization of the Neurovascular pathology in CADASIL: A model for subcortical vascular dementia.* Doctor of Philosophy, Newcastle University.

YAMAMOTO, Y., IHARA, M., THAM, C., LOW, R. W., SLADE, J. Y., MOSS, T., OAKLEY, A. E., POLVIKOSKI, T. & KALARIA, R. N. 2009. Neuropathological correlates of temporal pole white matter hyperintensities in CADASIL. *Stroke,* 40**,** 2004-11.

YAMANOUCHI, H., SUGIURA, S. & SHIMADA, H. 1989. Decrease of nerve fibres in the anterior corpus callosum of senile dementia of Alzheimer type. *J Neurol,* 236**,** 491-2.

YIP, A. G., MCKEE, A. C., GREEN, R. C., WELLS, J., YOUNG, H., CUPPLES, L. A. & FARRER, L. A. 2005. APOE, vascular pathology, and the AD brain. *Neurology,* 65**,** 259-65.

YOSHITA, M., FLETCHER, E., HARVEY, D., ORTEGA, M., MARTINEZ, O., MUNGAS, D. M., REED, B. R. & DECARLI, C. S. 2006. Extent and distribution of white matter hyperintensities in normal aging, MCI, and AD. *Neurology,* 67**,** 2192-8.

ZACCAI, J., BRAYNE, C., MCKEITH, I., MATTHEWS, F. & INCE, P. G. 2008. Patterns and stages of alpha-synucleinopathy: Relevance in a population-based cohort. *Neurology,* 70**,** 1042-8.

ZHANG, B., HIGUCHI, M., YOSHIYAMA, Y., ISHIHARA, T., FORMAN, M. S., MARTINEZ, D., JOYCE, S., TROJANOWSKI, J. Q. & LEE, V. M. 2004. Retarded axonal transport of R406W mutant tau in transgenic mice with a neurodegenerative tauopathy. *J Neurosci,* 24**,** 4657-67.

ZHENG, H., JIANG, M., TRUMBAUER, M. E., SIRINATHSINGHJI, D. J., HOPKINS, R., SMITH, D. W., HEAVENS, R. P., DAWSON, G. R., BOYCE, S., CONNER, M. W., STEVENS, K. A., SLUNT, H. H., SISODA, S. S., CHEN, H. Y. & VAN DER PLOEG, L. H. 1995. beta-Amyloid precursor protein-deficient mice show reactive gliosis and decreased locomotor activity. *Cell,* 81**,** 525-31.

ZHOU, G., REN, S., CHEN, N., DUAN, L., ZHANG, Z., FANG, S. & ZHAO, W. 2008. Cerebral white matter lesions and cognitive function in a non-demented Chinese veteran cohort. *J Int Med Res,* 36**,** 115-22.